

LIGNIN DEGRADATION AND MODIFICATION BY LACCASE/MEDIATOR SYSTEMS

Insights at the molecular level



Roelant Hilgers

Propositions

1. Monomeric lignin model compounds do not exist.
(this thesis)
2. Optimizing reaction conditions based on laccase activity is a poor strategy for lignin degradation by laccase/mediator systems.
(this thesis)
3. YouTube should actively flatten the curve of increasing incidents of online radicalization.
(Based on: Proceedings of the 2020 Conference on Fairness, Accountability, and Transparency. 2020. p. 131-141)
4. 'Catalytic synthesis' is a contradictio in terminis.
5. 'Sustainability' should be a compulsory subject in secondary education.
6. Transparency in the meat production chain starts with glass walls of abattoirs.

Propositions belonging to the thesis, entitled

Lignin degradation and modification by laccase/mediator systems

Insights at the molecular level

Roelant Hilgers

Wageningen, 4 September 2020

Lignin degradation and modification by laccase/mediator systems

Insights at the molecular level

Roelant Hilgers

Thesis committee

Promotor

Prof. Dr J.-P. Vincken
Professor of Food Chemistry
Wageningen University & Research

Co-promotor

Dr M.A. Kabel
Associate professor at the Laboratory of Food Chemistry
Wageningen University & Research

Other members

Prof. Dr J.H. Bitter, Wageningen University & Research
Prof. Dr A.S. Meyer, Technical University of Denmark
Prof. Dr P.C.A. Bruijninx, Utrecht University
Dr M.C.R. Franssen, Wageningen University & Research

This research was conducted under the auspices of the Graduate School VLAG (Advanced studies in Food Technology, Agrobiotechnology, Nutrition and Health Sciences).

Lignin degradation and modification by laccase/mediator systems

Insights at the molecular level

Roelant Hilgers

Thesis

submitted in fulfilment of the requirements for the degree of doctor
at Wageningen University

by the authority of the Rector Magnificus,

Prof. Dr A.P.J. Mol

in the presence of the

Thesis Committee appointed by the Academic Board

to be defended in public

on Friday 4 September 2020

at 4 p.m. in the Aula.

Roelant Hilgers

Lignin degradation and modification by laccase/mediator systems

Insights at the molecular level

242 pages

PhD thesis, Wageningen University, Wageningen, the Netherlands (2020)

With references, with summary in English

ISBN: 978-94-6395-385-6

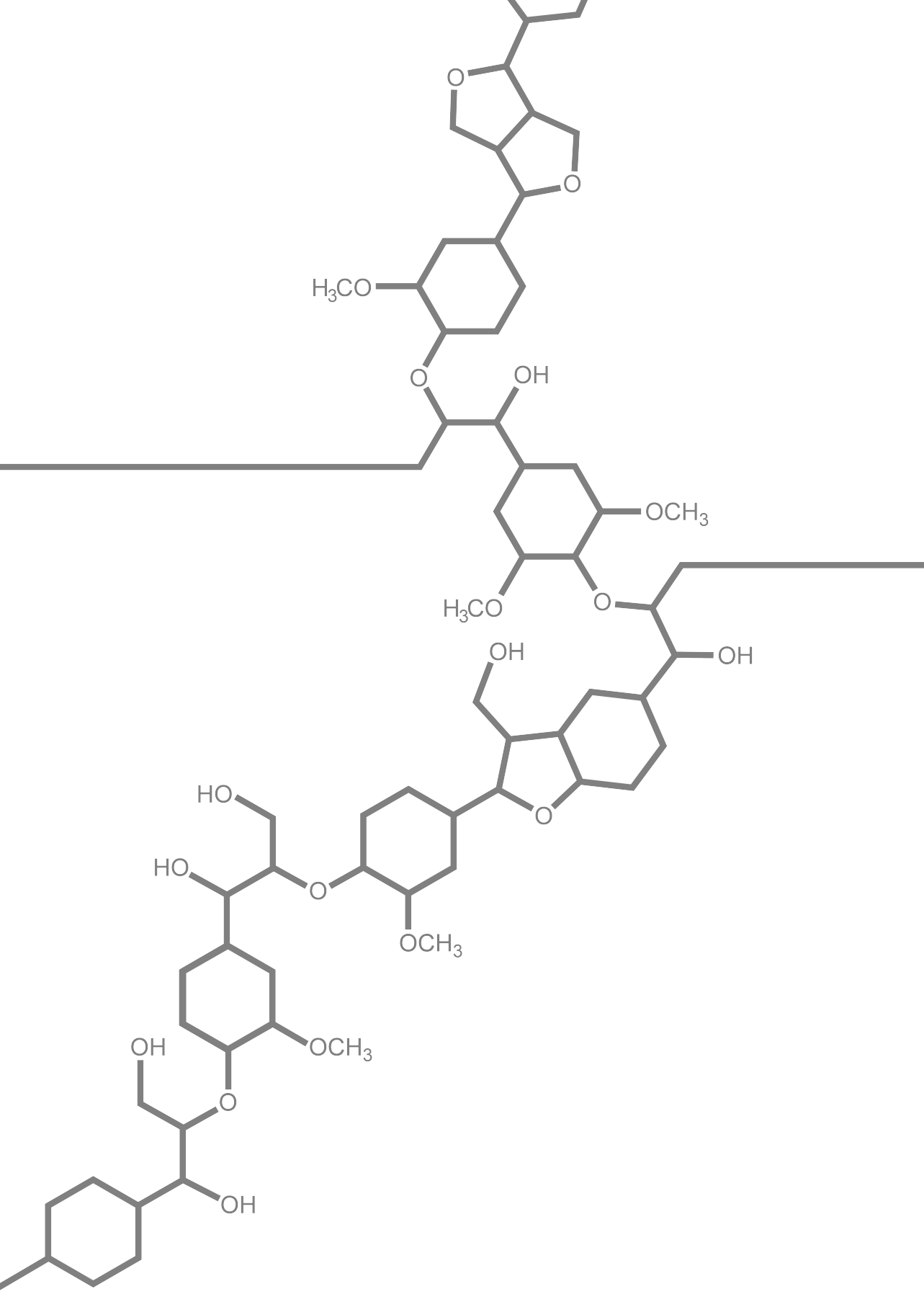
DOI: <https://doi.org/10.18174/520249>

Abstract

Lignin degradation and valorization is one of the major challenges in biorefinery. A potential green tool for lignin degradation or modification is the use of laccase/mediator systems (LMS). Treatment of lignin with LMS results in lignin radicals, which may react further via multiple pathways, resulting in lignin degradation, modification or polymerization. The overall outcome of LMS treatments of lignin is, currently, hard to predict, as the reactions of lignin induced by LMS treatments are insufficiently understood. In this thesis, we investigated the reactivity of lignin upon laccase and LMS treatments by using various lignin model compounds as well as lignocellulose and lignin isolates as substrates. We demonstrated that the balance between degradation, C_α-oxidation and polymerization of lignin is dependent on multiple factors, such as the choice of mediator and the initial structure of the lignin substrate. In addition, we revealed that buffer properties play a key role in the balance between C_α-oxidation and degradation of lignin structures by a laccase/hydroxybenzotriazole (HBT) system, and that altering buffer properties allows to enhance bond cleavage of a lignin structure by >1 order of magnitude. Laccase/HBT treatment of wheat straw and corn stover was shown to result in up to 51% delignification of the biomass. Based on the insights obtained from the model compound studies, and by using a combination of HSQC NMR spectroscopy and py-GC-MS, we showed, for the first time, that the laccase/HBT system degrades lignin via cleavage of C_β-O, O-4' and C_α-C_β bonds. Overall, by studying the reactivity of various lignin substructures, this thesis provided in-depth insights into the reactivity of lignin upon laccase and LMS treatments.

Table of contents

Chapter 1	General introduction	1
Chapter 2	Laccase/mediator systems: their reactivity toward phenolic lignin structures	29
Chapter 3	The impact of lignin sulfonation on its reactivity with laccase and laccase/HBT	53
Chapter 4	Boosting degradation of lignin β -O-4' linkages by laccase/HBT: the overlooked effect of buffer properties	81
Chapter 5	Understanding laccase/HBT-catalyzed grass delignification at the molecular level	107
Chapter 6	Facile enzymatic C _V -acylation of lignin model compounds	155
Chapter 7	On the reactivity of <i>p</i> -coumaroyl groups in lignin upon laccase and laccase/HBT treatments	179
Chapter 8	General discussion	201
Summary		225
Acknowledgements		231
About the author		237



CHAPTER

1

General introduction

1.1 Relevance of this research

With increasing concerns about global warming and the depletion of fossil resources, worldwide measures are taken to promote the transition from a fossil-based to a biobased economy. One of the strategies to contribute to this transition is the use of lignocellulosic biomass for the production of biofuels, biochemicals and biomaterials. A key step in this process is the selective degradation and removal of lignin, the most recalcitrant constituent of lignocellulose. It has been shown that lignin degradation and its removal from lignocellulose facilitates microbial and enzymatic saccharification of the polysaccharides present in lignocellulose.¹⁻³ This, eventually, results in a more efficient production of biofuels or biochemicals. An additional area of importance is the valorization of technical lignins, which are structurally modified lignins, currently of low value, produced at a scale of >1 Mtonne per year as by-product in the pulp and paper industry.⁴ Various chemical and physical strategies have been developed for lignin degradation and modification, but most of these require harsh conditions. As an alternative and sustainable approach, enzymatic lignin degradation and modification are receiving increasing attention. In this respect, laccases are considered highly relevant oxidative enzymes produced by many lignin-degrading micro-organisms. To boost their oxidative capacity, laccases are often combined with so-called mediators, to form a laccase/mediator system (LMS). Laccase and LMS have been shown to be promising tools for both delignification of lignocellulosic biomass, and for valorization of technical lignins. Nevertheless, the mechanisms behind laccase and LMS-based lignin conversions are poorly understood, which hampers further optimization. Therefore, the main aim of this thesis is to enhance the understanding of laccase and LMS-catalyzed lignin conversion at the molecular level.

1.2 Lignocellulose

Lignocellulose is a complex architecture of cellulose, hemicellulose and lignin, occurring in both woody and herbaceous plants, mainly in the secondary cell wall.⁵ These three constituents form a rigid three-dimensional network, providing strength to the plant (see **Fig. 1.1**). The relative abundance of cellulose, hemicellulose and lignin are, amongst other factors, strongly dependent on the botanical origin (**Table 1.1**).

Table 1.1 Relative abundance of cellulose, hemicellulose and lignin in softwood, hardwood and grasses (w/w % based on dry matter).⁶

Source	Cellulose (%)	Hemicellulose (%)	Lignin (%)
Softwood	45-50	25-35	25-35
Hardwood	40-55	24-40	18-25
Grasses	25-40	35-50	10-30

Cellulose is a polysaccharide consisting exclusively of β -(1 \rightarrow 4)-linked glucosyl units, with a degree of polymerization (DP) of up to 10,000, depending on the source.⁷ It is

assembled into partly crystalline fibers, mainly held together by hydrogen bonds.⁷⁻⁹ Hemicellulose is a collective name for a variety of heterogeneous and branched polysaccharides, such as arabinoxylans and glucomannans. The composition of the hemicellulose fraction is strongly dependent on the botanical origin of the lignocellulosic biomass. In contrast to cellulose, hemicelluloses have a relatively low DP (generally 50-300), and are generally amorphous.^{10,11} The hemicelluloses are associated with the cellulose fibers via hydrogen bonding.^{12,13}

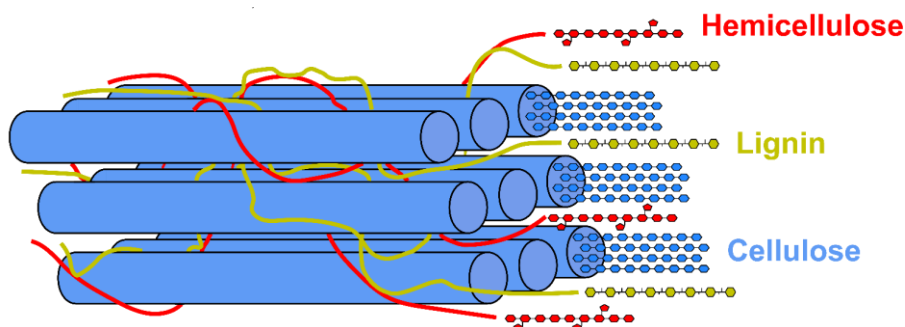


Fig. 1.1 Schematic representation of lignocellulose as present in secondary plant cell walls, based on Loqué et al.¹⁴

The third and, arguably, most complex constituent of lignocellulose is lignin, a heterogeneous aromatic polymer. It is associated with both cellulose and hemicellulose via non-covalent (mainly electrostatic) interactions and with hemicellulose via covalent linkages (see section 1.3).^{15,16}

1.3 The structure of lignin

1.3.1 Lignin biosynthesis and the structure of native lignin

The primary precursors of lignin are the phenylpropanoids sinapyl alcohol, coniferyl alcohol and *p*-coumaryl alcohol (**Fig. 1.2**). During lignin biosynthesis, these monomers are oxidized to radicals by peroxidases and/or laccases, after which they undergo endwise oxidative coupling to form a lignin polymer. Oxidation of the polymer chain end occurs, most likely, not directly by peroxidases or laccases, but via radical transfer between the polymer and small, freely diffusible phenoxyl radicals.^{17,18} Once the sinapyl, coniferyl and *p*-coumaryl alcohol building blocks are incorporated into the polymer, they are referred to as syringyl (S), guaiacyl (G) and *p*-hydroxyphenyl (H) subunits, respectively.^{18,19}

The relative abundance of S, G and H units in lignin differs largely between plant types. With some exceptions, softwood lignin essentially only contains G units, and low amounts of H units, whereas hardwood lignin is composed of both S and G units and traces of H units.^{18,19} Grass lignin contain S, G and H units, although the relative abundance of H units is rarely above 5%.¹⁹

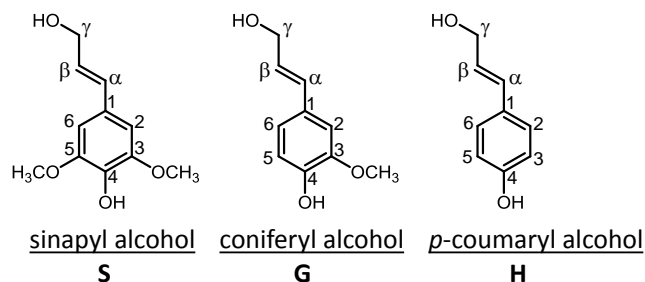


Fig. 1.2 Molecular structures of the three monolignols, the main precursors of lignin. Once incorporated in the lignin polymer, these monolignols form syringyl (S), guaiacyl (G) and *p*-hydroxyphenyl (H) subunits.

Upon radical coupling of monolignols to the growing polymer, a variety of C-O and C-C linkages are formed, most often involving the C_β atom of the monolignol. In all native lignins, the β-aryl ether (β-*O*-4' linkage) is the most abundant interunit linkage. In addition, most lignins contain considerable amounts of phenylcoumaran (β-5') and resinol (β-β') linkages. A schematic example of the lignin polymerization process, including formation of these three interunit linkages linkages, is shown in **Fig. 1.3**.

The type of interunit linkage formed upon radical coupling is directly influenced by the structure (i.e. S/G/H) of the radicals involved. For instance, as the formation of β-5' linkages requires a free (i.e. not methoxylated) C₅ atom, such bonds cannot be formed upon coupling to an S-type aromatic ring (see reaction 1 in **Fig. 1.3**). Consequently, the highest content of phenylcoumaran linkages is generally found in softwood lignins, in which S units are absent (**Table 1.2**). Furthermore, resinol formation requires two free C_β atoms, thus, each linear lignin chain can only have one resinol linkage.

Table 1.2 Relative abundance of lignin interunit linkages found in lignin from softwood, hardwood and grasses. Values are based on literature.¹⁹⁻²⁶ N.D. = No data.

Linkage	Relative abundance (%)		
	Softwood	Hardwood	Grasses
β-aryl ether (β- <i>O</i> -4')	45-50	60-89	74-84
Phenylcoumaran (β-5')	9-12	2-11	5-15
Resinol (β-β')	2-6	3-14	1-7
Tetrahydrofuran (β-β') ^a	N.D.	N.D.	≤5
Dibenzodioxocin	5-7	≤2	≤3
(5-5'/α- <i>O</i> -4'/β- <i>O</i> -4')			
Diaryl ether (4- <i>O</i> -5')	~2	~2	N.D.
Spirodienone (β-1'/α- <i>O</i> -α')	1-9	1-7	2-3

^a Present in (highly) C_V-acylated lignins. After β-β' coupling (step I in Fig. 1.3), a water molecule is inserted to enable rearomatization, as C_V-acylation prevents intramolecular rearomatization (step II in Fig. 1.3).

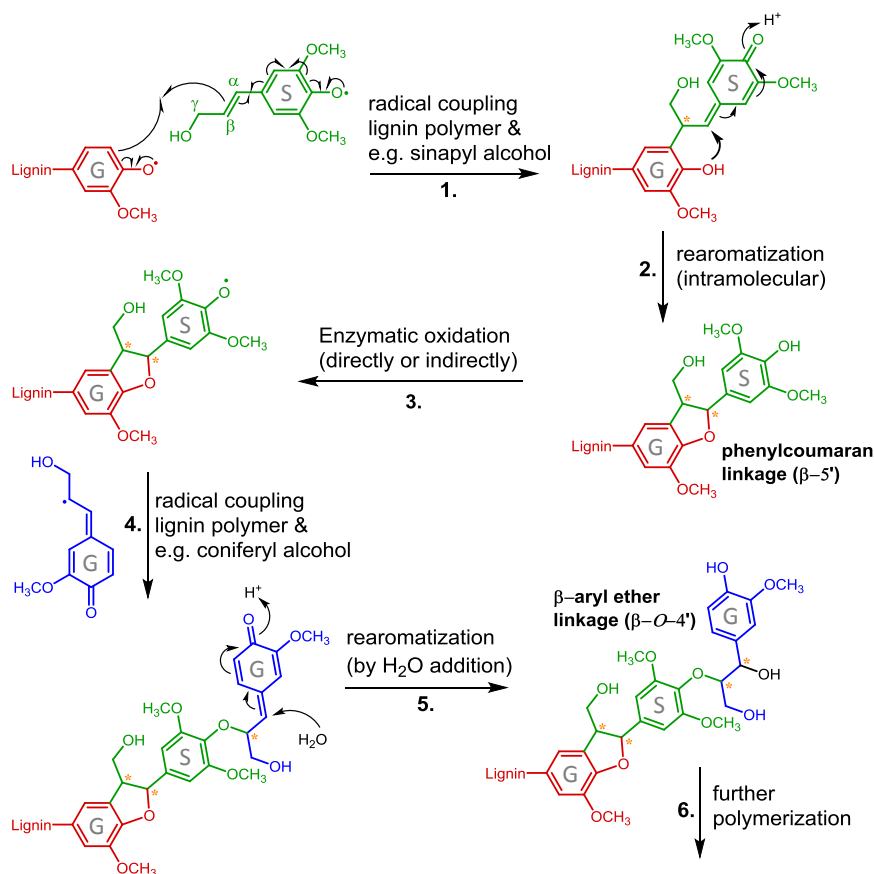


Fig. 1.3 Overview of the formation of phenylcoumaran (β -5'), β -aryl ether (β -O-4') and resinol (β - β') linkages during lignin biosynthesis. Chiral centers are indicated with a yellow asterisk. Note that reaction 1 cannot occur in case the polymer chain end (in red) is an S unit, and that resinol formation requires two free C_β atoms, limiting their incorporation in a linear lignin chain.

In addition to the three regular subunits, other substructures have been identified in lignin, the most important ones being:

- Tricin: a flavone that can be found in grass lignins, located at the end of the polymer. It is suggested to function as a starting point for lignin polymerization.^{19,27}
- Ferulate: with a free carboxyl group or esterified to arabinoxylans, can be integrally incorporated in grass lignin, via the same coupling reactions as the monolignols discussed above.^{18,28} Arabinoxylan-bound ferulate groups have also been suggested to function as nucleation sites for lignification of plant cell walls.²⁸ In any case, the incorporation of hemicellulose-ferulate esters into the lignin polymer results in cross-linking between hemicellulose and lignin, presumably increasing the recalcitrance towards degradation.²⁸
- *p*-Coumarate: occurs in grass lignin, acylating the C_V-position, mainly of S units.¹⁹ In contrast to ferulate, the *p*-coumarate groups are not prone to oxidative coupling, and occur largely as free pendant groups.^{19,28}
- *p*-Hydroxybenzoate: occurs in several hardwood lignins (i.e. those from palms, aspen, willow and poplar).¹⁹ Similar to *p*-coumarate groups in grasses, the *p*-hydroxybenzoate groups largely occur as free-phenolic pendant groups.^{19,28}
- Acetate: Occurs in both grass lignins and several hardwood lignins, acylating the C_V-position.

Example structures of lignin from grasses, hardwood and softwood, showing the subunits and interunit linkages discussed above, are shown in **Fig. 1.4**.

There are strong indications that the lignin polymers in lignocellulose are covalently coupled to hemicellulose via both ether and ester bonds. Although several structures of such linkages have been suggested, due to analytical challenges, only few unequivocal identifications have been reported.^{16,29} The exact structures of these linkages are not further discussed here, as this is considered out of scope in this research.

1.3.2 Production and structure of technical lignins

In biorefineries and in pulp and paper industry, pre-treatment processes are required to separate the constituents of lignocellulosic biomass. This, eventually, enables further processing of the different components to value-added products, such as biofuels, biochemicals or paper.³⁰ Typically, such pre-treatment processes are optimized for the valorization of the polysaccharides. Although lignin can be separated with high yield, its structure is severely modified.^{30,31} Several pre-treatment techniques are being used, which all result in lignin fractions of different purity and structure. At commercial scale, the largest scale pre-treatment processes are kraft pulping and sulfite pulping.⁴ During kraft pulping, lignocellulose (generally from wood) is heated (150-180 °C) in a solution of sodium sulfide under alkaline conditions.³² The resulting kraft lignin is a highly polydisperse mixture of branched oligomers and polymers.³³ The abundance of 'regular'

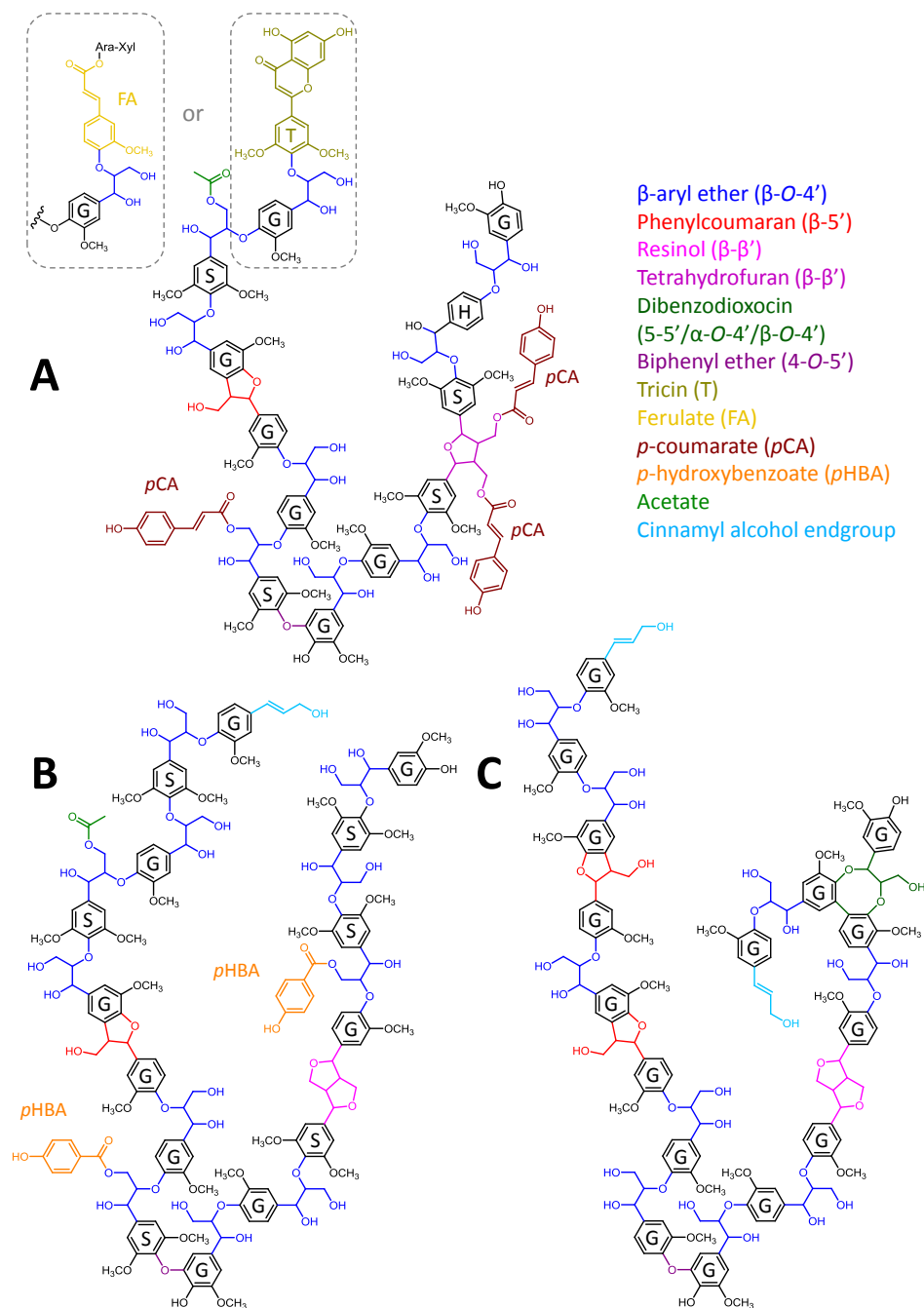


Fig. 1.4 Example structures representing native lignin from grasses (A), hardwood (B) and softwood (C), based on Ralph et al.¹⁹ Although efforts have been done to represent the individual subunits and linkages at levels that correspond to reported values in literature, a perfect representation is not possible in a model structure comprising only 16-17 subunits.

interunit linkages (i.e. those shown in **Table 1.2** and **Fig. 1.4**) is highly reduced, whereas biphenyl and diaryl ether linkages are formed instead.³³

Sulfite pulping can be performed at a wide pH range, and entails treatment of lignocellulosic biomass with a concentrated solution of (bi)sulfite at 130-160 °C. During this process, α -hydroxyl groups of lignin are substituted by sulfonate groups, resulting in water-soluble lignosulfonate as a by-product. Many of the original lignin substructures remain intact, although also in this process ether cleavage and (re)condensation reactions occur.^{34,35} The more condensed structure of technical lignins increases their recalcitrance and hampers valorization. Consequently, the commercial valorization of technical lignin is very low (only 2% in 2010)³⁶, and essentially limited to the use of lignosulfonates as e.g. emulsifiers and binding agents.¹¹

1.4 Enzymatic lignin degradation and modification

The degradation of lignin in nature occurs mainly, and most effectively, by white-rot fungi.³⁷⁻³⁹ To achieve this, white-rot fungi excrete various oxidative enzymes: lignin peroxidases (LiP, EC 1.11.1.14), manganese peroxidases (MnP, EC 1.11.1.13), versatile peroxidases (VP, EC 1.11.1.16) and laccases (EC 1.10.3.2).^{37,38,40} In addition, several accessory enzymes, such as aryl alcohol oxidases and glucose oxidases, are produced to generate hydrogen peroxide, fueling the ligninolytic peroxidases.^{37,41} In terms of redox potentials, LiP and VP are the most powerful ligninolytic enzymes.³⁸ However, their large scale production (via heterologous expression) is very challenging.⁴² In addition, peroxidases are prone to inactivation by hydrogen peroxide, which is at the same time required as co-substrate.⁴³ As these drawbacks are essentially absent for laccase, this enzyme is of high interest for lignin degradation and modification at industrial scale.^{41,43}

1.5 Laccase and laccase/mediator systems (LMS)

1.5.1 Laccase structure and activity

Laccases are multi-copper oxidases that can oxidize a wide variety of substrates, mainly aromatic structures. They can be found in fungi, as well as in bacteria, plants and insects,⁴⁴ although the most powerful laccases are produced by white-rot fungi.^{45,46} Fungal laccases generally have a molecular mass of 50-100 kDa and can be heavily glycosylated.^{46,47} In one catalytic cycle, the enzyme performs four one-electron substrate oxidations, coinciding with the reduction of molecular oxygen to water (**Fig. 1.5**).

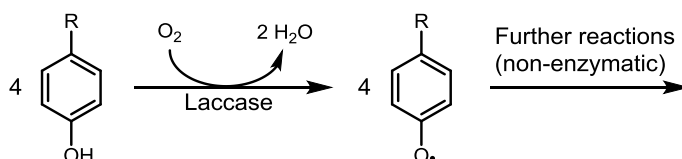


Fig. 1.5 Schematic representation of the catalytic activity of a laccase on a phenolic substrate.

The active site of laccases contains four copper atoms, which are classified as Type I, Type II and Type III, based on their spectroscopic and paramagnetic properties.⁴⁸ These four copper atoms are bound to three redox sites: T1, T2 and T3 (**Fig. 1.6**). A Type I copper is bound as a mononuclear cluster at T1. The T2 (mononuclear) and T3 (binuclear) sites, together form a trinuclear cluster. At T1, the oxidation of the substrate takes place. It is also responsible for the beautiful blue color of the enzyme, due to its strong absorbance around 600 nm.^{48,49} After each (one-electron) oxidation of a substrate, the substrate diffuses away from the active site, after which a new substrate can bind. The abstracted electron is transferred from the T1 copper, via a conserved His-Cys-His triad, to the trinuclear T2-T3 cluster, where O₂ is reduced to water (**Fig. 1.6**).^{48,50}

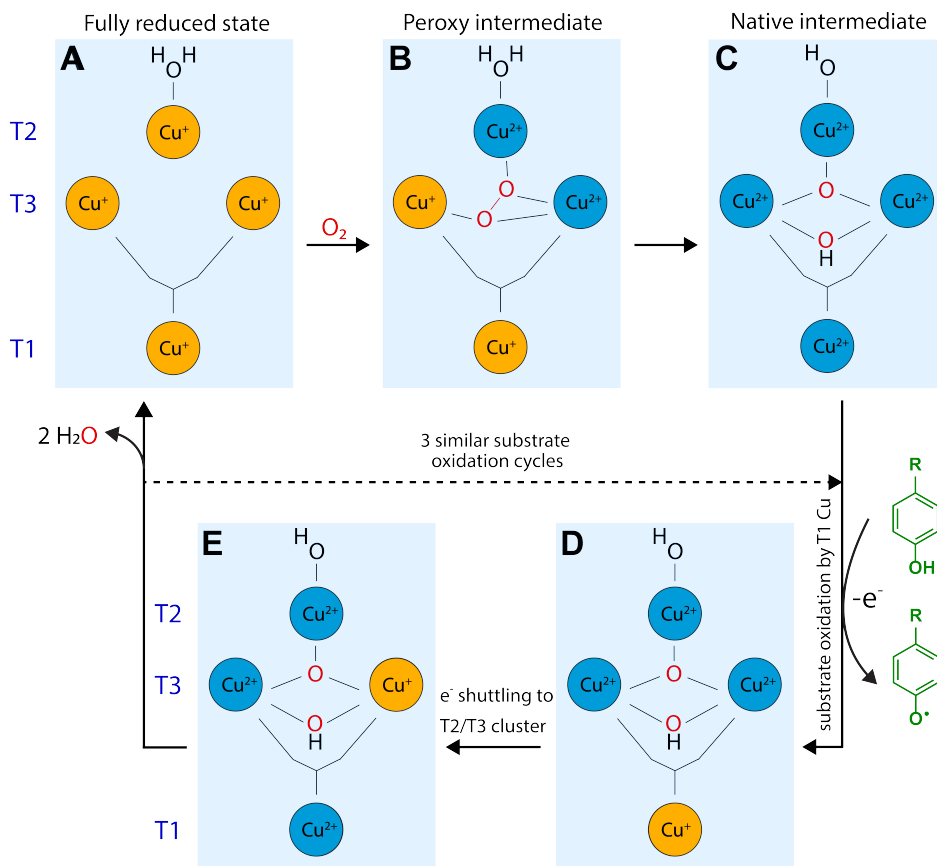


Fig. 1.6 Schematic representation of the active site of laccases and its operational mechanism, based on Solomon et al.⁵⁵ Upon binding of O₂, the four copper atoms are oxidized (A-C). A substrate is then bound close to the T1 copper, which abstracts an electron from the substrate (C-D). The abstracted electron is transferred to the trinuclear T2/T3 cluster (D-E), after which an additional substrate can be oxidized by the T1 copper. This cycle continues until all four copper atoms are reduced, i.e. after oxidation of four substrates (E-A), after which the same cascade of reactions starts over again. It should be noted that the exact state and configuration of the oxygen atoms in E depends on the oxidation state of the enzyme. For simplicity, the same configuration is shown as in the native intermediate (C).

Although the redox potentials of fungal laccases are high compared to plant and bacterial laccases, they do not exceed 800 mV vs. normal hydrogen electrode (NHE).^{46,48,51} Consequently, their substrate range is limited to substrates with relatively low redox potentials, generally below 1000 mV vs. NHE.^{48,51} With respect to lignin, this means that laccase are only powerful enough to oxidize the phenolic (and not the non-phenolic) substructures of the polymer, as only phenolic substructures have sufficiently low redox potentials. Therefore, it was long believed that laccase only plays a minor role in lignin degradation in nature. In 1990, however, Bourbonnais et al. showed that, in the presence of a suitable 'mediator', laccase could oxidize lignin-like structures with redox potentials well above 1000 mV vs. NHE (see section 1.5.2).⁵² This discovery also resulted in a renewed interest in laccase for biotechnological applications, such as lignin degradation and modification.⁵³

1.5.2 Laccase/mediator systems

Laccases can be combined with a so-called mediator to enable oxidation of high-redox potential substrates that are recalcitrant to the activity of laccase alone.^{52,53} In such a laccase/mediator system (LMS), the mediator is first oxidized by laccase, after which it diffuses away from the active site and oxidizes the substrate (i.e. the compound to be oxidized) (**Fig. 1.7**). An ideal mediator is a good laccase substrate that is stable in both oxidized and reduced form and does not inhibit the laccase activity.⁵³ This way, the LMS can perform multiple cycles, without significant loss of activity. In addition to redox issues, the addition of a mediator can also overcome steric issues related to the oxidation of substrates,⁵⁴ which is, obviously, of interest for oxidation of lignin in a complex lignocellulose matrix.

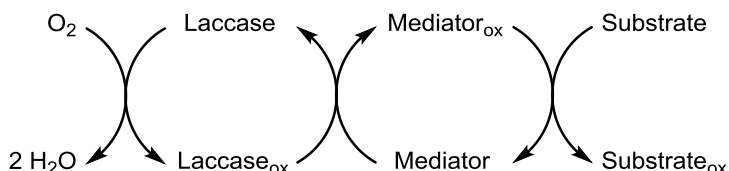


Fig. 1.7 Schematic representation of the principle of a laccase/mediator system (LMS). It should be noted that in the context of a LMS, the term 'substrate' is used for the to-be-oxidized compound, even though the mediator is the actual substrate of the enzyme.

Only a limited number of compounds meet these criteria, and can therefore be regarded as 'true' mediators. Among them are several transition metal complexes and a few organic compounds, such as 2,2'-azino-bis(3-ethylbenzothiazoline-6-sulfonic acid) (ABTS) and (2,2,6,6-tetramethylpiperidin-1-yl)oxyl (TEMPO). The high costs and insufficient environmental safety of the transition metal complexes limit their applicability in industry.⁵³ Although less stable in oxidized form, several N-OH containing compounds,

such as 1-hydroxybenzotriazole (HBT) and *N*-hydroxyphthalimide (HPI), have been shown to be very effective mediators as well (**Fig. 1.8**).

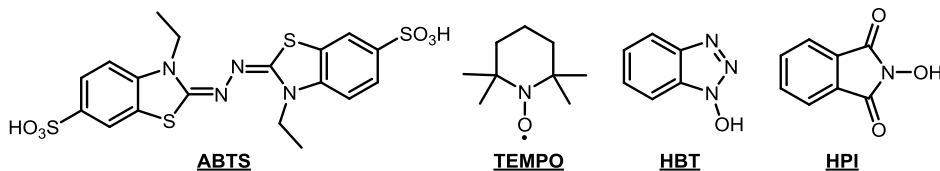


Fig. 1.8 Molecular structures of the most widely used organic laccase mediators.

The exact mechanism by which the mediator oxidizes the substrate is dependent on the type of mediator used. In the case of ABTS, first a rapid enzymatic oxidation of ABTS to its radical cation (ABTS^{•+}) occurs, after which it is slowly converted to the dication (ABTS²⁺). It has been proposed that ABTS²⁺, which has a high redox potential (1100 mV vs. NHE)⁵⁶ can subsequently oxidize non-phenolic compounds via direct electron transfer (ET) (**Fig. 1.9A**).^{56,57} Nevertheless, due to the limited stability of ABTS²⁺ under mild conditions, which are required for laccase activity, the exact structure of the mediator_{ox} species (see **Fig. 1.7**) has been questioned.⁵⁸ Via ET, the substrate is oxidized to a radical cation, which then reacts further non-enzymatically (see section 1.6).

The N-OH type mediators are proposed to operate via hydrogen atom transfer (HAT). After oxidation by laccase to aminoxyl radicals, they abstract a radical hydrogen atom from the benzylic carbon of non-phenolic lignin structures. Thereby, the aminoxyl radicals are reduced to their original form (**Fig. 1.9B**). The non-phenolic benzylic radicals that are formed undergo subsequent non-enzymatic reactions, of which the final outcome is dependent on the exact structure of the substrate (see section 1.6).

For TEMPO, an ionic mechanism has been proposed. First, laccase oxidizes TEMPO to an oxoammonium ion (step 1 in **Fig. 1.9C**). The latter species can, subsequently, be attacked by a hydroxyl group of the substrate (step 2), after which heterolytic cleavage of the formed N-O bond yields an oxidized substrate (bearing a carbonyl group), and the hydroxylamine form of TEMPO (step 3). The latter is then oxidized by laccase to form back the original (radical) form of TEMPO (step 4). As the key step of the TEMPO-catalyzed mechanism involves a nucleophilic attack by a hydroxyl group, rather than oxidation to a radical or radical cation, it is not selective for lignin structures, and also oxidizes carbohydrates.^{59,60}

In addition to the (synthetic) mediators described above, several natural phenolic compounds have been reported to show mediator activity, including small lignin related molecules like syringaldehyde, acetosyringone and methyl syringate.⁶¹⁻⁶³ The oxidation mechanism of such phenolic mediators is generally assumed to be HAT, similar to N-OH type mediators. This has, however, only been proven for hydroquinone and phenol red,⁶⁴ which are not related to lignin. As small phenolic compounds may be present during lignin degradation in nature, it has been proposed that such compounds act as laccase

mediators during fungal lignin biodegradation.^{40,65} In addition, 3-hydroxyanthranilic acid (3-HAA), a phenolic fungal metabolite, has been shown to act as a mediator, implying that fungi may also actively excrete laccase mediators during lignin biodegradation.⁶⁶ Nevertheless, degradation of a lignin model by laccase/3-HAA has only been demonstrated by using a C_α-oxidized lignin model as substrate, and other authors have shown that 3-HAA-deficient mutant fungi degraded lignin equally efficient as the wild type fungus.⁶⁸ Thus, hitherto, a direct involvement of LMS in fungal lignin degradation in nature has not been unequivocally proven.⁴¹

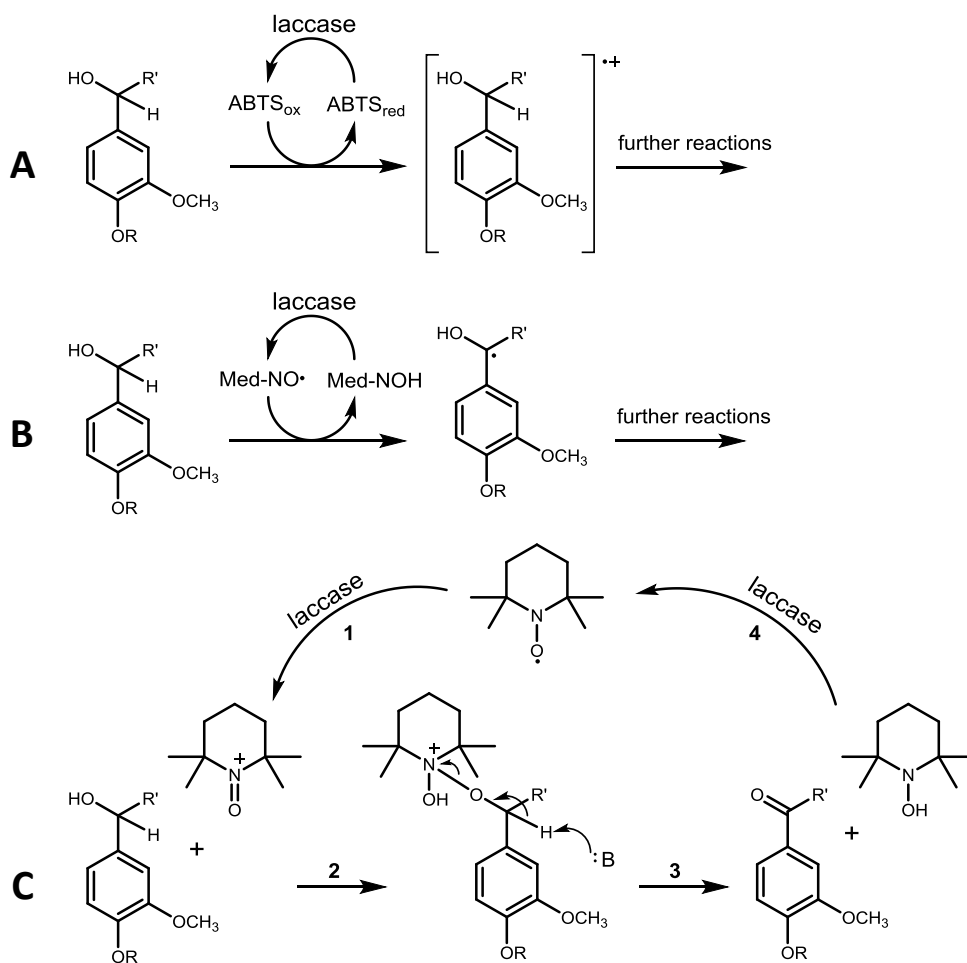


Fig. 1.9 Proposed mechanisms for oxidation of non-phenolic lignin-related compounds by different types of mediators: ET mechanism for ABTS (A), HAT mechanism for N-OH type mediators (B), and ionic mechanism for TEMPO (C).⁶⁷ R and R' refer to lignin polymer chains.

1.6 Conversion of lignin by laccase and LMS: insights from lignin model compound studies

1.6.1 The use of model compounds in reactivity studies

To study the reactivity of lignin in laccase and LMS treatments, often, low-molecular-weight lignin model compounds are used. The use of model compounds has two major benefits over the use of polymeric lignin or lignocellulosic biomass: i) Model compounds are, in contrast to polymeric lignin, readily soluble in water and many organic solvents, facilitating chromatography-based analysis (e.g. LC-MS and GC-MS), and ii) their well-defined structure enables detailed study of reactions and underlying mechanisms. An obvious drawback is that a relatively simple model compound can never completely reflect the complex and heterogeneous structure and reactivity of polymeric lignin. Nevertheless, the reactivity of model compounds may give valuable insights into the reactivity of polymeric lignin.

1.6.2 Reactions of lignin model compounds upon laccase and LMS treatments

As described in section 1.5, oxidation of lignin by laccase or LMS results in radical species (except for laccase/TEMPO), that react further via non-enzymatic routes (see **Fig. 1.5** and **Fig. 1.9**). These follow-up reactions have been studied by using both phenolic and non-phenolic model compounds, with structures reflecting S and/or G units of lignin. Many of those studies, however, have only used monomeric model compounds, such as vanillyl alcohol and veratryl alcohol.^{61,69,70} As such structures lack an interunit linkage, they give poor insight into the reactivity of lignin. Several other studies have used dimeric β -O-4'-linked model compounds (see **Fig. 1.10**), and thereby provided more insight into the reactions of lignin upon laccase and LMS treatment. An overview of the used dimeric model compounds and the corresponding outcomes are shown in **Fig. 1.10** and **Table 1.3**. The main outcomes reported are radical coupling, C_α-oxidation and/or bond cleavage.

As can be observed from **Table 1.3**, radical coupling is commonly observed for phenolic compounds, whereas it is not observed for non-phenolic models. The latter structures primarily undergo C_α-oxidation and several types of bond cleavage reactions. In addition to the phenolic/non-phenolic character of the model compound, also the S/G character of the rings seems to influence their reactivity. For example, non-phenolic G-S models seem to undergo bond cleavage more readily than their G-G analogues. It should be noted that there are strong indications that laccase can also induce bond cleavage in phenolic lignin structures, via cleavage of the C₁-C_α bond (i.e. alkyl aryl cleavage).⁷¹ Though, hitherto, this has not been proven for β -O-4' linked dimers.

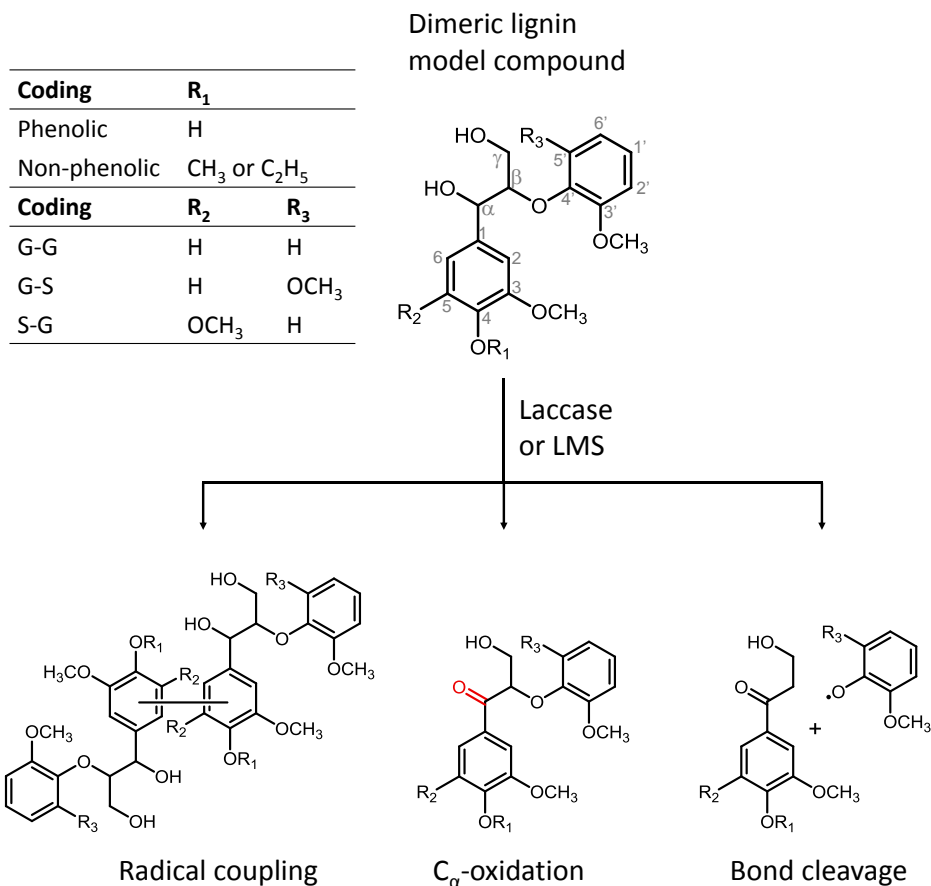


Fig. 1.10 Structure of dimeric β -O-4' linked model compounds used in literature, along with their coding used in Table 1.3, and observed reactions upon laccase and LMS incubations. For simplicity, only C _{β} -O cleavage is shown, although also cleavage of other bonds have been reported. Note that, although bond cleavage may also result in carbonyl formation at C _{α} , the term C _{α} -oxidation is used for carbonyl formation without cleavage of the interunit linkage.

Although not included in **Table 1.3**, also a few studies have been performed on dimeric (α -5' and 5-5' linked) models representing the structure of kraft lignin. Though presented as 'degradation', these structures were found to undergo demethylation, hydroxylation and side-chain oxidation, without cleavage of interunit bonds.^{72,73} Hitherto, no studies have been reported on the reactivity of dimeric (or oligomeric) lignosulfonate models. Thus, insights into the reactivity of lignosulfonate are limited to a couple of studies on lignosulfonate polymers (see section 1.7).

Table 1.3 Overview of the reported reaction outcomes of incubations of dimeric, β -*O*-4' linked model compounds with laccase or LMS. 3-HAA = 3-hydroxyanthranilic acid.

Substrate structure	Laccase source	Mediator	Buffer	Result	Ref
Phenolic model compounds					
G-G	<i>M. albomyces</i> & <i>T. hirsuta</i>	None		Oxidative coupling	74
G-G	<i>T. hirsuta</i>	A) None B) ABTS	Acetate pH 4.5 + 10% (v/v) acetone	A) Polymerization B) Co-polymerization of model/mediator	75
G-G	<i>T. versicolor</i>	None	Acetate pH 5.2	Oxidative coupling	76
S-G	<i>M. albomyces</i> & <i>T. hirsuta</i>	None		C _α -oxidation	74
Non-phenolic model compounds					
G-G	<i>T. villosa</i>	HBT	Acetate pH 4	C _α -oxidation C _α -C _β cleavage <i>O</i> -4' ether cleavage	77
G-G	Not reported	HBT or ABTS	Citrate pH 4.5	C _α -oxidation	78
G-G	<i>T. versicolor</i>	ABTS	Acetate pH 4	C _α -oxidation C _α -C _β cleavage	79
G-G	<i>T. versicolor</i>	HBT	Acetate pH 5	C _α -oxidation	80
G-G	<i>T. versicolor</i>	HBT or ABTS	Acetate pH 5	C _α -oxidation	81
G-G	<i>T. versicolor</i>	ABTS	Acetate pH 5	C _α -oxidation	52
G _{ox} -G ^a	<i>P. cinnabarinus</i>	3-HAA	Tartrate pH 4	Degradation to veratric acid and guaiacol	66
G-S	<i>T. versicolor</i>	HBT	McIlvaine pH 4	C _α -oxidation C _α -C _β cleavage C _β - <i>O</i> cleavage <i>O</i> -4' cleavage Ring cleavage	82
G-S _{ox} ^b	<i>T. versicolor</i>	HBT	Acetate pH 4	C _α -C _β cleavage C _β - <i>O</i> cleavage <i>O</i> -4' cleavage	83
G-S	<i>T. versicolor</i>	HBT	Acetate pH 5	C _α -oxidation C _α -C _β cleavage C _β - <i>O</i> cleavage <i>O</i> -4' cleavage Ring cleavage	80

^a G-G type model with a C_α-oxidized interunit linkage. ^b G-S type model with an aldehyde group at C₁'.

1.7 Activity of laccase and LMS towards polymeric lignin and lignocellulosic biomass

1.7.1 Challenges in analysis of polymeric lignin and lignocellulose

In order to understand the reactivity of lignin in laccase or LMS treatments, analytical methods are required for both quantification and structural characterization of lignin.

Quantification of lignin

At lab scale, quantification is generally performed gravimetrically by Klason lignin determination, which is based on removal of polysaccharides by severe sulfuric acid treatment. Recently, our lab introduced py-GC-MS, with ^{13}C labelled lignin as internal standard, as an alternative for lab-scale lignin quantification.^{84,85} In pulp and paper industry, the lignin content is estimated by determination of the Kappa number, which is based on the oxidation of lignin by permanganate.⁸⁶

Structural characterization of lignin

For structural analysis of lignin, various techniques are used, of which 2D NMR spectroscopy is the most important one. Especially HSQC experiments are commonly performed, sometimes in combination with e.g. HMBC for confirmation purposes. 2D NMR spectroscopy is the only technique that may provide in-depth insight into the structure of lignin, without destructing the sample. Insights into the structure and abundance of subunits (i.e. S, G, H, other) and interunit linkages are obtained.⁸⁷ Nevertheless, even with 2D NMR, monitoring structural changes in lignin is challenging. For instance, formation of 5-5' bonds (during radical coupling) is difficult to prove, as such structural motifs are not detectable in HSQC spectra. In addition, HSQC correlations of lignin may overlap with those of proteins and carbohydrates, which impedes reliable peak integration.⁸⁷

Another widely used technique for structural characterization of lignin is py-GC-MS, which involves pyrolytic deconstruction of biomass or lignin, followed by GC-MS analysis of the released volatile components. Thereby, direct insights into the structure of lignin subunits are obtained. Indirectly, some insights into the amount and type of interunit linkages can be obtained, although this requires in-depth understanding of the pyrolytic degradation reactions.^{88,89} Alternative and more selective degradation methods, such as thioacidolysis or DFRC (Derivatization Followed by Reductive Cleavage)^{90,91} can also be combined with e.g. GC analysis to provide specific structural information, but these methods do not give a complete insight into the structure of lignin.

Occasionally, Fourier-transform infrared spectroscopy (FTIR) is used to identify structural

changes upon lignin treatment. This technique, however, may give insights into the accumulation or decrease of specific functional groups, but does not provide detailed structural information.⁴⁵

Lastly, size-exclusion-chromatography (SEC) can be used to provide insights into the molecular weight of lignin. Nevertheless, this requires solubilization of the lignin, which is difficult to achieve without modification of its structure. In addition, residual polysaccharides may interfere with the analysis.⁹²

From the above it is clear that a complete mapping of the effect of laccase and LMS treatments of lignin is challenging. A reasonably complete overview of the changes in lignin quantity and structure requires a combination of multiple analytical techniques. In addition, it should be stressed that most of the above-mentioned techniques have mainly been used and tested on native lignin samples. Consequently, it remains unclear whether they are equally suitable for analysis of (heavily) modified or degraded lignin.

1.7.2 Delignification of lignocellulosic biomass

Despite of the analytic challenges discussed above, a number of studies have been performed on the effect of LMS treatments of lignocellulosic biomass, generally with the main aim to delignify the biomass and to improve enzymatic saccharification of the remaining polysaccharides. An overview of these studies, with their main outcomes is shown in **Table 1.4**. As can be observed, in most of these studies, delignification and/or improved saccharification were reported, indicating that LMS treatments are potential tools for sustainable delignification. In addition, these studies did not focus on understanding the mechanisms underlying lignin modification by LMS as lignin analysis within the complex matrix of lignocellulose is a challenge (indicated below).

It should be noted that more studies on LMS treatments of lignocellulose have been published, but in these studies, LMS treatments were combined with alkaline peroxide treatments to improve delignification.^{62,93-97} As these studies do not provide insight into the sole action of LMS, they are not displayed in **Table 1.4**.

Overall, it is clear that laccase, in combination with various mediators, can induce delignification of lignocellulosic biomass, and that this results in improved enzymatic saccharification of polysaccharides. Nevertheless, the underlying mechanisms are still poorly understood, due to the following reasons:

- Most studies focused on the lignin content and/or saccharification yield, and did not include an in-depth structural characterization (e.g. by performing 2D NMR).
- Studies that included (NMR-based) structural characterization often combined LMS treatments with alkaline peroxide treatments. These studies did not distinguish between the effects of both treatments.

- Upon biomass delignification, part of the lignin is solubilized. The solubilized lignin fraction is commonly not included in the analyses, even though its structure is likely to be more altered, and more indicative for the underlying degradation mechanisms than the insoluble residual lignin.

Table 1.4 Overview of the reported reaction outcomes of laccase and LMS treatments lignocellulosic biomass, adapted from Munk et al.⁴⁵ TMAH = Tetramethylammonium hydroxide thermochemolysis; Sac-As = Saccharification assay; TAL = Thioacidolysis; P = Polymerization; DP = Depolymerization; MeS = Methyl syringate; C_α-ox = C_α-oxidation; DL = Delignification; Sac = Saccharification yield.

Substrate	Laccase source	Mediator	Buffer	Analyses	Result	Ref
Corn stover ^a	<i>T. versicolor</i>	HBT	Acetate pH 4	TMAH-GC-MS, Sac-As	Sac↑	⁹⁸
Eucalyptus pulp	<i>P. cinnabarinus</i>	HBT	Tartrate pH 4	Klason, ¹ H NMR, TAL-GC, TAL-SEC, py-GC-MS	DP, DL, C _α -ox	⁹⁹
Eucalyptus pulp	<i>M. thermophila</i>	MeS	Phosphate pH 6	Klason, ¹ H NMR, TAL-GC, TAL-SEC, py-GC-MS	DP, DL, C _α -ox	⁹⁹
Wheat straw	<i>P. cinnabarinus</i>	HBT	Tartrate pH 4	Klason, Sac-As, HSQC NMR	DL, C _α -ox, Sac↑	¹⁰⁰
Spruce ^b	<i>C. unicolor</i>	None	Citrate pH 5	SEC, Sac-As	P, Sac↑	¹⁰¹
Giant reed ^b	<i>C. unicolor</i>	None	Citrate pH 5	SEC, Sac-As	P, Sac↓	¹⁰¹
Mixed wood pulp	<i>A. fumigatus</i>	HBT	Unbuffered pH 6	Kappa no., FTIR	DL	¹⁰²

^a Ensiled. ^b Steam pretreated.

1.7.3 Modification of technical lignins

Even though very few model compound studies have been published on the reactivity of technical lignins, multiple studies have been performed with the aim to modify technical lignins by using laccase or LMS and, thereby, improve their performance as e.g. binders or adhesives.

In the case of kraft lignin, laccase and LMS treatments resulted mostly in lignin polymerization (**Table 1.5**). Only in cases where ABTS was used as a mediator, depolymerization was observed, illustrating the large impact that the choice of mediator can have on the overall reaction outcome. In the case of lignosulfonate, polymerization was observed exclusively, both with and without addition of mediators. Although it is clear that laccase and LMS can be used to modify the structure of technical lignins, the overall outcome of incubations remains hard to predict, as the underlying reactions are insufficiently understood.

Table 1.5 Overview of the reported reaction outcomes of laccase and LMS treatments of technical lignins, adapted from Munk et al.⁴⁵ Although studies on other types of technical lignins have been performed, only lignosulfonate and kraft lignin are included in the table. LS = Lignosulfonate; P = Polymerization; DP = Depolymerization; SW = Softwood; HW = Hardwood; AS = Acetosyringone.

Substrate	Laccase source	Mediator	Buffer	Analyses	Result	Ref
LS	<i>M. thermophila</i>	None	Acetate pH 5 and 7.5	SEC, FTIR	P	103
LS	<i>T. hirsuta</i> & <i>T. villosa</i>	HBT	Unbuffered pH 4-8	SEC, FTIR, py-GC-MS, HSQC NMR	P, C-C bond formation	104
LS	<i>M. thermophila</i>	None, HBT, ABTS, TEMPO, other	Unbuffered pH 7	SEC	P	105
SW & HW Kraft lignin	<i>T. versicolor</i>	A) None B) ABTS	Acetate pH 5	SEC	A) P B) DP	106
HW Kraft lignin	<i>M. thermophila</i>	various	Phosphate pH 6	SEC, FTIR	P	107
SW & HW Kraft lignin	<i>M. albomyces</i> & <i>S. ipomoea</i>	AS	Phosphate & glycine pH 7-10	SEC	P	108
Agave kraft lignin	<i>F. proliferatum</i>	A) HBT B) ABTS	Unbuffered pH 6	SEC, HPLC	A) P B) DP	109

1.8 Aim and outline of this thesis

The overall aim of this thesis is to enhance the understanding of laccase and LMS-catalyzed lignin modification at the molecular level. This way, we hope to improve the predictability of laccase and LMS treatments, and to pave the way for further optimization of laccase-based lignin degradation and modification. A dual approach is used. On the one hand, model compounds are used to improve the fundamental understanding of the reactivity of specific lignin substructures. This also includes novel model compounds that represent lignin substructures of which the reactivity has not been investigated yet. On the other hand, we use lignocellulosic biomass and lignin isolates to investigate whether the findings of model compound studies can be extrapolated to LMS treatments of polymeric lignin.

In **Chapter 2**, we investigate the reactivity of a phenolic lignin model compound with laccase and two laccase/mediator systems. We show, using a combination of analytical techniques, how the addition of a mediator influences the reactions that phenolic lignin structures undergo in laccase treatments. In **Chapter 3**, we describe how sulfonation of phenolic and non-phenolic model compounds influences their reactivity in laccase and LMS treatments. Hereby, we provide new insights into the reactivity of lignosulfonates. In **Chapter 4** we show that LMS-catalyzed ether cleavage of a non-phenolic lignin

structure can be substantially enhanced by altering the pH and strength of the incubation buffer. In addition, based on an in-depth study into the underlying reaction mechanisms, we provide a detailed theory for these observations. In **Chapter 5**, we study the delignification of wheat straw and corn stover by a laccase/HBT system in unprecedented detail by using 2D NMR, py-GC-MS and several other techniques. We provide, for the first time, insights into LMS-catalyzed lignin degradation in actual plant biomass. In **Chapter 6**, we provide a facile enzymatic procedure for the synthesis of acylated lignin model compounds, which are not commercially available. Such models mimic highly abundant substructures of grass and hardwood lignins. In **Chapter 7**, we zoom in on the reactivity of *p*-coumaroylated lignin substructures. Their reactivity is studied using both the enzymatically synthesized model compounds (Chapter 6) and lignin isolated from wheat straw and corn stover. In **Chapter 8**, the results obtained in the previous chapters are put into perspective in an integrated discussion. The roles of mediators and the structure of lignin in LMS treatments are discussed, as well as the relevance of lignin model compound studies. In addition, challenges and ideas for further improvement of LMS treatments, required for eventual commercial applications are discussed.

1.9 References

- Li M, Pu Y and Ragauskas AJ. Current understanding of the correlation of lignin structure with biomass recalcitrance. *Frontiers in Chemistry* **2016**, *4*, 45.
- Behera S, Arora R, Nandhagopal N and Kumar S. Importance of chemical pretreatment for bioconversion of lignocellulosic biomass. *Renewable and Sustainable Energy Reviews* **2014**, *36*, 91-106.
- Gupta R, Mehta G, Khalsa YP and Kuhad RC. Fungal delignification of lignocellulosic biomass improves the saccharification of cellulose. *Biodegradation* **2011**, *22* (4), 797-804.
- Gosselink RJA, *Lignin as a renewable aromatic resource for the chemical industry (PhD Thesis Wageningen University)*. Wageningen, **2011**. ISBN 9789461731005.
- Abramson M, Shoseyov O and Shani Z. Plant cell wall reconstruction toward improved lignocellulosic production and processability. *Plant Science* **2010**, *178* (2), 61-72.
- Sun Y and Cheng J. Hydrolysis of lignocellulosic materials for ethanol production: a review. *Bioresource Technology* **2002**, *83* (1), 1-11.
- Klemm D, Heublein B, Fink HP and Bohn A. Cellulose: fascinating biopolymer and sustainable raw material. *Angewandte Chemie International Edition* **2005**, *44* (22), 3358-3393.
- Nishiyama Y, Langan P and Chanzy H. Crystal structure and hydrogen-bonding system in cellulose I β from synchrotron X-ray and neutron fiber diffraction. *Journal of the American Chemical Society* **2002**, *124* (31), 9074-9082.
- Nishiyama Y, Sugiyama J, Chanzy H and Langan P. Crystal structure and hydrogen bonding system in cellulose Ia from synchrotron X-ray and neutron fiber diffraction. *Journal of the American Chemical Society* **2003**, *125* (47), 14300-14306.
- Pu Y, Zhang D, Singh PM and Ragauskas AJ. The new forestry biofuels sector. *Biofuels, Bioproducts and Biorefining: Innovation for a sustainable economy* **2008**, *2* (1), 58-73.
- Schutyser W, Renders T, Van den Bosch S, Koelewijn S-F, Beckham GT and Sels BF. Chemicals from lignin: an interplay of lignocellulose fractionation, depolymerisation, and upgrading. *Chemical Society Reviews* **2018**, *47* (3), 852-908.
- Somerville C, Bauer S, Brininstool G, Facette M, Hamann T, Milne J, Osborne E, Paredes A, Persson S and Raab T. Toward a systems approach to understanding plant cell walls. *Science* **2004**, *306* (5705), 2206-2211.
- Zhang X, Yang W and Blasiak W. Modeling study of woody biomass: interactions of cellulose, hemicellulose, and lignin. *Energy & Fuels* **2011**, *25* (10), 4786-4795.
- Loque D, Scheller HV and Pauly M. Engineering of plant cell walls for enhanced biofuel production. *Current Opinion in Plant Biology* **2015**, *25*, 151-161.
- Kang X, Kirui A, Widanage MCD, Mentink-Vigier F, Cosgrove DJ and Wang T. Lignin-polysaccharide interactions in plant secondary cell walls revealed by solid-state NMR. *Nature Communications* **2019**, *10* (1), 1-9.
- Giummarella N, Pu Y, Ragauskas AJ and Lawoko M. A critical review on the analysis of lignin carbohydrate bonds. *Green Chemistry* **2019**, *21* (7), 1573-1595.
- Hatfield R, Ralph J and Grabber JH. A potential role for sinapyl *p*-coumarate as a radical transfer mechanism in grass lignin formation. *Planta* **2008**, *228* (6), 919.
- Vanholme R, Demedts B, Morreel K, Ralph J and Boerjan W. Lignin biosynthesis and structure. *Plant Physiology* **2010**, *153* (3), 895-905.
- Ralph J, Lapierre C and Boerjan W. Lignin structure and its engineering. *Current Opinion in Biotechnology* **2019**, *56*, 240-249.
- Rinaldi R, Jastrzebski R, Clough MT, Ralph J, Kennema M, Bruijninx PC and Weckhuysen BM. Paving the way for lignin valorisation: recent advances in bioengineering, biorefining and catalysis. *Angewandte Chemie International Edition* **2016**, *55* (29), 8164-8215.
- Del Río JC, Lino AG, Colodette JL, Lima CF, Gutiérrez A, Martínez ÁT, Lu F, Ralph J and Rencoret J. Differences in the chemical structure of the lignins from sugarcane bagasse and straw. *Biomass and Bioenergy* **2015**, *81*, 322-338.
- Del Río JC, Prinsen P, Rencoret J, Nieto L, Jiménez-Barbero J, Ralph J, Martínez ÁT and Gutiérrez A. Structural characterization of the lignin in the cortex and pith of elephant grass (*Pennisetum purpureum*) stems. *Journal of Agricultural and Food Chemistry* **2012**, *60* (14), 3619-3634.

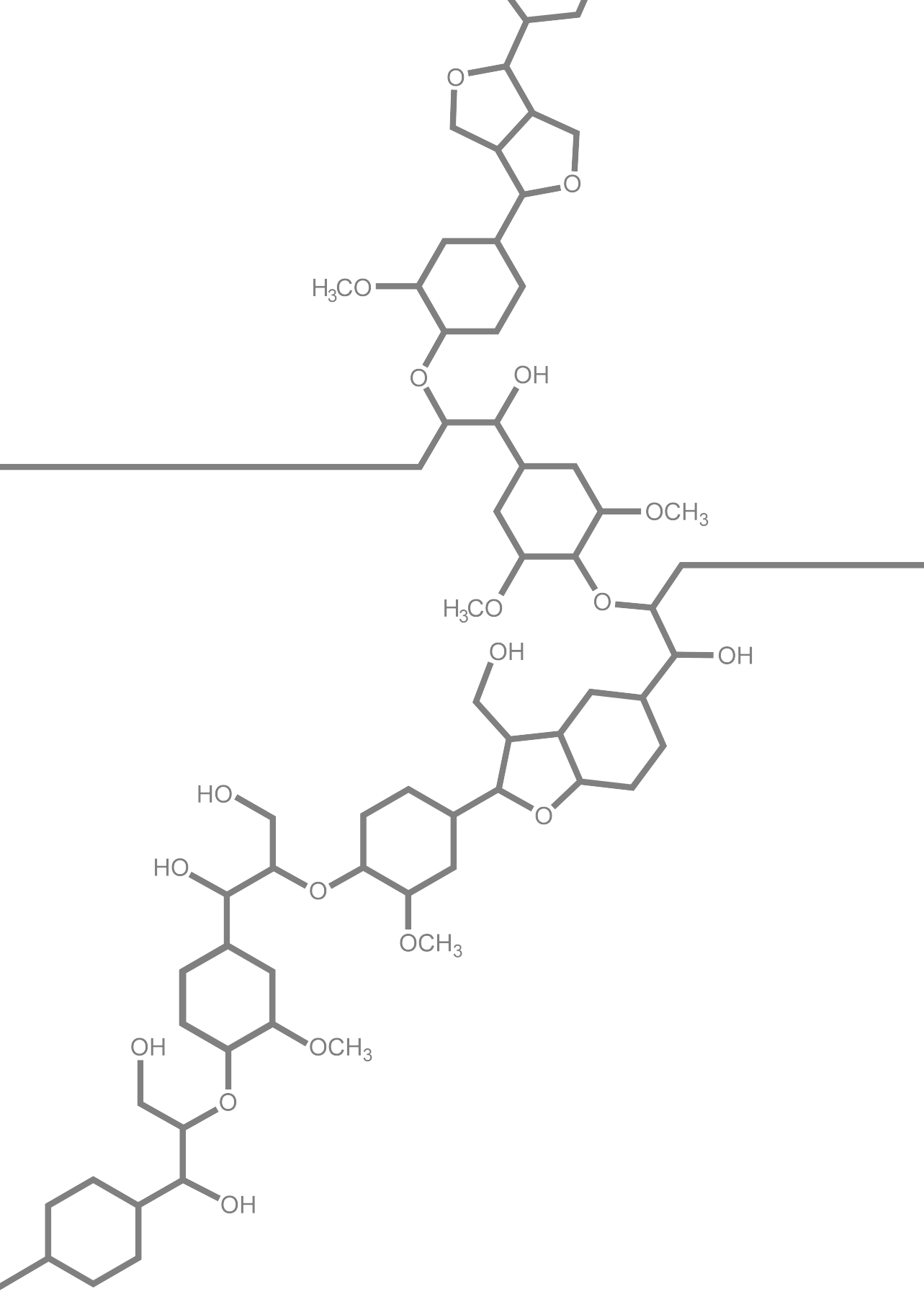
23. Del Río JC, Rencoret J, Prinsen P, Martínez AT, Ralph J and Gutiérrez A. Structural characterization of wheat straw lignin as revealed by analytical pyrolysis, 2D-NMR, and reductive cleavage methods. *Journal of Agricultural and Food Chemistry* **2012**, 60 (23), 5922-5935.
24. Zeng J, Helms GL, Gao X and Chen S. Quantification of wheat straw lignin structure by comprehensive NMR analysis. *Journal of Agricultural and Food Chemistry* **2013**, 61 (46), 10848-10857.
25. Dou J, Kim H, Li Y, Padmakshan D, Yue F, Ralph J and Vuorinen T. Structural characterization of lignins from willow bark and wood. *Journal of Agricultural and Food Chemistry* **2018**, 66 (28), 7294-7300.
26. Rencoret J, Marques G, Gutiérrez A, Nieto L, Jiménez-Barbero J, Martínez ÁT and Del Río JC. Isolation and structural characterization of the milled-wood lignin from *Paulownia fortunei* wood. *Industrial Crops and Products* **2009**, 30 (1), 137-143.
27. Lan W, Lu F, Regner M, Zhu Y, Rencoret J, Ralph SA, Zakai UI, Morreel K, Boerjan W and Ralph J. Tricin, a flavonoid monomer in monocot lignification. *Plant Physiology* **2015**, 167 (4), 1284-1295.
28. Ralph J. Hydroxycinnamates in lignification. *Phytochemistry Reviews* **2010**, 9 (1), 65-83.
29. Nishimura H, Kamiya A, Nagata T, Katahira M and Watanabe T. Direct evidence for α -ether linkage between lignin and carbohydrates in wood cell walls. *Scientific Reports* **2018**, 8 (1), 1-11.
30. Zakzeski J, Bruijninx PC, Jongerius AL and Weckhuysen BM. The catalytic valorization of lignin for the production of renewable chemicals. *Chemical Reviews* **2010**, 110 (6), 3552-3599.
31. Constant S, Wienk HLJ, Frissen AE, de Peinder P, Boelens R, Van Es DS, Grisel RJH, Weckhuysen BM, Huijgen WJJ, Gosselink RJA and Bruijninx PCA. New insights into the structure and composition of technical lignins: a comparative characterisation study. *Green Chemistry* **2016**, 18 (9), 2651-2665.
32. Luo H and Abu-Omar MM. Chemicals from lignin. *Encyclopedia of Sustainable Technologies; Elsevier: Amsterdam, The Netherlands* **2017**, 573-585.
33. Crestini C, Lange H, Sette M and Argyropoulos DS. On the structure of softwood kraft lignin. *Green Chemistry* **2017**, 19 (17), 4104-4121.
34. Glasser WG. About making lignin great again - some lessons from the past. *Frontiers in Chemistry* **2019**, 7, 565.
35. Aro T and Fatehi P. Production and application of lignosulfonates and sulfonated lignin. *ChemSusChem* **2017**, 10 (9), 1861-1877.
36. Higson A and Smith C. Renewable chemicals factsheet: lignin. *York: NNFFC* **2011**.
37. Ten Have R and Teunissen PJM. Oxidative mechanisms involved in lignin degradation by white-rot fungi. *Chemical Reviews* **2001**, 101 (11), 3397-3414.
38. Wong DW. Structure and action mechanism of ligninolytic enzymes. *Applied Biochemistry and Biotechnology* **2009**, 157 (2), 174-209.
39. Janusz G, Pawlik A, Sulej J, Świdarska-Burek U, Jarosz-Wilkolazka A and Paszczyński A. Lignin degradation: microorganisms, enzymes involved, genomes analysis and evolution. *FEMS Microbiology Reviews* **2017**, 41 (6), 941-962.
40. Martínez ÁT, Speranza M, Ruiz-Dueñas FJ, Ferreira P, Camarero S, Guillén F, Martínez MJ, Gutiérrez Suárez A and Del Río JC. Biodegradation of lignocellulosics: microbial, chemical, and enzymatic aspects of the fungal attack of lignin. *International Microbiology* **2005**, 8, 195-204.
41. Martínez ÁT, Ruiz-Duenas FJ, Martinez MJ, del Río JC and Gutierrez A. Enzymatic delignification of plant cell wall: from nature to mill. *Current Opinion in Biotechnology* **2009**, 20 (3), 348-357.
42. Ayala M, Pickard MA and Vazquez-Duhalt R. Fungal enzymes for environmental purposes, a molecular biology challenge. *Journal of Molecular Microbiology and Biotechnology* **2008**, 15 (2-3), 172-180.
43. Mate DM and Alcalde M. Laccase: a multi-purpose biocatalyst at the forefront of biotechnology. *Microbial Biotechnology* **2017**, 10 (6), 1457-1467.
44. Strong PJ and Claus H. Laccase: a review of its past and its future in bioremediation. *Critical Reviews in Environmental Science and Technology* **2011**, 41 (4), 373-434.

45. Munk L, Sitarz AK, Kalyani DC, Mikkelsen JD and Meyer AS. Can laccases catalyze bond cleavage in lignin? *Biotechnology Advances* **2015**, *33* (1), 13-24.
46. Morozova O, Shumakovich G, Gorbacheva M, Shleev S and Yaropolov A. "Blue" laccases. *Biochemistry (Moscow)* **2007**, *72* (10), 1136-1150.
47. Thurston CF. The structure and function of fungal laccases. *Microbiology* **1994**, *140* (1), 19-26.
48. Alcalde M. *Laccases: biological functions, molecular structure and industrial applications*. in *Industrial Enzymes: Structure, Function and Applications*, Polaina J and MacCabe AP, Eds. (Springer, **2007**), pp. 461-476.
49. Piontek K, Antorini M and Choinowski T. Crystal structure of a laccase from the fungus *Trametes versicolor* at 1.90-Å resolution containing a full complement of coppers. *Journal of Biological Chemistry* **2002**, *277* (40), 37663-37669.
50. Jones SM and Solomon EI. Electron transfer and reaction mechanism of laccases. *Cellular and Molecular Life Sciences* **2015**, *72* (5), 869-883.
51. Giardina P, Faraco V, Pezzella C, Piscitelli A, Vanhulle S and Sannia G. Laccases: a never-ending story. *Cellular and Molecular Life Sciences* **2010**, *67* (3), 369-385.
52. Bourbonnais R and Paice MG. Oxidation of non-phenolic substrates: an expanded role for laccase in lignin biodegradation. *FEBS Letters* **1990**, *267* (1), 99-102.
53. Morozova O, Shumakovich G, Shleev S and Yaropolov YI. Laccase-mediator systems and their applications: a review. *Applied Biochemistry and Microbiology* **2007**, *43* (5), 523-535.
54. d'Acunzo F, Galli C, Gentili P and Sergi F. Mechanistic and steric issues in the oxidation of phenolic and non-phenolic compounds by laccase or laccase-mediator systems. The case of bifunctional substrates. *New Journal of Chemistry* **2006**, *30* (4), 583-591.
55. Solomon EI, Augustine AJ and Yoon J. O₂ Reduction to H₂O by the multicopper oxidases. *Dalton Transactions* **2008**, (30), 3921-3932.
56. Bourbonnais R, Leech D and Paice MG. Electrochemical analysis of the interactions of laccase mediators with lignin model compounds. *Biochimica et Biophysica Acta (BBA)-General Subjects* **1998**, *1379* (3), 381-390.
57. Baiocco P, Barreca AM, Fabbrini M, Galli C and Gentili P. Promoting laccase activity towards non-phenolic substrates: a mechanistic investigation with some laccase-mediator systems. *Organic & Biomolecular Chemistry* **2003**, *1* (1), 191-197.
58. Branchi B, Galli C and Gentili P. Kinetics of oxidation of benzyl alcohols by the dication and radical cation of ABTS. Comparison with laccase-ABTS oxidations: an apparent paradox. *Organic & Biomolecular Chemistry* **2005**, *3* (14), 2604-2614.
59. Baratto L, Candido A, Marzorati M, Sagui F, Riva S and Danieli B. Laccase-mediated oxidation of natural glycosides. *Journal of Molecular Catalysis B: Enzymatic* **2006**, *39* (1-4), 3-8.
60. Marzorati M, Danieli B, Haltrich D and Riva S. Selective laccase-mediated oxidation of sugars derivatives. *Green Chemistry* **2005**, *7* (5), 310-315.
61. Rosado T, Bernardo P, Koci K, Coelho AV, Robalo MP and Martins LO. Methyl syringate: an efficient phenolic mediator for bacterial and fungal laccases. *Bioresource Technology* **2012**, *124*, 371-378.
62. Barneto AG, Aracri E, Andreu G and Vidal T. Investigating the structure-effect relationships of various natural phenols used as laccase mediators in the biobleaching of kenaf and sisal pulps. *Bioresource Technology* **2012**, *112*, 327-335.
63. Camarero S, Ibarra D, Martínez MJ and Martínez ÁT. Lignin-derived compounds as efficient laccase mediators for decolorization of different types of recalcitrant dyes. *Applied and Environmental Microbiology* **2005**, *71* (4), 1775-1784.
64. Calcaterra A, Galli C and Gentili P. Phenolic compounds as likely natural mediators of laccase: A mechanistic assessment. *Journal of Molecular Catalysis B: Enzymatic* **2008**, *51* (3), 118-120.
65. Johannes C and Majcherczyk A. Natural mediators in the oxidation of polycyclic aromatic hydrocarbons by laccase mediator systems. *Applied and Environmental Microbiology* **2000**, *66* (2), 524-528.
66. Eggert C, Temp U, Dean JFD and Eriksson K-EL. A fungal metabolite mediates degradation of non-phenolic lignin structures and synthetic lignin by laccase. *FEBS Letters* **1996**, *391* (1), 144-148.
67. Fabbrini M, Galli C and Gentili P. Comparing the catalytic efficiency of some mediators of laccase. *Journal of Molecular Catalysis B: Enzymatic* **2002**, *16* (5), 231-240.

68. Li K, Horanyi PS, Collins R, Phillips RS and Eriksson K-EL. Investigation of the role of 3-hydroxyanthranilic acid in the degradation of lignin by white-rot fungus *Pycnoporus cinnabarinus*. *Enzyme and Microbial Technology* **2001**, 28 (4-5), 301-307.
69. Crestini C, Jurasek L and Argyropoulos DS. On the mechanism of the laccase-mediator system in the oxidation of lignin. *Chemistry-A European Journal* **2003**, 9 (21), 5371-5378.
70. Li K, Xu F and Eriksson K-EL. Comparison of fungal laccases and redox mediators in oxidation of a nonphenolic lignin model compound. *Applied and Environmental Microbiology* **1999**, 65 (6), 2654-2660.
71. Kawai S, Umezawa T and Higuchi T. Degradation mechanisms of phenolic β -1 lignin substructure model compounds by laccase of *Coriolus versicolor*. *Archives of Biochemistry and Biophysics* **1988**, 262 (1), 99-110.
72. Crestini C and Argyropoulos DS. The early oxidative biodegradation steps of residual kraft lignin models with laccase. *Bioorganic & Medicinal Chemistry* **1998**, 6 (11), 2161-2169.
73. Elegir G, Daina S, Zoia L, Bestetti G and Orlandi M. Laccase mediator system: oxidation of recalcitrant lignin model structures present in residual kraft lignin. *Enzyme and Microbial Technology* **2005**, 37 (3), 340-346.
74. Lahtinen M, Kruus K, Heinonen P and Sipilä J. On the reactions of two fungal laccases differing in their redox potential with lignin model compounds: products and their rate of formation. *Journal of Agricultural and Food Chemistry* **2009**, 57 (18), 8357-8365.
75. Rittstieg K, Suurnäkki A, Suortti T, Kruus K, Guebitz GM and Buchert J. Polymerization of guaiacol and a phenolic β -O-4 substructure by *Trametes hirsuta* laccase in the presence of ABTS. *Biotechnology Progress* **2003**, 19 (5), 1505-1509.
76. Ramalingam B, Sana B, Seayad J, Ghadessy FJ and Sullivan MB. Towards understanding of laccase-catalysed oxidative oligomerisation of dimeric lignin model compounds. *RSC Advances* **2017**, 7 (20), 11951-11958.
77. Srebotnik E and Hammel KE. Degradation of nonphenolic lignin by the laccase/1-hydroxybenzotriazole system. *Journal of Biotechnology* **2000**, 81 (2), 179-188.
78. Rochefort D, Bourbonnais R, Leech D and Paice MG. Oxidation of lignin model compounds by organic and transition metal-based electron transfer mediators. *Chemical Communications* **2002**, (11), 1182-1183.
79. Bohlin C, Persson P, Gorton L, Lundquist K and Jönsson LJ. Product profiles in enzymic and non-enzymic oxidations of the lignin model compound erythro-1-(3, 4-dimethoxyphenyl)-2-(2-methoxyphenoxy)-1, 3-propanediol. *Journal of Molecular Catalysis B: Enzymatic* **2005**, 35 (4-6), 100-107.
80. Heap L, Green A, Brown D, van Dongen B and Turner N. Role of laccase as an enzymatic pretreatment method to improve lignocellulosic saccharification. *Catalysis Science & Technology* **2014**, 4 (8), 2251-2259.
81. Bourbonnais R, Paice MG, Freiermuth B, Bodie E and Borneman S. Reactivities of various mediators and laccases with kraft pulp and lignin model compounds. *Applied and Environmental Microbiology* **1997**, 63 (12), 4627-4632.
82. Kawai S, Nakagawa M and Ohashi H. Degradation mechanisms of a nonphenolic β -O-4 lignin model dimer by *Trametes versicolor* laccase in the presence of 1-hydroxybenzotriazole. *Enzyme and Microbial Technology* **2002**, 30 (4), 482-489.
83. Kawai S, Asukai M, Ohya N, Okita K, Ito T and Ohashi H. Degradation of a non-phenolic β -O-4 substructure and of polymeric lignin model compounds by laccase of *Coriolus versicolor* in the presence of 1-hydroxybenzotriazole. *FEMS Microbiology Letters* **1999**, 170 (1), 51-57.
84. Van Erven G, De Visser R, Merckx DWH, Strolenberg W, De Gijssel P, Gruppen H and Kabel MA. Quantification of lignin and its structural features in plant biomass using ^{13}C lignin as internal standard for pyrolysis-GC-SIM-MS. *Analytical Chemistry* **2017**, 89 (20), 10907-10916.
85. Van Erven G, De Visser R, De Waard P, Van Berkel WJH and Kabel MA. Uniformly ^{13}C labeled lignin internal standards for quantitative py-GC-MS analysis of grass and wood. *ACS Sustainable Chemistry & Engineering* **2019**, 7 (24), 20070-20076.
86. Tuomela M, Vikman M, Hatakka A and Itävaara M. Biodegradation of lignin in a compost environment: a review. *Bioresource Technology* **2000**, 72 (2), 169-183.

87. Mansfield SD, Kim H, Lu F and Ralph J. Whole plant cell wall characterization using solution-state 2D NMR. *Nature Protocols* **2012**, 7(9), 1579.
88. Del Río JC, Speranza M, Gutiérrez A, Martínez MJ and Martínez ÁT. Lignin attack during eucalypt wood decay by selected basidiomycetes: a Py-GC/MS study. *Journal of Analytical and Applied Pyrolysis* **2002**, 64(2), 421-431.
89. Dey Laskar D, Ke J, Zeng J, Gao X and Chen S. Py-GC/MS as a powerful and rapid tool for determining lignin compositional and structural changes in biological processes. *Current Analytical Chemistry* **2013**, 9(3), 335-351.
90. Lu F and Ralph J. Derivatization followed by reductive cleavage (DFRC method), a new method for lignin analysis: protocol for analysis of DFRC monomers. *Journal of Agricultural and Food Chemistry* **1997**, 45(7), 2590-2592.
91. Rolando C, Monties B and Lapierre C, in *Methods in lignin chemistry*. (Springer, Berlin, 1992), pp. 334-349.
92. Zinovyev G, Sulaeva I, Podzimek S, Rössner D, Kilpeläinen I, Summerskii I, Rosenau T and Potthast A. Getting closer to absolute molar masses of technical lignins. *ChemSusChem* **2018**, 11(18), 3259-3268.
93. Rico A, Rencoret J, Del Río JC, Martínez AT and Gutiérrez A. In-depth 2D NMR study of lignin modification during pretreatment of Eucalyptus wood with laccase and mediators. *BioEnergy Research* **2015**, 8(1), 211-230.
94. Rico A, Rencoret J, Del Río JC, Martínez AT and Gutiérrez A. Pretreatment with laccase and a phenolic mediator degrades lignin and enhances saccharification of Eucalyptus feedstock. *Biotechnology for Biofuels* **2014**, 7(1), 6.
95. Rencoret J, Pereira A, Del Río JC, Martínez AT and Gutiérrez A. Delignification and saccharification enhancement of sugarcane byproducts by a laccase-based pretreatment. *ACS Sustainable Chemistry & Engineering* **2017**, 5(8), 7145-7154.
96. Babot ED, Rico A, Rencoret J, Kalum L, Lund H, Romero J, Del Río JC, Martínez ÁT and Gutiérrez A. Towards industrially-feasible delignification and pitch removal by treating paper pulp with *Myceliophthora thermophila* laccase and a phenolic mediator. *Bioresource Technology* **2011**, 102(12), 6717-6722.
97. Gutiérrez A, Rencoret J, Cadena EM, Rico A, Barth D, Del Río JC and Martínez ÁT. Demonstration of laccase-based removal of lignin from wood and non-wood plant feedstocks. *Bioresource Technology* **2012**, 119, 114-122.
98. Chen Q, Marshall MN, Geib SM, Tien M and Richard TL. Effects of laccase on lignin depolymerization and enzymatic hydrolysis of ensiled corn stover. *Bioresource Technology* **2012**, 117, 186-192.
99. Du X, Li J, Gellerstedt G, Rencoret J, Del Río JC, Martínez AT and Gutiérrez A. Understanding pulp delignification by laccase-mediator systems through isolation and characterization of lignin-carbohydrate complexes. *Biomacromolecules* **2013**, 14(9), 3073-3080.
100. Rencoret J, Pereira A, Del Río JC, Martínez AT and Gutiérrez A. Laccase-mediator pretreatment of wheat straw degrades lignin and improves saccharification. *BioEnergy Research* **2016**, 9(3), 917-930.
101. Moilanen U, Kellock M, Galkin S and Viikari L. The laccase-catalyzed modification of lignin for enzymatic hydrolysis. *Enzyme and Microbial Technology* **2011**, 49(6-7), 492-498.
102. Vivekanand V, Dwivedi P, Sharma A, Sabharwal N and Singh RP. Enhanced delignification of mixed wood pulp by *Aspergillus fumigatus* laccase mediator system. *World Journal of Microbiology and Biotechnology* **2008**, 24(12), 2799.
103. Areskog D, Li J, Gellerstedt Gr and Henriksson G. Investigation of the molecular weight increase of commercial lignosulfonates by laccase catalysis. *Biomacromolecules* **2010**, 11(4), 904-910.
104. Prasetyo EN, Kudanga T, Østergaard L, Rencoret J, Gutiérrez A, Del Río JC, Santos JJ, Nieto L, Jiménez-Barbero J and Martínez AT. Polymerization of lignosulfonates by the laccase-HBT (1-hydroxybenzotriazole) system improves dispersibility. *Bioresource Technology* **2010**, 101(14), 5054-5062.
105. Huber D, Ortner A, Daxbacher A, Nyanhongo GS, Bauer W and Guebitz GM. Influence of oxygen and mediators on laccase-catalyzed polymerization of lignosulfonate. *ACS Sustainable Chemistry & Engineering* **2016**, 4(10), 5303-5310.

106. Bourbonnais R, Paice M, Reid I, Lanthier P and Yaguchi M. Lignin oxidation by laccase isozymes from *Trametes versicolor* and role of the mediator 2, 2'-azinobis (3-ethylbenzthiazoline-6-sulfonate) in kraft lignin depolymerization. *Applied and Environmental Microbiology* **1995**, *61* (5), 1876-1880.
107. Gouveia S, Fernández-Costas C, Sanromán MA and Moldes D. Enzymatic polymerisation and effect of fractionation of dissolved lignin from *Eucalyptus globulus* Kraft liquor. *Bioresource Technology* **2012**, *121*, 131-138.
108. Moya R, Saastamoinen P, Hernández M, Suurnäkki A, Arias E and Mattinen M-L. Reactivity of bacterial and fungal laccases with lignin under alkaline conditions. *Bioresource Technology* **2011**, *102* (21), 10006-10012.
109. Fernaund JRH, Carnicero A, Perestelo F, Cutuli MH, Arias E and Falcón MA. Upgrading of an industrial lignin by using laccase produced by *Fusarium proliferatum* and different laccase-mediator systems. *Enzyme and Microbial Technology* **2006**, *38* (1), 40-48.



Laccase/mediator systems: their reactivity toward phenolic lignin structures

Laccase/mediator systems (LMS) have been widely studied for their capacity to oxidize the non-phenolic subunits of lignin (70-90% of the polymer). The phenolic subunits (10-30% of the polymer), which can also be oxidized without mediators, have received considerably less attention. Consequently, it remains unclear to what extent the presence of a mediator influences the reactions of the phenolic subunits of lignin. To get more insight in this, UHPLC-MS was used to study the reactions of a phenolic lignin dimer (GBG), initiated by a laccase from *Trametes versicolor*, alone or in combination with the mediators HBT and ABTS. The role of HBT was negligible, as its oxidation by laccase occurred slowly in comparison to that of GBG. Laccase and laccase/HBT oxidized GBG at a comparable rate, resulting in extensive polymerization of GBG. In contrast, laccase/ABTS converted GBG at a higher rate, as GBG was oxidized both directly by laccase, but also by ABTS radical cations, which were rapidly formed by laccase. The laccase/ABTS system resulted in C_α-oxidation of GBG and coupling of ABTS to GBG, rather than polymerization of GBG. Based on these results, we propose reaction pathways of phenolic lignin model compounds with laccase/HBT and laccase/ABTS.

Based on: Roelant Hilgers, Jean-Paul Vincken, Harry Gruppen and Mirjam A. Kabel. Laccase/mediator systems: their reactivity toward phenolic lignin structures. *ACS Sustainable Chemistry & Engineering* **2018**, 6 (2), 2037-2046.

2.1 Introduction

Lignin is one of the most abundant polymers in nature as part of plant cell walls, and currently considered as sustainable precursor for chemicals or materials.¹⁻⁴ It is built up from sinapyl alcohol, coniferyl alcohol and *p*-coumaryl alcohol (S, G and H units, respectively), which couple via radical polymerization to form a variety of C-C and C-O interunit linkages. The β -O-4 linkage is the most abundant one, accounting for approximately 45 to 94 % of the total interunit linkages, in lignins mildly isolated from plant materials.³ Lignin contains phenolic and non-phenolic subunits, which account for 10-30 and 70-90% of the polymer, respectively.⁵

Although the valorization of lignin is still underexploited,³ three main routes are considered relevant. The first is via lignin polymerization, which may result in improved binders and adhesives.⁶ Second, lignin depolymerization may lead to high-value low-molecular-weight aromatics.^{1,2} A third option is the functionalization of lignin via grafting of specific molecules onto lignin.⁷ A green alternative for lignin valorization is via biocatalysis and, in particular, laccase is known as one of the key activities towards lignin. Various lignin modifications are reported for laccase, such as polymerization,^{4,8-10} depolymerization,¹¹⁻¹³ C_o-oxidation¹⁴ and demethylation.¹⁵ It is poorly understood, however, how to direct lignin modification by laccase towards one of these modifications. Thus, for an effective use of laccase in lignin valorization, it is essential to have a better understanding on how to control lignin modification by laccase.

Laccases (E.C. 1.10.3.2) are oxidases that couple the reduction of molecular oxygen to the one-electron oxidation of a wide variety of aromatic substrates. The most powerful laccases are produced by white-rot fungi, and can have redox potentials up to 800 mV vs. NHE.³ With respect to laccase activity towards lignin, it is important to distinguish the phenolic and non-phenolic subunits in lignin. The phenolic subunits can directly be oxidized by laccase, as the redox potentials of such subunits are sufficiently low. In contrast, the non-phenolic parts have redox potentials up to 1500 mV vs. NHE, and are therefore, recalcitrant to oxidation by laccase alone.¹⁶ Nevertheless, when laccase is combined with a so-called mediator, oxidation of non-phenolic lignin structures is possible as well.¹⁷ In such a laccase/mediator system (LMS), the mediator is first oxidized by the laccase, after which it can oxidize non-phenolic substrates via different mechanisms, such as electron transfer (ET) or radical hydrogen atom transfer (HAT).¹⁸ As a LMS is required for the oxidation of the non-phenolic subunits in lignin, and the phenolic subunits can be oxidized by laccase alone, research on lignin modification by LMS has mainly focused on the reactivity of non-phenolic lignin subunits,^{14,17-21} and several reaction pathways have been described for such incubations.^{1,22,23} Nevertheless, as lignin also contains a considerable amount of phenolic subunits, it is important to understand how these subunits react when incubated with LMS.

Research on lignin conversion by laccase and LMS is often performed using lignin model compounds. Phenolic lignin model compounds have been used, but most often in the

absence of mediators.²⁴⁻²⁶ A few studies have been published on the reactions of phenolic lignin model compounds in LMS incubations, and mainly polymerization was shown to occur. Conclusions about the degree of polymerization reached were obtained, but no insights about the structure of the (initially) formed reaction products could be provided.^{27,28} Consequently, it remains unclear how the phenolic subunits of lignin are modified by LMS and to what extent mediators play a role in such modifications.

In the current research, we used the phenolic β -O-4 linked lignin model compound, 1-(4-hydroxy-3-methoxyphenyl)-2-(2-methoxyphenoxy)propane-1,3-diol, (guaiacylglycerol- β -guaiacyl ether, GBG), to mimic the phenolic subunits in lignin. We employed RP-UHPLC-PDA-ESI-MSⁿ, to study detailed reaction pathways of GBG initiated by laccase (from *Trametes versicolor*) with or without a mediator. 2,2'-Azino-bis(3-ethylbenzothiazoline-6-sulphonic acid) (ABTS) and 1-hydroxybenzotriazole (HBT) were used as mediators, as these are the most commonly used mediators in literature. MALDI-TOF-MS was used to investigate the formation of larger reaction products.

2.2 Materials & Methods

2.2.1 Materials

Guaiacylglycerol- β -guaiacyl ether (GBG; **Fig. 2.1**) was obtained from TCI chemicals (Tokyo, Japan) and 2,5-dihydroxybenzoic acid (DHB) was obtained from Bruker Daltonics (Bremen, Germany). Laccase from *Trametes versicolor* and all other chemicals were purchased from Sigma Aldrich (St. Louis, MO, USA). The laccase was partially purified, after which the activity was determined spectrophotometrically by oxidation of ABTS¹⁷ (1 U = 1 μ mol ABTS oxidized per minute) (see Supporting Information for details). Water was prepared using a Milli-Q water purification system (Merck Millipore, Billerica, MA).

2.2.2 Incubation of GBG with laccase and laccase/mediator systems

GBG was dissolved at 0.5 mM in sodium phosphate buffer (50 mM, pH 4) with or without an equimolar concentration of ABTS or HBT. Laccase was added to reach a final substrate and mediator concentration of 0.4 mM and a laccase activity of 0.1 U mL⁻¹. The mixtures were incubated at 40 °C and 400 rpm in a thermomixer (Eppendorf, Hamburg, Germany). After 1, 2, 5, 10, 15, 20, 30 and 60 min, and after 24 h, 50 μ L of the sample was transferred to another tube, and 5 μ L sodium azide (20 mM) was added to stop the reaction.²⁹ As no azide-related products were detected, and reaction products were stable in the presence of an excess of azide, the addition of azide was considered not to influence the reaction product profile (results not shown). The resulting samples were diluted 10 times in MilliQ water and were centrifuged (10000 $\times g$, 5 min, 20 °C) prior to analysis by RP-UHPLC-PDA-MSⁿ. A detailed description of the RP-UHPLC-PDA-MSⁿ analysis can be found in the Supporting Information.

2.2.3 Incubation of GBG with ABTS radical cations

GBG was dissolved at 0.5 mM in sodium phosphate buffer (50 mM, pH 4). ABTS (2 mM) was incubated with 0.20 U mL⁻¹ laccase (2 min, 40 °C) and directly centrifuged over an Amicon Ultra-4 centrifugal filter (Merck Millipore) with a normalized molecular weight limit of 10 kDa. The dark green filtrate was incubated with the GBG solution at a ratio of 1:4 (2 min, 40 °C). As a control, the same incubation was done using ABTS that was not treated with laccase.

2.2.4 Sample Preparation for Matrix-Assisted Laser Desorption Ionization–Time of Flight Mass Spectrometry (MALDI-TOF)

The samples were prepared as described in 2.2.3, with the adaptation that the reaction was stopped after 7, 15 and 60 min. Samples were diluted 2 times in methanol, and a saturated solution of DHB was used as matrix. In a second experiment, similar incubations with laccase and laccase/HBT were stopped after 2, 5, 10, 15 and 20 min. For details about MALDI-TOF settings see Supporting Information.

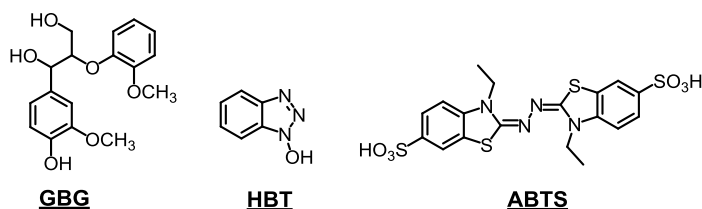


Fig 2.1 Molecular structures of guaiacylglycerol-β-guaiacyl ether (GBG), 1-hydroxybenzotriazole (HBT), and 2,2'-azino-bis(3-ethylbenzothiazoline-6-sulfonic acid) (ABTS).

2.3 Results & Discussion

2.3.1 Reaction products of GBG incubated with laccase

GBG (**Fig. 2.1**) was, first, incubated with laccase without addition of mediators. From the UHPLC-MS chromatograms, two main reaction products were observed upon incubation of GBG, both having their largest intensities during the first 20 min (**Fig. 2.2**, **Table 2.1** and **Fig. S2.1**). In addition, remaining GBG was detected (only trace amounts after 2 min). Using accurate mass determination the reaction products were found to correspond with molecular formulas C₃₄H₃₈H₁₂ and C₅₁H₅₆O₁₈ (**Table 2.1**). Based on their molecular formulas and the fact that the fragmentation patterns showed high similarities with GBG (**Table 2.1** and **Fig. 2.3**), these products were annotated as a dimer of GBG (molecular weight (Mw)=2×GBG-2H) and a trimer of GBG (Mw=3×GBG-4H; **Table 2.1**), formed via radical coupling. Recently, oligomerization of GBG was reported by others, and it was shown that coupling between two GBG radicals occurs via C-C bond formation.³⁰ The

same was suggested for the subsequent formation of a trimer, although no experimental evidence was given. Therefore, we have specified the coupling position in the dimer, but not of the second coupling in the trimer in **Fig. 2.3**. In addition to the dimer and trimer, only traces of other reaction products were observed (**Table S2.1**). After 24 h, precipitation was observed and no peaks were detected in the chromatograms, suggesting ongoing polymerization of the initially formed dimer and trimer. Thus, the activity of laccase alone was found to result in polymerization of GBG. This conclusion is in line with results on laccase activity towards phenolic model compounds reported by others.^{27,30}

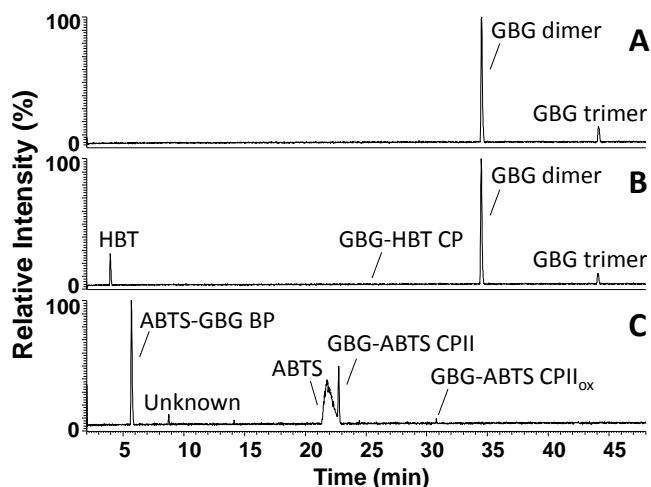


Fig. 2.2 RP-UHPLC-MS chromatograms (negative mode) of GBG incubated for 5 min with laccase (A), laccase/HBT (B), and laccase/ ABTS (C). Chromatograms of other time points can be found in the Supporting Information.

2.3.2 Reaction products of GBG incubated with a laccase/HBT system

When GBG was incubated with laccase in combination with HBT, the reaction products formed were very comparable to those formed in the presence of laccase alone (**Fig. 2.2**, **Table 2.1** and **Fig. S2.1**). The same dimer and trimer were identified based on retention time, accurate mass and fragmentation pattern (**Fig. 2.2** and **Table 2.1**). Also the amounts were comparable, based on UV₂₈₀ peak area. In addition to the dimer and trimer, a small peak (hardly visible) corresponding to the molecular formula $C_{23}H_{23}N_3O_7$ was observed. This, in combination with a fragmentation pattern similar to that of GBG (**Table 2.1** and **Fig. 2.3**), suggested the formation of a GBG-HBT radical coupling product (GBG-HBT CP, **Fig. 2.3**). After prolonged incubation times (1 h) $C_{23}H_{21}N_3O_7$ was detected, which, most likely, corresponded to further oxidation of GBG-HBT CP to GBG-HBT CP_{ox} (**Fig. 2.3**). It was recently shown for the first time that N-OH type mediators, such as HBT, couple to lignin upon addition of laccase.⁷ Our results confirm that such

coupling can occur at the phenolic moieties of lignin, but also indicate that the extent of coupling between GBG and HBT is small as compared to GBG oligomerization. The proposed structures of all coupling products are depicted in **Fig. 2.3**, together with their proposed MS² fragmentation pathways. After 24 h, no GBG-related peaks were detected anymore and precipitation was observed. Approximately 45% of the original HBT was still present, as determined from UV₂₈₀ peak areas (data not shown). Part of it was converted to benzotriazole (BT), which is inactive as a mediator.³¹ This conversion of HBT to BT has been described by others^{31,32} and also occurred in a control reaction with only HBT and laccase without GBG present (data not shown). Most likely, BT is formed upon a reaction of HBT radicals with aromatic amino acids of the enzyme.³²

2.3.3 Reaction products of GBG incubated with a laccase/ABTS system

When GBG was incubated with laccase and ABTS, a larger variety of reaction products was detected compared to the incubations described above (**Fig. 2.2**, **Table 2.1** and **Fig. S2.1**). Molecules with molecular formulas C₁₇H₁₈O₆ and C₃₅H₃₅N₄O₁₂S₄ were detected, especially after short reaction times (1-15 min). These were annotated as C₆-oxidized GBG and a radical coupling product between oxidized GBG and ABTS (GBG_{ox} and GBG-ABTS CPI_{ox} in **Table 2.1** and **Fig. 2.3**), respectively. A relatively small peak corresponding to a coupling of non-oxidized GBG and ABTS (GBG-ABTS CPI) has been observed as well, but inconsistently. Likely, the latter coupling product is prone to react further. The structure and fragmentation pattern of GBG-ABTS CPI can be found in **Fig. S2.4**. In addition, reaction products with molecular formulas C₂₆H₂₇N₃O₉S₂, C₂₆H₂₅N₃O₉S₂ were found. Based on these formulas and their fragmentation patterns, these products were annotated as GBG-ABTS CPII and GBG-ABTS CPII_{ox}, respectively (**Table 2.1** and **Fig. 2.3**). Similar coupling products, between a phenolic compound and part of the ABTS molecule, have been reported for hydroxybenzoic acids³³ and catechin,³⁴ using NMR and mass spectrometry, respectively. To our knowledge, this is the first time that such coupling products are shown for lignin model compounds. The main MS² fragments (*m/z* 242 and 214 in negative mode) match with the fragments reported for the catechin-ABTS products (*m/z* 244 and 216 in positive mode).³⁴ As the adducts identified with NMR spectroscopy²⁹ resulted from C-N coupling (rather than O-N coupling), the adducts in **Fig. 2.3** are also shown with a C-N bond between the GBG and ABTS moiety. In addition to these coupling products, a major peak was detected corresponding to C₉H₉NO₄S₂. As this molecule was hardly formed in a control reaction with only ABTS and laccase (data not shown), it was considered to be an ABTS cleavage product (ABTS CLP) formed upon coupling of GBG and ABTS. Lastly, a reaction product was detected with molecular formula C₂₅H₂₅N₄O₈S₄. This could correspond to a radical coupling product of guaiacol and ABTS. It should be mentioned that for the formation of such a product cleavage of GBG to form guaiacol is required, either before or during coupling with ABTS. Besides the detection of C₂₅H₂₅N₄O₈S₄, no indications were found for cleavage of GBG.

Table 2.1 Compounds detected with UHPLC-PDA-ESI-ITMS and UHPLC-PDA-ESI-FTMS after incubation of GBG with laccase from *T. versicolor* in the presence or absence of ABTS and HBT. MS² fragments and λ_{max} were determined using UHPLC-PDA-ESI-ITMS. All other values were obtained using UHPLC-PDA-ESI-FTMS. Relative intensities of MS² fragments are shown between brackets. N.D. = Not detected.

RT (min)	Tent. annot.	Molecular formula	Ion	Observed/calculated mass	Mass error (ppm)	MS ² fragments	λ_{max} (nm)
Reaction products of GBG incubated with laccase alone							
20.8	GBG	C ₁₇ H ₂₀ O ₆	[M+Na] ⁺	320.12556/ 320.12599	-1.34	295 (55), 302 (16), 201 (8), 147 (6), 219 (5), 176 (4)	278
34.8	GBG dimer	C ₃₄ H ₃₈ O ₁₂	[M-H] ⁻	638.23720/ 638.23633	1.36	589 (100), 483 (62), 513 (28), 435 (26), 329 (20), 465 (12), 541 (12), 359 (8)	278
44.7	GBG trimer	C ₅₁ H ₅₆ O ₁₈	[M-H] ⁻	956.34775/ 956.34666	1.13	907 (100), 889 (60), 919 (30), 859 (20)	N.D.
Reaction products of GBG incubated with laccase/HBT							
3.9	HBT	C ₆ H ₅ N ₃ O	[M-H] ⁻	135.04329/ 135.04326	0.23	106 (100), 78 (4)	306, 276,
			[M+H] ⁺			91 (63), 80 (40), 53 (18), 107 (8)	269
7.2	BT	C ₆ H ₅ N ₃	[M+H] ⁺	119.04832/ 119.04835	-0.23	N.D.	260, 280
20.9	GBG	C ₁₇ H ₂₀ O ₆	[M+Na] ⁺	320.12556/ 320.12599	-1.34	295, 302, 201, 219, 147, 176	278
25.1	GBG-HBT CP	C ₂₃ H ₂₃ N ₃ O ₇	[M-H] ⁻	453.15375/ 453.15360	0.33	404 (100), 328 (38), 298 (30)	330
31.9	GBG-HBT CP _{ox}	C ₂₃ H ₂₁ N ₃ O ₇	[M-H] ⁻	451.13838/ 451.13795	0.95	420 (100), 310 (27), 326 (15)	N.D.
34.4	GBG dimer	C ₃₄ H ₃₈ O ₁₂	[M-H] ⁻	638.23720/ 638.23633	1.36	589 (100), 483 (62), 513 (28), 435 (26), 329 (20), 465 (12), 541 (12), 359 (8)	278
44.7	GBG trimer	C ₅₁ H ₅₆ O ₁₈	[M-H] ⁻	956.34775/ 956.34666	1.13	907 (100), 889 (60), 919 (30), 859 (20)	N.D.
Reaction products of GBG incubated with laccase/ABTS							
5.6	ABTS CLP	C ₉ H ₉ NO ₄ S ₂	[M-H] ⁻	258.99757/ 258.99730	1.05	229 (37)	256, 292, 285
8.7	Unknown	Unknown	[M-H] ⁻	329.99756		302 (100), 238 (29), 222 (9)	278
17.0	Unknown	C ₂₅ H ₂₅ N ₄ O ₈ S ₄	[M-2H] ⁻	637.05667/ 637.05553	1.79	363 (100), 378 (95), 228 (34), 605 (31), 405 (26), 257 (25), 335 (18)	305
21.4	ABTS	C ₁₈ H ₁₈ N ₄ O ₆ S ₄	[M-2H] ²⁻	514*		N.D.	342
22.7	GBG- ABTS CPII	C ₂₆ H ₂₇ N ₃ O ₉ S ₂	[M-H] ⁻	589.11946/ 589.118876	0.99	242 (100), 214 (61), 228 (10)	550

Table 2.1 continued

RT (min)	Tent. annot.	Molecular formula	Ion	Observed/ calculated mass	Mass error (ppm)	MS ² fragments	λ_{\max} (nm)
24.4	GBG-ABTS CPI _{ox}	C ₃₅ H ₃₅ N ₄ O ₁₂ S ₄	[M-3H] ²⁻	831.11369/ 831.11289	0.96	572 (100), 228 (43), 256 (42)	305, 278
			[M-2H] ⁻			N.D.	
28.3	GBG _{ox}	C ₁₇ H ₁₈ O ₆	[M-H] ⁻	318.11017/ 318.11034	-0.52	287 (100), 193 (71)	280, 311
			[M+H] ⁺			167 (100), 149 (70), 271 (68), 151 (59), 195 (44), 269 (32), 177 (26), 289 (22)	
			[M+Na] ⁺			311 (100), 218 (16), 146 (11), 187 (6)	
30.7	GBG-ABTS CPI _{ox}	C ₂₆ H ₂₅ N ₃ O ₉ S ₂	[M-H] ⁻	587.10366/ 587.10322	0.76	242, 214, 556, 228	585, 448, 328

*Only data from UHPLC-PDA-ESI-ITMS were used, as FTMS only showed in-source fragmentation.

In contrast to the incubation with laccase alone and laccase with HBT, no GBG was detected at all incubation times, suggesting a fast conversion of GBG into reaction products. The dimer and trimer found for incubations with laccase alone and laccase/HBT were absent at all incubation times when ABTS was used. After 24 h, approximately 29% of the initial amount ABTS was still present (data not shown). Whereas others reported polymerization as the main result of laccase/ABTS activity towards phenolic substrates,^{27,28} our results suggest that GBG preferably couples to ABTS, rather than to another GBG molecule.

2.3.4 Reaction pathways of laccase and laccase/HBT with GBG

When To get more insight into the course of the reactions occurring during incubation of GBG with laccase and the laccase/mediator systems, product formation was monitored at 9 different time points within the first hour. Hereto, peak areas from extracted ion chromatograms of the reaction products (**Table 2.1**) relative to the time point with the highest area, were plotted as function of incubation time (**Fig. 2.4**). For clarity, only GBG-related reaction products are shown.

Fig. 2.4A and **B** show that, under the conditions used, a fast conversion of GBG to oligomeric products occurred. Already in the first minute, 67 and 69% of the GBG was converted by laccase and laccase/HBT, respectively. For both laccase and laccase/HBT it was shown that the dimer and the trimer gradually decreased in abundance and disappeared within one hour. The decrease of the dimer in the first 20 min occurred together with an increase in higher oligomers, indicating further polymerization (**Fig. S2.2**). In the incubation with laccase/HBT, the coupling product GBG-HBT CP increased during the first 30 min, and then decreased again.

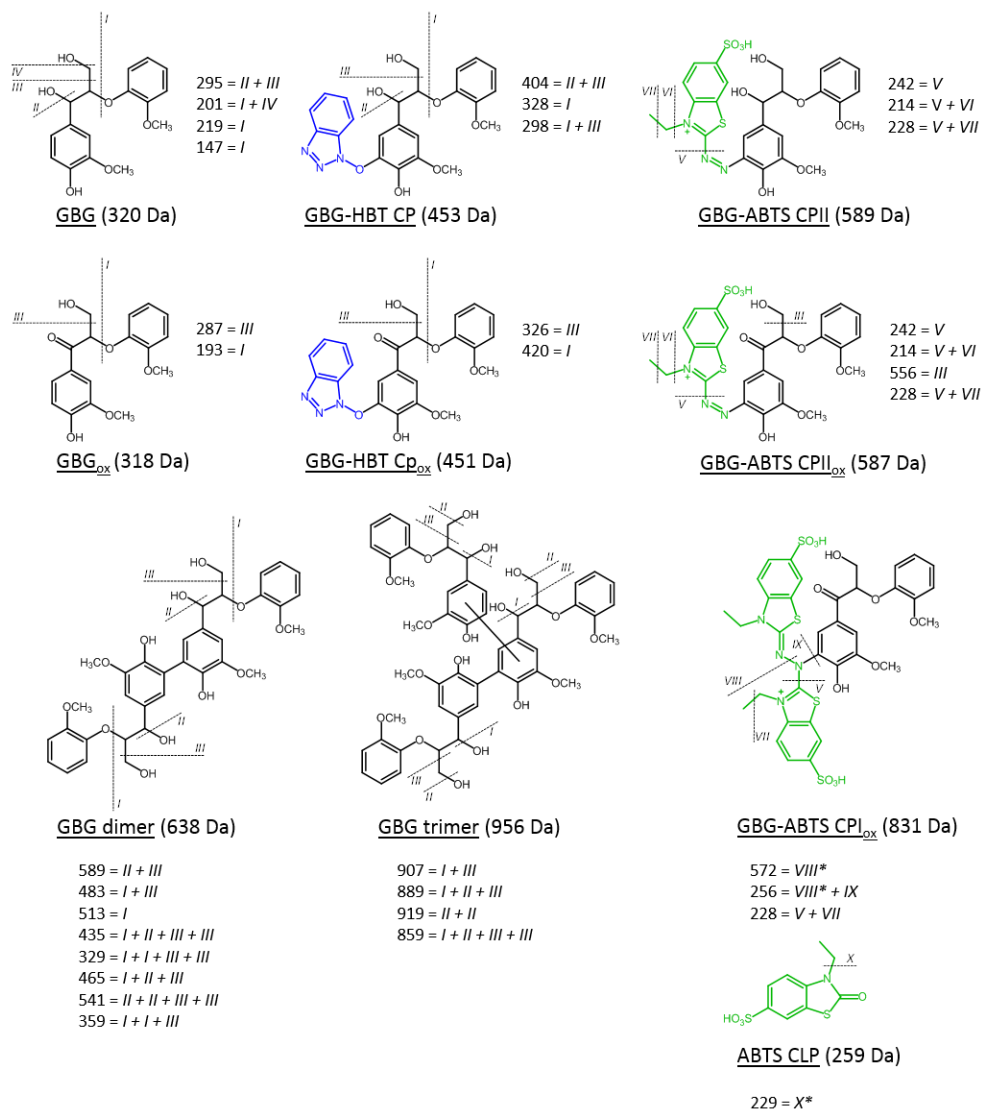


Fig. 2.3 Proposed structures of reaction products of GBG after incubation with laccase and LMS. The dotted lines represent the proposed fragmentation pattern, resulting in the MS² fragments reported in Table 2.1. The fragmentation pattern of GBG and GBG-ABTS CPI_{ox} originate from the parent ions [M+Na]⁺ and [M-3H]²⁺, respectively. All other patterns originate from the parent ion [M-H]⁻. In the coupling products and oligomers, the positions of coupling could not be identified based on MS² spectra, and are therefore based on literature.^{31,34-35} The position of the second interunit bond in the GBG trimer is not specified, as there is no experimental evidence for either C-C or C-O linkage. Fragmentations with an * (in GBG-ABTS CPI_{ox} and ABTS CLP) are suggested to be radical fragmentations.

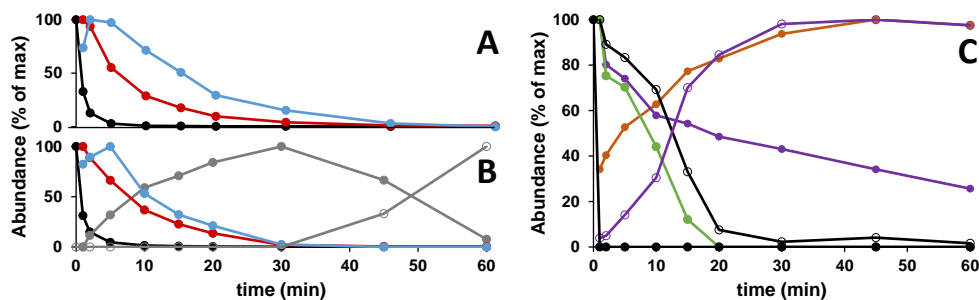


Fig. 2.4 Normalized MS peak areas in time of reaction products formed upon incubation of GBG with laccase alone (A), laccase/HBT (B), and laccase/ABTS (C). Areas were obtained from extracted ion chromatograms: GBG (m/z 343) (black dot), GBG dimer (m/z 637) (red dot), GBG trimer (m/z 955) (blue dot), GBG-HBT CP (m/z 452) (grey dot), GBG-HBT CP_{ox} (m/z 450) (open dot, grey line), GBG_{ox} (m/z 319 and 341) (open dot, black line), GBG-ABTS CPI_{ox} (m/z 414) (green dot), GBG-ABTS CPII (m/z 588) (purple dot), GBG-ABTS CPII_{ox} (m/z 586) (open dot, purple line) and ABTS CLP (m/z 258) (orange dot). For the abundance (Y axis), the time point with the largest peak area was set to 100%. For the other time points, the abundance was calculated as the peak area relative to the area of this largest peak. Amounts withdrawn per time point and injected to UHPLC-MS analysis were the same for all time points.

The decrease of GBG-HBT CP coincided with an increase in its oxidized equivalent GBG-HBT CP_{ox}, confirming that GBG-HBT CP is oxidized further to GBG-HBT CP_{ox}. For such a conversion from alcohol to ketone at C_α, a benzylic radical should be formed. This may have occurred via radical hydrogen abstraction by a HBT radical. As a phenolic lignin structure itself could also act as HAT-type mediator,³⁵ radical hydrogen abstraction may also have occurred by a phenoxyl radical of a GBG-related structure. If the latter indeed occurred, the oxidant probably was an oligomeric GBG radical, as all GBG was converted before conversion of GBG-HBT CP to GBG-HBT CP_{ox} took place (**Fig. 2.4**).

These findings indicate that upon incubation with both laccase and laccase/HBT, extensive polymerization of GBG takes place. Radical coupling between GBG and HBT occurred, but only to a small extent. The coupling product was further oxidized, and is probably prone to further polymerization. The rate of conversion of GBG and its oligomers does not seem to be influenced by the presence of HBT, suggesting that the role of HBT is negligible when laccase/HBT is used on phenolic substrates. A schematic overview of the proposed reactions is depicted in **Fig. 2.5**.

2.3.5 Reaction pathways of laccase/ABTS with GBG

Similar to the incubations with laccase and laccase/HBT, the reaction of GBG with laccase/ABTS was monitored over time. **Fig. 2.4C** shows that all GBG was converted within the first minute of incubation. Based on this and on the annotations discussed above, it can be stated that the laccase/ABTS system differs from laccase and laccase/HBT in two ways: (i) GBG is converted faster (higher rate), and (ii) GBG is converted into different reaction products (other pathways).

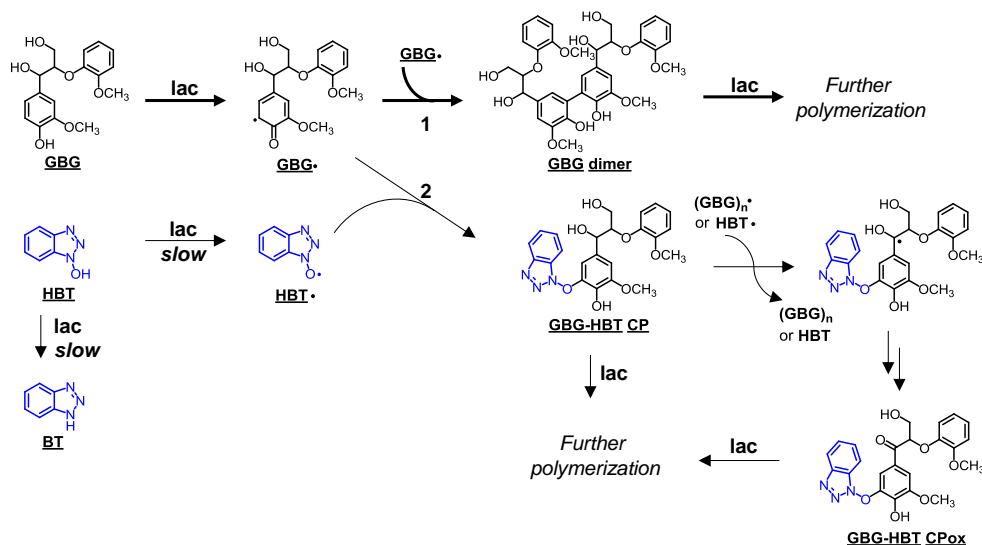


Fig. 2.5 Overview of proposed reactions occurring after incubation of GBG with laccase alone or a laccase/HBT system. The thick arrows represent the major reaction pathway. The reactions represented by thin arrows do occur, but slower and/or to a smaller extent. In the case of laccase alone, all GBG reacts via route 1. In the case of a laccase/HBT system, GBG reacts via route 1 and 2, but route 1 is favored due to the slow oxidation of HBT. Oxidation of GBG-HBT CP is proposed to occur via radical hydrogen abstraction by either a HBT radical (HBT•) or an oligomeric GBG radical ((GBG)_n•). The C–C coupling in the dimer is based on Ramalingam et al.³¹ For clarity, reductions of O₂ to H₂O by laccase are not shown in the figure.

A possible explanation for the higher conversion rate might be the rapid formation of ABTS radical cations (ABTS^{•+}), which might undergo a redox reaction with GBG. ABTS^{•+} has been shown to induce oxidative polymerization of creosol, a phenolic monomeric lignin model compound²⁸ and to undergo a redox reaction with vanillyl alcohol.³⁷ To check whether a similar interaction between GBG and ABTS^{•+} occurred, GBG was incubated with laccase-free ABTS^{•+}. GBG was indeed converted upon addition of ABTS^{•+}, resulting in several reaction products: GBG_{ox}, GBG dimer, oxidized GBG dimer and GBG-ABTS CPI (Fig. S2.3). The annotation of the latter two products can be found in Table S2.2 and Fig. S2.4. As no GBG conversion was observed in a control reaction with neutral ABTS (Fig. S2.3B), it was concluded that the higher GBG conversion rate by the laccase/ABTS system is caused by the fact that GBG is oxidized via two mechanisms: directly by laccase and via a redox reaction with ABTS^{•+}. It cannot be excluded that also the dication ABTS²⁺ (formed via disproportionation of ABTS^{•+}) is involved in the oxidation of GBG. Nevertheless, as it has been shown with cyclic voltammetry that vanillyl alcohol can rapidly be oxidized by ABTS^{•+},³⁶ we assume that the same applies to GBG.

Fig. S2.3 also shows that C_α-oxidized GBG is formed upon addition of ABTS^{•+}. The fact that C_α-oxidized products were not observed in incubations with laccase alone implies that C_α-oxidation is caused by ABTS^{•+} rather than laccase. **Fig. 2.4C** shows that the concentrations of GBG_{ox}, GBG-ABTS CPI_{ox} are highest after 1 min of incubation, and that their concentration decreased relatively fast during the first 20 min. GBG-ABTS CPII was also highest after 1 min, but its decrease was slower. In contrast, the concentrations of GBG-ABTS CPII_{ox} and ABTS CLP gradually increased during the first hour of incubation, suggesting that they were formed upon conversion of the other reaction products. After 24 h, most reaction products from **Fig. 2.4C** had disappeared, except for ABTS CLP and GBG-ABTS CPII_{ox}. The areas of these peaks had even increased with 33 and 23%, respectively (data not shown). These results indicate that GBG formed coupling products with ABTS in the presence of laccase, after which a part of the ABTS moiety was cleaved off. The ultimate product formed after coupling of ABTS and GBG was GBG-ABTS CPII_{ox}. To our knowledge, coupling of ABTS to lignin and lignin model compounds has been suggested by others,^{8,27} but the structure of such lignin-ABTS coupling products has not been elaborated so far.

Based on the above, an overview of the course of the reactions leading to the formation of GBG-ABTS CPII_{ox} was constructed (**Fig. 2.6**). We suggest that after oxidation, GBG[•] undergoes two follow-up reactions: (i) Radical coupling with ABTS^{•+} to form an intermediate product GBG-ABTS CPI, or (ii) A second oxidation (by ABTS^{•+}) to form GBG_{ox}. In the latter case, GBG_{ox} can be further oxidized (by laccase or ABTS^{•+}) to GBG_{ox}[•], which then also couples to ABTS^{•+} to form GBG-ABTS CPI_{ox}. GBG-ABTS CPI and GBG-ABTS CPI_{ox} are subsequently converted to GBG-ABTS CPII and GBG-ABTS CPII_{ox}, upon which ABTS CLP was split off as a byproduct. The exact mechanism behind this is unknown, but it is suggested to involve an oxidation step, as the intermediates (GBG-ABTS CPI and GBG-ABTS CPI_{ox}) did not react further after inactivation of the laccase (**Fig. 2.4**). Eventually, the formed GBG-ABTS CPII can be oxidized to the ultimate reaction product GBG-ABTS CPII_{ox}.

2.3.6 Formation of larger oligomeric products

To investigate whether larger reactions products were formed upon incubation with laccase or LMS, MALDI-TOF spectra were recorded. After 1 hour of incubation with laccase and laccase/HBT, GBG oligomers up to DP 8 and DP 7 were detected, respectively (**Fig. 2.7**). As precipitation of reaction products occurred in both incubations, and the mixture still contained small amounts of insoluble material after dilution in methanol, it cannot be excluded that insoluble oligomers of higher DP were formed. Besides the GBG oligomers, no other peaks were detected, suggesting that incubation of GBG with laccase or laccase/HBT (almost) solely resulted in oligomerization of GBG. In contrast, a completely soluble reaction mixture was obtained after incubation with laccase/ABTS, in which all of the GBG oligomers were absent.

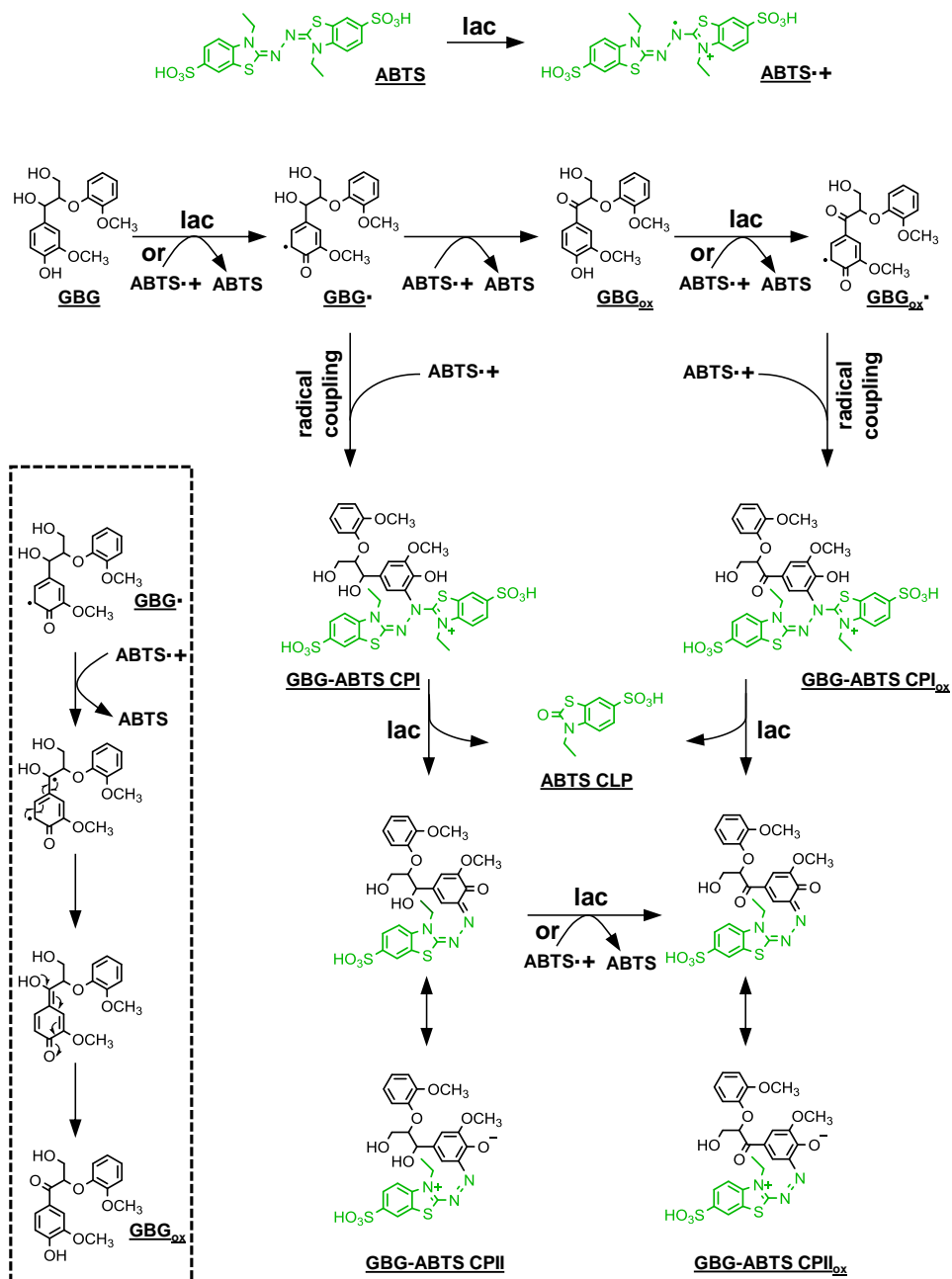


Fig. 2.6 Overview of proposed reactions occurring after incubation of GBG with a laccase/ABTS system. GBG can be oxidized directly by laccase or indirectly via ABTS^{•+}, which is formed by laccase. The GBG radicals may react further to GBG_{ox} or may undergo radical coupling with ABTS^{•+}. After coupling of GBG and ABTS, further rearrangements take place in which part of the ABTS molecule is cleaved from the reaction product. The inset shows the proposed mechanism of GBG_{ox} formation from GBG[•]. For clarity, reductions of O₂ to H₂O by laccase are not shown in the figure.

Instead, reaction products with m/z 657, 977, 989 and 1275 were detected. Assuming that these m/z values, like all GBG oligomers, originate from Na^+ adducts, it seems plausible that m/z 657 and 977 correspond to a GBG dimer with two oxidized C_α groups ($\text{Mw}=2\times\text{GBG}-6\text{H}$) and a GBG trimer with one oxidized C_α group ($\text{Mw}=3\times\text{GBG}-6\text{H}$), respectively. Although these products were not detected using UHPLC-MS, a GBG dimer and oxidized dimer were detected upon incubation with $\text{ABTS}^{+\cdot}$ (**Fig. S2.3**). It can therefore not be excluded that GBG is converted into (oxidized) oligomers in the laccase/ABTS system. Another indication for this is that all GBG had reacted during the first minute, but approximately 45% of the ABTS was still present after 1 hour. Since an equimolar ratio of GBG and ABTS was used, it is impossible that all GBG coupled to ABTS, and that GBG-ABTS CPII_{ox} is the only reaction product. Furthermore, polymerization of a phenolic model compound with laccase and ABTS has been shown before, using SEC²⁷ and MALDI-TOF.²⁸

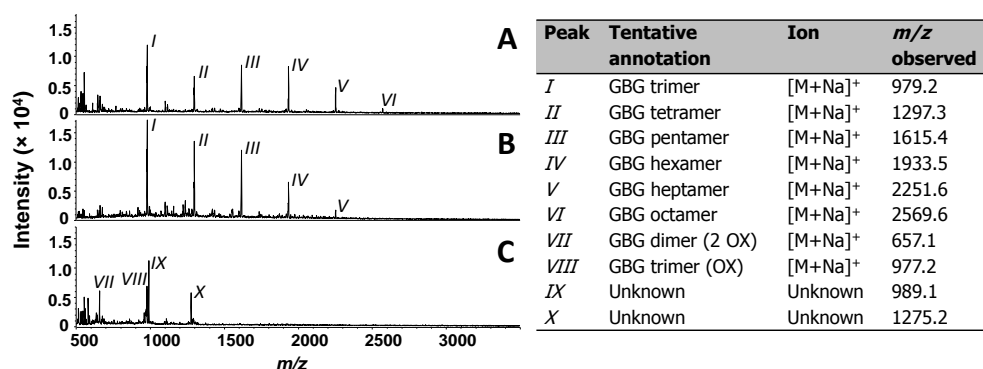


Fig. 2.7 MALDI-TOF spectra (left) of GBG after 60 min incubation with laccase alone (A), laccase/HBT (B) and laccase/ABTS (C) measured in positive mode, and corresponding tentative peak annotations (right). OX = C_α hydroxyl oxidized to ketone.

2.3.7 The role of the mediator in LMS incubations of GBG

Lignin contains 70-90% non-phenolic and 10-30% phenolic subunits.⁵ As the phenolic lignin structures can be oxidized by laccase alone, the question remains whether and how the mediator plays a role in the reaction rate and pathway when phenolic structures are incubated with LMS. Based on the results discussed above, it can be concluded that the role of HBT is very limited, in contrast to ABTS, which strongly influenced both rate and pathway. Whereas the efficiency of a mediator towards non-phenolic lignin structures has been reported to depend on its stability as a radical, and to its potency to abstract a radical from a non-phenolic substrate³⁷⁸ (via electron transfer or radical hydrogen atom transfer), we hypothesized that the role of the mediator towards phenolic substrates is dominated by the rate of its oxidation. The large difference in redox potentials, i.e. 1.08 V vs. NHE for HBT and 0.69 V vs. NHE for $\text{ABTS}/\text{ABTS}^{+\cdot}$,³⁸ suggests that the oxidation of

HBT by laccase occurs much slower than that of ABTS to $\text{ABTS}^{\cdot+}$. This was confirmed by oxygen consumption measurements of both mediators and GBG with laccase (**Fig. S2.5**). Oxygen consumption of ABTS is 1.9 times faster than that of GBG, whereas no substantial oxygen consumption of HBT with laccase was detected within the time frame used. So, although oxidized HBT may probably undergo a (redox) reaction with GBG, the conversion of GBG by laccase alone is already complete before a substantial amount of HBT is oxidized. Consequently, the role of HBT is negligible in this system. In contrast, the fast conversion of ABTS to $\text{ABTS}^{\cdot+}$ allows $\text{ABTS}^{\cdot+}$ to compete with GBG radicals in coupling reactions and to induce C_α -oxidations before GBG radicals start to polymerize. These results indicate that the influence of the mediator on the conversion of a phenolic lignin structure is highly dependent on its oxidation rate by laccase. It should be noted that the formation of substrate-mediator adducts may also be influenced by the bulkiness and presence of reactive groups on the mediator, but the comparison between HBT and ABTS does not give any insights in this.

2.4 Conclusions

The mediators HBT and ABTS strongly differed regarding their influence on GBG conversion by laccase. The influence of HBT was negligible, but ABTS strongly increased the conversion rate of GBG and altered the followed reaction pathways. Whereas laccase and laccase/HBT incubations resulted in extensive polymerization of GBG, incubation with the laccase/ABTS system mainly resulted in C_α -oxidation and coupling between GBG and ABTS. This difference in influence between HBT and ABTS can be explained by the much higher oxidation rate of ABTS by laccase, as compared to that of HBT. Extrapolating to polymeric lignin, our results suggest that the use laccase/ABTS will most likely result in a large degree of ABTS grafting on the phenolic lignin subunits, whereas such grafting reactions are less likely to occur with laccase/HBT. As the GBG-ABTS adducts were found to be relatively stable, this suggests that, once ABTS has been grafted on phenolic lignin subunits, further polymerization by laccase is blocked. These insights can be helpful for choosing the optimal mediator in a LMS, in which the mediator should not only be selected based on its efficiency in oxidation of non-phenolic lignin subunits, but also on its reactivity with the phenolic subunits.

2.5 References

1. Christopher LP, Yao B and Ji Y. Lignin biodegradation with laccase-mediator systems. *Frontiers in Energy Research* **2014**, *2*, 12.
2. Bugg TD and Rahmanpour R. Enzymatic conversion of lignin into renewable chemicals. *Current Opinion in Chemical Biology* **2015**, *29*, 10-17.
3. Munk L, Sitarz AK, Kalyani DC, Mikkelsen JD and Meyer AS. Can laccases catalyze bond cleavage in lignin? *Biotechnology Advances* **2015**, *33* (1), 13-24.
4. Areskog D, Li J, Gellerstedt G and Henriksson G. Investigation of the molecular weight increase of commercial lignosulfonates by laccase catalysis. *Biomacromolecules* **2010**, *11* (4), 904-910.
5. Lundquist K and Parkås J. Different types of phenolic units in lignins. *BioResources* **2011**, *6* (2), 920-926.
6. Huber D, Ortner A, Daxbacher A, Nyanhongo GS, Bauer W and Guebitz GM. Influence of oxygen and mediators on laccase-catalyzed polymerization of lignosulfonate. *ACS Sustainable Chemistry & Engineering* **2016**, *4* (10), 5303-5310.
7. Munk L, Punt AM, Kabel MA and Meyer AS. Laccase catalyzed grafting of N-OH type mediators to lignin via radical-radical coupling. *RSC Advances* **2017**, *7* (6), 3358-3368.
8. Bourbonnais R, Paice M, Reid I, Lanthier P and Yaguchi M. Lignin oxidation by laccase isozymes from *Trametes versicolor* and role of the mediator 2, 2'-azinobis (3-ethylbenzthiazoline-6-sulfonate) in kraft lignin depolymerization. *Applied and Environmental Microbiology* **1995**, *61* (5), 1876-1880.
9. Moya R, Saastamoinen P, Hernández M, Suurnäkki A, Arias E and Mattinen M-L. Reactivity of bacterial and fungal laccases with lignin under alkaline conditions. *Bioresource Technology* **2011**, *102* (21), 10006-10012.
10. Prasetyo EN, Kudanga T, Østergaard L, Rencoret J, Gutiérrez A, Del Río JC, Santos JI, Nieto L, Jiménez-Barbero J and Martínez AT. Polymerization of lignosulfonates by the laccase-HBT (1-hydroxybenzotriazole) system improves dispersibility. *Bioresource Technology* **2010**, *101* (14), 5054-5062.
11. Fernaud JRH, Carnicero A, Perestelo F, Cutuli MH, Arias E and Falcón MA. Upgrading of an industrial lignin by using laccase produced by *Fusarium proliferatum* and different laccase-mediator systems. *Enzyme and Microbial Technology* **2006**, *38* (1), 40-48.
12. Shleev S, Persson P, Shumakovich G, Mazhugov Y, Yaropolov A, Ruzgas T and Gorton L. Interaction of fungal laccases and laccase-mediator systems with lignin. *Enzyme and Microbial Technology* **2006**, *39* (4), 841-847.
13. Xia Z, Yoshida T and Funaoka M. Enzymatic synthesis of polyphenols from highly phenolic lignin-based polymers (lignophenols). *Biotechnology Letters* **2003**, *25* (1), 9-12.
14. Bourbonnais R, Paice MG, Freiermuth B, Bodie E and Borneman S. Reactivities of various mediators and laccases with kraft pulp and lignin model compounds. *Applied and Environmental Microbiology* **1997**, *63* (12), 4627-4632.
15. Bourbonnais R and Paice MG. Demethylation and delignification of kraft pulp by *Trametes versicolor* laccase in the presence of 2, 2'-azinobis-(3-ethylbenzthiazoline-6-sulphonate). *Applied Microbiology and Biotechnology* **1992**, *36* (6), 823-827.
16. Couto SR and Herrera JLT. Industrial and biotechnological applications of laccases: a review. *Biotechnology Advances* **2006**, *24* (5), 500-513.
17. Bourbonnais R and Paice MG. Oxidation of non-phenolic substrates: an expanded role for laccase in lignin biodegradation. *FEBS Letters* **1990**, *267* (1), 99-102.
18. Baiocco P, Barreca AM, Fabbri M, Galli C and Gentili P. Promoting laccase activity towards non-phenolic substrates: a mechanistic investigation with some laccase-mediator systems. *Organic & Biomolecular Chemistry* **2003**, *1* (1), 191-197.
19. Muheim A, Fiechter A, Harvey PJ and Schoemaker HE. On the mechanism of oxidation of non-phenolic lignin model compounds by the laccase-ABTS couple. *Holzforschung* **1992**, *46* (2), 121-126.
20. Eggert C, Temp U, Dean JFD and Eriksson K-EL. A fungal metabolite mediates degradation of non-phenolic lignin structures and synthetic lignin by laccase. *FEBS Letters* **1996**, *391* (1), 144-148.

21. Astolfi P, Brandi P, Galli C, Gentili P, Gerini MF, Greci L and Lanzalunga O. New mediators for the enzyme laccase: mechanistic features and selectivity in the oxidation of non-phenolic substrates. *New Journal of Chemistry* **2005**, 29 (10), 1308-1317.
22. Kawai S, Nakagawa M and Ohashi H. Aromatic ring cleavage of a non-phenolic β -O-4 lignin model dimer by laccase of *Trametes versicolor* in the presence of 1-hydroxybenzotriazole. *FEBS Letters* **1999**, 446 (2-3), 355-358.
23. Kawai S, Asukai M, Ohya N, Okita K, Ito T and Ohashi H. Degradation of a non-phenolic β -O-4 substructure and of polymeric lignin model compounds by laccase of *Coriolus versicolor* in the presence of 1-hydroxybenzotriazole. *FEMS Microbiology Letters* **1999**, 170 (1), 51-57.
24. Kawai S, Umezawa T, Shimada M and Higuchi T. Aromatic ring cleavage of 4,6-di-(tert-butyl)-guaiaicol, a phenolic lignin model compound, by laccase of *Coriolus versicolor*. *FEBS Letters* **1988**, 236 (2), 309-311.
25. Kawai S, Umezawa T and Higuchi T. Degradation mechanisms of phenolic β -1 lignin substructure model compounds by laccase of *Coriolus versicolor*. *Archives of Biochemistry and Biophysics* **1988**, 262 (1), 99-110.
26. Areskog D, Li J, Nousiainen P, Gellerstedt G, Sipilä J and Henriksson G. Oxidative polymerisation of models for phenolic lignin end-groups by laccase. *Holzforschung* **2010**, 64 (1), 21-34.
27. Rittstieg K, Suurnäkki A, Suortti T, Kruus K, Guebitz GM and Buchert J. Polymerization of guaiacol and a phenolic β -O-4 substructure by *Trametes hirsuta* laccase in the presence of ABTS. *Biotechnology Progress* **2003**, 19 (5), 1505-1509.
28. Potthast A, Rosenau T, Koch H and Fischer K. The reaction of phenolic model compounds in the laccase-mediator system (LMS) investigations by matrix assisted laser desorption ionization time-of-flight mass spectrometry (MALDI-TOF-MS). *Holzforschung* **1999**, 53 (2), 175-180.
29. Johannes C and Majcherczyk A. Laccase activity tests and laccase inhibitors. *Journal of Biotechnology* **2000**, 78 (2), 193-199.
30. Ramalingam B, Sana B, Seayad J, Ghadessy FJ and Sullivan MB. Towards understanding of laccase-catalysed oxidative oligomerisation of dimeric lignin model compounds. *RSC Advances* **2017**, 7 (20), 11951-11958.
31. Li K, Helm RF and Eriksson KEL. Mechanistic studies of the oxidation of a non-phenolic lignin model compound by the laccase/1-hydroxybenzotriazole redox system. *Biotechnology and Applied Biochemistry* **1998**, 27 (3), 239-243.
32. Sealey J and Ragauskas AJ. Investigation of laccase/N-hydroxybenzotriazole delignification of kraft pulp. *Journal of Wood Chemistry and Technology* **1998**, 18 (4), 403-416.
33. Matsumura E, Yamamoto E, Numata A, Kawano T, Shin T and Murao S. Structures of the laccase-catalyzed oxidation products of hydroxy-benzoic acids in the presence of ABTS [2,2'-Azino-di-(3-ethylbenzothiazoline-6-sulfonic acid)]. *Agricultural and Biological Chemistry* **1986**, 50 (5), 1355-1357.
34. Osman A, Wong K and Fernyhough A. ABTS radical-driven oxidation of polyphenols: Isolation and structural elucidation of covalent adducts. *Biochemical and Biophysical Research Communications* **2006**, 346 (1), 321-329.
35. Cañas AI and Camarero S. Laccases and their natural mediators: biotechnological tools for sustainable eco-friendly processes. *Biotechnology Advances* **2010**, 28 (6), 694-705.
36. Bourbonnais R, Leech D and Paice MG. Electrochemical analysis of the interactions of laccase mediators with lignin model compounds. *Biochimica et Biophysica Acta (BBA)-General Subjects* **1998**, 1379 (3), 381-390.
37. Fabbrini M, Galli C and Gentili P. Comparing the catalytic efficiency of some mediators of laccase. *Journal of Molecular Catalysis B: Enzymatic* **2002**, 16 (5), 231-240.

2.6 Supporting Information

2.6.1 Laccase purification and activity determination

The crude laccase (3.7 g, 2.17% protein as determined by DUMAS using the method described by Teuling et al.¹) was partially purified using anion-exchange chromatography with a 260 mL DEAE-Sepharose column. Elution was carried out with a sodium phosphate buffer (pH 6.0, linear gradient from 0 to 1 M NaCl over 20 column volumes, 27 mL min⁻¹). The fractions with high laccase activity were pooled, desalted and concentrated using Amicon Ultra centrifugal filters with a cut-off of 10 kDa (Merck Millipore) to give a blue enzyme solution. The activity of the laccase was determined spectrophotometrically by oxidation of ABTS.¹⁷ A 1 mL quartz cuvette was filled with 0.5 mM ABTS in a sodium acetate buffer (pH 5, 100 mM). A solution of laccase was added and the increase in absorbance at 420 nm was monitored over time ($\epsilon = 36000 \text{ M}^{-1} \text{ cm}^{-1}$). The laccase activity was expressed in units (1 U = 1 μmol ABTS oxidized per minute).

2.6.2 RP-UHPLC-PDA analysis

Reaction products were separated using an Accela UHPLC system (Thermo Scientific, San Jose, CA, USA) equipped with a pump, degasser, autosampler and photodiode array (PDA) detector. Samples (5 μL) were injected onto an Acquity UPLC BEH C18 column (150 x 2.1 mm, particle size 1.7 μm) (Waters, Milford, MA, USA). The flow rate was 400 $\mu\text{L min}^{-1}$ at 45 °C. Water (A) and acetonitrile (B) were used as eluents, both acidified with 0.1% formic acid. The following gradient was used: 0-1.5 min at 5% B (isocratic), 1.5-47 min from 5 to 35% B (linear gradient), 47-48 min from 35 to 99% B (linear gradient), 48-53 min at 99% B (isocratic), 53-54 min from 99 to 5% B (linear gradient) and 54-59 min at 5% B (isocratic). The PDA detector was set to record wavelengths between 200 and 700 nm.

2.6.3 Electrospray Ionization – Ion Trap Mass Spectrometry (ESI-ITMS)

Mass spectrometric data were obtained using an LTQ Velos Pro mass spectrometer (Thermo Scientific) equipped with a heated ESI probe coupled to the UHPLC system. Nitrogen was used as sheath gas and auxiliary gas. Data were collected in both positive and negative ionization mode over the m/z range 120-2.000. Data dependent MS2 analysis was performed using collision-induced dissociation with a normalized collision energy of 35%. The system was tuned using LTQ Tune Plus 2.7 (Thermo Scientific) upon direct injection of GBG in both positive and negative ionization mode. The ion transfer tube temperature was 300 °C, source heater temperature was 250 °C and the source voltage was 3.5 kV. Data were processed using Xcalibur 2.2 (Thermo Scientific).

2.6.4 Electrospray Ionization – Fourier Transform Mass Spectrometry (ESI-FTMS) (accurate mass determination)

For accurate mass determination, reaction products were separated using a Vanquish UHPLC system (Thermo Scientific). The same samples were used as for ESI-IT-MS, after a 10-fold further dilution in MilliQ water. The injection volume was 1 μL . The column, eluents and gradient were identical to those described for RP-UHPLC-PDA analysis. The column compartment heater was set to 45 $^{\circ}\text{C}$, the eluent preheater was set to 45 $^{\circ}\text{C}$ and the post-column cooler was set to 40 $^{\circ}\text{C}$. A Thermo Q Exactive Focus hybrid quadrupole-orbitrap mass spectrometer (Thermo Scientific) equipped with a heated ESI probe coupled to the Vanquish RP-UHPLC system was used to acquire accurate mass data. Half of the flow was directed toward the MS. Full MS data were recorded in both negative and positive ionization mode over a range of m/z 100-1500 at a resolution of 70000. The mass spectrometer was calibrated in both positive and negative mode using Tune 2.8 software (Thermo Scientific) by direct infusion of Pierce LTQ ESI positive and negative ion calibration solutions (Thermo Scientific). Nitrogen was used as sheath gas (30 arbitrary units) and auxiliary gas (20 arbitrary units). The capillary temperature was 320 $^{\circ}\text{C}$; the probe heater temperature was 280 $^{\circ}\text{C}$; the source voltage was 2.8 kV; and the S-lens RF level was 50. Data processing was done using Xcalibur 2.2 (Thermo Scientific) and Compound Discoverer 2.0 (Thermo Scientific). Molecular formulas of reaction products were determined with a set of requirements unique for each incubation. In incubations with GBG and laccase alone, the determination of molecular formulas was restricted to C, H and O atoms, and a maximum mass error of 5 ppm. In the case of GBG with laccase and HBT, also nitrogen atoms were allowed, with a maximum of 6 N atoms per molecule. For GBG with laccase and ABTS, nitrogen and sulfur were included, with a maximum of 8 N and S atoms per molecule. In all cases, this led to a list of candidates, with only one plausible formula.

2.6.5 Matrix-Assisted Laser Desorption Ionization – Time Of Flight Mass Spectrometry (MALDI-TOF-MS)

Spots were prepared by mixing 1 μL DHB with 1 μL sample on a MTP 384 ground steel target plate (Bruker Daltonics). Drying was accelerated using a hairdryer. Mass spectra (m/z 500-3500) were obtained in positive mode using an Ultraflextreme workstation (Bruker Daltonics), equipped with a Smartbeam II laser of 355 nm. A laser intensity of 30-40 % was used with ion source voltages of 20.00 and 17.86 kV, reflector voltages of 20.96 and 10.84 kV and a lens voltage of 7.59 kV. The system was calibrated using maltodextrin.

Table S2.1 Reaction products detected in trace amounts with RP-UHPLC-MS after incubation of GBG with laccase in presence or absence of HBT. These products were absent in incubations containing ABTS.

RT (min)	Tentative annotation	Mol. formula	Ion	Observed/ calculated mass	Mass error (ppm)	MS ² fragments	Incubation
33.8	Unknown	C ₃₃ H ₃₄ O ₁₃	[M-H] ⁻	638.20003/ 638.19995	0.13	453, 441	Lac, Lac/HBT
34.0	Unknown	C ₃₃ H ₃₄ O ₁₃	[M-H] ⁻	638.20003/ 638.19995	0.13	453, 441	Lac, Lac/HBT
37.3	Unknown	C ₃₃ H ₃₄ O ₁₂	[M-H] ⁻	622.20457/ 622.20503	-0.58	573, 497, 467	Lac, Lac/HBT
37.7	GBG dimer (isomer)	C ₃₄ H ₃₈ O ₁₂	[M+FA] ⁻ [M-H] ⁻	638.23720/ 638.23633	1.37	637 589, 465, 483, 513, 435, 359, 329	Lac, Lac/HBT
37.6	Unknown	C ₃₃ H ₃₄ O ₁₂	[M-H] ⁻	622.20457/ 622.20503	-0.58	573, 497, 467	Lac, Lac/HBT
40.2	C ₆ -oxidized GBG dimer*	C ₃₄ H ₃₆ O ₁₂	[M-H] ⁻	636.22054/ 636.22068	-0.22	587, 605, 557	Lac, Lac/HBT
46.8	Unknown	C ₅₂ H ₅₆ O ₂₀	[M-H] ⁻	1000.33858/ 1000.33650	0.61	953, 775, 757, 935, 727, 829	Lac, Lac/HBT

* The oxidized dimer may be formed via radical hydrogen abstraction at one of the benzylic positions of the GBG dimer shown in Fig. 2.3. The oxidant is proposed to be a phenoxyl radical of GBG or a phenoxyl radical of a GBG oligomer.

Table S2.2 Reaction products of GBG detected with RP-UHPLC-ITMS after incubation with ABTS^{•+}, which are not already shown in Table 2.1 and Fig. 2.3.

RT (min)	Tentative annotation	Ion	m/z	MS ² fragments
19.0	GBG-ABTS CPI	[M-3H] ²⁻ [M-2H] ⁻	415 831	574, 228, 256
39.7	GBG dimer _{ox}	[M-H] ⁻	635	587, 605, 481, 451, 511, 557

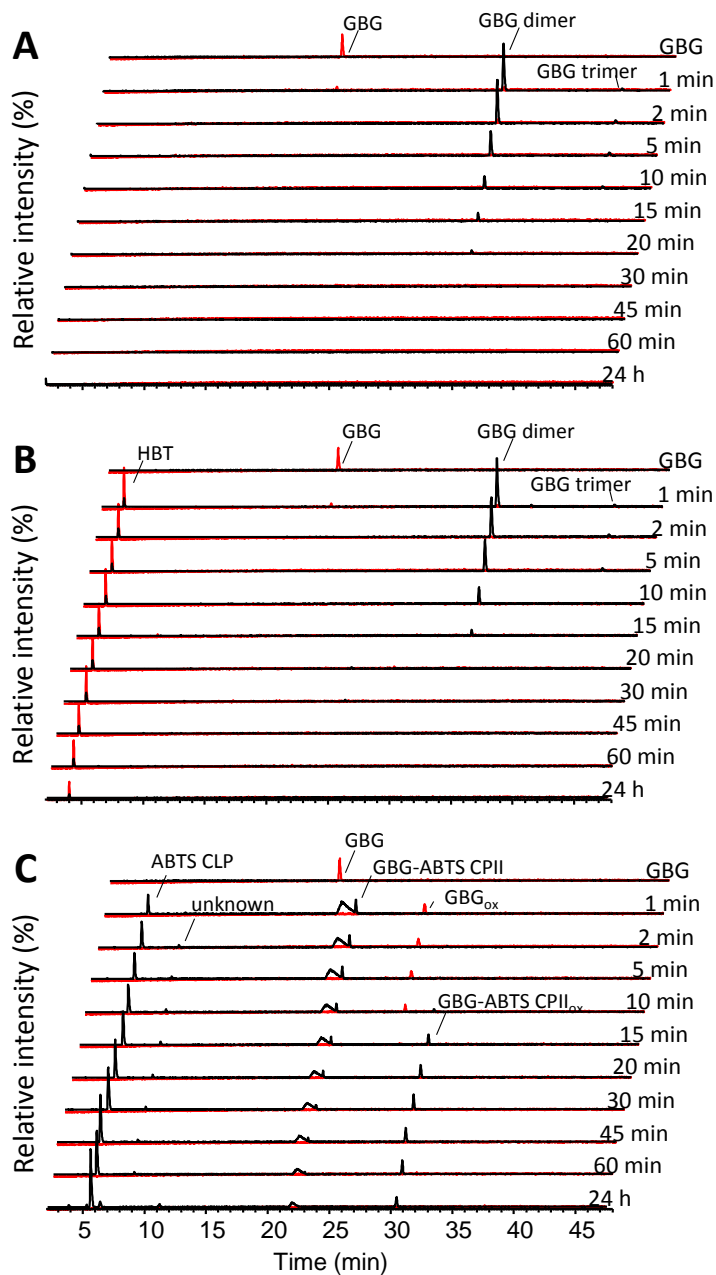


Fig. S2.1 UHPLC-MS chromatograms in time of GBG incubations with laccase (A), laccase/HBT (B) and laccase/ABTS (C) measured in positive (red) and negative ionization mode (black).

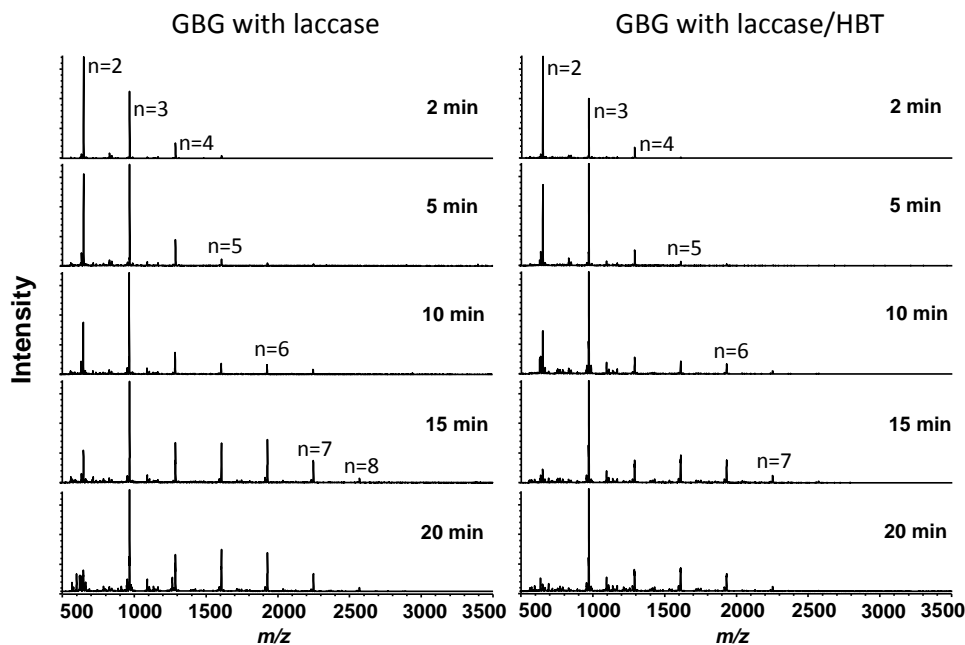


Fig. S2.2 MALDI-TOF-MS analysis of GBG incubated with laccase alone (left) and laccase/HBT (right). Both incubations resulted in oligomerization of GBG. All annotated peaks corresponded to Na^+ adducts of GBG oligomers, with n =the degree of polymerization.

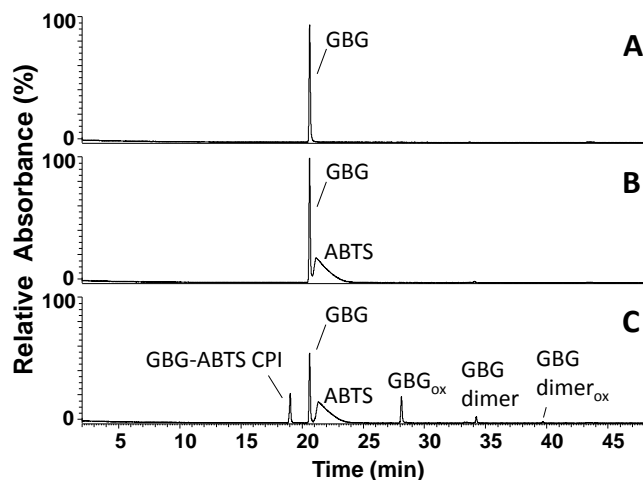


Fig. S2.3 RP-UHPLC-UV chromatograms (280 nm) of GBG (A), GBG incubated with ABTS (B) and GBG incubated with ABTS^+ (C). Annotations of GBG-ABTS CPI and GBG dimer_{ox} can be found in Table S2 and Fig. S2.3.

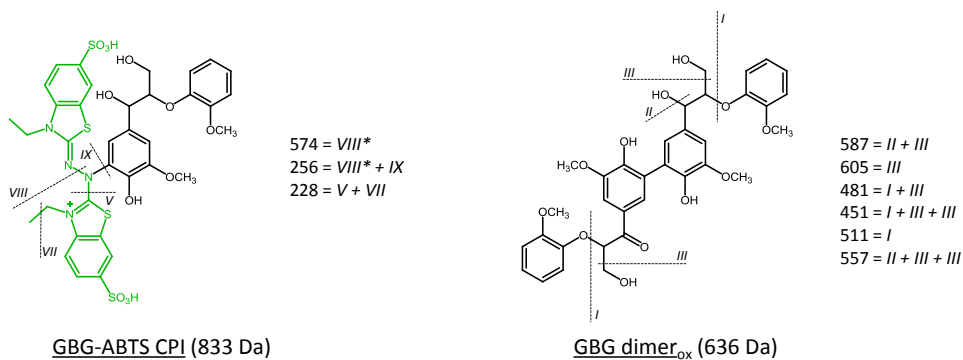


Fig. S2.4 Proposed structures and MS² fragmentation pathways of reaction products of GBG after incubation with ABTS⁺, which are not already shown in Table 2.1 and Fig. 2.3. Fragmentations with an * are suggested to be radical fragmentations.

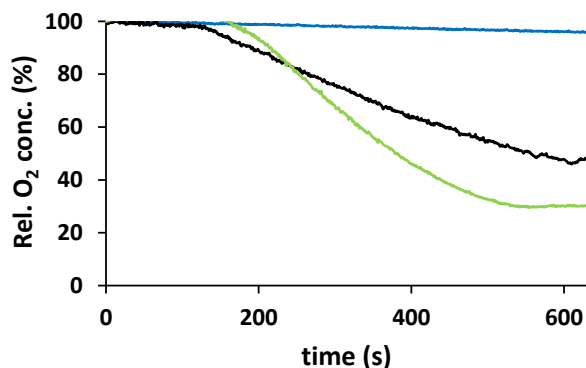
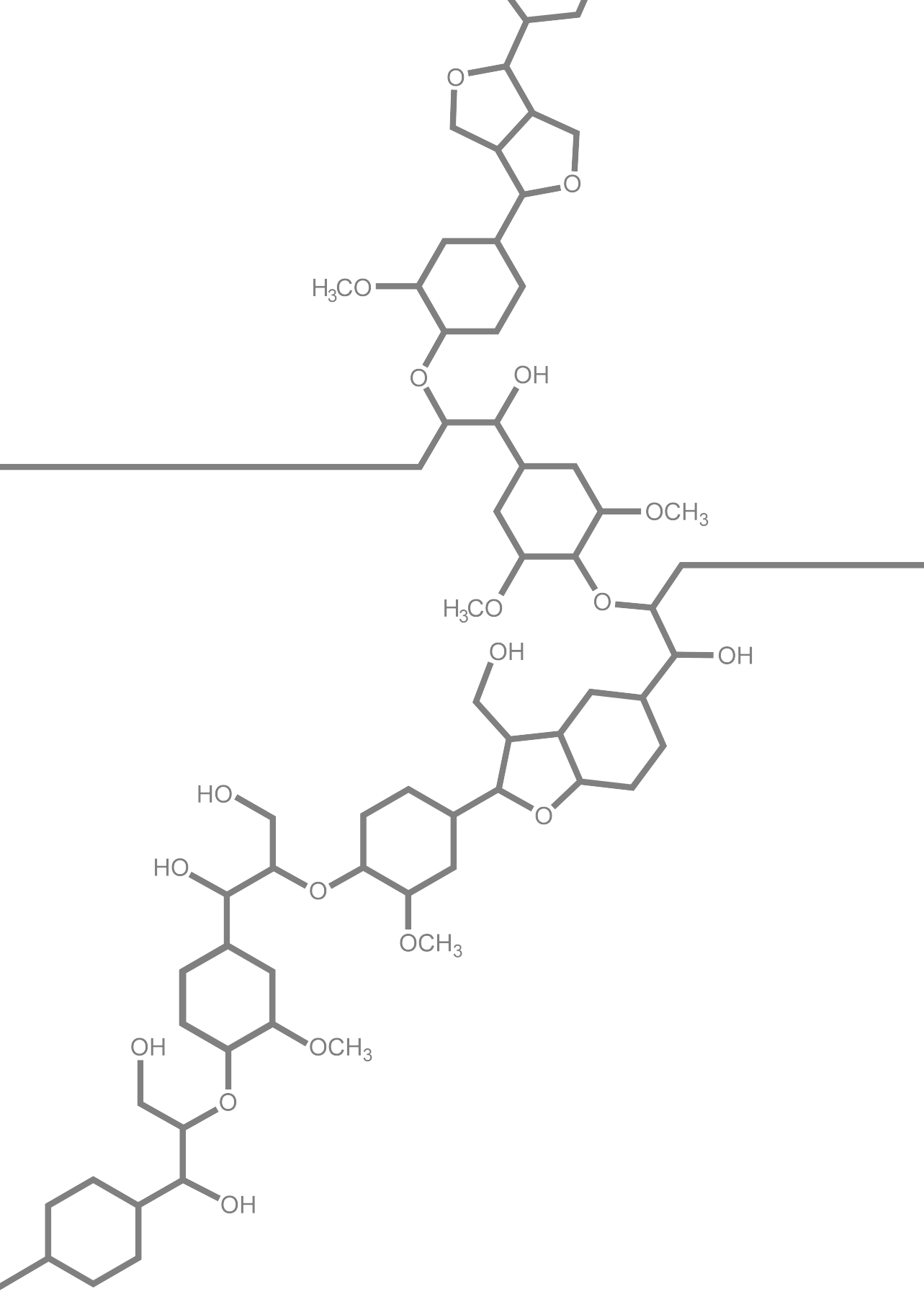


Fig. S2.5 Oxygen consumption of GBG (black), ABTS (green) and HBT (blue) incubated with 1 U mL⁻¹ laccase. Oxygen consumption was measured using an Oxytherm System (Hansatech Kings Lynn, UK). GBG, HBT and ABTS were used as substrates at 1 mM in a sodium phosphate buffer (50 mM) at pH 4. After equilibration, laccase was added to obtain an activity of 1 U mL⁻¹. Incubations were performed in a total volume of 1 mL at 25 °C. Data acquisition was performed using Oxygraph Plus software (Hansatech).

References Supporting Information

- Teuling E, Schrama JW, Gruppen H and Wierenga PA. Effect of cell wall characteristics on algae nutrient digestibility in Nile tilapia (*Oreochromis niloticus*) and African catfish (*Clarus gariepinus*). *Aquaculture* **2017**, 479, 490-500.



The impact of lignin sulfonation on its reactivity with laccase and laccase/HBT

Lignin is a highly abundant aromatic polymer in nature, but its controlled cleavage or cross-linking is a major challenge and currently hindering industrial applicability. Laccase (L) and laccase/mediator systems (LMS) are promising tools for enzymatic lignin modification, but to date, their overall reaction outcome is hard to predict and control. This research aimed to understand the reactivity of native and sulfonated β -O-4' linked lignin structures in L and LMS treatments. *Trametes versicolor* laccase, and the mediator hydroxybenzotriazole (HBT) were used, and reaction products were analyzed using UHPLC-MSⁿ and MALDI-TOF-MS. Polymerization was observed for both the native and sulfonated phenolic compounds, suggesting that sulfonation does not affect radical coupling of the phenolic lignin subunits. In contrast, sulfonation of the *non*-phenolic lignin structure prevented C_α-oxidation and cleavage by L/HBT, which was explained by an increased C_α-H bond dissociation energy of ~10 kcal/mol upon sulfonation. Overall, our results indicate that lignin sulfonation drives the overall outcome of LMS incubations towards polymerization.

Based on: Roelant Hilgers, Megan Twentyman-Jones, Annemieke van Dam, Harry Gruppen, Han Zuilhof, Mirjam A. Kabel and Jean-Paul Vincken. The impact of lignin sulfonation on its reactivity with laccase and laccase/HBT. *Catalysis Science & Technology* **2019**, 9 (6), 1535-1542.

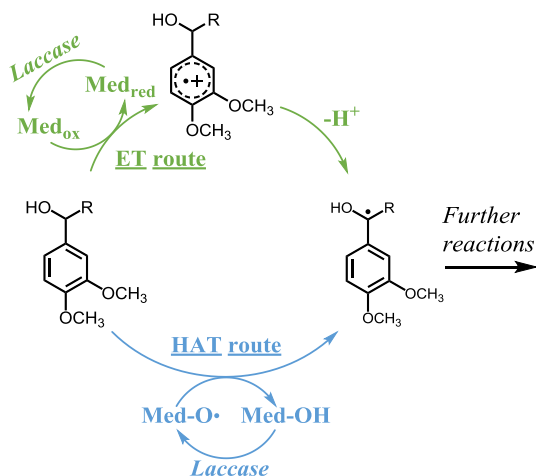
3.1 Introduction

Lignin is one of the main polymeric constituents of plant cell walls and is considered a renewable precursor for chemicals and materials.¹⁻⁴ Plants synthesize lignin via radical coupling of the precursors sinapyl alcohol, coniferyl alcohol and *p*-coumaroyl alcohol (S, G and H units, respectively). Upon polymerization, a variety of C-C and C-O interunit linkages is formed, of which the β -O-4' linkage is the most abundant one, accounting for 45-94% of the total interunit linkages.³ Polymeric lignin consists of 10-30% phenolic subunits, mainly being the endcaps of the polymer, and 70-90% non-phenolic subunits, forming the lignin backbone.⁵

Currently, lignin is still underutilized in industrial applications. Depending on the intended application, lignin can be valorized via different routes, such as polymerization, depolymerization and grafting.⁶⁻⁸ Preferably, valorization should occur via sustainable approaches, such as enzymatic modifications. One of the few enzymes known to be active toward lignin is laccase (E.C. 1.10.3.2), an oxidase that couples the reduction of molecular oxygen to the one-electron oxidation of a wide variety of aromatic substrates. Laccases have relatively low redox potentials: the most powerful laccases, produced by white-rot fungi, have redox potentials up to 800 mV vs. NHE.³ In contrast, the non-phenolic subunits have redox potentials up to 1500 mV vs. NHE and are, therefore, recalcitrant to oxidation by laccase alone.⁹ Consequently, laccases can only oxidize the phenolic subunits of lignin. Nevertheless, when laccase is combined with a mediator, also the non-phenolic lignin structures can be oxidized.¹⁰ In such a laccase/mediator system (LMS), laccase oxidizes the mediator, which, in turn, can react with a non-phenolic lignin subunit, via different mechanisms, dependent on the mediator. Among the most widely used mediators are the synthetic compounds HBT and ABTS, but also small lignin-derived phenolic compounds, such as syringaldehyde and methyl syringate.¹¹⁻¹⁸ HBT and natural phenolics have been reported to oxidize non-phenolic lignin subunits via a radical hydrogen atom transfer (HAT) mechanism, whereas ABTS is suggested to operate via electron transfer (ET) (**Scheme 3.1**).¹⁹ In the HAT mechanism, the oxidized mediator is generally an oxygen centered radical species that abstracts a radical hydrogen atom from the benzylic position of the lignin structure, forming back the non-radical mediator species and a benzylic radical. The efficiency of this reaction depends on the bond dissociation energies (BDEs) of the mediator O-H bond and the lignin C_α-H bond. In contrast, in the ET mechanism, the mediator is an oxidized species that abstracts an electron from the lignin structure, forming back the reduced mediator species and a radical cation. The radical cation then spontaneously loses a proton to form a benzylic radical. The efficiency of the ET reaction depends on the redox potentials of the mediator and the lignin structure.²⁰ After oxidation by laccase or LMS, lignin may undergo a variety of follow-up reactions, such as radical coupling, C_α-oxidation and cleavage reactions.

In literature, LMS incubations on lignin are studied in several ways and with several purposes: (i) on biomass or pulp, in order to degrade lignin and increase the yield of

saccharification of the polysaccharides present, and (ii) on technical lignins, in order to upgrade their structure for various applications. Among the technical lignins, lignosulfonate is by far the most available one,²¹ and is, therefore, an interesting target for lignin valorization. The main difference between native lignin and lignosulfonate is that the majority of C₆-positions in lignosulfonate are substituted by a sulfonate group instead of a hydroxyl group. Lignosulfonate and native lignin also seem to differ regarding their reactions in the presence of LMS. So far, LMS incubations with lignosulfonate have only been reported to result in polymerization, whereas comparable LMS treatments mainly led to depolymerization and C₆-oxidation of native lignin.³ Currently, it is unknown why these substrates react in such a different manner in LMS incubations. This is partly due to the fact that the reaction pathways of LMS-induced lignin modifications have mainly been studied using lignin model compounds that resemble the structural motifs of native lignin. The information obtained via these studies, although valuable, cannot directly be extrapolated to reactions of lignosulfonate, due to the large degree of C₆-sulfonation in the latter. To date, it remains unknown whether and how C₆-sulfonation influences the reactivity of lignin structures. To be able to predict or even control the reaction outcome of LMS incubations of lignin and lignosulfonate in the future, it is essential to understand how their structural features influence the reactivity with laccase and LMS.



Scheme 3.1 Mechanisms of ET and HAT oxidation routes in laccase/mediator systems. A non-phenolic lignin model is used as an example substrate. Adapted from Baiocco et al.¹⁹

Therefore, in this study, we compared the reactivity of two types of lignin model compounds in laccase and laccase/HBT incubations: one type representing the structure of native lignin, and the other type representing the structure of lignosulfonate. To mimic native lignin, two β -O-4' linked lignin model compounds were used. Guaiacylglycerol- β -guaiacyl ether (GBG; 1-(4-hydroxy-3-methoxyphenyl)-2-(2-methoxyphenoxy)propane-

1,3-diol) was used to mimic the phenolic lignin end caps, and veratrylglycerol- β -guaiacyl ether (VBG; 1-(3,4-dimethoxyphenyl)-2-(2-methoxyphenoxy)propane-1,3-diol) was used to mimic the non-phenolic lignin backbone (**Fig. 3.1**). Their sulfonated analogues SGBG (3-hydroxy-1-(4-hydroxy-3-methoxyphenyl)-2-(2-methoxyphenoxy)propane-1-sulfonic acid) and SVBG (1-(3,4-dimethoxyphenyl)-3-hydroxy-2-(2-methoxyphenoxy)propane-1-sulfonic acid) (**Fig. 3.1**) were synthesized and used to mimic the end caps and backbone of lignosulfonate. We picked HBT as a mediator for two reasons: (i) It has been widely used in LMS incubations of both native lignin and lignosulfonate,^{12,18,22-24} which enables a direct comparison between our model compound study and results reported for LMS incubations of polymeric lignins, and (ii) it operates via the HAT mechanism, which makes it possible to extrapolate our results to incubations with natural phenolics as mediators.

3.2 Materials & Methods

3.2.1 Materials

Guaiacylglycerol- β -guaiacyl ether (GBG; **Fig. 3.1**) was obtained from TCI chemicals (Tokyo, Japan), veratrylglycerol- β -guaiacyl ether (VBG; **Fig. 3.1**) was purchased from ABCR (Karlsruhe, Germany) and 2,5-dihydroxybenzoic acid (DHB) was bought from Bruker Daltonics (Bremen, Germany). Laccase, HBT, ABTS, SPE cartridges and all other chemicals were purchased from Sigma Aldrich (St. Louis, MO, USA). Laccase was partially purified as described earlier,²⁵ after which the activity was determined spectrophotometrically by oxidation of ABTS (1 U = 1 μ mol ABTS oxidized per minute at pH 5). Water was prepared using a Milli-Q water purification system (Merck Millipore, Billerica, MA).

3.2.2 Sulfonation and purification of lignin model compounds

GBG was sulfonated by heating a GBG solution (20 mL, 2 mM) for 4 h at 130 °C in the presence of sodium bisulfite (3.5 M) at pH 2.5. Similarly, VBG was sulfonated by heating for 4 h at 150 °C and pH 1.5. Reactions were performed in a Monowave 400 microwave reactor (Anton Paar, Graz, Austria). Of both incubations, five batches were prepared, which were pooled afterwards. The sulfonated lignin model compounds were desalted and purified prior to use in experiments (see Supporting Information for details). To verify that the model compounds were sulfonated, the purified sulfonated compounds were analyzed by performing 2D HSQC and HMBC NMR spectroscopy (see Supporting Information for details). After sulfonation and purification, diastereomeric mixtures were obtained with an isomer ratio of 1:3 for both SGBG and SVBG, based on UHPLC-UV₂₈₀ peak areas.

3.2.3 Incubation of lignin model compounds with laccase and laccase/mediator systems

The phenolic model compounds, GBG and SGBG, were dissolved at 0.05 mM in sodium acetate buffer (50 mM, pH 4) with or without an equimolar concentration of HBT. Laccase

was added to reach a final substrate and mediator concentration of 0.04 mM and a laccase activity of 0.04 U mL⁻¹ in a total volume of 1 mL. The mixtures were incubated at 40 °C and 400 rpm in a thermomixer (Eppendorf, Hamburg, Germany). After 2, 5, 10, 20, 35 and 60 min, 100 µL of the incubation mixture was collected and 10 µL of 20 mM sodium azide was added to this aliquot to stop the reaction. Incubations with the non-phenolic model compounds, VBG and SVBG, were performed similarly, with the adaptations that the HBT concentration was 0.4 mM and the reactions were stopped after 1, 3, 6 and 24 h. The samples were centrifuged (10,000*g*, 5 min, 20 °C) and analyzed by using RP-UHPLC-PDA-MSⁿ. Incubations for MALDI-TOF-MS were performed similarly, with substrate and mediator concentrations of 0.4 mM and a laccase activity of 0.2 U mL⁻¹ in all incubations. Detailed descriptions of the RP-UHPLC-PDA-MSⁿ and MALDI-TOF-MS methods can be found in the Supporting Information. In addition, separate oxygen consumption measurements were performed using HBT, GBG and SGBG as substrates (see Supporting Information for details).

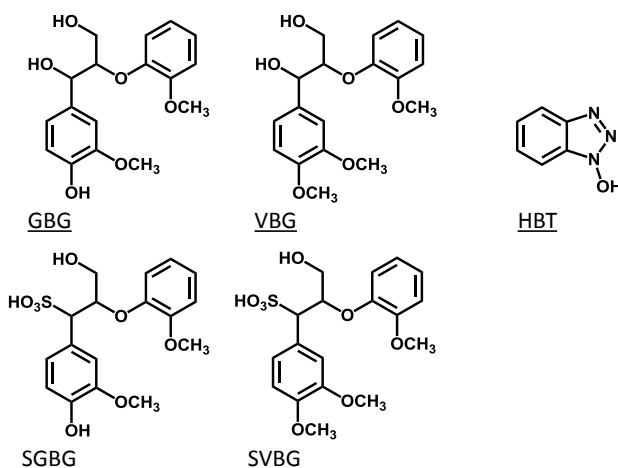


Fig. 3.1 Molecular structures of the lignin model compounds GBG, VBG, SGBG and SVBG, and the mediator HBT.

3.2.4 Computational analyses

All computational analyses were performed with the B97D functional and 6-311+G(d,p) basis set, as implemented in Gaussian 16 (version B1), using a SMD solvent model for water.²⁶

Homolytic C-H bond dissociation energies were calculated by elongating the desired C-H bond to 5 Å (in triplet state), and subtracting the single-point energy of this geometry from the (singlet) optimized geometry.

The ionization energy of all four compounds in the neutral state was determined as the difference between the single-point energies of the uncharged ground state and that of the corresponding radical cation in the geometry of the optimized neutral ground state.

3.3 Results

3.3.1 Reactions of phenolic lignin model compounds with laccase and laccase/HBT

The phenolic model compounds GBG and SGBG (**Fig. 3.1**) were first incubated with laccase in the absence of HBT. After oxidation by laccase, both GBG and SGBG underwent radical coupling to form dimers ($M_w=2\times\text{GBG}-2\text{H}$) (**Fig. 3.2**, **Fig. 3.3**, **Table 3.1** and **Fig. S3.5/S3.6/S3.9**). It should be noted that the GBG and SGBG dimers consist of four aromatic rings. From that perspective, they should be considered tetramers. Although dimerization may occur via either C-C or C-O coupling, dimerization of GBG resulted in only one clear peak. Based on previous research, this product was annotated as a C-C coupled GBG dimer.²⁷ A second GBG dimer peak was only present in trace amounts. This dimer showed a slightly different fragmentation pattern (**Fig. S3.10**) and was tentatively annotated as the C-O coupling product. A peak corresponding to a GBG trimer was also detected, especially after prolonged incubation times. Treatment of SGBG yielded several dimeric products, which were poorly separated by UHPLC. Due to the poor separation and relatively low intensity, the exact number of SGBG dimers formed was difficult to determine. Nevertheless, two areas of SGBG dimers could be distinguished in the chromatogram (region A and B in **Fig. 3.2E**), which showed slightly different fragmentation patterns (**Fig. S3.11**).

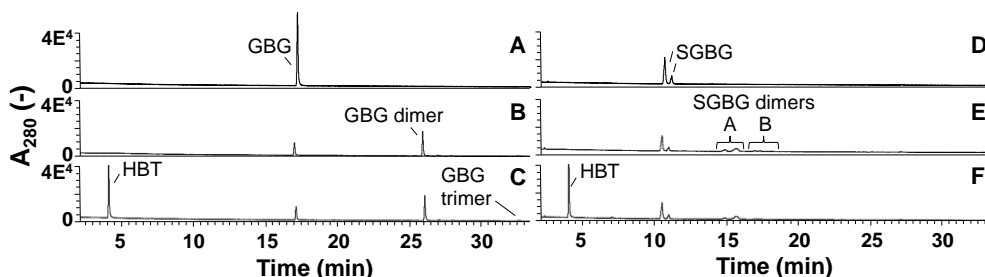


Fig. 3.2 RP-UHPLC-UV280 chromatograms of GBG (A-C) and SGBG (D-F) incubated for 2 min without laccase (A and D), with laccase alone (B and E) and laccase/HBT (C and F). Note that the substrate SGBG was used as a diastereomeric mixture, resulting in two chromatographic peaks. Chromatograms of other time points can be found in the Supporting Information.

It was speculated that region A, containing the major SGBG dimer peaks, corresponded to C-C coupling products, and that region B, containing the minor SGBG peaks, corresponded to C-O coupling products. Within the two areas, multiple peaks were present, which can be explained by the fact that the SGBG substrate was a mixture of two diastereomers. Upon coupling, the number of diastereomers is increased, resulting in a more complex mixture of reaction products. In addition to dimers, also oligomeric reaction products were detected, by using MALDI-TOF-MS (**Fig. S3.12/S3.13**). Although laccase treatment of other phenolic lignin models has been reported to result in C_0 -oxidized products,²⁸ no indications for this were found in the present study.

Prolonged incubation of GBG (>60 min) was also tested, but mainly resulted in precipitation of the reaction products. Upon incubation of GBG and SGBG with the laccase/HBT system, the same dimers and oligomers, as were formed in the incubations with laccase alone, were found. In addition, trace amounts of coupling products between substrates and HBT were detected (GBG-HBT and SGBG-HBT) (**Table 3.1** and **Fig. S3.9**). An overview of the major reaction pathways of GBG and SGBG in laccase and laccase/HBT incubations is shown in **Fig. 3.3**.

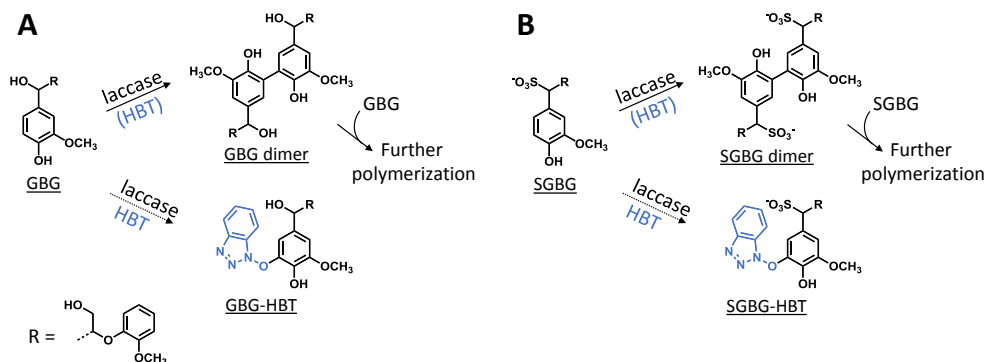


Fig. 3.3 Schematic representation of the outcomes of laccase and LMS incubations of GBG (A) and SGBG (B). The solid arrows show the major reaction pathway and the dotted arrows display the minor reaction pathway. Detailed information on identification of the compounds can be found in Table 3.1 and Fig. S3.9.

In addition to product formation, the substrate conversion was monitored over time (**Fig. 3.4**). In the absence of HBT, laccase converted 68% of the GBG and 52% of the SGBG in 2 min, based on UV₂₈₀ peak area. This indicated that laccase oxidizes GBG faster than SGBG. The same trends were observed for the laccase/HBT incubations: After 2 min, the laccase/HBT system converted 69% and 51% of GBG and SGBG, respectively.

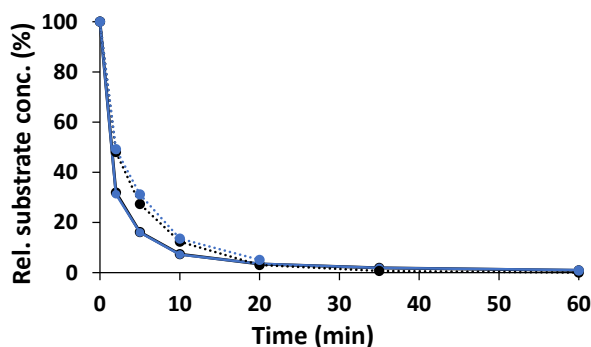


Fig. 3.4 Conversion of GBG (solid lines) and SGBG (dotted lines) in time by laccase (black) and laccase/HBT (blue). Rel. substrate conc. refers to the substrate concentration in the incubation relative to the substrate concentration at t=0.

Table 3.1 Compounds detected with RP-UHPLC-PDA-ESI-ITMS and RP-UHPLC-PDA-ESI-FTMS after incubation of the phenolic lignin model compounds GBG and SGBG with laccase from *T. versicolor* in the presence or absence of HBT. The MS² fragments are given with their relative abundance (%) in parentheses. When no fragment with an abundance of 100% is reported, the most abundant fragment ion was equal to the parent ion. Proposed fragmentation patterns can be found in Fig. S3.9.

Tent. annotat.	Mol. formula	RT (min)	Ion	Observed/calculated mass (Da)	Mass error (ppm)	MS ² fragments	λ_{\max} (nm)	Incub.
Reaction products of GBG								
GBG	C ₁₇ H ₂₀ O ₆	17.2	[M+Na] ⁺	320.12602/ 320.12599	0.11	295 (44), 302 (12), 147 (8), 201 (8), 219 (8)	277	Lac, Lac/HBT
GBG dimer	C ₃₄ H ₃₈ O ₁₂	26.0	[M-H] ⁻	638.23707/ 638.23633	1.17	589 (100), 483 (64), 513 (28), 435 (26), 329 (20), 541 (14), 465 (12), 359 (8)	277	Lac, Lac/HBT
Unknown	C ₂₄ H ₂₃ NO ₉	27.0	[M-H] ⁻	469.13765/ 469.13728	0.78	424 (100), 312 (38), 409 (36), 287 (26), 268 (16), 296 (14), 344 (12), 272 (8)	308	Lac, Lac/HBT
GBG trimer	C ₅₁ H ₅₆ O ₁₈	32.5	[M-H] ⁻	956.34718/ 956.34666	0.54	907 (100), 889 (52), 919 (26), 859 (18)	N.D.	Lac, Lac/HBT
GBG-HBT	C ₂₃ H ₂₃ N ₃ O ₇	19.7	[M-H] ⁻	453.15328/ 453.15360	-0.7	404 (100), 328 (42), 298 (38)	330	Lac/HBT
Reaction products of SGBG								
SGBG	C ₁₇ H ₂₀ O ₈ S	10.6, 11.1	[M-H] ⁻	384.08827/ 384.08789	1.00	259 (100), 179 (68), 203 (38), 165 (30), 229 (22), 195 (6)	276	Lac, Lac/HBT
SGBG dimers	C ₃₄ H ₃₈ O ₁₆ S ₂	15.0, 15.8, 17.1,	[M-2H] ²⁻	766.16073/ 766.16013	0.79	561 (100), 320 (64), 123 (24), 273 (20), 449 (16), 577 (18), 437 (10)	277	Lac, Lac/HBT
SGBG-HBT	C ₂₃ H ₂₃ N ₅ O ₉ S	15.2	[M-H] ⁻	517.11580 517.11550	0.56	312 (100), 392 (60), 298 (34), 203 (10)	332	Lac/HBT
HBT and related								
HBT	C ₆ H ₅ N ₃ O	3.8	[M-H] ⁻ [M+H] ⁺	135.04325/ 135.04325	-0.07	106 (100), 78 (6) 91 (32), 80 (30), 107 (20), 53 (18)	306, 276, 268	Lac/HBT
BT	C ₆ H ₅ N ₃	6.9	[M+H] ⁺	119.04827/ 119.04835	-0.65	N.D.	258, 280	Lac/HBT

3.3.2 Reactions of non-phenolic lignin model compounds with laccase and laccase/HBT

As expected, in incubations with laccase alone, no VBG and SVBG was converted (**Fig. 3.5**). In the laccase/HBT incubation, the native model compound VBG was mainly converted to its ketone analogue VBG_{ox}. In addition, small peaks corresponding to C₁₁H₁₄O₄ and C₁₂H₁₆O₄ were formed (**Fig. 3.5** and **3.6**, **Table 3.2**, **Fig. S3.15**). These peaks were tentatively annotated as cleavage products VBG CLP I and VBG CLP II, respectively. The former cleavage product is suggested to be formed via β ether cleavage, which has been reported before.^{29,30} The exact structure of VBG CLP II could not be elucidated. In contrast to their phenolic analogues, VBG and SVBG did not form coupling products with HBT, suggesting that coupling to HBT occurs at the aromatic ring rather than at the benzylic position. After 24 h, 47% of the VBG was converted, based on UV₂₈₀ peak area. In contrast, the laccase/HBT system was unable to convert SVBG. Even after 24 h, the areas of the SVBG peaks remained unchanged. A schematic overview of the incubation outcomes of VBG and SVBG is shown in **Fig. 3.6**.

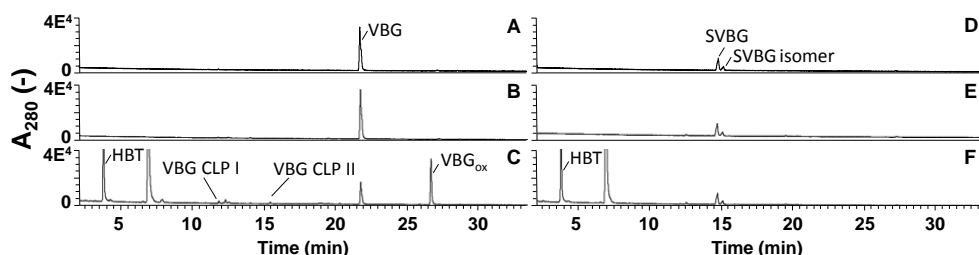


Fig. 3.5 RP-UHPLC-UV₂₈₀ chromatograms of VBG (A-C) and SVBG (D-F) incubated for 24 h without laccase (A and D), with laccase alone (B and E) and laccase/HBT (C and F). The unlabelled peaks correspond to degradation products of the mediator. Chromatograms of other time points can be found in the Supporting Information.

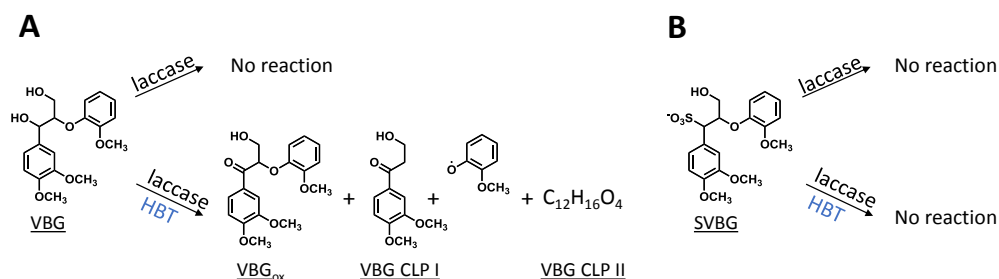


Fig. 3.6 Schematic representation of the outcomes of laccase and LMS incubations of VBG (A) and SVBG (B). Whereas VBG is oxidized by both LMS, SVBG is completely inert in all incubations. The structure of VBG CLP II (C₁₂H₁₆O₄) could not be elucidated.

Table 3.2 Compounds detected with RP-UHPLC-PDA-ESI-ITMS and RP-UHPLC-PDA-ESI-FTMS after incubation of the non-phenolic lignin model compounds VBG and SVBG with laccase from *T. versicolor* in the presence or absence of HBT. The MS² fragments are given with their relative abundance (%) in parentheses. When no fragment with an abundance of 100% is reported, the most abundant fragment ion was equal to the parent ion. Proposed fragmentation patterns can be found in Fig. S3.15.

Tent. annotat.	Mol. formula	RT (min)	Ion	Observed/calculated mass (Da)	Mass error (ppm)	MS ² fragments	λ_{\max} (nm)	Incub.
Reaction products of VBG								
VBG	C ₁₈ H ₂₂ O ₆	21.7	[M+Na] ⁺	334.14123/ 334.14164	1.21	309 (42), 215 (8), 147 (4), 233 (4)	276	Lac, Lac/HBT
VBG CLP I	C ₁₁ H ₁₄ O ₄	11.9	[M+H] ⁺	210.08920/ 210.08921	0.04	139 (100), 165 (20), 124 (10)	275, 303	Lac/HBT
VBG CLP II	C ₁₂ H ₁₆ O ₄	15.4	[M+H] ⁺ [M+Na] ⁺	224.10467/ 224.10486	-0.85	165 (100), 139 (18), 181 (8) N.D.	276, 308	Lac/HBT
VBG _{ox}	C ₁₈ H ₂₀ O ₆	26.6	[M+H] ⁺ [M+Na] ⁺	332.12563/ 332.12599	-1.08	149 (100), 167 (84), 285 (84), 165 (74), 181 (72), 209 (52), 177 (30), 303 (28), 121 (20), 192 (12) 325 (100), 232 (18), 201 (10)	279, 312	Lac/HBT
Reaction products of SVBG								
SVBG	C ₁₈ H ₂₂ O ₈ S	14.8, 15.1	[M-H] ⁻	398.10353/ 398.10354	-0.02	273 (100), 203 (20), 123 (18), 215 (18), 329 (8)	277	Lac, Lac/HBT
HBT and related								
HBT	C ₆ H ₅ N ₃ O	3.8	[M-H] ⁻ [M+H] ⁺	135.04325/ 135.04325	-0.07	106 (100), 78 (6) 91 (32), 80 (30), 107 (20), 53 (18)	306, 276, 268	Lac/HBT
BT	C ₆ H ₅ N ₃	6.9	[M+H] ⁺	119.04827/ 119.04835	-0.65	N.D.	258, 280	Lac/HBT

3.4 Discussion

3.4.1 The effect of sulfonation of phenolic lignin model compounds on their conversion by laccase and laccase/HBT

The reaction pathways of GBG and SGBG were highly similar. Both model compounds underwent oligomerization in the laccase and laccase/HBT incubations. Hence, sulfonation of the phenolic end caps in lignin does not affect their proneness to undergo radical coupling reactions. Thus, both native and sulfonated lignin may undergo polymerization when oxidized by laccase. The presence of HBT had only a minor effect on the reaction pathway (**Fig. 3.3**), which can be explained by the fact that laccase

oxidizes GBG and SGBG much faster than it oxidizes HBT (**Fig. S3.14**). Consequently, GBG and SGBG are already converted before a substantial amount of HBT is oxidized. Laccase converted SGBG more slowly than it converted GBG. The conversion rate of phenolic substrates by laccase has been reported to be dependent on the difference in redox potentials of the laccase and the substrate.³¹ To check whether the sulfonation may have affected the redox potential of the phenolic model compounds, we calculated their ionization energies in water using B97D/6-311+G(d,p) calculations and an SMD solvent model for water (**Table 3.3**). As the ionization energies of GBG and SGBG are very similar, it is unlikely that the lower conversion rate of SGBG as compared to GBG is due to different redox properties of the compounds. An alternative explanation might be that the sulfonation decreases the affinity of the substrate for the active site of the laccase. It has been reported that the substrate binding cavity of a laccase from *T. versicolor*, is dominated by negative charges.³² As the sulfonic acid group on SGBG is also negatively charged, electrostatic repulsion may occur, resulting in a lower binding affinity and, consequently, to a lower conversion rate.

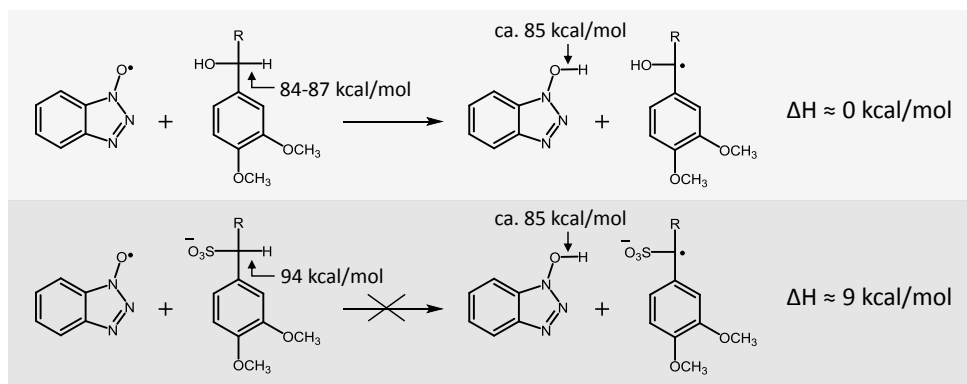
3.4.2 The effect of sulfonation of non-phenolic lignin model compounds on their reactions by laccase/HBT

Whereas laccase/HBT slowly converted VBG to both its ketone analogue and cleavage products, it was unable to convert SVBG. Since in a laccase/HBT system oxidation of the substrate by the mediator occurs via a HAT mechanism,¹⁹ the reaction is dependent on the difference in bond dissociation energy (BDE) between the O-H bond of HBT and the C_α-H bond in the lignin model compound. In order to explain the difference in reactivity of VBG and SVBG, we calculated the C_α-H BDE of both molecules (**Table 3.3**). As can be observed, the C_α-H BDE of SVBG (94 kcal/mol) is substantially higher than that of VBG (87 kcal/mol), indicating that radical hydrogen abstraction is less favourable in the sulfonated structure. According to literature, the BDE of the O-H bond in HBT is approximately 85 kcal/mol.³³

Table 3.3 Calculated ionization energies in water (IE) and C_α-H bond dissociation energies (BDE) of the model compounds used. N.D. = Not determined.

	C _α -H BDE (kcal/mol)	IE (kcal/mol)
GBG	84	121
SGBG	94	118
VBG	87	N.D.
SVBG	94	N.D.

As this value is in the same range as that of VBG, it seems plausible that radical hydrogen abstraction by the HBT radical can occur in the case of VBG. In contrast, the BDE of SVBG is too high for the HBT radical to abstract a radical hydrogen atom, making it inert to the laccase/HBT system, in line with our experiments (**scheme 3.2**).



Scheme 3.2 Sulfonation of lignin structures increases the C_α-H BDE, and thereby makes non-phenolic lignin structures inert to conversion by the laccase/HBT system.

3.4.3 Sulfonation of lignin polymers: implications for reactivity with laccase and LMS

Several studies have investigated the effect of laccase and LMS on polymeric lignin, and both polymerization and depolymerization have been reported as outcomes.³ It has been suggested that polymerization and depolymerization are in competition with each other, and that this competition may be influenced by reaction conditions and the presence of mediators.³ Obviously, the final outcome of this competition is dependent on the reactions of both the phenolic and non-phenolic structures in lignin. It is a general trend that the activity of laccase alone leads to lignin polymerization, whereas the activity of LMS leads to depolymerization.³ This can be rationalized, as laccase alone can only oxidize the phenolic subunits, which tend to undergo radical coupling, leading to lignin polymerization. LMS also oxidizes the non-phenolic structures, which generally leads to C_α-oxidation or bond cleavage.

Remarkably, when lignosulfonate is used as a substrate, both laccase and LMS incubations are shown to induce polymerization.^{4,6,22,23,34} To date, there was no mechanistic explanation for this observation, since the effects of laccase and LMS have only been investigated on polymeric lignosulfonate. These studies reported changes in molecular weight or overall changes in chemical structure, but did not describe detailed reaction pathways. To overcome this knowledge gap, in the present study, we used phenolic and non-phenolic sulfonated lignin model compounds. This enabled us to rationalize the observation that lignosulfonate is polymerized by both laccase and LMS: Polymerization, which generally occurs upon oxidation of phenolic lignin subunits, can

still occur when lignin is sulfonated. In contrast, cleavage of the β -O-4' bond, which generally occurs upon oxidation of non-phenolic lignin subunits, is impaired after sulfonation. This drives the polymerization/depolymerization competition to an overall result of lignin polymerization, even in the presence of mediators. Obviously, the extent of this effect is dependent on the degree of sulfonation of the lignosulfonate preparation and the ratio phenolic/non-phenolic subunits. In addition, it should be taken into account that the model compounds used, consist of G-units linked by a β -O-4' bond. In lignin and lignosulfonate, S and H units and other interunit linkages may be present, which may also play a role in the overall reaction outcome.

3.5 Conclusions

This work reports the effect of sulfonation of lignin model compounds on their reactivity in laccase and LMS incubations. Phenolic lignin model compounds, both native and sulfonated, underwent radical coupling reactions, indicating that laccase is able to induce polymerization of both native and sulfonated lignin. Sulfonation of a non-phenolic β -O-4' linked lignin model compound had a larger impact on its reactivity: whereas C_o-oxidation and cleavage of the native model compound were observed in LMS incubations, the sulfonated model compound was completely unreactive in laccase and laccase/HBT incubations. Overall, since sulfonation prevents cleavage of the non-phenolic lignin backbone, while keeping radical coupling of phenolic end groups possible in LMS incubations, we conclude that sulfonation of lignin drives the overall outcome of LMS incubations toward polymerization. The insights obtained from this study can be used to rationalize and predict the effect of laccase and LMS on native lignin and lignosulfonate.

3.6 References

1. Christopher LP, Yao B and Ji Y. Lignin biodegradation with laccase-mediator systems. *Frontiers in Energy Research* **2014**, 2, 12.
2. Bugg TD and Rahmanpour R. Enzymatic conversion of lignin into renewable chemicals. *Current Opinion in Chemical Biology* **2015**, 29, 10-17.
3. Munk L, Sitarz AK, Kalyani DC, Mikkelsen JD and Meyer AS. Can laccases catalyze bond cleavage in lignin? *Biotechnology Advances* **2015**, 33 (1), 13-24.
4. Areskog D, Li J, Gellerstedt G and Henriksson G. Investigation of the molecular weight increase of commercial liginosulfonates by laccase catalysis. *Biomacromolecules* **2010**, 11 (4), 904-910.
5. Lundquist K and Parkås J. Different types of phenolic units in lignins. *BioResources* **2011**, 6 (2), 920-926.
6. Ortner A, Hofer K, Bauer W, Nyanhongo GS and Guebitz GM. Laccase modified liginosulfonates as novel binder in pigment based paper coating formulations. *Reactive and Functional Polymers* **2018**, 123, 20-25.
7. Chen Q, Marshall MN, Geib SM, Tien M and Richard TL. Effects of laccase on lignin depolymerization and enzymatic hydrolysis of ensiled corn stover. *Bioresource Technology* **2012**, 117, 186-192.
8. Munk L, Punt AM, Kabel MA and Meyer AS. Laccase catalyzed grafting of N-OH type mediators to lignin via radical-radical coupling. *RSC Advances* **2017**, 7 (6), 3358-3368.
9. Couto SR and Herrera JLT. Industrial and biotechnological applications of laccases: a review. *Biotechnology Advances* **2006**, 24 (5), 500-513.
10. Bourbonnais R and Paice MG. Oxidation of non-phenolic substrates: an expanded role for laccase in lignin biodegradation. *FEBS Letters* **1990**, 267 (1), 99-102.
11. Rico A, Rencoret J, Del Río JC, Martínez AT and Gutiérrez A. Pretreatment with laccase and a phenolic mediator degrades lignin and enhances saccharification of Eucalyptus feedstock. *Biotechnology for Biofuels* **2014**, 7 (1), 6.
12. Rencoret J, Pereira A, Del Río JC, Martínez AT and Gutiérrez A. Laccase-mediator pretreatment of wheat straw degrades lignin and improves saccharification. *BioEnergy Research* **2016**, 9 (3), 917-930.
13. Rosado T, Bernardo P, Koci K, Coelho AV, Robalo MP and Martins LO. Methyl syringate: an efficient phenolic mediator for bacterial and fungal laccases. *Bioresource Technology* **2012**, 124, 371-378.
14. Camarero S, Ibarra D, Martínez ÁT, Romero J, Gutiérrez A and Del Río JC. Paper pulp delignification using laccase and natural mediators. *Enzyme and Microbial Technology* **2007**, 40 (5), 1264-1271.
15. Cañas AI and Camarero S. Laccases and their natural mediators: biotechnological tools for sustainable eco-friendly processes. *Biotechnology Advances* **2010**, 28 (6), 694-705.
16. Shleev S, Persson P, Shumakovich G, Mazhugo Y, Yaropolov A, Ruzgas T and Gorton L. Interaction of fungal laccases and laccase-mediator systems with lignin. *Enzyme and Microbial Technology* **2006**, 39 (4), 841-847.
17. Bourbonnais R and Paice MG. Demethylation and delignification of kraft pulp by *Trametes versicolor* laccase in the presence of 2, 2'-azinobis-(3-ethylbenzthiazoline-6-sulphonate). *Applied Microbiology and Biotechnology* **1992**, 36 (6), 823-827.
18. Gutiérrez A, Rencoret J, Cadena EM, Rico A, Barth D, José C and Martínez ÁT. Demonstration of laccase-based removal of lignin from wood and non-wood plant feedstocks. *Bioresource Technology* **2012**, 119, 114-122.
19. Baiocco P, Barreca AM, Fabbini M, Galli C and Gentili P. Promoting laccase activity towards non-phenolic substrates: a mechanistic investigation with some laccase-mediator systems. *Organic & Biomolecular Chemistry* **2003**, 1 (1), 191-197.
20. Galli C, Gentili P and Lanzalunga O. Hydrogen abstraction and electron transfer with aminoxyl radicals: synthetic and mechanistic issues. *Angewandte Chemie International Edition* **2008**, 47 (26), 4790-4796.
21. Gosselink RJA, *Lignin as a renewable aromatic resource for the chemical industry* (PhD Thesis Wageningen University). Wageningen, 2011. ISBN 9789461731005.

22. Huber D, Ortner A, Daxbacher A, Nyanhongo GS, Bauer W and Guebitz GM. Influence of oxygen and mediators on laccase-catalyzed polymerization of lignosulfonate. *ACS Sustainable Chemistry & Engineering* **2016**, 4 (10), 5303-5310.
23. Prasetyo EN, Kudanga T, Østergaard L, Rencoret J, Gutiérrez A, Del Río JC, Santos JI, Nieto L, Jiménez-Barbero J and Martínez AT. Polymerization of lignosulfonates by the laccase-HBT (1-hydroxybenzotriazole) system improves dispersibility. *Bioresource Technology* **2010**, 101 (14), 5054-5062.
24. Heap L, Green A, Brown D, van Dongen B and Turner N. Role of laccase as an enzymatic pretreatment method to improve lignocellulosic saccharification. *Catalysis Science & Technology* **2014**, 4 (8), 2251-2259.
25. Hilgers RJ, Vincken J-P, Gruppen H and Kabel MA. Laccase/mediator systems: Their reactivity towards phenolic lignin structures. *ACS Sustainable Chemistry & Engineering* **2018**, 6 (2), 2037-2046.
26. Frisch MJ, Trucks GW, Schlegel HB, Scuseria GE, Robb MA, Cheeseman JR, Scalmani G, Barone V, Petersson GA and Nakatsuji H. Gaussian 16, revision B. 01; Wallingford, CT, 2016.
27. Ramalingam B, Sana B, Seayad J, Ghadessy FJ and Sullivan MB. Towards understanding of laccase-catalysed oxidative oligomerisation of dimeric lignin model compounds. *RSC Advances* **2017**, 7 (20), 11951-11958.
28. Lahtinen M, Heinonen P, Oivanen M, Karhunen P, Kruus K and Sipilä J. On the factors affecting product distribution in laccase-catalyzed oxidation of a lignin model compound vanillyl alcohol: experimental and computational evaluation. *Organic & Biomolecular Chemistry* **2013**, 11 (33), 5454-5464.
29. Kawai S, Asukai M, Ohya N, Okita K, Ito T and Ohashi H. Degradation of a non-phenolic β -O-4 substructure and of polymeric lignin model compounds by laccase of *Coriolus versicolor* in the presence of 1-hydroxybenzotriazole. *FEMS Microbiology Letters* **1999**, 170 (1), 51-57.
30. Srebotnik E and Hammel KE. Degradation of nonphenolic lignin by the laccase/1-hydroxybenzotriazole system. *Journal of Biotechnology* **2000**, 81 (2), 179-188.
31. Xu F. Oxidation of phenols, anilines, and benzenethiols by fungal laccases: correlation between activity and redox potentials as well as halide inhibition. *Biochemistry* **1996**, 35 (23), 7608-7614.
32. Piontek K, Antorini M and Choinowski T. Crystal structure of a laccase from the fungus *Trametes versicolor* at 1.90-Å resolution containing a full complement of coppers. *Journal of Biological Chemistry* **2002**, 277 (40), 37663-37669.
33. Astolfi P, Brandi P, Galli C, Gentili P, Gerini MF, Greci L and Lanzalunga O. New mediators for the enzyme laccase: mechanistic features and selectivity in the oxidation of non-phenolic substrates. *New Journal of Chemistry* **2005**, 29 (10), 1308-1317.
34. Gillgren T, Hedenström M and Jönsson LJ. Comparison of laccase-catalyzed cross-linking of organosolv lignin and lignosulfonates. *International Journal of Biological Macromolecules* **2017**, 105, 438-446.
35. Ralph SA, Ralph J and Landucci L. NMR database of lignin and cell wall model compounds. **2009**, available at URL www.glbrc.org/databases_and_software/nmrdatabase/.
36. Lutnaes BF, Myrvold BO, Lauten RA and Endeshaw MM. ^1H and ^{13}C NMR data of benzylsulfonic acids - model compounds for lignosulfonate. *Magnetic Resonance in Chemistry* **2008**, 46 (3), 299-305.

3.7 Supporting Information

3.7.1 Purification of sulfonated lignin model compounds

After the sulfonation step in the microwave reactor, the incubation mixtures were cooled down to room temperature and desalted by using solid phase extraction. Supelclean ENVI-Carb cartridges (Sigma Aldrich, St. Louis, MO, USA) were activated with 80% ACN and washed with water. Subsequently, the incubation mixture was applied onto the cartridge and the cartridges were washed with 10 column volumes of water to remove salts. The model compounds were then eluted using 3 column volumes of 100% ACN, and dried under a nitrogen flow. The residue was dissolved in 1 mL water and was further purified by using a Reveleris Flash system (Grace Davison Discovery Sciences, Columbia, MD, USA), equipped with a 4 g Reveleris RP Flash cartridge, ELSD detector and UV detector. The eluents used were water (eluent A) and ACN (eluent B), both containing 1% (v/v) formic acid. After activation of the cartridge with eluent B, and washing with 5 column volumes of eluent A, the desalted reaction mixtures were injected. The sulfonated model compounds were then separated from byproducts using the following gradient profiles: For SGBG, 0-1 min at 3% B (isocratic), 1-9.3 min from 3 to 16% B (linear gradient), 9.3-9.6 min from 16 to 100% B (linear gradient), 9.6-11 min at 100% B (isocratic); For SVBG: 0-1 min at 5% B (isocratic), 1-9.3 min from 5 to 18% B (linear gradient), 9.3-9.6 min from 18 to 100% B (linear gradient), 9.6-11 min at 100% B (isocratic). The flow was set at 18 mL min⁻¹ and fractions of 4 mL were collected. The resulting fractions were diluted 10 times with water and analyzed by using RP-UHPLC-PDA-MS. Fractions that contained the sulfonated model compounds and that were free of byproducts were pooled. Remaining ACN was evaporated under reduced pressure, after which the model compound solutions were freeze-dried and stored in a desiccator.

3.7.2 2D HSQC NMR analysis of the lignin model compounds

In order to verify that the model compounds SGBG and SVBG were sulfonated at the C_α-position, the lignin model compounds were analyzed by using 2D NMR. For GBG and VBG, approximately 1 mg was dissolved in 500 μL DMSO-*d*₆, and for SGBG and SVBG, approximately 150 μg was dissolved in 450 μL DMSO-*d*₆. The NMR experiments were recorded at 25 °C by using hsqcetgpsisp2.2 and hmbcgpndqf pulse sequences on a Bruker AVANCE III 600 MHz NMR spectrometer (Bruker BioSpin, Rheinstetten, Germany) equipped with a 5 mm cryo-probe. The internal temperature of the probe was set at 298 K. Spectral widths were 6,000 Hz (10-0 ppm) for the ¹H-dimension and 25,000 Hz (165-0 ppm) for the ¹³C dimension. The solvent peak (DMSO-*d*₆) was used as an internal reference (δ_c 39.5 ppm; δ_H 2.49 ppm).

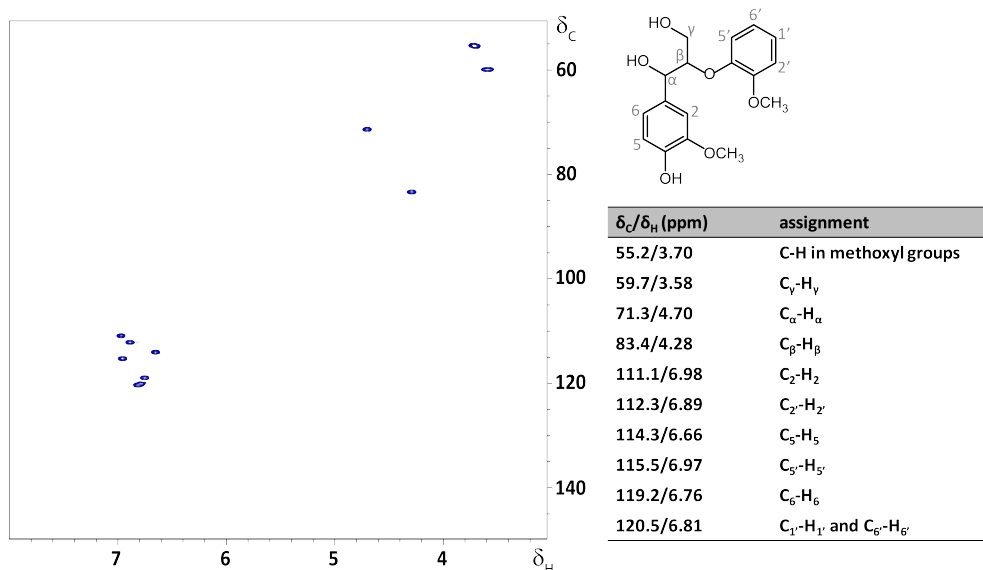


Fig. S3.1 2D HSQC NMR spectrum and peak annotations of the model compound GBG. Both the side chain and aromatic region are included. Peak assignment was based on Ralph et al.³⁵

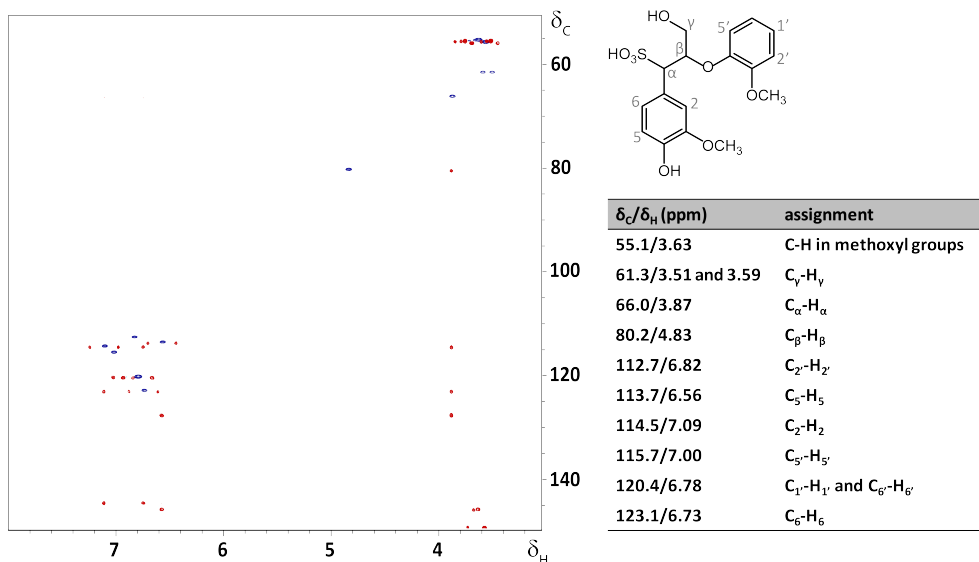


Fig. S3.2 2D HSQC (blue) and HMBC (red) NMR spectrum and peak annotations of the model compound SGBG. Both the side chain and aromatic region are included. Peak assignment was done based on the combination of HSQC and HMBC data, and by comparison of the chemical shifts with the chemical shifts of sulfonated lignin models reported by Lutnaes et al.³⁶ The peak in light blue corresponds to the least abundant diastereomer of SGBG ($C_{1'}-H_{1'}$ and $C_6'-H_6'$).

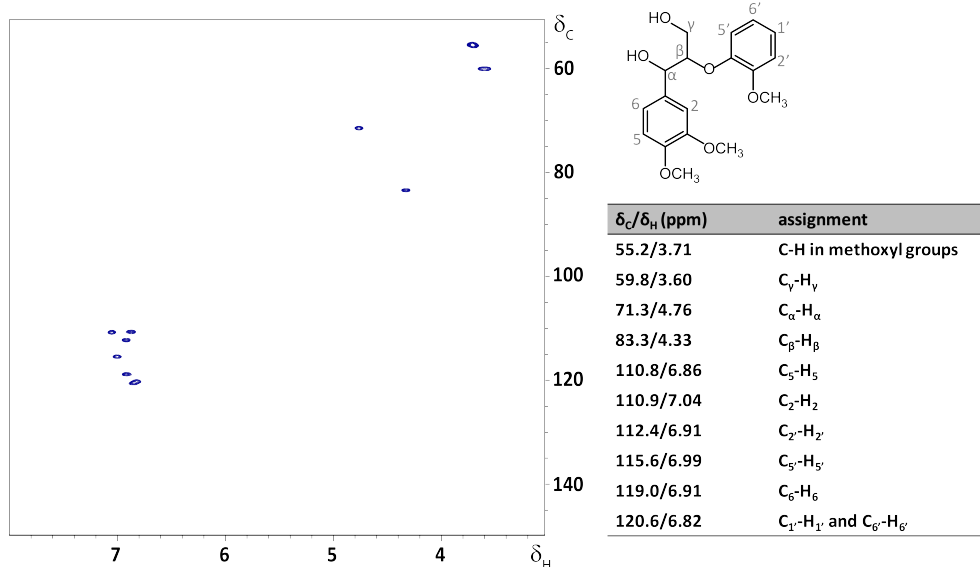


Fig. S3.3 2D HSQC NMR spectrum and peak annotations of the model compound VBG. Both the side chain and aromatic region are included. Peak assignment was based on Ralph et al.³⁵

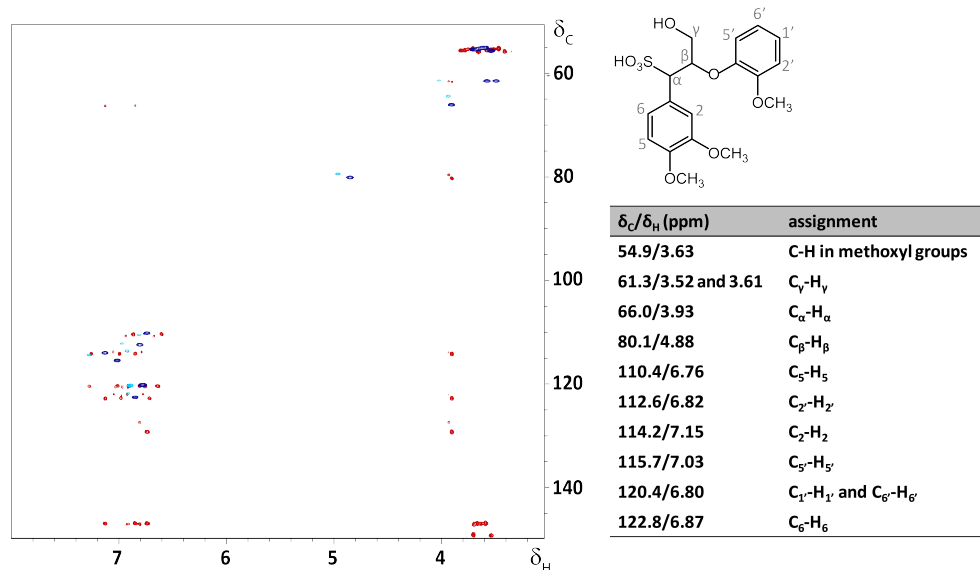


Fig. S3.4 2D HSQC (blue) and HMBC (red) NMR spectrum and peak annotations of the model compound SVBG. Both the side chain and aromatic region are included. Peak assignment was done based on the combination of HSQC and HMBC data, and by comparison of the chemical shifts with the chemical shifts of sulfonated lignin models reported by Lutnaes et al.³⁶ In the table, only the chemical shifts of the most abundant diastereomer are included. In the table, only the chemical shifts of the most abundant diastereomer are included. The peaks of the other diastereomer are indicated in light blue.

3.7.3 RP-UHPLC-PDA analysis

Reaction products were separated by using an Accela UHPLC system (Thermo Scientific, San Jose, CA, USA) equipped with a pump, degasser, autosampler and photodiode array (PDA) detector. Samples (5 μL) were injected onto an Acquity UPLC BEH C18 column (150 x 2.1 mm, particle size 1.7 μm) (Waters, Milford, MA, USA). The flow rate was 400 $\mu\text{L min}^{-1}$ at 45 $^{\circ}\text{C}$. Water (A) and acetonitrile (B) were used as eluents, both acidified with 0.1% (v/v) formic acid. The following gradient was used: 0-1.5 min at 5% B (isocratic), 1.5-32 min from 5 to 35% B (linear gradient), 32-33 min from 35 to 100% B (linear gradient), 33-38 min at 100% B (isocratic), 38-39 min from 99 to 5% B (linear gradient) and 39-44 min at 5% B (isocratic). The PDA detector was set to record wavelengths between 200 and 700 nm.

3.7.4 Electrospray Ionization – Ion Trap Mass Spectrometry (ESI-IT-MS)

Mass spectrometric data were obtained with an LTQ Velos Pro mass spectrometer (Thermo Scientific) equipped with a heated ESI probe coupled to the UHPLC system. Nitrogen was used as sheath gas and auxiliary gas. Data were collected in both positive and negative ionization mode over the m/z range 120-2,000. Data dependent MS^2 analysis was performed on the most intense ion by using collision-induced dissociation with a normalized collision energy of 35%. To gain MS^2 spectra of the second and third most abundant ions, dynamic exclusion was used, with a repeat count of six MS^2 spectra per parent ion within a time frame of 15 s. The most intense ion was selected. The system was tuned with LTQ Tune Plus 2.7 (Thermo Scientific) upon direct injection of GBG in both positive and negative ionization mode. The ion transfer tube temperature was 300 $^{\circ}\text{C}$, source heater temperature was 250 $^{\circ}\text{C}$ and the source voltage was 3.5 kV. Data were processed with Xcalibur 2.2 (Thermo Scientific).

3.7.5 Electrospray Ionization – Fourier Transform Mass Spectrometry (Accurate mass determination)

For accurate mass determination, reaction products were separated using a Vanquish UHPLC system (Thermo Scientific). The same samples were used as for ESI-IT-MS, after a 10-fold further dilution in MilliQ water. The injection volume was 1 μL . The column, eluents and gradient were identical to those described for RP-UHPLC-PDA analysis. The column compartment heater was set to 45 $^{\circ}\text{C}$, the eluent preheater was set to 45 $^{\circ}\text{C}$ and the post-column cooler was set to 40 $^{\circ}\text{C}$. A Thermo Q Exactive Focus hybrid quadrupole-orbitrap mass spectrometer (Thermo Scientific) equipped with a heated ESI probe coupled to the Vanquish RP-UHPLC system was used to acquire accurate mass data. Half of the flow was directed toward the MS. Full MS data were recorded in both negative and positive ionization mode over a range of m/z 100-1,500 at a resolution of 70,000. The mass spectrometer was calibrated in both positive and negative mode using Tune 2.8

software (Thermo Scientific) by direct infusion of Pierce LTQ ESI positive and negative ion calibration solutions (Thermo Scientific). Nitrogen was used as sheath gas (30 arbitrary units) and auxiliary gas (20 arbitrary units). The capillary temperature was 320 °C; the probe heater temperature was 280 °C; the source voltage was 2.8 kV; and the S-lens RF level was 50. Data processing was done using Xcalibur 2.2 (Thermo Scientific) and Compound Discoverer 2.0 (Thermo Scientific). Molecular formulas of reaction products were determined with a set of requirements unique for each incubation. In incubations with GBG or VBG and laccase alone, the determination of molecular formulas was restricted to C, H and O atoms, and a maximum mass error of 5 ppm. In the case of GBG or VBG with laccase and HBT, also nitrogen atoms were allowed, with a maximum of 6 N atoms per molecule. The requirements for reaction products of the sulfonated model compounds were the same, with the adaptation that 8 sulfur atoms were allowed in all cases. For every peak, this led to a list of candidates, with only one plausible formula.

3.7.6 Matrix-Assisted Laser Desorption Ionization – Time Of Flight Mass Spectrometry (MALDI-TOF-MS)

Prior to analysis, a cation exchange resin (AG 50W-X8 DOWEX) was added to the samples for at least 3 h. Under continuous flow of a hairdryer, 1 µL of 25 mg mL⁻¹ 2,5-dihydroxybenzoic acid (DHB) was mixed with 1 µL sample on a MTP 384 ground steel target plate (Bruker Daltonics). Mass spectra (m/z 500-3,500) were acquired using a Bruker UltraFlextreme MALDI-TOF (Bruker Daltonics) instrument equipped with a Smartbeam2 nitrogen laser (337 nm) operated in reflector mode with an acceleration voltage of 25 kV. Ion voltages were set to 20.00 and 17.90 kV, reflector voltages to 20.80 and 10.90 kV and the lens voltage to 7.85 kV. Ionization in positive mode was carried out with a laser beam intensity of 20-30% at 500 Hz. Each mass spectrum (m/z 500 – 3,500) was obtained from four additions of 250 laser shots to a total of 1,000 shots. Calibration was carried out with a 1 mg/ml maltodextrin solution (DP 20; Mw 400 – 3,500 Da). Data was processed using FlexAnalysis 3.3 (Bruker Daltonics).

3.7.7 Oxygen consumption

Oxygen consumption was measured with an Oxytherm System (Hansatech Kings Lynn, UK). Lignin model compounds and mediators were used as substrates at 0.4 mM in a sodium acetate buffer (50 mM) at pH 4. Also in incubations containing both a model compound and a mediator, the individual concentrations were 0.4 mM. After equilibration, laccase was added to obtain an activity of 1 U mL⁻¹. Here, a higher laccase activity was used than in the incubations described in the article, in order to obtain a more clear decrease in O₂ concentration within the short time frame of the measurement. Incubations were performed in a total volume of 1 mL at 25 °C. Data were acquired by using Oxygraph Plus software (Hansatech).

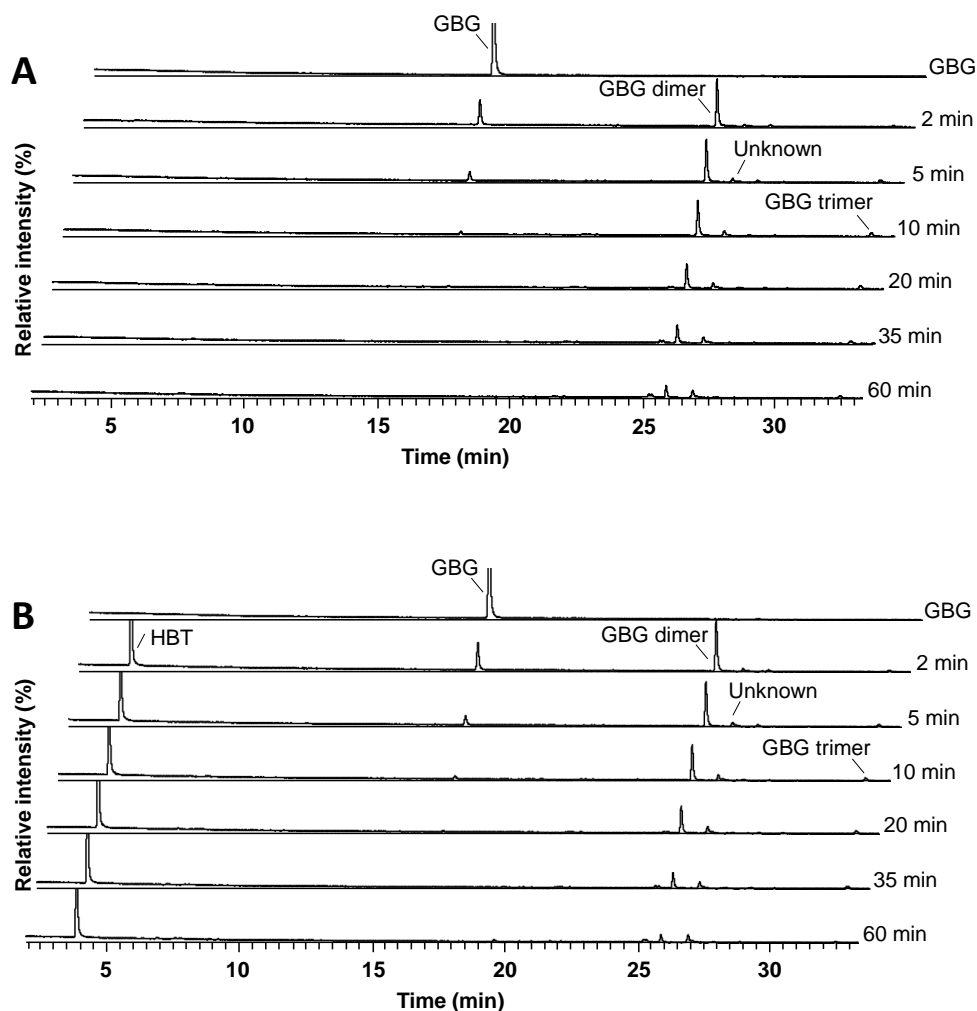


Fig. S3.5 RP-UHPLC-UV₂₈₀ chromatograms in time of GBG incubated with laccase (A) and laccase/HBT (B).

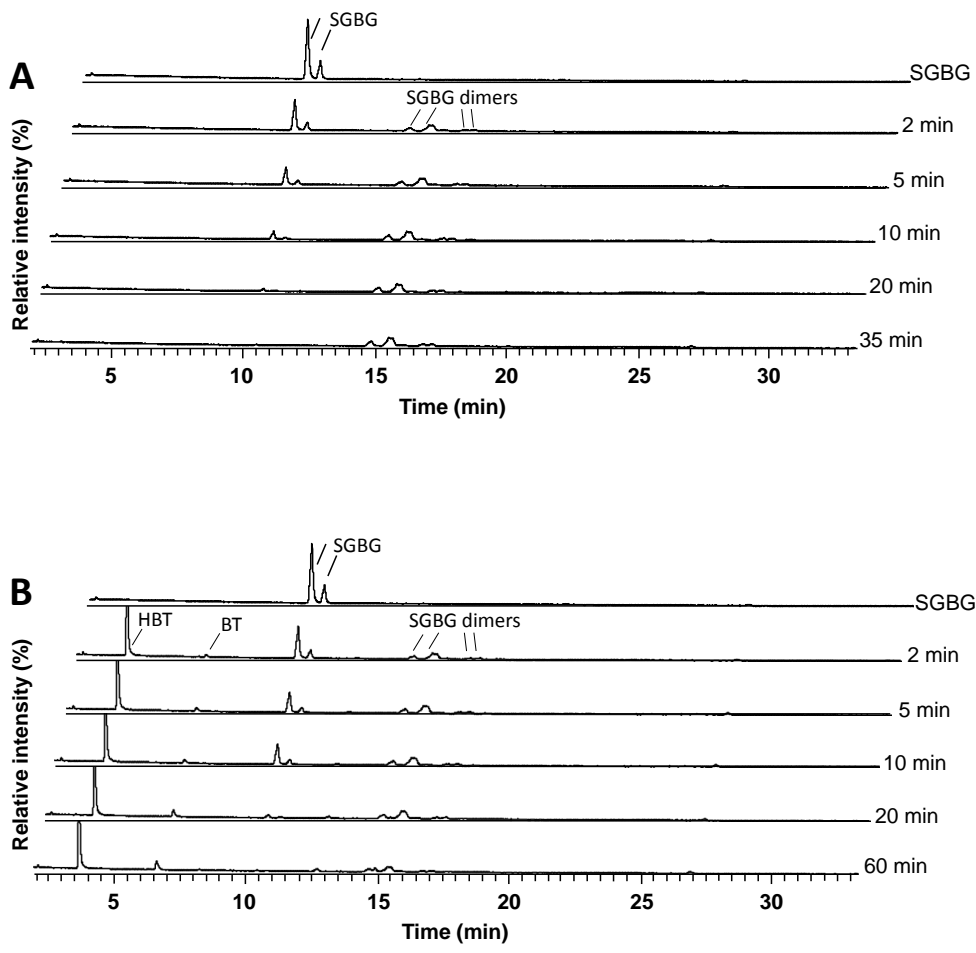


Fig. S3.6 RP-UHPLC-UV₂₈₀ chromatograms in time of SGBG incubated with laccase (A) and laccase/HBT (B).

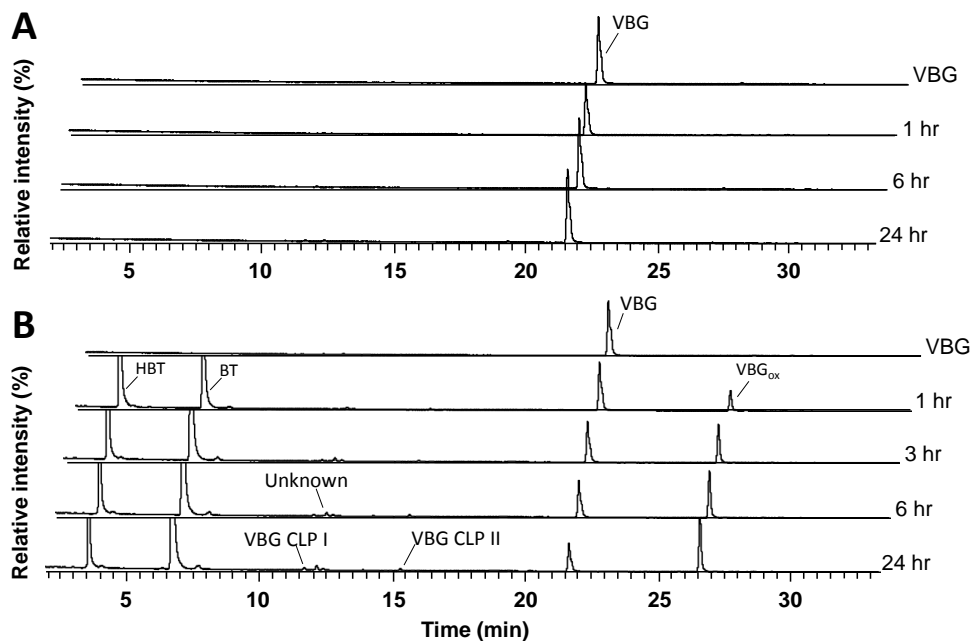


Fig. S3.7 RP-UHPLC-UV₂₈₀ chromatograms in time of VBG incubated with laccase (A) and laccase/HBT (B).

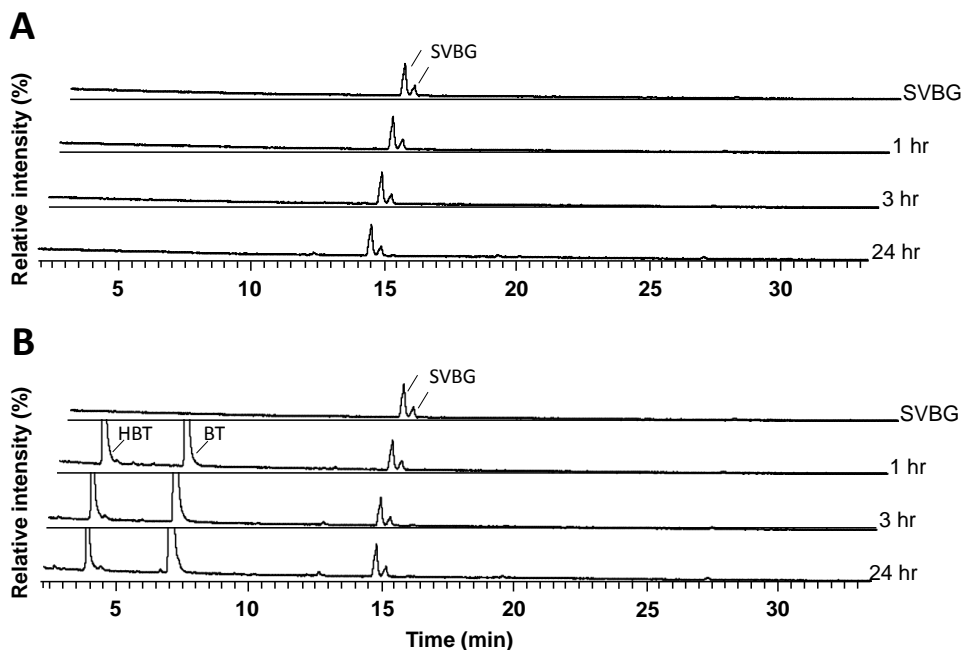


Fig. S3.8 RP-UHPLC-UV₂₈₀ chromatograms in time of SVBG incubated with laccase (A) and laccase/HBT (B).

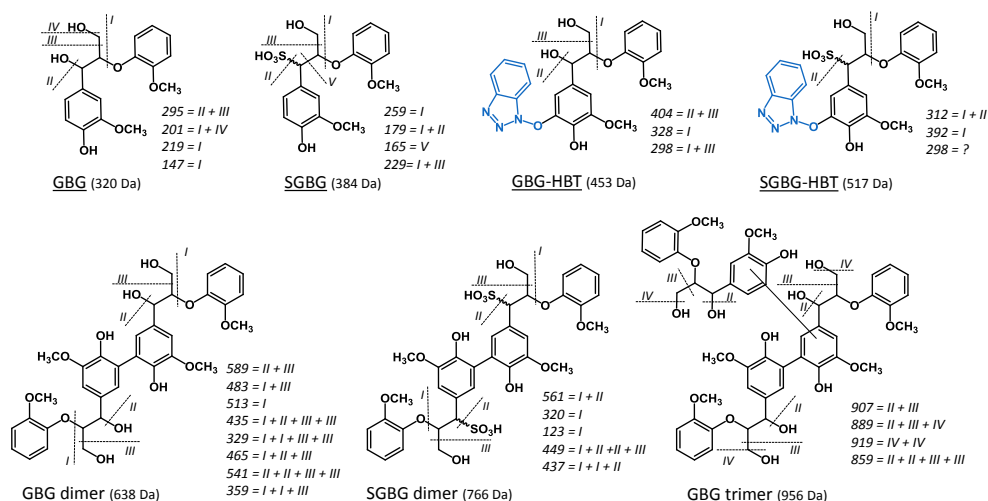


Fig. S3.9 Proposed fragmentation patterns of GBG, SGBG and their reaction products formed after incubation with laccase and laccase/HBT. The dotted lines represent the proposed fragmentation pattern, resulting in the MS² fragments reported in Table 3.1. The patterns correspond to fragmentation of parent ions [M+Na]⁺ for GBG, [M-2H]²⁻ for SGBG dimer, and [M-H]⁻ for all other molecules.

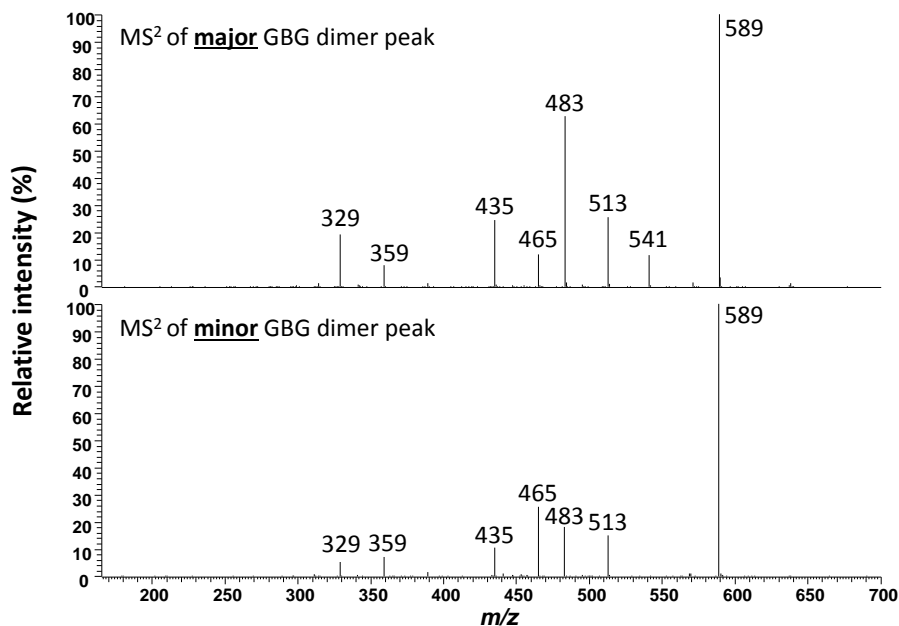


Fig. S3.10 MS² fragmentation patterns of the major GBG dimer (Rt=16.0 min) and minor GBG dimer (Rt=17.9 min) formed upon incubation with laccase. Both fragmentation patterns originate from a parent ion of m/z 637 in negative mode.

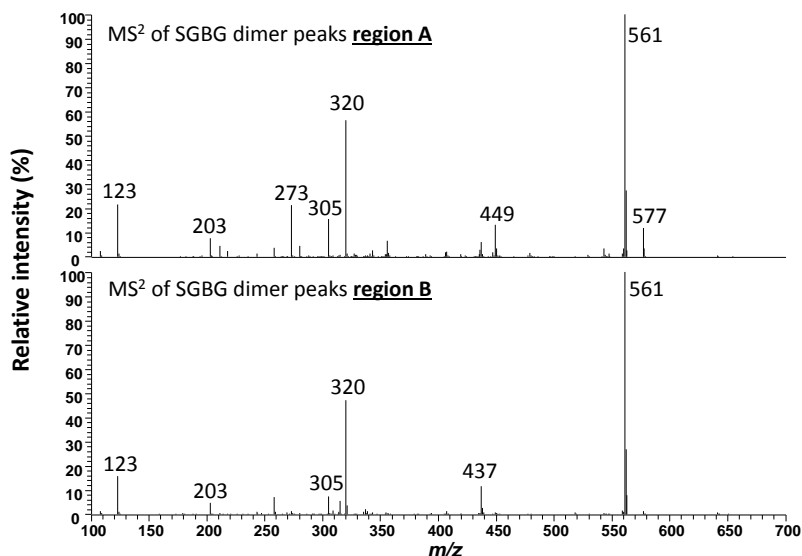
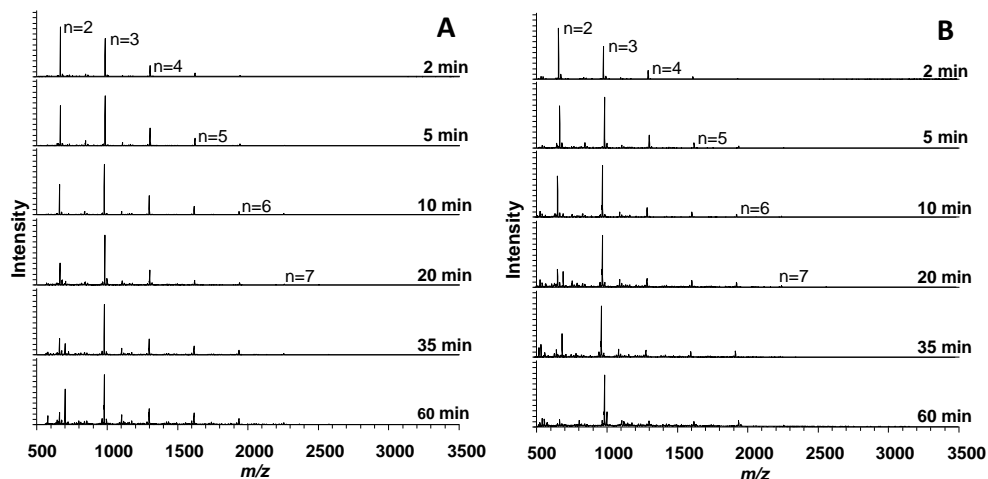


Fig. S3.11 MS² fragmentation patterns of the two regions of SGBG dimers (region A and B) shown in Fig. 2. Both fragmentation patterns originate from a parent ion of m/z 382 ($=[M-2H]^{2-}$) in negative mode.



Peak	Tentative annotation	Ionization	m/z	Observed in incubation
$n=2$	GBG dimer	$[M+Na]^+$	661.2	Lac; lac/HBT
$n=3$	GBG trimer	$[M+Na]^+$	979.3	Lac; lac/HBT
$n=4$	GBG tetramer	$[M+Na]^+$	1297.4	Lac; lac/HBT
$n=5$	GBG pentamer	$[M+Na]^+$	1615.6	Lac; lac/HBT
$n=6$	GBG hexamer	$[M+Na]^+$	1933.7	Lac; lac/HBT
$n=7$	GBG heptamer	$[M+Na]^+$	2251.8	Lac; lac/HBT

Fig. S3.12 MALDI-TOF-MS spectra in time of GBG incubated with laccase (A) and laccase/HBT (B). The table shows the observed m/z values and their corresponding tentative annotations.

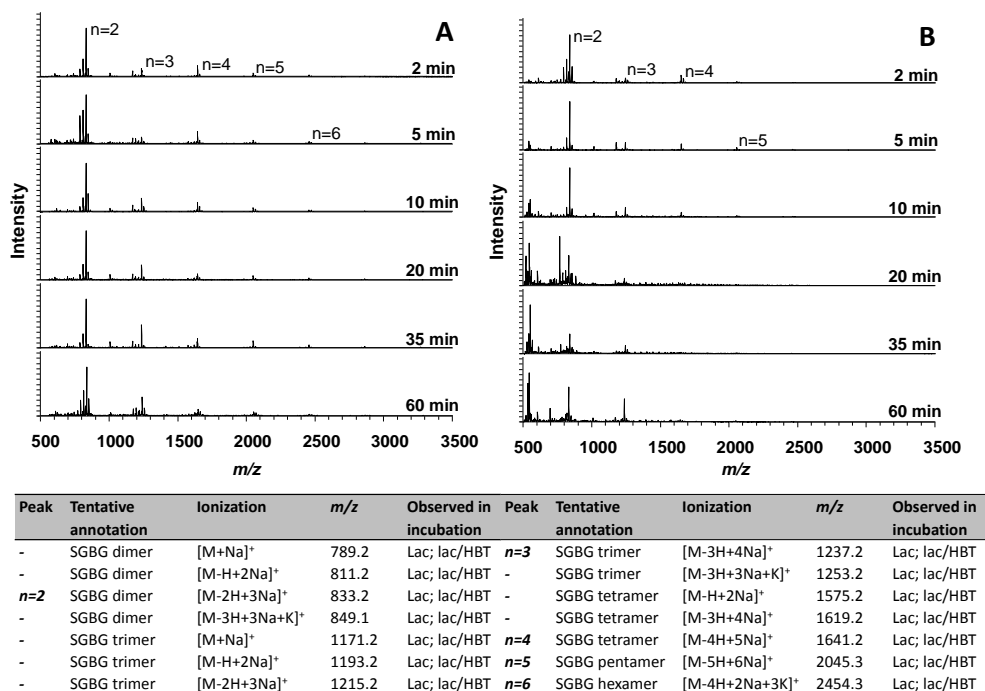


Fig. S3.13 MALDI-TOF-MS spectra in time of SGBG incubated with laccase (A) and laccase/HBT (B). The table shows the observed m/z values and their corresponding tentative annotations.

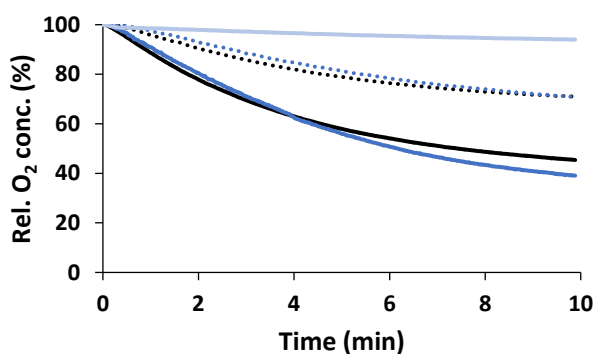


Fig. S3.14 Oxygen consumption of lignin model compounds, mediators and combinations thereof in the presence of laccase: GBG (solid, black); SGBG (dotted, black); GBG+HBT (solid, blue); SGBG+HBT (dotted, blue); HBT (solid, light blue).

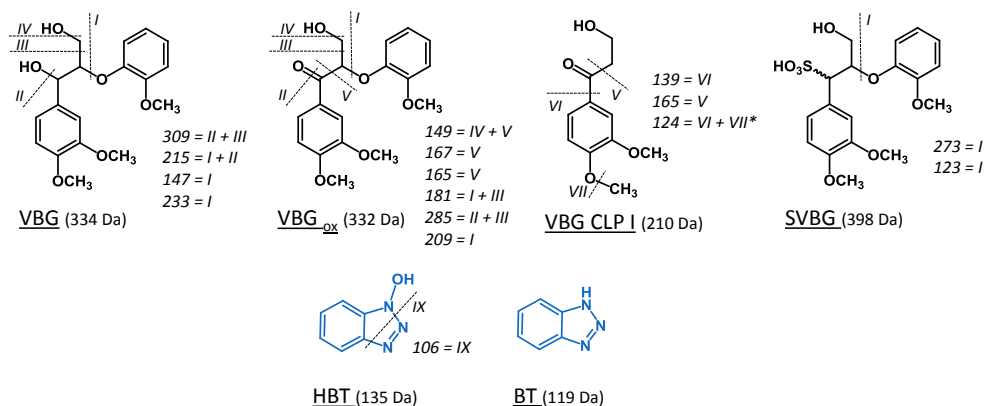
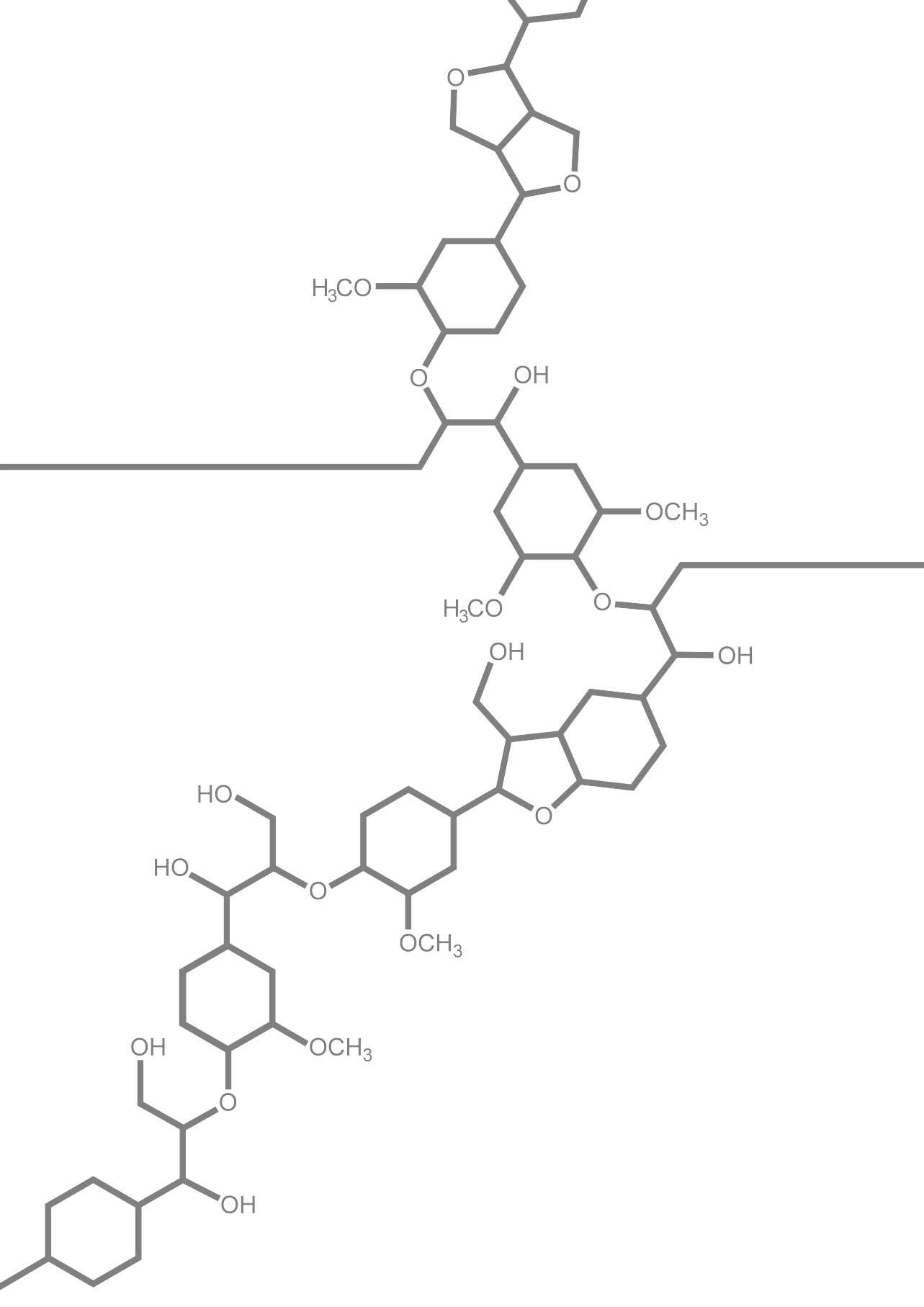


Fig. S3.15 Proposed fragmentation patterns of VBG, SVBG, HBT and of reaction products of VBG formed in laccase/HBT incubations. The dotted lines represent the proposed fragmentation pattern, resulting in the MS² fragments reported in Table 3.2. The patterns correspond to fragmentation of parent ions [M+Na]⁺ for VBG, [M+H]⁺ for VBG_{ox}, VBG CLP I and BT, and [M-H]⁻ for SVBG and HBT. * This fragmentation is suggested to be a radical fragmentation.

References Supporting Information

1. Ralph SA, Ralph J and Landucci L. NMR database of lignin and cell wall model compounds. **2009**, available at URL www.glbrc.org/databases_and_software/nmrdatabase/.
2. Lutnaes BF, Myrvold BO, Lauten RA and Endeshaw MM. ¹H and ¹³C NMR data of benzyldisulfonic acids - model compounds for lignosulfonate. *Magnetic Resonance in Chemistry* **2008**, 46 (3), 299-305.



Boosting degradation of lignin β -O-4' linkages by laccase/HBT: the overlooked effect of buffer properties

Over the past years, laccase/mediator systems (LMS) have received a lot of attention as potential green tools for lignin degradation. Nevertheless, it has often been reported that C_α-oxidation, rather than bond cleavage, is the main result of LMS treatment. Remarkably few studies have attempted to influence this product profile and thereby enhance the effectivity of LMS in cleaving lignin structures. Here, we show for the first time that the ratio between β -O-4' ether cleavage and C_α-oxidation can be substantially increased, from <10% to 80% ether cleavage, by altering buffer pH and buffer strength. The underlying reactions were further studied with experimental and computational (Density Functional Theory; DFT) approaches. Based on the outcomes, we propose detailed reaction mechanisms for the reactions underlying ether cleavage and C_α-oxidation. We propose that increasing buffer pH and strength, enhances H-bonding between the lignin model and buffer anions, which drives the overall reaction outcome towards ether cleavage.

Based on: Roelant Hilgers, Annemieke van Dam, Han Zuilhof, Jean-Paul Vincken and Mirjam A. Kabel. Controlling the competition: boosting laccase/HBT-catalyzed cleavage of a β -O-4' linked lignin model. *ACS Catalysis* **2020**, 10, 8650-8659.

4.1 Introduction

Lignin is a highly abundant aromatic polymer in plant cell walls, and its selective degradation is a major challenge in biorefinery. Lignin mainly consists of syringyl (S), guaiacyl (G) and *p*-hydroxyphenyl (H) units, coupled via a variety of inter-unit linkages, of which the β -*O*-4' linkage is most abundant (45-94% of the total inter-unit linkages).¹ The polymer consists of phenolic subunits (10-30%), mainly being the endcaps of the polymer, and non-phenolic subunits (70-90%), forming the backbone.² Although lignin can be degraded by using thermochemical treatments, green alternatives are preferred, and are receiving increasing attention.

A potential green approach for selective lignin degradation is the use of laccase/mediator systems (LMS). Laccases (EC 1.10.3.2) are oxidases with redox potentials of <800 mV¹ that use molecular oxygen to perform one-electron oxidations of aromatic substrates. Laccases can oxidize the phenolic lignin subunits, which have sufficiently low redox potentials, but oxidation of the non-phenolic subunits having redox potentials up to 1500 mV is hampered.³ To overcome the inertness of non-phenolic subunits, a mediator can be added to form a LMS. In such a system, laccase oxidizes the mediator, which subsequently oxidizes the non-phenolic lignin structure. The most widely used mediator is 1-hydroxybenzotriazole (HBT).

HBT is generally assumed to oxidize non-phenolic lignin structures via hydrogen atom transfer (HAT),^{4,5} although it has been suggested that electron transfer (ET) may also occur in the case of relatively electron-rich lignin substructures.⁶ Oxidation of lignin substructures via HAT and ET results in the formation of benzylic radicals and radical cations, respectively. These radicals react further (non-enzymatically) via several routes, depending on the structure of the substrate.⁷⁻¹¹ Studies on LMS treatments of non-phenolic β -*O*-4' linked lignin model compounds mainly report C α -oxidation¹² and bond cleavage as outcomes,^{9-11,13,14} and it has been suggested that their formation occurs via competing routes.^{1,9} Typically, C α -oxidation is the major reaction outcome, whereas cleavage products are only formed in minor amounts.^{11,13,14} Obviously, when LMS treatments are performed with the aim to degrade lignin, this product distribution is undesirable, and should be shifted in favor of bond cleavage.

In principle, to increase the efficiency of LMS-catalyzed lignin degradation, two strategies could be followed: i) maximizing the total extent of oxidation by increasing the catalytic performance of the LMS, or ii) steering the non-enzymatic follow-up reactions towards bond cleavage (at the cost of C α -oxidation). Whereas multiple studies have been published related to the catalytic performance of different laccases and mediators (in line with the first approach),¹⁵⁻¹⁹ to the best of our knowledge, no studies have been published that follow the second approach. In addition, as LMS treatments are often performed at those conditions under which the laccase is optimally active, it is largely unknown whether and how reaction conditions can affect the reaction product profile.

Here, we show that altering buffer pH and buffer strength can dramatically enhance degradation of a non-phenolic lignin model, veratrylglycerol- β -guaiacyl ether (VBG), by a laccase/HBT system. Furthermore, based on additional experiments and a computational (DFT) study, we provide new insights into the competition between C α -oxidation and ether bond cleavage and the underlying mechanisms.

4.2 Materials & Methods

4.2.1 Materials

Veratrylglycerol- β -guaiacyl ether (VBG) was purchased from ABCR (Karlsruhe, Germany). Laccase from *Trametes versicolor*, HBT, ABTS and all other chemicals were purchased from Sigma Aldrich (St. Louis, MO, USA). The laccase was partially purified as described earlier.²⁰ Laccase activity was determined spectrophotometrically by oxidation of ABTS (1 U = 1 μ mol ABTS oxidized per minute at pH 5). The partially purified laccase had a specific activity of approximately 50 U/mg. Water was prepared by using a Milli-Q water purification system (Merck Millipore, Billerica, MA).

4.2.2 Buffers used in this study

In this study, citrate/phosphate buffers were used at various pH values and buffer strengths. In this article, a X/Y mM citrate/phosphate buffer refers to a buffer prepared from X mM citric acid and Y mM dibasic phosphate stock solutions. It should be noted that the actual concentrations of citrate and phosphate are pH dependent.

4.2.3 Incubation of VBG with the laccase/HBT system

Incubations at varying pH values

Stock solutions of 0.2 mM VBG, 1 mM HBT, and 10 U/mL laccase were prepared in MQ water. Citrate/phosphate buffers were prepared at pH 3, 4, 5, 6 and 7 by mixing 50 mM citric acid and 100 mM dibasic sodium phosphate at different ratios. VBG, HBT, laccase and buffer were then mixed in a ratio of 1:1:1:2, to obtain final concentrations of 0.04 mM VBG, 0.2 mM HBT, 2 U/mL laccase and 20/40 mM citrate/phosphate buffer. All samples were prepared in duplicate. The mixtures were incubated at 40 °C and 400 rpm in a thermomixer (Eppendorf, Hamburg, Germany). After 2, 6, 24 and 48 h, 40 μ L of the incubation mixture was collected and 10 μ L of 20 mM sodium azide was added to the aliquots to stop the reaction. The samples were centrifuged (10,000 \times g, 5 min, 20 °C) and analyzed by using RP-UHPLC-PDA-MSⁿ. Calibration curves of VBG (5-50 μ M), and the main reaction products CLP (0.2-20 μ M) and VBG_{ox} (1-40 μ M) (see section: large-scale preparation and purification of reaction products) were prepared in triplicate, and were included in the RP-UHPLC-PDA-MS analysis to quantify VBG, VBG_{ox} and CLP after incubation. To estimate the formed quantities of the reaction product CLP II, the calibration curve of CLP was used. From these calibration curves, the extinction

coefficients of CLP and VBG_{ox} relative to that of VBG were determined. In further experiments, only calibration curves of VBG were included, and quantities of CLP and VBG_{ox} were calculated based on their relative extinction coefficients.

Incubations at varying buffer strengths

Samples were prepared according to the procedure described above, with final citrate/phosphate buffer concentrations of 5/10, 20/40, 40/80 and 80/160 mM (citrate/phosphate) and incubated for 48 h. Similarly, incubations were performed in MQ water instead of buffer. The pH of these incubation mixtures was adjusted to 4 or 6 by addition of HCl and NaOH. During incubation, the pH change of these samples was less than 0.15 pH point. Incubations (48 h) in concentrated citrate buffers (only at pH 4 and 6) were performed with a final citrate concentrations of 2 M and a laccase activity of 4 U/mL. For comparison, incubations (48 h) in a 20/40 mM citrate/phosphate buffer were performed with an equal laccase dose (i.e. 4 U/mL).

4.2.4 Large-scale production and purification of reaction products

To enable quantification of the main reaction products, a large-scale incubation of VBG with laccase/HBT was performed, after which the reaction products were purified. Hereto, two batches of 50 mg VBG and 125 mg HBT were incubated in 40 mL citrate/phosphate buffers (20/40 mM) at pH 4 and 6. Laccase was added to obtain a final activity of 10 U/mL. After 48 h, the reaction mixtures were centrifuged (5000 x *g*, 20 °C, 10 min) and the reaction products were separated using Flash chromatography. Hereto, the centrifuged reaction mixtures were injected on a Reveleris Flash system (Grace Davison Discovery Sciences, Columbia, MD, USA), equipped with a 4 g Reveleris RP Flash cartridge, ELSD detector and UV detector. The eluents used were water (eluent A) and ACN (eluent B), both containing 1% (v/v) formic acid. After activation of the cartridge with eluent B, and washing with 5 column volumes of eluent A, the reaction mixtures were injected. The reaction products and remaining VBG were then separated using the following elution profile: 0-5 min at 0% B (isocratic), 5-33 min from 0 to 32% B (linear gradient), 33-33.6 min from 32 to 100% B (linear gradient), 33.6-36 min at 100% B (isocratic). The flow was set at 18 mL/min and fractions of 4 mL were collected. The resulting fractions were diluted 10 times with water and analyzed by using RP-UHPLC-PDA-MS. Fractions that contained the reaction products and that were free of byproducts were pooled. Remaining ACN was evaporated under reduced pressure, after which the model compound solutions were freeze-dried and stored in a desiccator.

The fractions containing pure CLP or VBG_{ox} were pooled and freeze-dried. The obtained CLP and VBG_{ox} were analyzed using RP-UHPLC-PDA-MS and 2D NMR (HSQC, HMBC and COSY) to confirm purity and identity of the products. Since no completely pure fractions of CLP II could be obtained, the most pure fraction was freeze-dried and analyzed using HSQC and HMBC NMR.

4.2.5 2D NMR analysis

The purified reaction products were analyzed by using 2D NMR. Hereto, VBG_{ox} (490 μ g), CLP (360 μ g) and CLP II (300 μ g, partly purified) were dissolved in 450 μ L DMSO-*d*₆ after which the solutions were transferred to Shigemi NMR tubes. The NMR experiments were recorded at 25 °C by using hsqcetgpsisp2.2 and hmbcgpndqf pulse sequences on a Bruker AVANCE III 600 MHz NMR spectrometer (Bruker BioSpin, Rheinstetten, Germany) equipped with a 5 mm cryo-probe. For VBG_{ox} and CLP, a cosygpqf pulse sequence was used as well. The internal temperature of the probe was set at 298 K. The solvent peak (DMSO-*d*₆) was used as an internal reference (δ_c 39.5 ppm; δ_H 2.49 ppm). Data acquisition and processing was performed by using Topspin 4.0.1 (Bruker).

4.2.6 RP-UHPLC-PDA-MS analysis

Analysis of reaction mixtures were performed using a Vanquish UHPLC system (Thermo Scientific, San Jose, CA, USA) coupled to a PDA detector and either a Thermo LTQ Velos Pro ion-trap mass spectrometer or a Thermo Q Exactive Focus hybrid quadrupole-orbitrap mass spectrometer. Previously reported methods were used for both UHPLC-PDA-MS systems,¹⁴ with the only adaptation being the elution profile: 0-1.5 min at 5% B (isocratic), 1.5-28 min from 5 to 35% B (linear gradient), 28-28.8 min from 35 to 100% B (linear gradient), 28.8-33.3 min at 100% B (isocratic), 33.3-34 min from 100 to 5% B (linear gradient) and 34-38 min at 5% B (isocratic).

4.2.7 Preparation of C α -deuterated VBG (VBG_{C α -D})

For the preparation of C α -deuterated VBG, purified VBG_{ox} was used as starting material. Hereto, 2 mg VBG_{ox} was dissolved in 2 mL of 5% methanol, and approximately 1 mg NaBD₄ was added. The mixture was left at room temperature for 1 h, after which the C α -deuterated VBG (VBG_{C α -D}) was extracted three times with 0.5 mL diethyl ether. The diethyl ether was evaporated under a continuous flow of N₂, and VBG_{C α -D} was dissolved in 5% methanol. The purity was checked by using RP-UHPLC-PDA-MS. A single peak was observed with *m/z* 358, corresponding to the [M+Na]⁺ ion of VBG_{C α -D}. No remaining VBG_{ox}, non-deuterated VBG or other impurities were observed. The deuterated VBG was freeze-dried and stored in a desiccator until further use.

4.2.8 Determination of kinetic isotope effects

Kinetic isotope effects (KIE) were determined at pH 3, 4, 5 and 6 by performing intermolecular competition experiments. Hereto, VBG and VBG_{C α -D} were incubated for 48 h with the laccase/HBT system, starting with equimolar concentrations of 0.04 mM (see section 'Incubation of VBG with the laccase/HBT system: incubations at varying pH values' for details). The KIE was then determined by quantification of VBG and VBG_{C α -D} using high resolution RP-UHPLC-PDA-MS.

4.2.9 Computational analyses

All quantum chemical calculations were performed with the B97D functional and 6-311+G(d,p) basis set, as implemented in Gaussian 16 (version B1), using a SMD solvent model for water.²¹

4.3 Results & Discussion

4.3.1 Conversion of VBG by the laccase/HBT system

Incubations of VBG with laccase/HBT were performed in citrate/phosphate buffers at pH 3-7. In all cases, three reaction products were detected: The C₆-ketone analogue of VBG (VBG_{ox}), and two ether cleavage products (CLP and CLP II) (**Fig. 4.1** and **4.2**; see **Table S4.1** and **Fig. S4.1-4.3** for UHPLC-MS and NMR based identification). VBG_{ox} was found to be the major product, which is in line with previous findings in literature.^{11,13,14} During the incubation, HBT was partly converted to benzotriazole (BT). It should be noted that, upon formation of CLP and CLP II, other cleavage products should have been formed as well (i.e. products containing the other aromatic ring of VBG). These products were not detected, most likely because they reacted further to multiple other products.

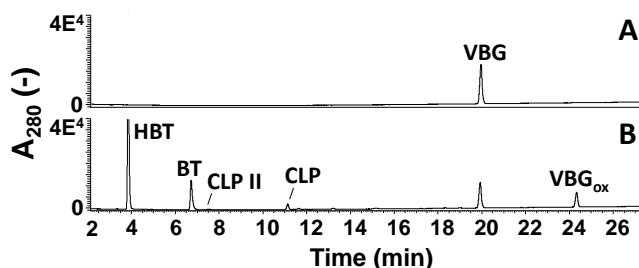


Fig. 4.1 RP-UHPLC-UV₂₈₀ chromatograms of VBG (A) and VBG incubated for 48 h with laccase/HBT in a 20/40 mM citrate/phosphate buffer at pH 6 (B). BT = benzotriazole. Chromatograms of incubations at other pH values and incubations times and data used for product identification can be found in the Supporting Information.

4.3.2 The effect of pH and buffer strength on product distribution

Laccase/HBT incubations performed at pH 3-7 in 20/40 mM citrate/phosphate buffers were followed over time (**Fig. S4.4**). Regarding the extent of VBG conversion, pH 4 and 5 were found to be the optimum pH values, showing 45 and 54% conversion, respectively, after 48 h (**Fig. 4.3**). The relatively high conversion may justify why most lignin and lignin model compound incubations in literature are performed at these, for the laccase more optimal, pH values.^{10,11,22-26} Nevertheless, the pH was shown to strongly affect the product distribution. At pH 3 and 4, mainly VBG_{ox} was formed and the cleavage products were only formed to a minor extent (i.e. both < 6% of the reaction products). At higher pH values, the product distribution shifted in favor of the cleavage products,

mainly due to an increased formation of CLP (**Fig. 4.3**). At pH 6 and 7, the cleavage products together accounted for 38% of the reaction products. Regarding absolute amounts, the optimal pH for cleavage of VBG was pH 6, due to a higher laccase activity at pH 6 than at pH 7. The formation of CLP II was highest at low pH values, but rather low yields ($\leq 1\%$) were found in all incubations, indicating that cleavage of the O-4' bond occurs only to a very limited extent. Therefore, in further investigations, we focused on the formation of VBG_{ox} and CLP.

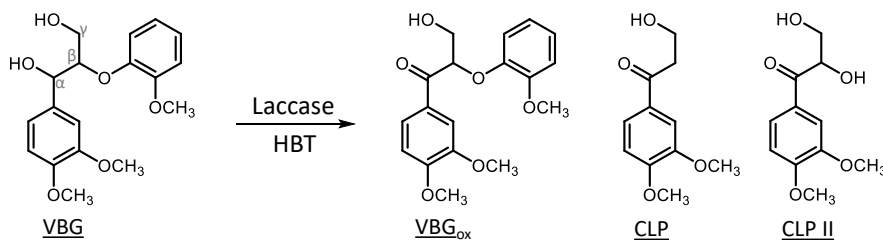


Fig. 4.2 Reaction products of VBG formed upon incubation with the laccase/HBT system. Identification of the reaction products was based on RP-UHPLC-PDA-MS and NMR (see Supporting Information).

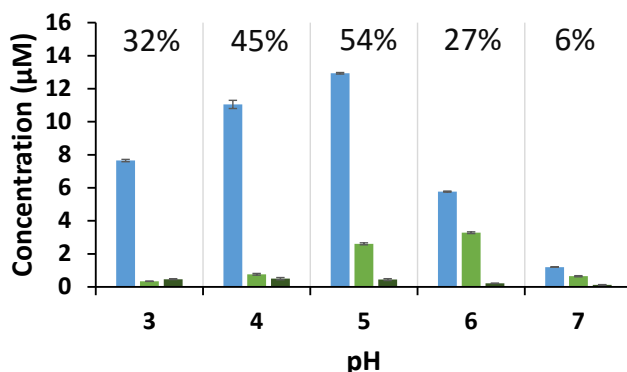


Fig. 4.3 Molar concentration of the reaction products VBG_{ox} (blue), CLP (green) and CLP II (dark green) after incubation with laccase/HBT for 48 h in 20/40 mM citrate/phosphate buffers. Percentages refer to the conversion of VBG. The error bars represent the standard deviation of two independent incubations.

Although it seemed that the pH influenced the reaction product profile, it is important to note that by increasing the buffer pH, also the phosphate/citrate ratio and the dissociation of citrate and phosphate increased. Therefore, we investigated whether the observed differences in product ratios (see **Fig. 4.3**) were effects of pH or (also) of the concentration of specific ions. Hereto, the incubations of VBG were repeated in 5/10 mM, 40/80 mM and 80/160 mM citrate/phosphate buffers. Interestingly, the molar ratio CLP/VBG_{ox} was found to increase not only with increasing pH, but also with increasing buffer strength (**Fig. 4.4**). In absence of a buffer, a pH effect was still observed, although

the ratio $\text{CLP}/\text{VBG}_{\text{ox}}$ was significantly lower than in buffered incubations. These results indicate that the product ratio is not determined by a 'simple' pH dependence, but that the ratio $\text{CLP}/\text{VBG}_{\text{ox}}$ is considerably affected by the presence of buffer ions.

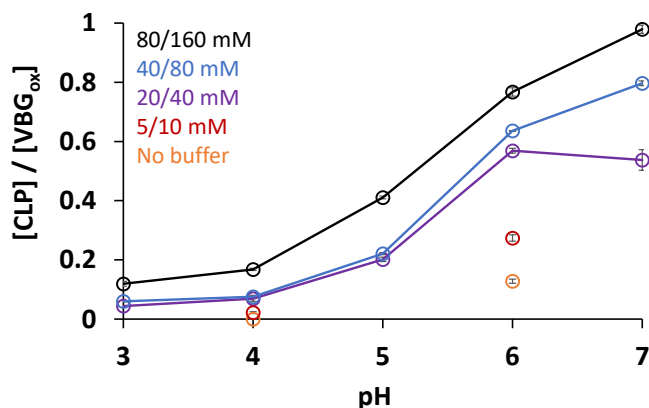


Fig. 4.4 Molar ratios between CLP and VBG_{ox} after incubation of VBG for 48 h with laccase/HBT in buffers prepared from 5/10 mM (red), 20/40 mM (purple), 40/80 mM (blue) and 80/160 mM citrate/phosphate (black) or non-buffered solutions of which the pH was adjusted using NaOH and HCl (yellow). The error bars represent the standard deviation of two independent incubations.

Based on the insights described above, we attempted to further enhance ether cleavage of VBG by performing incubations in highly concentrated (2 M) citrate buffers at pH 4 and 6. After 48 h, 34–40% of the VBG was converted, and $\text{CLP}/\text{VBG}_{\text{ox}}$ ratios as high as 0.9 and 3.9 were obtained at pH 4 and 6, respectively (**Fig. 4.5**). The latter ratio is 138 times higher than that obtained in the control experiment (20/40 mM citrate/phosphate buffer at pH 4), and demonstrates the enormous impact of the buffer properties on the reaction outcome. Interestingly, after 48 h of incubation, the residual laccase activity was larger in the concentrated citrate buffers than in the weak citrate/phosphate buffers (**Table S4.3**). Hence, the increased extent of ether bond cleavage does not occur at the cost of enzyme stability.

4.3.3 Experimental insights into the effect of reaction conditions on product distribution

Competing or sequential formation of VBG_{ox} and CLP?

Our next step was to understand in more detail how the buffer properties affect the product distribution in laccase/HBT incubations. Firstly, we verified that the two dominant reaction products (i.e. VBG_{ox} and CLP) are true end products of the incubation, and that they are formed through competing, rather than sequential reactions. To this aim, purified VBG_{ox} and CLP were incubated with laccase/HBT at pH 4 and 6. After 24 h, no conversion was found for both products, confirming that both VBG_{ox} and CLP are end

products of the laccase/HBT treatment, formed via competing reaction pathways (**Fig. S4.5**).

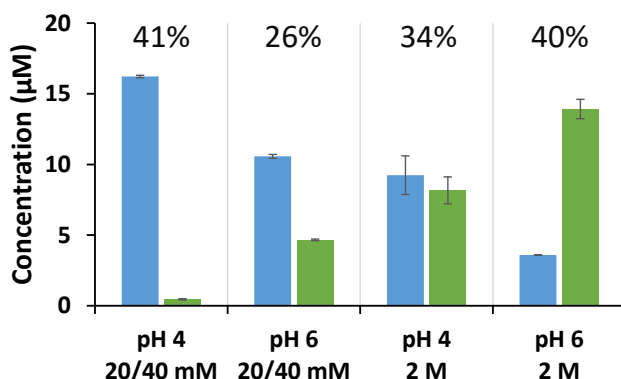


Fig. 4.5 Molar concentrations of the reactions products VBG_{ox} (blue) and CLP (green) after incubation of VBG with laccase/HBT in 20/40 mM citrate/phosphate or 2 M citrate buffers for 48h. Percentages refer to the conversion of VBG. The error bars represent the standard deviation of two independent incubations.

The role of laccase activity

As the results shown in **Fig. 4.3** were obtained from incubations with the same amount (and not activity) of laccase at all pH values, we checked whether the observed pH effects were caused indirectly by the effect of pH on laccase activity towards HBT. Although laccase loading slightly affected the ratio CLP/VBG_{ox} (**Fig. S4.6**), the differences were too small to explain the results shown in **Fig. 4.3**. Thus, it was concluded that CLP and VBG_{ox} should be formed from laccase-independent, competing reactions.

Buffer or salt effects in the competing reactions?

The ratio CLP/VBG_{ox} was found to increase with increasing pH and buffer strength. As both buffer strength and pH are positively correlated with ionic strength, due to increased concentration and dissociation of ions, respectively, we investigated whether the ratio CLP/VBG_{ox} could also be enhanced by increasing the ionic strength with a non-buffer salt (i.e. KNO₃). As can be observed from **Fig. 4.6**, the addition of 0.5 M KNO₃ did not significantly affect the product ratio. From this, it can be inferred that the product ratio is not affected by the ionic strength of the reaction medium, but rather by the concentration of specific buffer ions.

Do buffer pH and strength affect the oxidation mechanism?

To define the exact starting point of the observed competition reactions, we investigated whether oxidation of VBG by the HBT radical would result in the formation of benzylic radicals (via HAT) and/or radical cations (via ET). Although it is generally assumed that the laccase/HBT system operates via a HAT mechanism, evidence for this has only been obtained by using monomeric lignin model substrates, and only at pH 5.^{4,27} In another

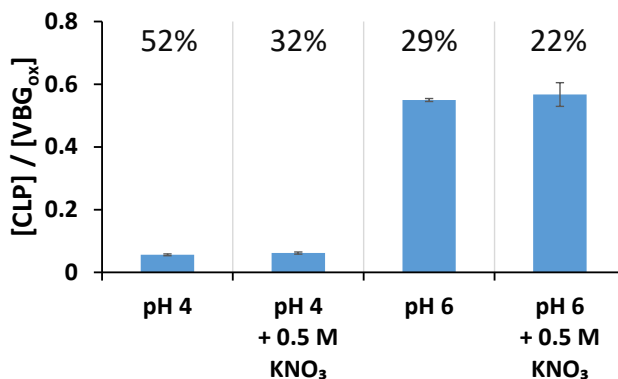


Fig. 4.6 Molar product ratios (CLP/VBG_{ox}) after incubation of VBG for 48 h with laccase/HBT in buffers at pH 4 and 6 prepared from 20/40 mM citrate/phosphate, and in the same buffers supplemented with 0.5 M KNO₃. The error bars represent the standard deviation of two independent incubations. The percentages refer to the conversion of VBG.

study, in which a dimeric lignin model was used, it has been suggested that laccase/HBT can operate via both HAT and ET.⁶ We, therefore, investigated whether a HAT or an ET mechanism would be more plausible in the case of VBG oxidation, and whether a shift in oxidation mechanism could occur when changing the buffer pH. To this end, we determined the kinetic isotope effect (KIE) of VBG and its C_α-deuterated analogue (VBG_{Cα-D}) in intermolecular competition experiments in 20/40 mM citrate/phosphate buffers at pH 3, 4, 5 and 6 (see **Fig. 4.7**).

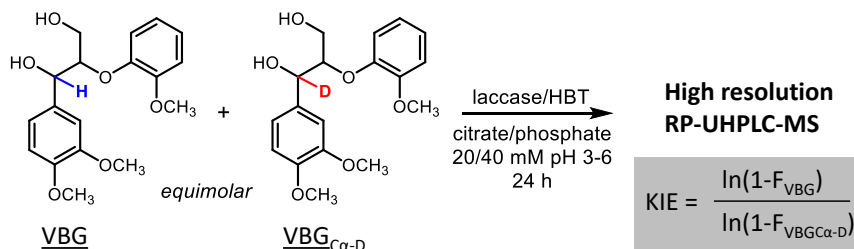


Fig. 4.7 Schematic overview of the kinetic isotope effect (KIE) determination. The KIE was determined by comparing conversion rates of VBG and its C_α-deuterated analogue VBG_{Cα-D} in an intermolecular competition experiment. The KIE was then determined by using the formula shown in the figure, wherein F = fraction of substrate converted.²⁸

In case of a HAT mechanism, a substantial primary KIE can be expected, as cleavage of the C_α-H/D bond occurs at the rate-limiting step. In contrast, no substantial KIE is expected in the case of ET, as the C_α-H/D bond is not involved in the rate-limiting step.⁴ Relatively large KIEs (4.1-6.3) were found for all pH values. As these KIE values clearly point into the direction of a HAT mechanism, and as no clear increasing or decreasing trend in KIE was observed with increasing pH, a shift in oxidation mechanism seems

implausible. Thus, we concluded that the competition between CLP and VBG_{ox} formation starts after formation of a VBG benzylic radical.

Table 4.1 Kinetic isotope effects obtained from an intermolecular competition between oxidation of VBG and C α -deuterated VBG (VBG_{C α -D}) upon incubation with laccase/HBT for 48 h. Averages and standard deviations of two independent incubations are shown.

pH	3	4	5	6
KIE (H/D)	5.1 \pm 0.7	5.1 \pm 0.3	6.3	4.1 \pm 0.5

4.3.4 Computational insights into the competing reaction mechanisms

To gain further insights into the competing reactions of the VBG benzylic radical, we zoomed in on the reaction mechanisms underlying C α -oxidation and C β -O ether cleavage. Mechanisms have been suggested for both reactions, although few efforts have been made to provide evidence for these mechanisms.^{6,29} To check the plausibility of the suggested mechanisms and to obtain more insights into the structures of the transition states (TS) and intermediates, we performed a Density Functional Theory (DFT) study to determine the relative enthalpies of all structures involved.

C α -oxidation

For C α -oxidation, a mechanism has been suggested in literature that involves addition of O₂ to the benzylic radical, after which the C α -ketone is formed by splitting off a hydroperoxyl radical (**Fig. 4.8**, pathway A).^{6,29} As the energy-minimized starting point of this step (i.e. structure 1 + O₂) has quartet spin, while the resulting peroxy radical intermediate (structure 3) has doublet spin, TS 2 is likely to have a blended spin state. We, therefore, started out by potential energy scans assuming either quartet spin (coming from structure 1 and O₂) or doublet spin (coming from structure 3). The quartet-state trajectory yielded a clear TS upon specific geometric restrictions (see **Fig. S4.7**), while the doublet trajectory did not yield a TS. Since the quartet trajectory was higher in energy than the doublet one, this was analyzed in detail, so as to obtain an upper limit to the TS energy. The resulting (quartet) TS structure (**Fig. S4.7**, **Table S4.2**) has a relative energy of 29.7 kcal/mol compared to the starting materials. As O₂ addition is overall exothermic by 52.6 kcal/mol, it was concluded that O₂ addition is irreversible. The second step of pathway A involves splitting off a hydroperoxyl radical. For this step, a clear TS (structure 4) containing a five-membered ring was found, indicating that the hydroperoxyl radical leaving group is formed through intramolecular H-transfer. The activation energy of this second step equals 17.5 kcal/mol. Thus, depending on how much doublet spin character is involved in TS 2, the activation energy of pathway A is predicted to be in the range of 17.5-29.7 kcal/mol. Although the calculated enthalpy gain of splitting of a hydroperoxyl radical is essentially zero, the reaction is probably driven forward by entropy gain and/or further reactions of the hydroperoxyl radical.

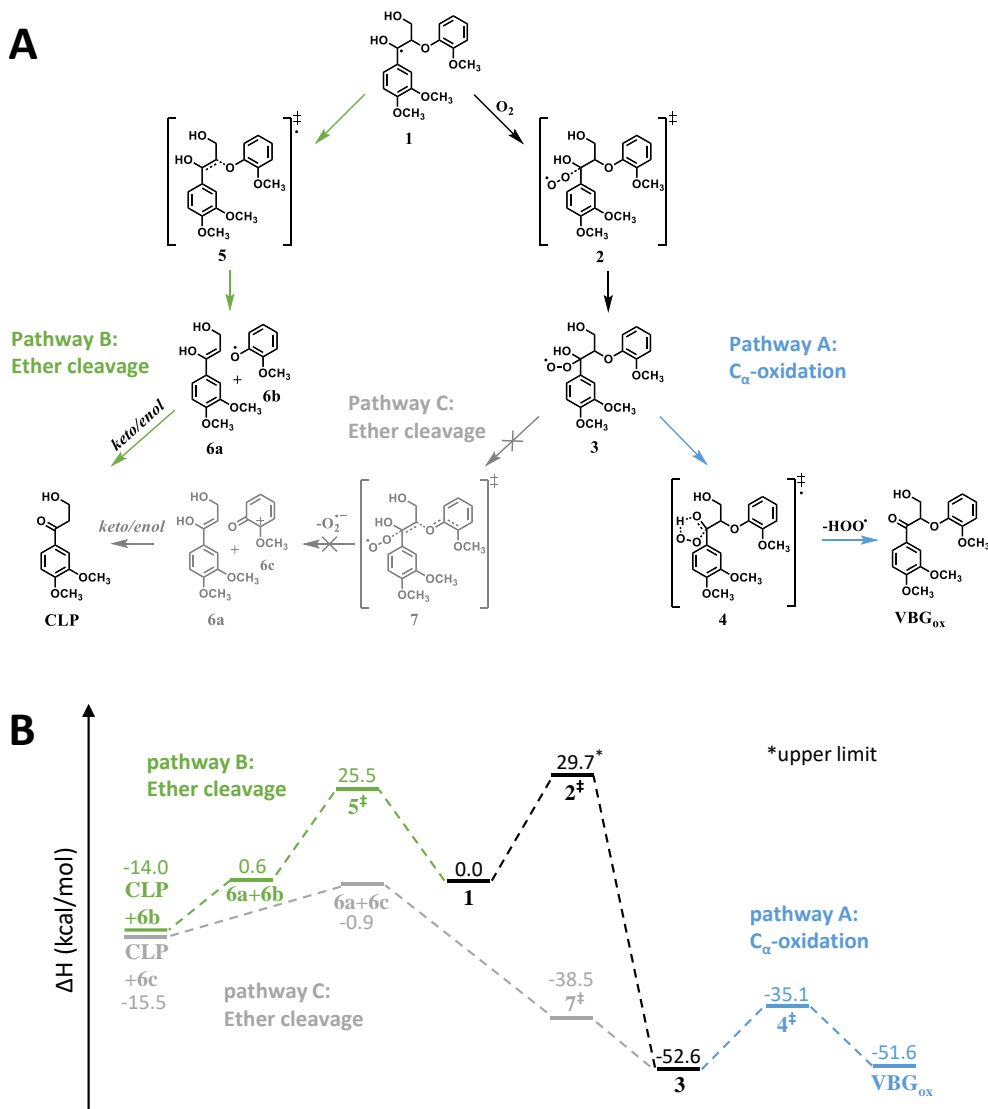


Fig. 4.8 Proposed reaction mechanisms in literature (panel A) for C_α-oxidation (pathway A) and C_β-O cleavage (pathway B&C) of the VBG benzylic radical, with calculated relative enthalpies of intermediates, transition states and products (panel B). As structure 6b and 6c rapidly react further, the final relative enthalpies of the cleavage pathways (B and C) are expected to be significantly lower than the presented values. Based on the calculations, pathway B is a more plausible cleavage mechanisms than pathway C (grey). * This enthalpy should be interpreted as an upper limit.

C_β-O ether cleavage

For C_β-O ether cleavage, two different mechanisms have been reported in literature. The first mechanism involves a homolytic cleavage of the C_β-O bond directly from the benzylic

radical (**Fig. 4.8**, pathway B), whereas the second mechanism involves O₂ addition followed by heterolytic cleavage of the C _{β} -O bond (**Fig. 4.8**, pathway C).^{6,29}

In pathway B, the relative enthalpy of the TS for the C _{β} -O bond cleavage was calculated to be 25.5 kcal/mol (structure 5). As the subsequent keto-enol tautomerization is expected to be very fast, and thus not rate-limiting,³⁰ no further TS was calculated. The overall activation energy of pathway B, thus, equals 25.5 kcal/mol. Although the calculated enthalpy gain of pathway B only equals 14.0 kcal/mol, it should be noted that the formed guaiacol radical (structure 6b) rapidly reacts further, which is expected to further decrease the relative enthalpy of the products. Based on the overall energy gain, and a surmountable activation energy, pathway B seems to be a plausible route. Pathway C has a slightly higher overall energy gain than pathway B. However, the intermediate after splitting off the superoxide (structure 6c) lies 51.5 kcal/mol higher than its precursor (structure 3), making this pathway unlikely to occur.

4.3.5 Towards an explanation for the buffer-dependent competition

Based on the DFT study, a competition between pathway A and pathway B seems possible. However, based on the reactions shown in **Fig. 4.8**, it is not directly clear how this competition would be influenced by the buffer pH and/or strength. Theoretically, as O₂ solubility decreases at high salt levels,³¹ pathway A could be slowed down at increased buffer strength and pH. Nevertheless, no significant effects of buffer salts on O₂ solubility are expected in weak buffers, nor did we find any significant differences in O₂ concentrations between buffers at pH 3 and 7 using Oxygraph measurements (data not shown). In addition, if the O₂ solubility would have been the main reason underlying the observed buffer effects, it would be expected that also high concentrations of other salts would affect the product profile. As can be clearly observed from **Fig. 4.6**, this was not the case. Since it was found that only buffer ions, and not KNO₃, affected the product ratio, a more plausible scenario is that specific buffer ions interact with the lignin structure during the course of the reaction, and thereby influence the competition between ether cleavage and C _{α} -oxidation. Interestingly, based on the pK_a equalization principle,³² strong H-bonding can be expected between the secondary alcohol proton in structure 1 and 3 and the citrate trianion or phosphate dianion (see Supporting Information for detailed explanation). As the concentrations of these anions increase with increasing pH (in the used pH range) and buffer strength, it is plausible that these anions are indeed involved in the observed buffer effect.

Furthermore, by performing DFT calculations, we investigated whether H-bonding between the VBG benzylic radical (structure 1) and citrate would be more favorable for the citrate trianion than for the dianion. Although, in both cases, such intermolecular H-bonding would require disruption of the intramolecular H-bond between the C _{α} -OH and C _{γ} -OH groups of structure 1, we found that H-bonding between structure 1 and the citrate trianion is overall favorable by 3.9 kcal/mol (Fig. 9). In contrast, for the citrate dianion it is unfavorable by 1.9 kcal/mol, i.e. in that case the intramolecular H-bond would be

preferred (data not shown). This finding strengthens our suggestion that only specific anions are involved in H-bonding to the lignin structure.

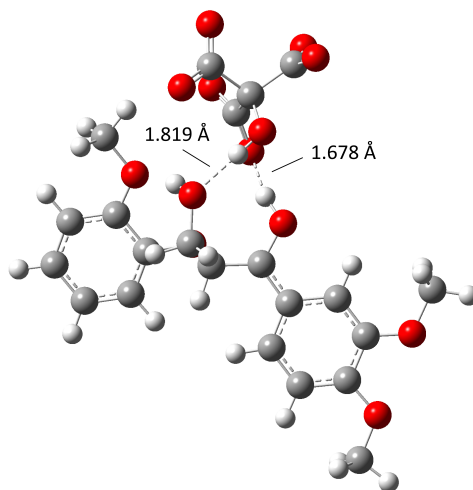


Fig. 4.9 Optimized geometry of the VBG benzylic radical (structure 1) and the citrate³⁻. The molecules are linked via two H-bonds: one between the C_α-OH proton of the VBG radical and a citrate carboxylate group (bond length = 1.678 Å), and one between the C_γ-OH oxygen and the tertiary alcohol proton of citrate (bond length = 1.819 Å). The overall enthalpy gain obtained by H-bonding is 3.9 kcal/mol. In case of citrate²⁻, H-bonding to structure 1 is enthalpically unfavorable by 1.9 kcal/mol. It should be noted that the O-atom of the aryl-ether is present, but largely hidden behind the C_γ-atom.

Two scenarios can be described via which such H-bonding between anions and lignin could affect the observed competition (**Fig. 4.10**).

Firstly, it has been shown that the rate of O₂ addition to (benzylic) radicals can be substantially diminished by e.g. steric or electronic stabilization of the radical.^{33,34} As H-bonding of buffer anions to the secondary alcohol proton would bring the anions in close proximity of the radical-bearing carbon atom, it is not inconceivable that such H-bonding somehow increases the stability of the radical, and thereby decreases the rate of O₂ addition. A lower O₂ addition rate would slow down pathway A, but not pathway B, resulting in relatively more ether cleavage (**Fig. 4.10A**). As there is currently no good model to predict O₂ addition rates to radicals, it remains to be investigated whether H-bonding between buffer anions and lignin radicals indeed slows down O₂ addition.

The second possibility is that the competition between C_β-O ether cleavage and C_α-oxidation takes place after the addition of O₂. Although pathway C was shown to be implausible, it could be speculated that there is an alternative and more favorable ether cleavage pathway, starting from the peroxy intermediate (structure 3 in **Fig. 4.8**). If that is the case, it is highly conceivable that H-bonding between buffer anions and structure 3 would affect the competition, in favor of ether cleavage. As the second step

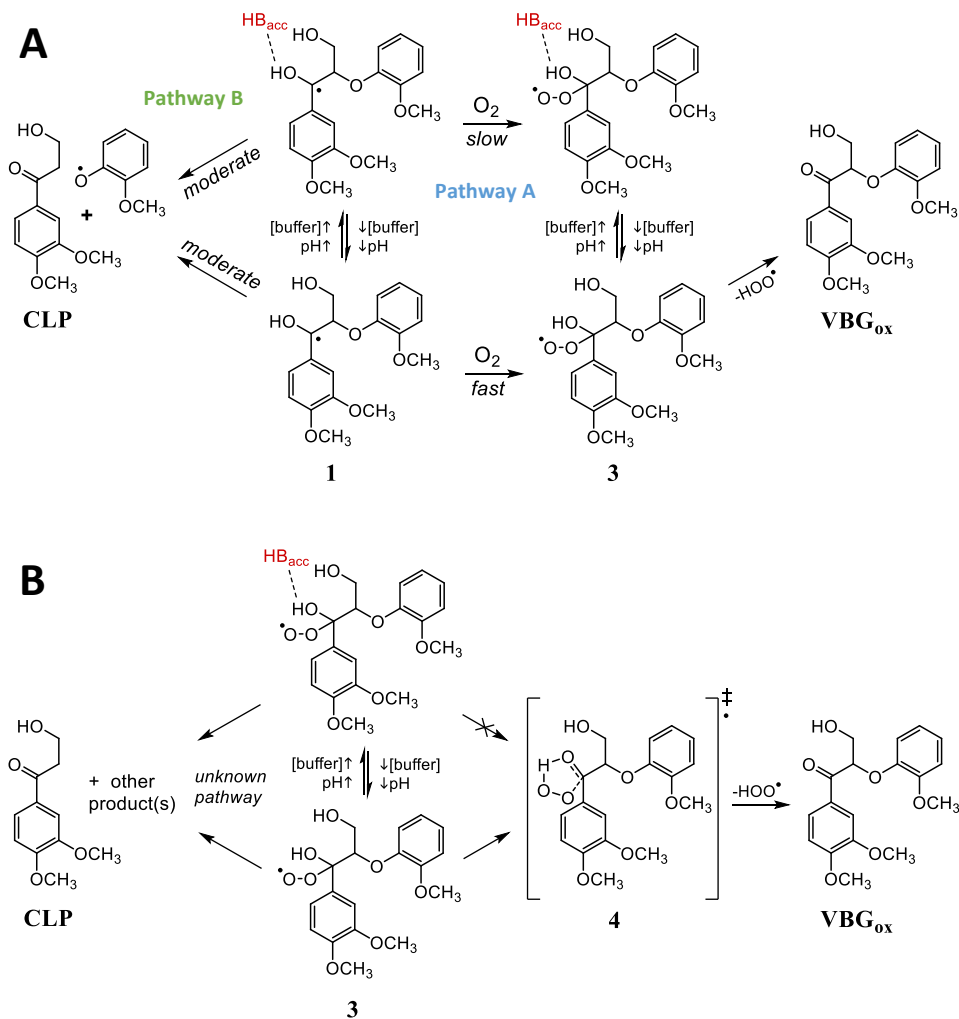


Fig. 4.10 Two possible scenarios for the effect of H-bonding on the competition between C_β-O ether cleavage and C_α-oxidation. H-bonding between VBG benzylic radicals and buffer anions may slow down the rate of O₂ addition, resulting in relatively more ether cleavage (A). Alternatively, an alternative C_β-O ether cleavage pathway may exist after O₂ addition. In that case, H-bonding to the VBG peroxy radical may impair formation of TS 4 and, thereby, slow down VBG_{ox} formation, resulting in relatively more ether cleavage (B). Based on the pK_a equalization principle,³² it is expected that citrate³⁻ and HPO₄²⁻ can form reasonably strong hydrogen bonds with the secondary alcohol proton. It should be noted that, also in scenario A, the hydroperoxy radical is expected to only be split off from a non-H-bonding peroxy intermediate. Nevertheless, as O₂ addition is irreversible, the competition between ether cleavage and C_α-oxidation in scenario A is not dependent on the rate of hydroperoxy split-off, but purely governed by the rates of ether cleavage and O₂ addition. HB_{acc} = Hydrogen bond acceptor.

of pathway A involves an intramolecular H-transfer (TS 4 in Fig. 4.8), strong H-bonding of the secondary alcohol proton to buffer anions would slow down this reaction step by impairing the formation of TS 4 (Fig. 4.10B). Valgimigli et al. reported previously that the rate of a comparable reaction is, indeed, decreased by H-bond formation between substrate and solvent.³⁵ Whether an alternative and favorable ether cleavage pathway exists after O₂ addition remains to be investigated.

4.4 Conclusions

In conclusion, we have shown that the competition between ether cleavage and C_α-oxidation of a non-phenolic β-O-4' linked lignin structure in LMS incubations is highly dependent on the reaction conditions. Both the relative and absolute extent of ether cleavage can be dramatically enhanced by increasing buffer pH and buffer strength. Furthermore, based on both experimental and computational efforts, we have provided new insights into the reaction mechanisms underlying C_α-oxidation and ether cleavage, and proposed that increased H-bonding between buffer anions and the C_α-OH group of the lignin structure drives the outcome of LMS treatment towards ether bond cleavage. We expect that these insights will be useful in further studies and optimizations of oxidative lignin degradation in industrial settings.

4.5 References and notes

1. Munk L, Sitarz AK, Kalyani DC, Mikkelsen JD and Meyer AS. Can laccases catalyze bond cleavage in lignin? *Biotechnology Advances* **2015**, *33* (1), 13-24.
2. Lundquist K and Parkås J. Different types of phenolic units in lignins. *BioResources* **2011**, *6* (2), 920-926.
3. Couto SR and Herrera JLT. Industrial and biotechnological applications of laccases: a review. *Biotechnology Advances* **2006**, *24* (5), 500-513.
4. Baiocco P, Barreca AM, Fabbri M, Galli C and Gentili P. Promoting laccase activity towards non-phenolic substrates: a mechanistic investigation with some laccase-mediator systems. *Organic & Biomolecular Chemistry* **2003**, *1* (1), 191-197.
5. d'Acunzo F, Baiocco P and Galli C. A study of the oxidation of ethers with the enzyme laccase under mediation by two N-OH-type compounds. *New Journal of Chemistry* **2003**, *27* (2), 329-332.
6. Kawai S, Nakagawa M and Ohashi H. Degradation mechanisms of a nonphenolic β -O-4 lignin model dimer by *Trametes versicolor* laccase in the presence of 1-hydroxybenzotriazole. *Enzyme and Microbial Technology* **2002**, *30* (4), 482-489.
7. Kawai S, Umezawa T, Shimada M and Higuchi T. Aromatic ring cleavage of 4,6-di-(tert-butyl)-guaiacol, a phenolic lignin model compound, by laccase of *Coriolus versicolor*. *FEBS Letters* **1988**, *236* (2), 309-311.
8. Kawai S, Nakagawa M and Ohashi H. Aromatic ring cleavage of a non-phenolic β -O-4 lignin model dimer by laccase of *Trametes versicolor* in the presence of 1-hydroxybenzotriazole. *FEBS Letters* **1999**, *446* (2-3), 355-358.
9. Kawai S, Umezawa T and Higuchi T. Degradation mechanisms of phenolic β -1 lignin substructure model compounds by laccase of *Coriolus versicolor*. *Archives of Biochemistry and Biophysics* **1988**, *262* (1), 99-110.
10. Kawai S, Asukai M, Ohya N, Okita K, Ito T and Ohashi H. Degradation of a non-phenolic β -O-4 substructure and of polymeric lignin model compounds by laccase of *Coriolus versicolor* in the presence of 1-hydroxybenzotriazole. *FEMS Microbiology Letters* **1999**, *170* (1), 51-57.
11. Srebotnik E and Hammel KE. Degradation of nonphenolic lignin by the laccase/1-hydroxybenzotriazole system. *Journal of Biotechnology* **2000**, *81* (2), 179-188.
12. Although ether cleavage may eventually also result in the formation of ketone groups at the C_a-position, in this paper the term C_a-oxidation is used to describe the conversion of C_a-OH to a C_a=O without concomitant ether cleavage.
13. Heap L, Green A, Brown D, van Dongen B and Turner N. Role of laccase as an enzymatic pretreatment method to improve lignocellulosic saccharification. *Catalysis Science & Technology* **2014**, *4* (8), 2251-2259.
14. Hilgers R, Twentyman-Jones M, van Dam A, Gruppen H, Zuilhof H, Kabel MA and Vincken J-P. The impact of lignin sulfonation on its reactivity with laccase and laccase/HBT. *Catalysis Science & Technology* **2019**, *9* (6), 1535-1542.
15. Li K, Xu F and Eriksson K-EL. Comparison of fungal laccases and redox mediators in oxidation of a nonphenolic lignin model compound. *Applied and Environmental Microbiology* **1999**, *65* (6), 2654-2660.
16. Fabbri M, Galli C and Gentili P. Comparing the catalytic efficiency of some mediators of laccase. *Journal of Molecular Catalysis B: Enzymatic* **2002**, *16* (5), 231-240.
17. Moldes D, Díaz M, Tzanov T and Vidal T. Comparative study of the efficiency of synthetic and natural mediators in laccase-assisted bleaching of Eucalyptus kraft pulp. *Bioresource Technology* **2008**, *99* (17), 7959-7965.
18. Ibarra D, Romero J, Martínez MJ, Martínez AT and Camarero S. Exploring the enzymatic parameters for optimal delignification of Eucalypt pulp by laccase-mediator. *Enzyme and Microbial Technology* **2006**, *39* (6), 1319-1327.
19. Barreca AM, Fabbri M, Galli C, Gentili P and Ljunggren S. Laccase-mediated oxidation of a lignin model for improved delignification procedures. *Journal of Molecular Catalysis B: Enzymatic* **2003**, *26* (1-2), 105-110.

20. Hilgers RJ, Vincken J-P, Gruppen H and Kabel MA. Laccase/mediator systems: Their reactivity towards phenolic lignin structures. *ACS Sustainable Chemistry & Engineering* **2018**, *6* (2), 2037-2046.
21. Frisch MJ, Trucks GW, Schlegel HB, Scuseria GE, Robb MA, Cheeseman JR, Scalmani G, Barone V, Petersson GA and Nakatsuji H. Gaussian 16, revision B. 01; Wallingford, CT, 2016.
22. Shleev S, Persson P, Shumakovich G, Mazhugo Y, Yaropolov A, Ruzgas T and Gorton L. Interaction of fungal laccases and laccase-mediator systems with lignin. *Enzyme and Microbial Technology* **2006**, *39* (4), 841-847.
23. Camarero S, Ibarra D, Martínez ÁT, Romero J, Gutiérrez A and Del Río JC. Paper pulp delignification using laccase and natural mediators. *Enzyme and Microbial Technology* **2007**, *40* (5), 1264-1271.
24. Gutiérrez A, Rencoret J, Cadena EM, Rico A, Barth D, Del Río JC and Martínez ÁT. Demonstration of laccase-based removal of lignin from wood and non-wood plant feedstocks. *Bioresource Technology* **2012**, *119*, 114-122.
25. Rencoret J, Pereira A, Del Río JC, Martínez AT and Gutiérrez A. Laccase-mediator pretreatment of wheat straw degrades lignin and improves saccharification. *BioEnergy Research* **2016**, *9* (3), 917-930.
26. Kawai S, Iwatsuki M, Nakagawa M, Inagaki M, Hamabe A and Ohashi H. An alternative β -ether cleavage pathway for a non-phenolic β -O-4 lignin model dimer catalyzed by a laccase-mediator system. *Enzyme and Microbial Technology* **2004**, *35* (2-3), 154-160.
27. d'Acunzo F, Baiocco P, Fabbri M, Galli C and Gentili P. The radical rate-determining step in the oxidation of benzyl alcohols by two N-OH-type mediators of laccase: the polar N-oxyl radical intermediate. *New Journal of Chemistry* **2002**, *26* (12), 1791-1794.
28. Melander L and Saunders W, *Reaction rates of isotopic molecules*. Wiley: New York, **1980**.
29. Ten Have R and Teunissen PJM. Oxidative mechanisms involved in lignin degradation by white-rot fungi. *Chemical Reviews* **2001**, *101* (11), 3397-3414.
30. Clayden J, Greeves N, Warren S and Wothers P, *Organic Chemistry*. 2 ed.; Oxford university press: **2012**.
31. Ming G and Zhenhao D. Prediction of oxygen solubility in pure water and brines up to high temperatures and pressures. *Geochimica et Cosmochimica Acta* **2010**, *74* (19), 5631-5640.
32. Gilli P, Pretto L, Bertolasi V and Gilli G. Predicting hydrogen-bond strengths from acid-base molecular properties. The pKa slide rule: toward the solution of a long-lasting problem. *Accounts of Chemical Research* **2008**, *42* (1), 33-44.
33. Bejan EV, Font-Sanchis E and Scaiano JC. Lactone-derived carbon-centered radicals: formation and reactivity with oxygen. *Organic letters* **2001**, *3* (25), 4059-4062.
34. Wright JS, Shadnia H and Chepelev LL. Stability of carbon-centered radicals: effect of functional groups on the energetics of addition of molecular oxygen. *Journal of computational chemistry* **2009**, *30* (7), 1016-1026.
35. Valgimigli L, Amorati R, Fumo MG, DiLabio GA, Pedulli GF, Ingold KU and Pratt DA. The unusual reaction of semiquinone radicals with molecular oxygen. *The Journal of Organic Chemistry* **2008**, *73* (5), 1830-1841.

4.6 Supporting Information

4.6.1 H-bond formation between the VBG radicals and buffer anions: Expectations based on the pK_a equalization principle

According to the pK_a equalization principle (or pK_a slide rule), the strength of hydrogen bonds is dependent on the difference between the pK_a values of the hydrogen bond donor (HBD) and acceptor (HBA).¹ The smaller the pK_a difference between HBD and HBA, the stronger the hydrogen bond. The pK_a of the secondary alcohol group of VBG is unknown, but it is expected to be similar to that of benzyl alcohol and 1-phenylethanol, which have pK_a values of 14.9 and 15.5, respectively.² The pK_a values of the VBG benzylic radical and peroxy radical (structures 1 and 3), however, are expected to be several pH points lower, due to the strong electron withdrawing nature of the radical and peroxy group.³ Assuming a pK_a of ~ 10 for the secondary OH structures 1 and 3, strong charge-assisted H-bond formation can be expected between structure 1/3 and citrate³⁻ (pK_a citrate²⁻/citrate³⁻ = 6.4) or HPO_4^{2-} (pK_a $H_2PO_4^-/HPO_4^{2-}$ = 7.2). Such H-bonds are much stronger than between structure 1/3 and H_2O (pK_a H_3O^+/H_2O = -1.74).

Table S4.1 Compounds detected using UHPLC-PDA-ESI-ITMS and UHPLC-PDA-ESI-FTMS after incubation of VBG with laccase from *T. versicolor* and HBT.

Annotat.	Mol. formula	RT (min)	Ion	Observed/ calculated mass (Da)	Mass error (ppm)	MS ² fragments
HBT	C ₆ H ₅ N ₃ O	3.74	[M+H] ⁺	135.04329/135.04326	0.22	119, 91, 80, 116, 53
BT	C ₆ H ₅ N ₃	6.64	[M+H] ⁺	119.04836/119.04835	0.08	102, 92, 65
CLP II	C ₁₁ H ₁₄ O ₅	7.41	[M+H] ⁺	226.08409/226.08413	-0.16	N.D.
CLP	C ₁₁ H ₁₄ O ₄	11.09	[M+H] ⁺	210.08925/210.08921	0.19	139, 193, 165
VBG	C ₁₈ H ₂₂ O ₆	19.95	[M+Na] ⁺	334.14149/334.14164	-0.45	309, 339
VBG _{ox}	C ₁₈ H ₂₀ O ₆	24.39	[M+H] ⁺	332.12599/332.12599	0.00	315, 181, 167, 149, 285, 209

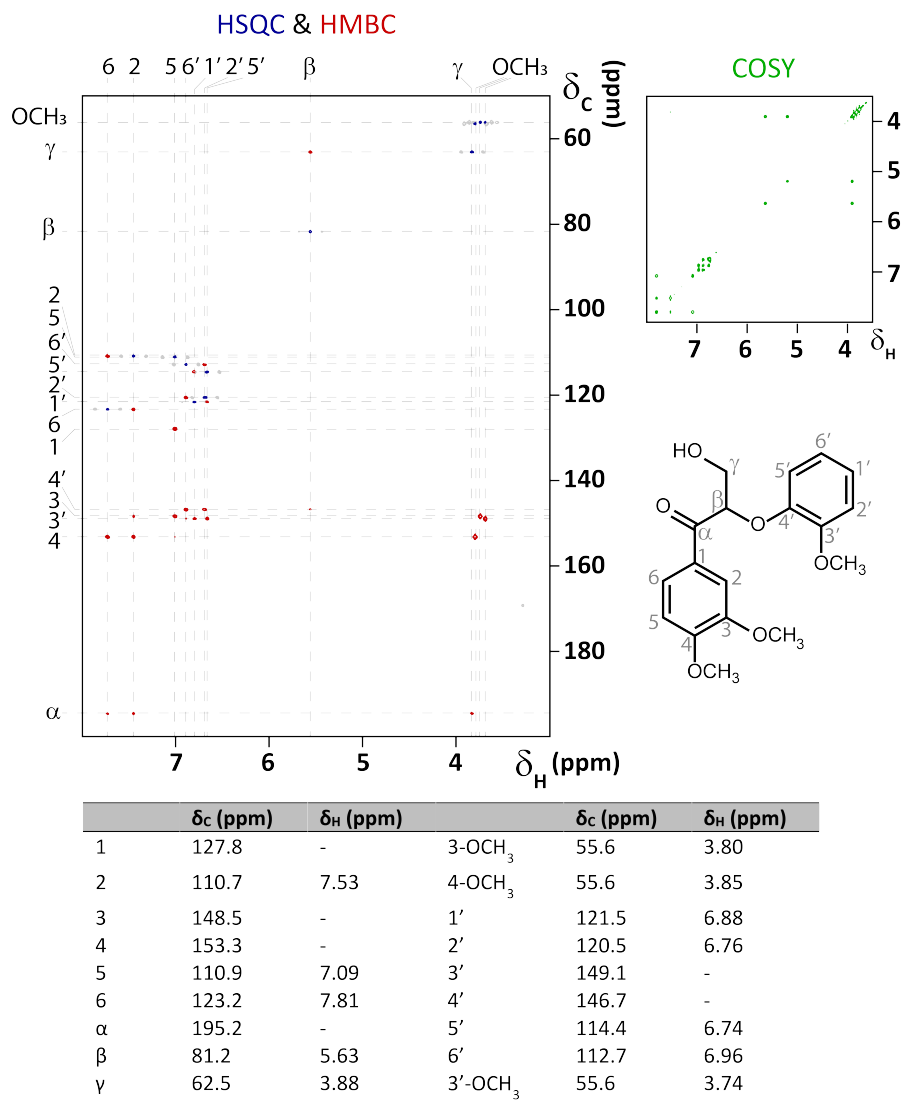


Fig. S4.1 HSQC (blue), HMBC (red) and COSY (green) spectra of purified VBG_{ox}. Grey peaks correspond to one-bond correlations from the HMBC experiment.

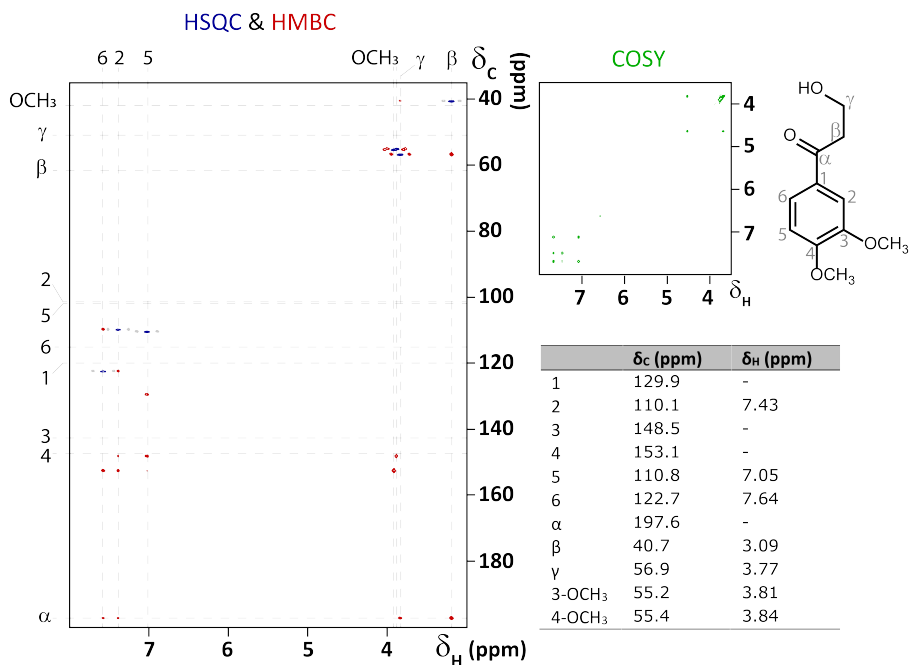


Fig. S4.2 HSQC (blue), HMBC (red) and COSY (green) spectra of purified CLP. Grey peaks correspond to one-bond correlations from the HMBC experiment.

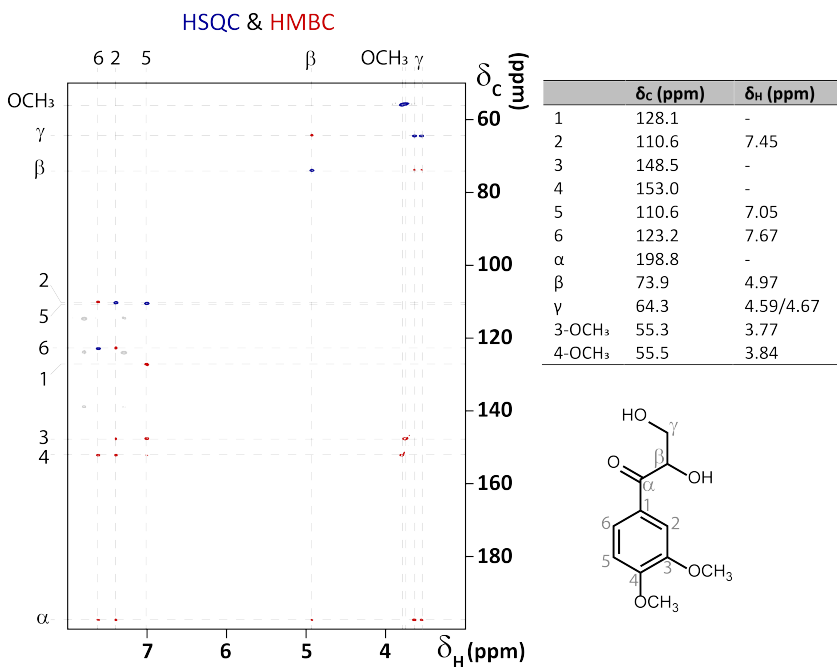


Fig. S4.3 HSQC (blue) and HMBC (red) spectra of partially purified CLP II. Grey peaks correspond to one-bond correlations from the HMBC experiment and an unknown impurity.

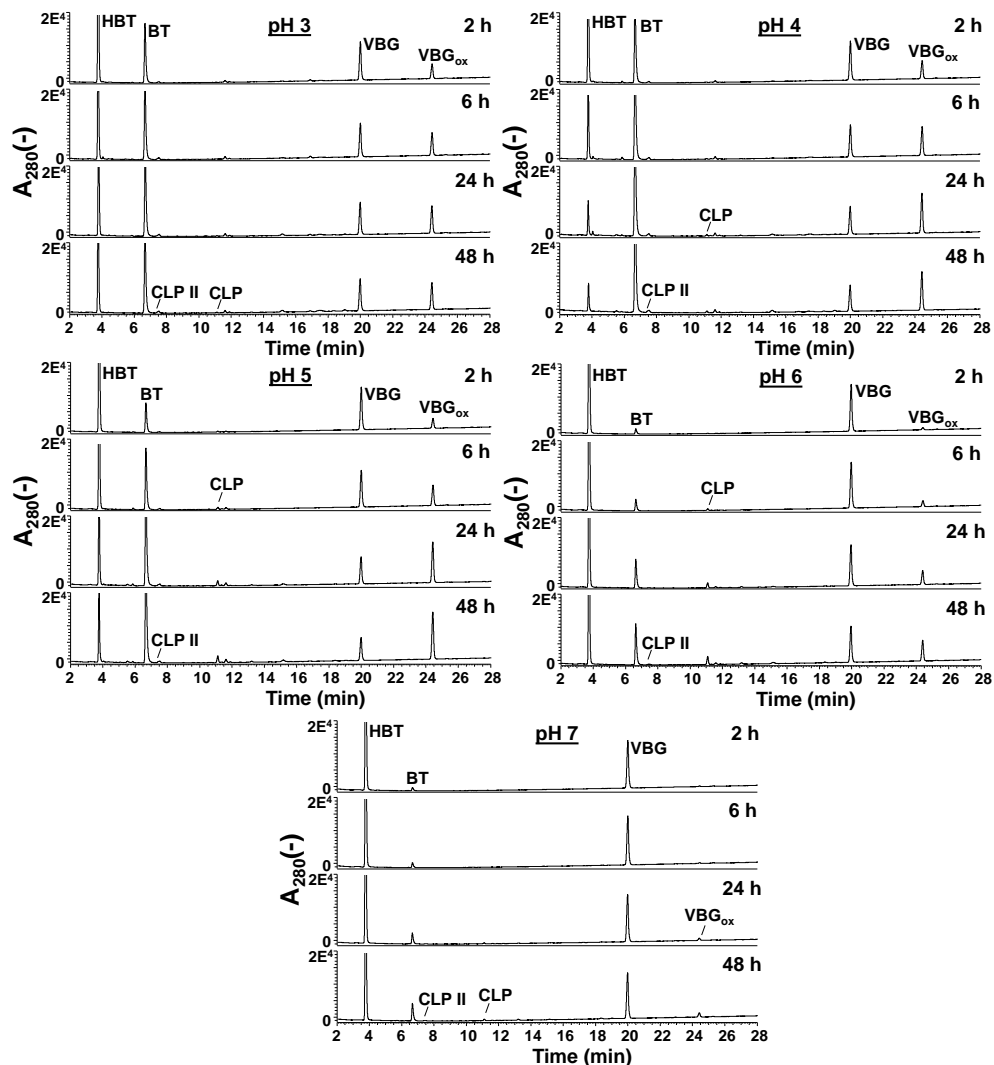


Fig. S4.4 RP-UHPLC-UV₂₈₀ chromatograms of VBG incubated for 2, 6, 24 and 48 h with laccase/HBT at in 20/40 mM citrate/phosphate buffers at pH 3-7.

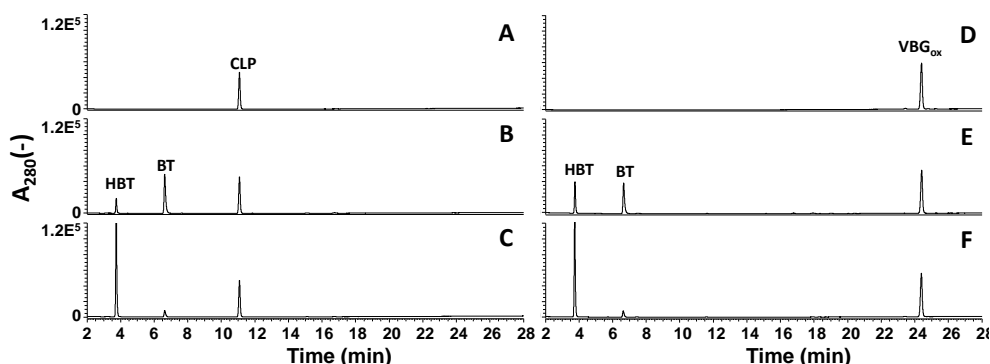


Fig. S4.5 RP-UHPLC-UV₂₈₀ chromatograms of purified CLP (A-C) and VBG_{ox} (D-F) after 24 h of incubation in 20/40 mM citrate/phosphate buffers in the presence or absence of laccase/HBT. A&D: Controls without laccase/HBT, B&E: Incubation with laccase/HBT at pH 4, and C&F: Incubation with laccase/HBT at pH 6.

4.6.2 Oxygen consumption measurement

Oxygen consumption measurements were performed by using a Hansatech Oxytherm system (Hansatech Kings Lynn, UK). HBT solutions (20 mM) were prepared in citrate/phosphate buffer (20/40 mM) at pH 4 and pH 5. The solutions (1 mL) were added to the measuring cell and were left to equilibrate at 40 °C under magnetic stirring (75 rpm). Once the oxygen concentration was stable, laccase was added at a final concentration of 2 U/mL. The relative rates (at pH 4 and 5) were calculated from the O₂ consumption between 20 and 220 s after laccase addition. Data acquisition was performed using the associated Oxygraph Plus software.

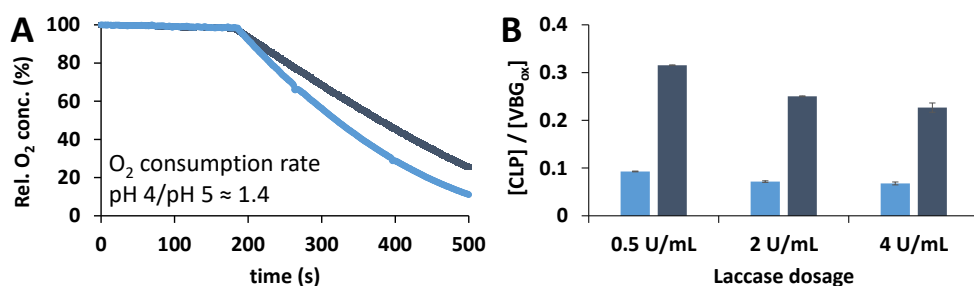


Fig. S4.6 Relative laccase activity toward HBT at pH 4 (blue) and 5 (navy) based oxygen consumption measurements (A) and molar ratios CLP/VBG_{ox} at pH 4 (blue) and 5 (navy) with varying laccase dosages (B). Although laccase loading slightly affected the product distribution, the figure shows that the effect of an 8-fold increase in laccase dosage is rather small compared to the effect of pH. As the laccase activity toward HBT is only 1.4-fold higher at pH 4 than at pH 5, it can be concluded that the observed pH effect is not (indirectly) caused by the effect of pH on laccase activity.

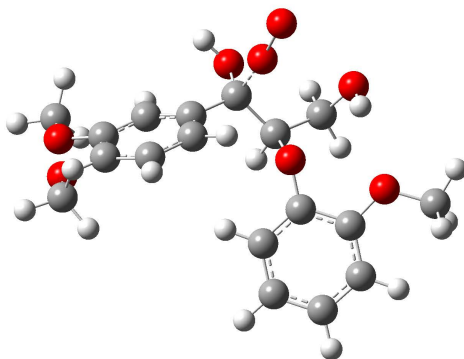


Fig. S4.7 Optimized geometry of the transition state (TS) of O₂ addition to the VBG benzylic radical, assuming quartet spin (TS 2 in Fig. 4.8). The quartet spin trajectory yielded a clear TS only if the O-O bond length in the incoming O₂ molecule was restricted at 1.57 Å and the H-O bond of the secondary hydroxyl group was restricted at 0.97 Å. Without doing so, TS 4 instead of TS 2 was found (see Fig. 4.8).

Table S4.2 Cartesian coordinates of the optimized geometry of TS 2

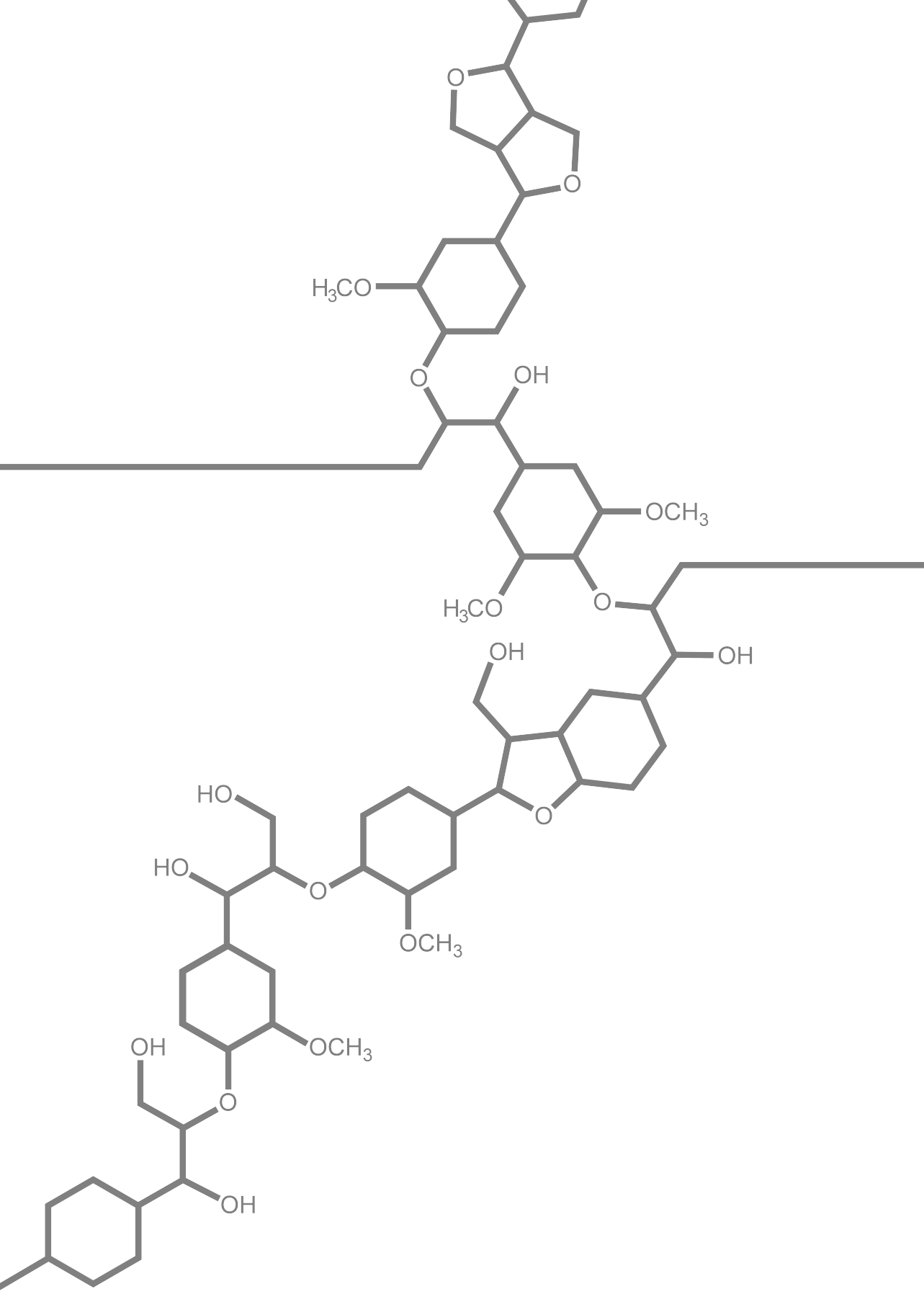
atom	X	Y	Z	atom	X	Y	Z
C	1.303512	-0.03576	1.209347	H	2.518265	-1.40857	-1.66234
C	2.361979	0.834927	1.49746	H	-0.73754	-0.47034	-1.65906
C	3.490709	0.903712	0.668318	H	-2.93384	-1.30225	-1.7602
C	3.553271	0.068738	-0.48595	H	-1.85073	-2.71384	-1.9459
C	2.491632	-0.79775	-0.76463	H	-5.08507	2.607132	-0.21456
C	1.356343	-0.85804	0.076675	H	-3.67073	4.393891	-1.1675
C	0.219704	-1.76514	-0.28696	H	-1.21613	4.035638	-1.47799
O	4.561827	1.720824	0.873609	H	-0.19997	1.837347	-0.7924
C	-1.05298	-1.06743	-0.78346	H	-3.08508	-1.99326	0.48525
C	-2.22102	-1.96617	-1.23501	H	5.741516	-0.37688	-2.87277
O	-1.50358	-0.18572	0.263031	H	4.762562	-1.69803	-2.14433
C	-2.0627	1.004987	-0.15396	H	3.961886	-0.42296	-3.12696
C	-3.45366	1.201472	0.025232	H	-5.91474	-0.6727	1.098828
C	-4.01985	2.433836	-0.3427	H	-5.811	1.098157	1.395637
C	-3.21352	3.446476	-0.88619	H	-6.04223	0.477884	-0.27727
C	-1.84064	3.246414	-1.0633	C	4.537565	2.570147	2.026264
C	-1.26841	2.021434	-0.68938	H	3.684019	3.265609	1.985623
O	-2.85563	-2.66139	-0.17838	H	4.480814	1.975884	2.952035
O	4.674372	0.197445	-1.25592	H	5.477695	3.129474	1.997496
C	4.779293	-0.63021	-2.41714	O	0.522782	-2.7948	-1.15114
O	-4.14722	0.145368	0.551807	H	1.331197	-3.22117	-0.83002
C	-5.56585	0.283236	0.696598	O	-0.3973	-3.29038	2.57884
H	0.44404	-0.08636	1.868289	O	-0.17157	-2.54168	1.220137
H	2.303289	1.458727	2.384976				

Table S4.3 Residual laccase activities after 48 h of incubation with VBG and HBT in different buffers.

Buffer pH	Buffer molarity & type	Residual laccase activity (%)
4	20/40 mM citrate/phosphate	0.2
4	2 M citrate	6.6
6	20/40 mM citrate/phosphate	1.1
6	2 M citrate	12.4

References Supporting Information

1. Gilli P, Pretto L, Bertolasi V and Gilli G. Predicting hydrogen-bond strengths from acid-base molecular properties. The pKa slide rule: toward the solution of a long-lasting problem. *Accounts of Chemical Research* **2008**, 42, 33-44.
2. Genovese A, Gambuti A, Lamorte SA and Moio L. An extract procedure for studying the free and glycosilated aroma compounds in grapes. *Food Chemistry* **2013**, 136, 822-834.
3. Von Sonntag C. *Free-radical-induced DNA damage and its repair*. Springer, **2006**.



Understanding laccase/HBT-catalyzed grass delignification at the molecular level

Laccase/mediator systems (LMS) are potential green tools to improve the valorization of lignocellulosic biomass by selective degradation of lignin. Despite extensive attention devoted to lignin degradation by LMS in literature, knowledge on the underlying mechanisms is largely limited to model compound studies. Here, we report a mechanistic study on the delignification of wheat straw (WS) and corn stover (CS) by a laccase/HBT system. Quantitative ^{13}C -IS py-GC-MS analysis revealed that WS and CS were delignified in the range of 28-51% (w/w). Based on a combination of py-GC-MS, 2D NMR, SEC and RP-UHPLC-MS, extensive structural characterization of both residual and solubilized lignin structures was performed, from which we reconstructed the degradation pathway of native lignin by laccase/HBT. For the first time, we show that degradation of native lignin in the plant cell wall matrix by LMS occurs via both $\text{C}_\alpha\text{-C}_\beta$ cleavage and ether cleavage of $\beta\text{-O-4'}$ aryl ethers, and that the latter primarily occurs via cleavage of the $\beta\text{-O}$ bond. C_γ -coumaroylated substructures were found to be more recalcitrant towards degradation than non-acylated substructures. In addition to lignin degradation, our results provide evidence for grafting of HBT onto lignin.

Based on: Roelant Hilgers, Gijs van Erven, Vincent Boerkamp, Irina Sulaeva, Antje Potthast, Mirjam A. Kabel and Jean-Paul Vincken. Understanding laccase/HBT-catalyzed grass delignification at the molecular level. *Green Chemistry* **2020**, 22 (5), 1735-1746.

5.1. Introduction

Agricultural by-products, such as wheat straw (WS) and corn stover (CS), are promising sources of polysaccharides for e.g. biochemical and biofuel production. Nevertheless, the co-occurrence of lignin in these lignocellulosic materials hinders efficient (enzymatic) conversion of the polysaccharides.¹ Hence, degradation or removal of lignin prior to polysaccharide conversion is advantageous.^{2,3} Although multiple chemical and/or physical delignification strategies have been reported, most of these require harsh conditions.^{2,4} Therefore, green alternatives are receiving increasing attention, such as biological pre-treatments (e.g. by using white-rot fungi) or fractionation with deep eutectic solvents.⁵⁻⁷ Another promising approach, especially with respect to industrial applicability, is enzymatic lignin degradation.⁸

Lignin is an aromatic polymer, built up via polymerization of the phenylpropanoids sinapyl alcohol, coniferyl alcohol and *p*-coumaryl alcohol. When incorporated in the lignin polymer, these building blocks form syringyl (S), guaiacyl (G) and *p*-hydroxyphenyl (H) subunits, respectively. Grass lignins also contain acetate, *p*-coumaric acid and ferulic acid, and also tricin may be incorporated.^{9,10} Polymerization of the phenylpropanoids results in a variety of interunit linkages, of which the β -O-4 linkage is the most abundant.¹¹ As most interunit linkages are formed via radical coupling of the phenolic hydroxyl groups of the phenylpropanoids, the majority (70-90%) of subunits in the lignin polymer are non-phenolic, while only 10-30% of the subunits are phenolic.¹²

Several classes of enzymes are known to be active toward lignin, including laccases and various peroxidases (i.e. lignin peroxidases, versatile peroxidases and manganese peroxidases). For industrial delignification of biomass, laccases are preferred to peroxidases, as laccases use molecular O₂ rather than H₂O₂ as electron acceptor, and are, in contrast to peroxidases, not inactivated by their electron acceptor.¹³ Due to their relatively low redox potential (≤ 800 mV vs. NHE),³ the phenolic subunits in lignin are most prone to direct laccase activity. In contrast, the non-phenolic subunits have higher redox potentials (> 1400 mV),^{14,15} and are, therefore, resistant to oxidation by laccase alone. Nevertheless, when laccase is combined with an appropriate mediator, its oxidizing capacity can be extended to non-phenolic lignin structures. In such a laccase/mediator system (LMS), laccase oxidizes the mediator, which subsequently undergoes a redox reaction with a (non-phenolic) lignin subunit. One of the most effective mediators known is 1-hydroxybenzotriazole (HBT).¹⁵⁻¹⁷

After oxidation by the mediator, the formed lignin radical can react further via a variety of pathways. These pathways have, so far, mainly been investigated by using low molecular weight model compounds, resembling substructures of lignin.¹⁸⁻²⁶ Dependent on the structure of the lignin radical, bond cleavage, radical coupling and a number of other modifications have been reported, and it has been suggested that these reaction pathways are in competition with each other. Obviously, this competition determines whether LMS treatment eventually results in overall polymerization or depolymerization.

Although these insights from model compound studies are valuable, so far, it remains unclear to what extent these insights can be extrapolated to LMS-induced lignin degradation *in situ*.

Over the past years, various studies have been published that report successful degradation or removal of lignin from biomass and paper pulp upon LMS treatment.²⁷⁻³⁹ In most of these studies, however, high laccase and mediator concentrations were used, which is undesirable from both economical and sustainability perspectives. In addition, these studies focused on the effectiveness of the LMS treatments, without performing in-depth structural characterization of the LMS treated lignin. Structural characterization may reveal accumulation of both degraded and recalcitrant substructures, and thereby provide insights into the mechanisms and bottlenecks underlying LMS based delignification. These insights are essential in order to increase the efficiency of LMS based biomass delignification. Although a number of previous studies included structural characterization of LMS treated lignin (e.g. by 2D NMR spectroscopy), limited insights were obtained into the effect of LMS on lignin structure, due to the following reasons: (i) Structural characterization was focused on the structure of residual lignin, rather than that of solubilized lignin, even in cases where lignin removal up to 50% was reported, and (ii) LMS treatments were often combined with alkaline peroxide treatments, which are known to induce structural changes in oxidized lignin.⁴⁰

In this study, our goal was to provide more insights into the mechanisms and bottlenecks underlying LMS-induced delignification of grasses. Wheat straw and corn stover were treated with a laccase/HBT system, after which lignin fractionation and purification was performed to allow detailed characterization of both residual and solubilized lignin populations. Treatments were done at both pH 4 and 6, as the used laccase has been reported to show optimal enzyme activity at pH 4, but optimal lignin model compound oxidation in a LMS at pH 6.⁴¹ A combination of py-GC-MS, 2D NMR, SEC and RP-UHPLC-MS was used to provide both quantitative and qualitative information on the structure of LMS treated lignin and enabled us to deduce the underlying ligninolysis mechanisms.

5.2. Materials & Methods

5.2.1. Materials

Wheat straw (*Triticum aestivum*, WS) and corn stover (*Zea mays*, CS) were kindly provided by CNC (Milsbeek, The Netherlands). Uniformly ¹³C-labeled wheat straw lignin isolate (¹³C-IS, 97.7 atom% ¹³C) was available in our laboratory from previous research,⁴² as well as 1-(3,4-dimethoxyphenyl)-3-hydroxypropan-1-one and 1-(3,4-dimethoxyphenyl)-2,3-dihydroxypropan-1-one.⁴³ Laccase from *Trametes versicolor* was purchased from Sigma Aldrich (St. Louis, MO, USA) and was used without any further purification. Laccase activity was measured spectrophotometrically by oxidation of ABTS (1 U = 1 μmol oxidized ABTS min⁻¹, see Supporting Information). Rovabio® Advance was obtained from Adisseo (Antony, France) and ViscoStar 150L was purchased from Dyadic

(Jupiter, FL, USA). All other chemicals were of analytical grade, purchased from commercial suppliers, and used without further purification. Water was purified using a MilliQ system (Millipore, Billerica, MA, USA).

5.2.2. Preparation of biomass for incubations

WS and CS were milled with a Centrifugal Mill ZM 200 (Retsch, Haan, Germany) (< 0.7 mm), after which acetone soluble material was removed using Soxhlet extraction. Subsequently, the acetone insoluble solids were dried overnight at 20 °C, followed by 3 h at 40 °C to remove the last traces of acetone. The residues were milled by using a Retsch PM100 planetary ball mill. Hereto, a 500 mL ZrO₂ grinding jar was charged with 30 g of sample and 100 ZrO₂ balls with a diameter of 10 mm. The net milling time was 1 h at an intensity of 600 rpm. To limit overheating, a 30 min break was inserted after every 15 min of milling. It should be noted that milling in a 500 mL jar setup proceeds with a higher intensity compared to the (routine) 50 mL scale, resulting in the same extent of milling in a much shorter time. The ball-milled biomass was washed multiple times with 100-300 mL aliquots of water until nearly colorless supernatants were obtained. The water-washed residues were lyophilized to yield milled wheat straw (MWS) and milled corn stover (MCS).

5.2.3. Laccase/mediator treatments

Laccase/HBT treatments of MWS and MCS were performed based on the experimental conditions reported by Rencoret et al.²⁸ Samples were prepared in duplicate at pH 4 and 6 in 75 mL Parr 2890HC reactors (Parr, Moline, IL, USA). Hereto, approximately 1.5 g MWS or MCS was suspended in 25 mL 0.2 M citric acid buffer. HBT was added at a concentration of 78 mM and incubations were started by adding laccase at doses of 50 U g⁻¹ MWS/MCS (pH 4 and 6) or 125 U g⁻¹ MWS/MCS (only pH 6). Incubations were performed at 40 °C under magnetic stirring (550 rpm) and 2 bar O₂ atmosphere. After 16 h, fresh laccase was added (half of the original dose) and the samples were incubated for another 8 h under the same conditions. Additional control incubations of MWS and MCS without laccase and HBT were also performed. After a total incubation time of 24 h, the suspensions were centrifuged ($4,700 \times g$, 10 min, 20 °C). The residue was washed five times with water at a 3.75 % (w/w) loading, and finally lyophilized to obtain the residue of laccase/HBT treatment (RES, see **Fig. 5.1**). The supernatants of the reaction suspensions, and the supernatants of the five washing steps were pooled and lyophilized to obtain water extractable lignin (WEL, **Fig. 5.1**). In addition to the above described incubations, an incubation with only laccase (3.1 U mL⁻¹) and HBT (78 mM) was performed in citric acid buffer at pH 5 (as a compromise pH) for 24 h at 40 °C. This sample was used as a control in NMR and RP-UHPLC-PDA-MS analyses.

5.2.4. Preparation of cellulolytic enzyme lignin (CEL) and water extractable cellulolytic enzyme lignin (WECEL)

For preparation of CEL (**Fig. 5.1**), approximately 650 mg (for WS) or 550 mg (for CS) RES was suspended in sodium acetate buffer (0.05 M, pH 4.8) to a 5% (w/w) loading. Subsequently, a xylanase-enriched enzyme cocktail (ViscoStar 150L) was added to a concentration of 0.01% (w/w), obtaining a 1/500 ratio (w/w; enzyme/biomass). The suspension was incubated under rotary shaking (20 rpm) for 24 h at 50 °C, after which it was centrifuged ($60,000 \times g$, 15 min, 20 °C). The residue was incubated for a second time, using fresh ViscoStar 150L and fresh buffer. The supernatant of the first incubation was stored at 4 °C. After incubation and centrifugation, the residue was washed three times with water at ~0.5% (w/w) solid loading, and lyophilized to yield cellulolytic enzyme lignin (CEL). The supernatants of both ViscoStar treatments and the supernatant from the three wash steps were combined and lyophilized to obtain water extractable cellulolytic enzyme lignin (WECEL).

5.2.5. Purification of WEL and WECEL

In order to remove free and lignin-bound carbohydrates, remaining HBT and related products, WECEL and WEL fractions were purified. As the amount of lignin in WEL fractions of control incubations was negligible, only WEL fractions of laccase/HBT treated WS and CS were purified. In the case of WECEL, both controls and laccase/HBT treated samples were included. For purification, treatment duplicates of the lyophilized WECEL and WEL fractions were pooled, after which 550-600 mg WS WECEL, 450-550 mg CS WECEL and 850-1270 mg WS and CS WEL (i.e. 50% of the obtained WEL) were weighed and dissolved at 5% (w/w) solid loading in 0.2 M citric acid buffer at pH 5.5 containing $57 \mu\text{g mL}^{-1}$ of a xylanase-enriched enzyme cocktail containing also ferulic acid esterase activity (Rovabio® Advance). The solutions were incubated for 24 h at 40 °C under rotary shaking (20 rpm), and lyophilized afterwards. The dried samples were suspended in 1% (v/v) formic acid and centrifuged ($4,700 \times g$, 20 °C, 5 min). The pellet was washed three times with 0.5 mL 1% (v/v) formic acid. All supernatants were pooled and fractionated by using reversed phase Flash chromatography (see Supporting Information for detailed procedure). The purified fractions, WECEL_{pure} and WEL_{pure} were used for further analyses.

5.2.6. Quantitative ¹³C-IS py-GC-MS

Quantification of lignin was performed by using a previously described py-GC-MS method, based on the use of a uniformly ¹³C-labeled lignin internal standard.^{42,44} In addition, the py-GC-MS data were used to fingerprint structural changes in lignin upon laccase/HBT treatment. A detailed description of the method can be found in the Supporting Information.

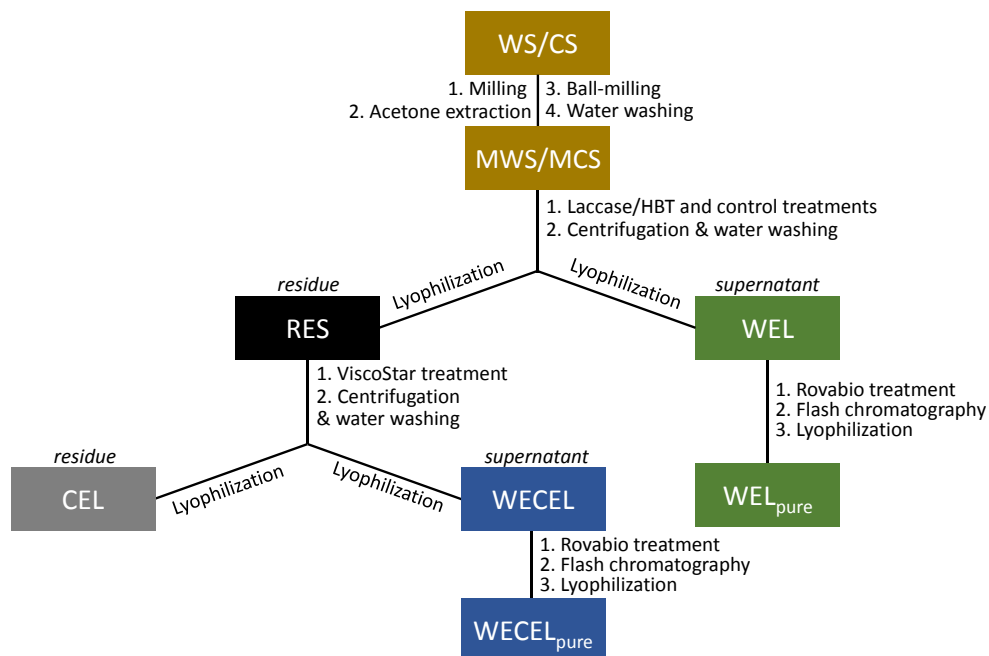


Fig. 5.1 Schematic overview of the incubations, fractionations and purifications in this study. (M)WS = (Milled) wheat straw; (M)CS = (Milled) corn stover; RES = Residue; WEL = Water-extractable lignin; CEL = Cellulolytic enzyme lignin; WECEL = Water-extractable cellulolytic enzyme lignin.

5.2.7. Klason lignin determination

Klason lignin determination was performed in duplicate based on a previously described method.⁴⁵ Here, 400 mg dried RES was weighed and 4 mL of 72% w/w sulfuric acid was added. Samples were incubated for 1 h at 30 °C, after which they were diluted with 44 mL water and incubated for 3 h at 100 °C. During both hydrolysis steps, samples were shaken and vortexed every 30 min. After hydrolysis, the suspensions were filtered over G4 glass filters. The residue was extensively washed with water until pH paper indicated that no residual acid was present. After drying overnight at 105 °C, the residue was weighed. The ash content (triplicates) of this residue was then determined by subjecting 1 mg portions of the sample, weighed on an XP6 excellence-plus microbalance (Mettler Toledo, Columbus, OH, USA) for 7 h to a temperature of 550 °C. The weight of the resulting residues relative to weight of the starting material (i.e. 1 mg) was taken as the ash content. The protein content was measured in duplicate according to the Dumas method using a Flash EA 1112 N analyzer (Thermo Scientific). Methionine was used as calibration standard, and a nitrogen to protein conversion factor of 6.25 was used. It should be noted that part of the nitrogen in laccase/HBT treated samples may have originated from HBT instead of protein. Since the contribution of HBT could not be accurately estimated, the calculated protein concentrations were reported without further

correction. The acid-soluble lignin content was not determined, due to interference of UV absorption of HBT.

5.2.8. 2D NMR spectroscopy

Structural characterization of the lignin fractions was performed by using 2D NMR analyses (HSQC and HMBC). Analysis of CEL samples was performed in gel state, based on a previously published method.⁴⁶ WECEL_{pure} and WEL_{pure} samples were measured in dissolved state. Detailed descriptions of the methods and integration procedures can be found in the Supporting Information. As no HSQC spectra of sufficient quality could be recorded for the RES fractions, relative abundances of structural features in the residue were determined based on the CEL and WECEL_{pure} fractions, which were both obtained from RES. Hereto, mass-weighted averages of HSQC integrals of CEL and WECEL_{pure} fractions were determined according to equation 1:

$$\int_{\text{res}} = (M_{\text{CEL}} * \int_{\text{CEL}} + M_{\text{WECEL}_{\text{pure}}} * \int_{\text{WECEL}_{\text{pure}}}) / (M_{\text{CEL}} + M_{\text{WECEL}_{\text{pure}}}) \quad (1)$$

Where \int_{res} is the mass-weighted averaged HSQC integral for residual lignin; M_{CEL} and $M_{\text{WECEL}_{\text{pure}}}$ are the masses of lignin in the CEL and WECEL_{pure} fraction, respectively; \int_{CEL} and $\int_{\text{WECEL}_{\text{pure}}}$ are the HSQC integrals obtained for the CEL and WECEL_{pure} fraction, respectively.

5.2.9. RP-UHPLC-PDA-MS

WECEL_{pure} fractions were analyzed to screen for lignin-HBT coupling products. Hereto, WECEL_{pure} fractions were dissolved at 1 mg mL⁻¹, centrifuged (12,500 × *g*, 5 min, 20 °C) and analyzed using RP-UHPLC-PDA-MS. A detailed description of the method can be found in the Supporting Information.

5.2.10. Size-exclusion chromatography

Size-exclusion chromatography (SEC) was performed on CEL and WECEL_{pure} samples. Hereto, fractions were dissolved at 4-8 mg mL⁻¹ in DMSO containing 0.5 w/v% LiBr, and were filtered through a 0.45 µm PTFE syringe filter. WECEL_{pure} completely dissolved, whereas some residue was observed in the case of CEL fractions. The soluble material was analyzed by using SEC-MALS_(IR) analysis, as described by Zinovyev et al.⁴⁷

5.3. Results & Discussion

5.3.1. Delignification of MWS MCS

After laccase/HBT treatment of MWS and MCS, the water-washed and lyophilized residues (i.e. WS and CS-RES fractions) were weighed and analyzed by using quantitative py-GC-MS analysis with ¹³C wheat straw lignin as internal standard. The analysis indicated that the laccase/HBT treatment resulted in a delignification of 44-51% and 36-44% for MWS

and MCS, respectively, whereas only 0-5% delignification was observed in control incubations without laccase/HBT (**Fig. 5.2**). These values are in a similar range as those reported in a previous study on laccase/HBT based wheat straw delignification and confirm that grasses can be effectively delignified by laccase/HBT treatments.²⁸ The used py-GC-MS based lignin quantification method has been validated for quantification of both wheat straw and corn stover lignin,^{42,44} but this was the first time the method was used for lignin quantification in LMS treated biomass. Therefore, for comparison, a Klason lignin determination was performed on the WS-RES fractions incubated at pH 4. Although the latter method suggested a MWS delignification of 32% at pH 4 (**Table S5.5**), which is, admittedly, lower than the values obtained by using py-GC-MS, both methods show a significant decrease in lignin content after laccase/HBT treatment. As both lignin quantification methods have their drawbacks (see Supporting Information for a more detailed discussion), and only py-GC-MS provides additional structural information, we used this method for lignin quantification on all other samples in this study. Although no lignin quantification could be performed for the unpurified WEL fractions,⁴⁸ it was assumed that all removed lignin ended up in the WEL fractions (see **Fig. 5.1**), as no volatile reaction products were expected to be formed.

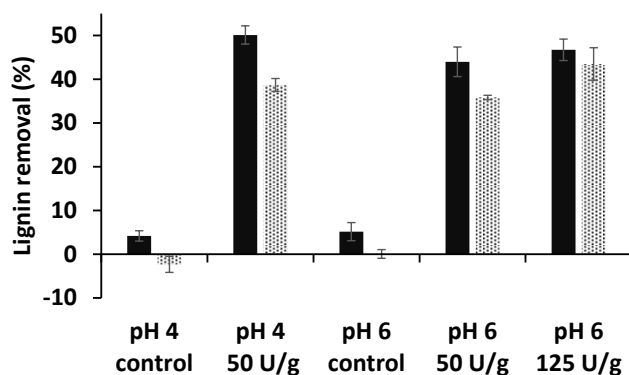


Fig. 5.2 Estimated lignin removal from milled wheat straw (solid bars) and milled corn stover (dotted bars) by laccase/HBT treatments based on quantitative ¹³C-IS py-GC-MS analysis (see Supporting Information for details).

5.3.2. Purification of lignin fractions

After LMS treatment, the residue (RES) and supernatant (WEL) were further fractionated and purified to facilitate structural lignin analysis by 2D NMR. Hereto, cellulolytic enzyme lignin (CEL) was prepared from RES, which resulted in a 2.0 to 2.7-fold increase in lignin content (**Table S5.9-S5.12**). The resulting supernatant (WECCEL) contained the released carbohydrates, but also a significant amount of lignin (i.e. 31-64% of the lignin originating from RES), indicating that also WECCEL lignin should be analyzed for a complete overview the residual lignin structure. To facilitate analysis, WECCEL was purified

by treatment with a xylanase-enriched enzyme cocktail containing additional ferulic acid esterase activity, and subsequent Flash chromatography. Based on py-GC-MS analysis it was estimated that this purification increased the lignin content from $\leq 10.6\%$ (w/w) in WECEL to $\geq 50.4\%$ (w/w) in WECEL_{pure} (Table S5.13-S5.16). The same strategy was used to remove sugars and mediator from WEL fractions, which resulted in WEL_{pure} fractions with estimated lignin contents of 6.6-23.2% (w/w) (Table S5.17). The summed lignin yields of the three final fractions (i.e. CEL, WECEL_{pure} and WEL_{pure}) were estimated to be 93-100% for control incubations and 39-67% for laccase/HBT incubations (see Table S5.9-S5.17), though it should be noted that the yields of the laccase/HBT treated fractions are expected to be underestimations (see discussion in Supporting Information).

5.3.3. Overall extent of lignin oxidation and degradation in CEL, WECEL_{pure} and WEL_{pure} fractions

As a measure for the extent of lignin oxidation in the purified WS and CS fractions (i.e. CEL, WECEL_{pure} and WEL_{pure}), the relative abundance of C_α-oxidized structures was determined based on semi-quantitative processing of 2D HSQC NMR spectra (see Fig. S5.1 for spectra and Table S5.3 for all assignments). It was observed that laccase/HBT treatment increased the relative content of C_α-oxidized subunits in all fractions, due to oxidation of both S and G-units (Fig. 5.3A and Fig. S5.2). The extent of C_α-oxidation was also estimated based on the abundance of C_α-oxidized products in py-GC-MS analysis of the same fractions (Fig. 5.3B). Although absolute values differed from the HSQC analysis, a very similar trend was observed: C_α-oxidation increased in all fractions, but the extent was vastly different for each fraction. Whereas CEL fractions of laccase/HBT treated MWS only showed 3-18% C_α-oxidation (based on HSQC NMR), for WECEL_{pure} and WEL_{pure} fractions, C_α-oxidation was 24-40% and 69-75%, respectively.

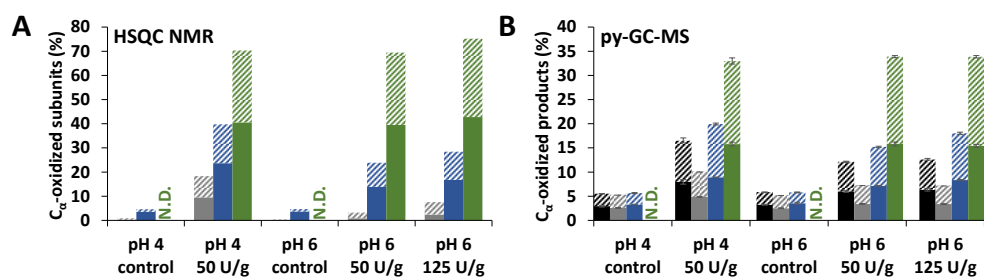


Fig. 5.3 Relative abundance of C_α-oxidized subunits as determined by using HSQC NMR (A) and estimated based on py-GC-MS (B) in RES (black), CEL (grey), WECEL_{pure} (blue) and WEL_{pure} (green) fractions of laccase/HBT treated MWS and controls. RES was only analyzed by using py-GC-MS. Solid and striped bars correspond to G and S units, respectively. Because of their low abundance, H-units are not included. Error bars in B represent the standard deviation of two treatment duplicates and two analytical duplicates. N.D. = Not determined. C_α-oxidation upon treatment of MCS showed similar trends and can be found in Fig. S5.2.

To verify that delignification of MWS and MCS was truly caused by cleavage of interunit linkages, the amount of intact interunit linkages per 100 aromatic subunits (S, G, H and oxidized analogues) was determined from the HSQC spectra. Indeed, in all fractions of laccase/HBT treated samples a decrease (up to 51%) in intact interunit linkages was observed (**Fig. 5.4A** and **Fig. S5.3**). We also estimated the amount of interunit linkages based on the py-GC-MS data. Hereto, the relative amount of pyrolysis products with intact 3-carbon side chains (PhC_γ) were taken, after correction for cleavage markers (i.e. diketones and vinylketones, as shown previously).^{5,43} Although the absolute values differed from those obtained using HSQC NMR, similar trends were observed (**Fig. 5.4B**). Interestingly, the amount of interunit linkages in WEL_{pure} was 2-4 times lower than in CEL and $\text{WECEL}_{\text{pure}}$.

Overall, the results shown in **Fig. 5.3** and **5.4** indicated that oxidized and degraded substructures accumulated in WEL_{pure} (i.e. solubilized lignin) and to a lower extent in $\text{WECEL}_{\text{pure}}$. Consequently, analysis of only residues, as often performed in literature,^{28,29,38,49} would heavily underestimate the overall effect of the laccase/HBT treatment on the structure of lignin, especially since a considerable amount of lignin is solubilized upon laccase/HBT treatment (**Fig. 5.2**).

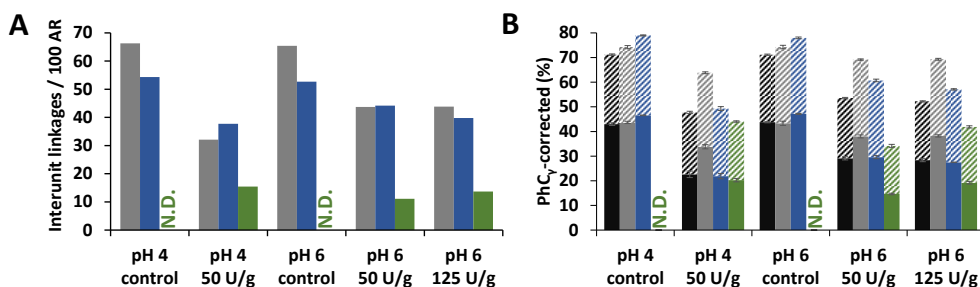


Fig. 5.4 HSQC NMR based (A) and py-GC-MS based (B) estimation of intact interunit linkages in RES (black), CEL (grey), $\text{WECEL}_{\text{pure}}$ (blue) and WEL_{pure} (green) fractions of laccase/HBT treated WS and controls. RES was only analyzed by using py-GC-MS. Data corresponding to CS showed similar trends (Fig. S5.3). In B, solid and striped bars refer to G and S units, respectively. Error bars in B represent the standard deviation of two treatment duplicates and two analytical duplicates. N.D. = Not determined.

5.3.4. Detailed insights into laccase/HBT induced reactions of lignin

To shed more light on the degradation pathways underlying the observed delignification, we zoomed in on the structural features of the most oxidized lignin fractions of laccase/HBT-treated MWS and MCS (i.e. $\text{WECEL}_{\text{pure}}$ and WEL_{pure}), and compared those to the structural features of the $\text{WECEL}_{\text{pure}}$ fraction of the corresponding control (**Fig. 5.5**). Although the spectra of laccase/HBT fractions showed multiple correlations that could

not be annotated (grey correlations in **Fig. 5.5**), the vast majority of these correlations also occurred in spectra from the Rovabio enzyme cocktail and the control incubation containing only laccase and HBT (**Fig. S5.5**). Thus, these correlations were mostly unrelated to lignin and were, therefore, not included in further processing of the spectra. From the lignin-related correlations in the aliphatic region it was observed that the decreased abundance of interunit linkages upon laccase/HBT treatment (**Fig. 5.4**) was caused by a decrease in β -*O*-4' linkages, as well as phenylcoumaran (β -5') and resinol (β - β') linkages (**Fig. 5.5A-C**). Concurrently, several new C-H correlations appeared, which were annotated based on comparison to HSQC spectra of purified degradation products of a lignin model dimer, and additional HMBC experiments (**Fig. S5.6**). Based on these annotations, it was concluded that three new structural features appeared: (i) C_o-oxidized intact β -*O*-4' linkages, (ii) hydroxypropiovanillone/syringone residues (HPV/HPS), and (iii) dihydroxy-propiovanillone/syringone residues (DHPV/S) (**Fig. 5.5**). HPV/S and DHPV/S resulted from cleavage of the β -*O* and *O*-4' bonds of β -*O*-4' linkages, respectively, and have been reported in studies on LMS-induced degradation of dimeric lignin model compounds.^{19,23,25} To the best of our knowledge, our research is the first to show evidence for such degradation pathways in a LMS treatment of actual lignocellulosic biomass.

In addition to the new structural features mentioned above, one of the formed correlations (F in **Fig. 5.5**) was tentatively annotated as a cyclohexadienone ketal (CHK).⁴³ Such structures have been reported as products from one-electron oxidation of β -*O*-4' linked model compounds,⁵⁰ but could in our study only be tentatively annotated, as no other evidence for CHK formation was found than the HSQC correlation at δ_C/δ_H 51.6/3.60.

The aromatic region also showed new C-H correlations after laccase/HBT treatment (**Fig. 5.5D-F**). In addition to C_o-oxidized S and G units, several new correlations appeared that showed overlap with HSQC correlations of HBT or its degradation products (**Fig. S5.5**). The presence of HBT-related correlations in WECEL_{pure} and WEL_{pure} fractions could be explained by the fact that, even after purification, some residual (free) HBT and its degradation product benzotriazole (BT) were present (**Table S5.6**). Nevertheless, as these HSQC correlations were, with lower intensity, also visible in the laccase/HBT treated CEL fractions (**Fig. S5.1**), and because the CEL fractions were extensively washed with water, it indicated that grafting of HBT on WS and CS lignin occurred during incubation, as has been suggested more often in literature.^{51,52} Corroborating evidence for HBT grafting was found in RP-UHPLC-MS analysis of WECEL_{pure} fractions, which revealed the formation of reaction products that were tentatively annotated as lignin-HBT coupling products, based on their molecular formula with 3 nitrogen and >>6 carbon atoms (**Table S5.6**). Therefore, the grey peaks in **Fig. 5.5E** and **F**, likely, predominantly correspond to a combination of free, degraded and lignin-grafted HBT.

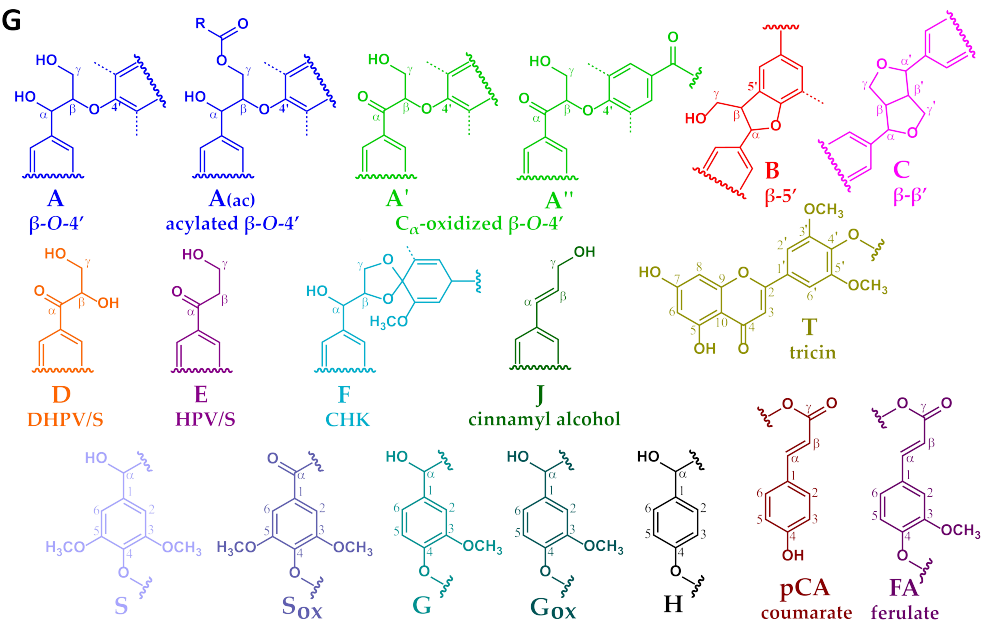
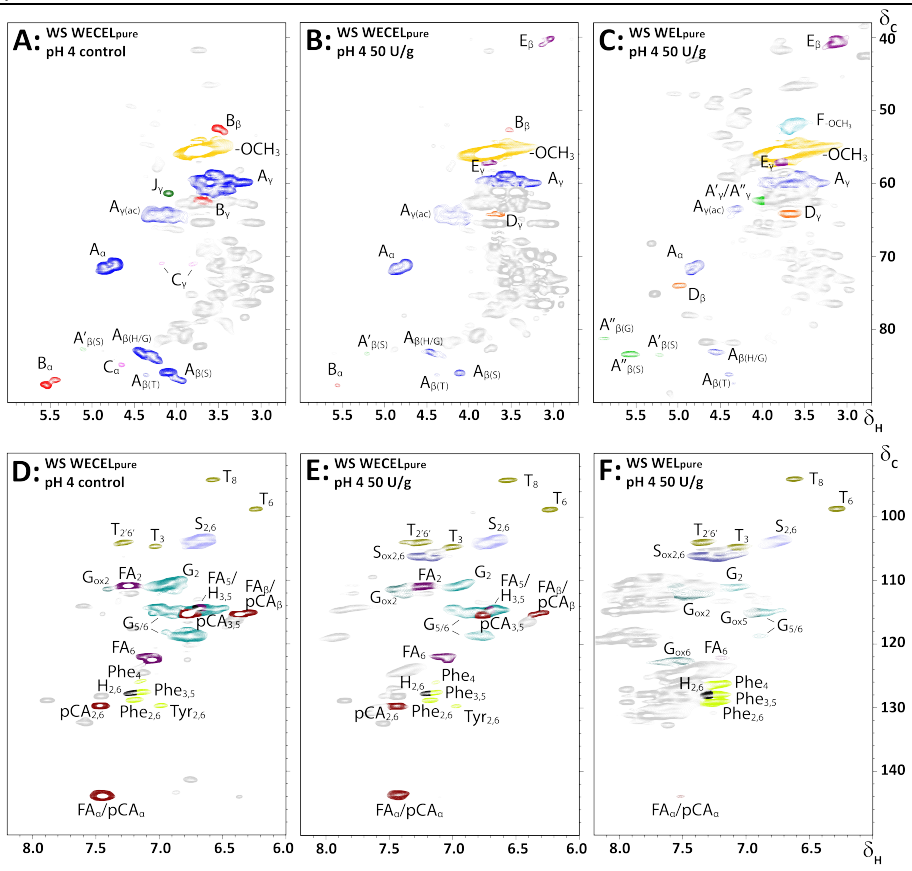


Fig. 5.5 (see previous page) Aliphatic (A-C) and aromatic (D-F) regions of HSQC spectra of (un)treated WS at pH 4: WECEL_{pure} of control incubation (A&D), WECEL_{pure} of laccase/HBT treatment (B&E) and WEL_{pure} of laccase/HBT treatment (C&F). Lignin substructures corresponding to the colored annotations are shown in (G). Dashed lines correspond to –H or –OCH₃. Annotations Phe and Tyr correspond to phenylalanine and tyrosine residues, respectively. Grey correlations are unassigned signals, mainly originating from Rovabio Advance and (reaction products of) HBT. Annotation was done based on literature and by comparison with purified degradation products of a lignin model compound (see Fig. S5.5).^{43,53-56} Note that F is a tentative annotation, and that the displayed structure is only one of the possible cyclohexadienone structures (see van Erven et al. for other possible structures).⁴³ A complete list of annotations can be found in Table S5.3. HSQC spectra of other incubations (pH 6 and CS) showed similar correlations (data not shown).

In addition to HSQC NMR, SEC-MALS_(IR) was performed on the CEL and WECEL_{pure} fractions to investigate the effect of the LMS treatment on the molecular weight distribution. No significant effect was observed in the case of CEL fractions. Remarkably, WECEL_{pure} fractions showed a slightly increased molecular weight after LMS treatment (**Fig. S5.4**). This suggests that degradation coincided with (re)polymerization.

As lignin model compound studies have shown that, in addition to ether cleavage products, also benzoic acids could be formed (via C_α-C_β cleavage) upon LMS treatment,^{23,25} and such structures would lack diagnostic correlations in HSQC spectra, we compared HMBC spectra of the WECEL_{pure} and WEL_{pure} fractions. The HMBC spectra indeed showed that, in addition to phenylketones, benzoic acids were formed upon laccase/HBT treatment, and that they were absent in the control sample (**Fig. 5.6**). In WEL_{pure} a small peak was also observed at δ_C 192 ppm, that was annotated as an aldehyde based on the presence of a correlation at δ_C/δ_H 192/9.8 in the corresponding HSQC spectrum (data not shown).⁵⁷ Nevertheless, as this HSQC correlation was also observed in WECEL_{pure} control samples, and laccase/HBT treatment did not result in more than 1 aldehyde group per 100 aromatic rings, we concluded that aldehyde formation was not a main degradation pathway during LMS treatment. Remarkably, very clear correlations were observed that corresponded to S-ketones and S-acids (δ_H 7.1-7.3), whereas the intensity of their G-analogues was very low. Possibly, G-units selectively undergo (re)polymerization and grafting, and that, via C-O coupling at C₅, this results in aromatic rings with HSQC correlations that overlap with those of S-units.^{58,59} Nevertheless, this hypothesis does not match with HSQC spectra, which showed formation of both C_α-oxidized G and S units, and py-GC-MS data, which showed that the cleavage markers (i.e. vinyl ketones and diketones)⁴³ are formed from both G and S units (**Tables S5.9-S5.17**). Therefore, the reason behind this discrepancy remains to be elucidated.

5.3.5. Relative susceptibility of lignin substructures to laccase/HBT activity

To get more insights into the relative susceptibility of lignin substructures towards degradation by laccase/HBT, lignin mass-weighted averages of the HSQC integrals of the residual lignin fractions (i.e. CEL and WECEL_{pure}) were determined (see Methods section

for calculation). Based on these integrals, relative abundances of structural features in the residual lignin were calculated (**Table 5.1**). The most apparent observations are discussed below.

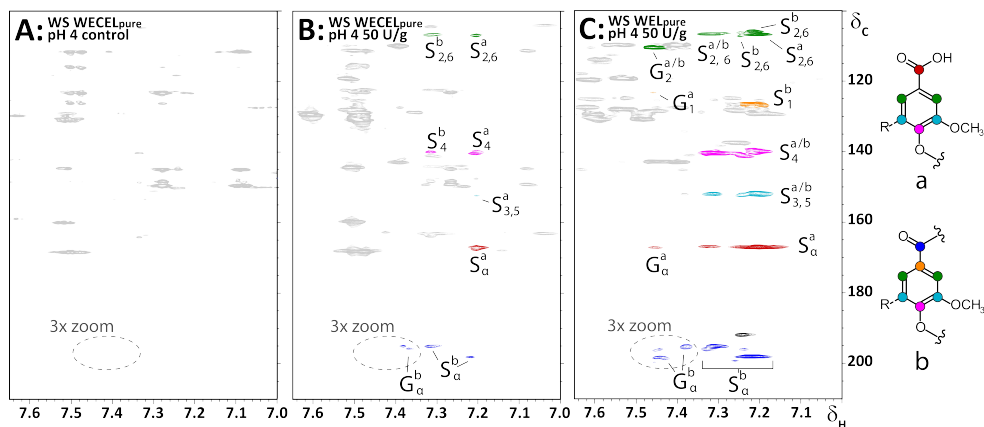


Fig. 5.6 Aromatic regions of ^1H - ^{13}C HMBC spectra obtained from WECEL_{pure} (A&B) and WEL_{pure} (C) fractions of WS incubated at pH 4. A = control, B&C = laccase/HBT treated. Annotation was done based on comparison with reported chemical shifts of lignin model compounds.⁶⁰ The black correlation at δ_{C} 192 ppm in C most likely corresponds to an aldehyde, but is only present in small amounts (see main text). Substructures corresponding to the annotated correlations are shown on the right. A full 3x zoomed version of the WEL_{pure} fraction, showing more ketone correlations, can be found in Fig. S5.7.

Firstly, **Table 5.1** shows that, although the overall decrease in intact linkages was mainly caused by degradation of β - O -4' linkages, the relative abundances of the interunit linkages suggested a preferential degradation of phenylcoumaran and resinol linkages. Although it is unknown whether these linkages are truly degraded or only modified, at least these findings show that not only β - O -4' linkages, but also β -5' and β - β' linkages are targets of the LMS treatment.

Secondly, in all laccase/HBT treated samples the S/G ratio of the residue increased, and this has previously been suggested to result from a preferential removal of G-units.^{28,29} At first sight, the increased S/G ratio indeed hints at a preferential removal of G-units, and this seems to be confirmed by the results shown in **Fig. 5.4B** and **Fig. S5.3B**, which indicates that mainly linkages are degraded that have their C_α atom connected to a G-unit (G-X linkage). Nevertheless, in case of preferential removal of G-units from the residue, an accumulation of G-units (low S/G ratio) is expected in the solubilized lignin. This is clearly not the case, as the S/G ratios in WEL_{pure} fractions are all higher than the S/G ratios of the residual lignin (**Table S5.7**). Another explanation for the observed increase in S/G ratio could be a higher degree of side-reactions of G-units (e.g. grafting and repolymerization at the C5 position), after which they may be excluded from data processing. A preferential removal of G-units and degradation of G-X linkages is therefore not proven.

Table 5.1 Structural features of residual lignin after laccase/HBT and control treatments as measured by HSQC NMR. Values displayed in this table are lignin mass-weighted averaged values from CEL and WECEL_{pure} fractions (see Methods section for calculation). Structural features of lignin in WECEL_{pure} fractions can be found in Table S5.7. ^a Amount of linkages per 100 aromatic units (S+S_{ox}+G+G_{ox}+H). ^b Numbers between brackets refer to relative abundance.

Laccase (U g ⁻¹)	Wheat straw						Corn stover					
	pH 4			pH 6			pH 4			pH 6		
	0	50		0	50		0	50		0	50	125
Lignin subunits (%)												
H	3	3		3	3		3	5		3	4	4
G	64	37		65	51		58	40		59	50	49
G _{ox}	1	19		1	8		5	13		4	7	9
S	31	28		31	31		34	32		34	32	32
S _{ox}	1	13		1	7		1	10		0	7	6
S/G	0.48	0.75		0.47	0.63		0.57	0.81		0.57	0.68	0.67
Hydroxycinnamates^a												
pCA	10	11		10	11		69	98		68	87	86
FA	26	22		27	19		74	28		72	22	26
Flavonoids^a												
Tricin	10	10		15	7		6	6		8	4	4
Interunit linkages^{a,b}												
β-O-4' (A)	52 (82)	28 (82)		51 (82)	42 (85)		46 (91)	27 (92)		40 (91)	30 (88)	23 (88)
β-O-4' _{ox} (A'/A'')	1 (2)	4 (12)		2 (3)	2 (5)		1 (1)	1 (2)		1 (1)	3 (7)	1 (5)
β-5' (B)	8 (13)	2 (6)		8 (12)	4 (9)		4 (7)	2 (6)		3 (8)	2 (5)	2 (8)
β-β' (C)	2 (3)	0 (0)		2 (3)	1 (2)		0 (0)	0 (0)		0 (0)	0 (0)	0 (0)
Total (100%)	63	35		63	50		50	29		44	35	26
Cleavage products^a												
DHPV/DHPS (D)	0.0	0.7		0.0	0.0		0.0	0.0		0.0	0.0	0.0
HPV/HPS (E)	0.3	3.4		0.0	1.0		0.0	0.6		0.0	0.5	0.8

Thirdly, the results shown in **Table 5.1** indicate that μ CA moieties accumulate in the residual lignin, in particular in CS. This accumulation is confirmed by an increased abundance of 4-vinylphenol in py-GC-MS analysis of laccase/HBT treated samples (**Table S5.18**).⁶¹ Hence, it was concluded that μ CA-esterified linkages were more recalcitrant toward degradation by laccase/HBT than other linkages. This may explain the somewhat lower degree of delignification in incubations of MCS (**Fig. 5.2**), since the μ CA content of CS is much higher than that of WS (**Table 5.1**). Extrapolating this observation to other lignocellulosic materials, it could be expected that materials with a low degree of μ CA-acylation, such as barley straw and rye straw,⁶² are better targets for LMS based delignification strategies than highly μ CA-acylated materials like sugarcane bagasse.⁵⁵ Lastly, a remarkable pH effect was observed for the degradation of tricin after laccase/HBT treatment. Whereas the relative abundance of tricin remained unaltered at pH 4, a decrease was observed at pH 6. As no accumulation of tricin was observed in the WEL_{pure} fraction, tricin was truly degraded, rather than only solubilized. In summary, these insights show that the laccase/HBT acts on a broad range of lignin substructures, and that the relative susceptibility is dependent on both the local structure of lignin and the reaction conditions.

5.3.6. Mechanisms underlying grass delignification by laccase/HBT

Overall, our results indicate that the β -O-4' linkages of MWS and MCS lignin undergo four types of reactions in laccase/HBT treatments: (i) C $_{\alpha}$ -C $_{\beta}$ cleavage, yielding carboxylic acid residues (route A in **Fig. 5.7**); (ii) O-4' cleavage, yielding DHPV/S residues (route B in **Fig. 5.7**); (iii) β -O cleavage, yielding HPV/S residues (route C in **Fig. 5.7**); and C $_{\alpha}$ -oxidation of intact linkages (route D in **Fig. 5.7**). As HPV/S residues and C $_{\alpha}$ -oxidized β -O-4' linkages are formed to a much larger extent than DHPV/S residues (**Table 5.1** and **Table S5.7**), we concluded that C $_{\alpha}$ -oxidation and β -O cleavage are the major reactions induced by laccase/HBT treatments and that O-4' cleavage only occurs to a minor extent. A quantitative comparison between these pathways and C $_{\alpha}$ -C $_{\beta}$ cleavage was not possible, as benzoic acids (formed via C $_{\alpha}$ -C $_{\beta}$ cleavage) lacked diagnostic HSQC correlations.

Lignin oxidation by HBT radicals is generally suggested to occur via hydrogen atom transfer (HAT), which results in the formation of benzylic radicals.¹⁴ The formation of carboxylic acids, HPV/S and C $_{\alpha}$ -oxidized linkages can, indeed, be explained from benzylic radical intermediates (**Fig. 5.7**). The formation of DHPV/S, however, is more likely to occur via a radical cation intermediate. The latter is formed via direct electron transfer (ET), rather than HAT. Although the redox potentials of non-phenolic lignin subunits (> 1.4 V vs. NHE)^{14,15} are higher than that of HBT (1.08 V vs. NHE),¹⁵ a slow ET between HBT radicals and non-phenolic lignin subunits with relatively low redox potentials seems

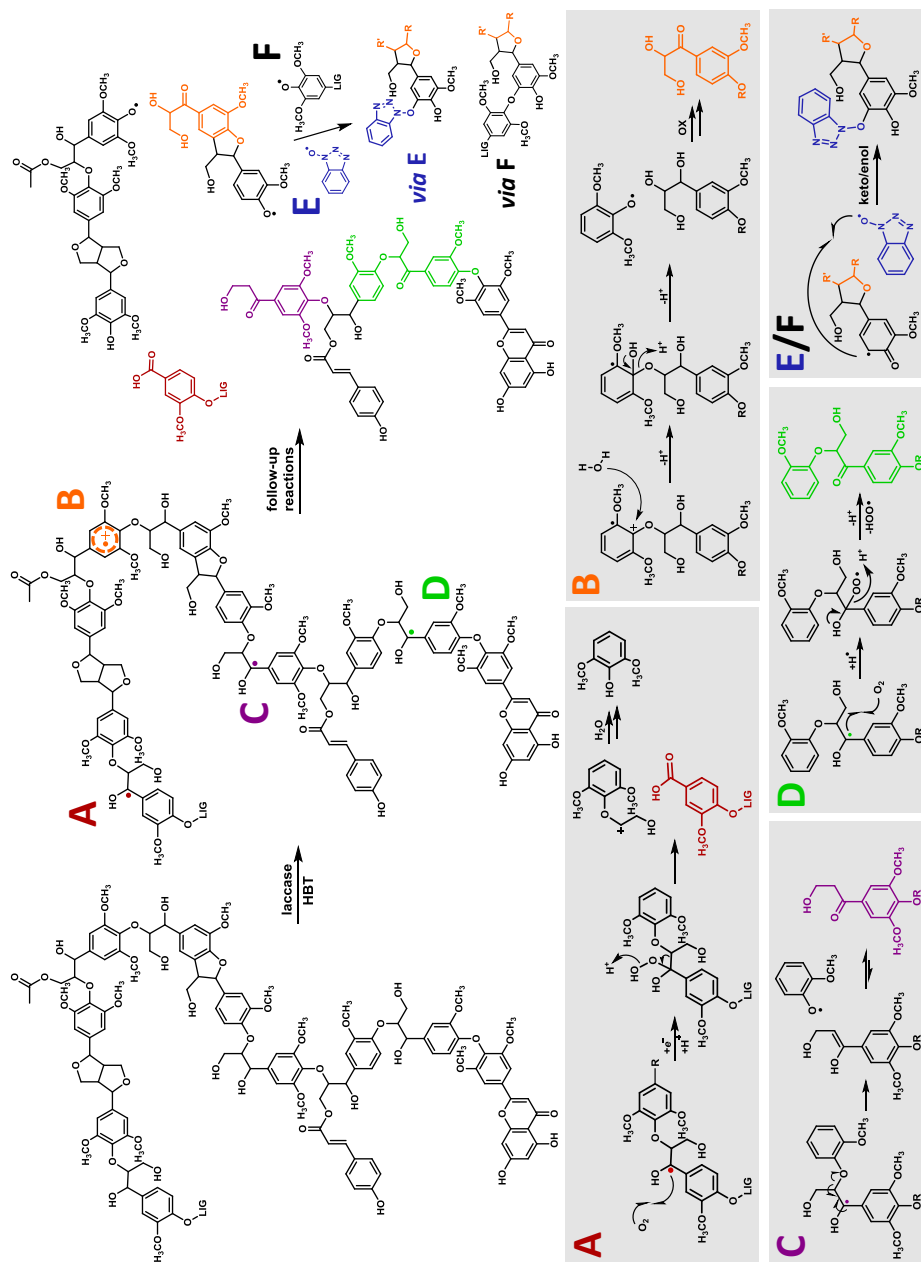


Fig. 5.7 General overview of the observed structural changes upon laccase/HBT treatment of MWS and MCS and suggested corresponding reactions mechanisms, shown on substructures of the lignin structure in the upper panel. A = $C_{\alpha}-C_{\beta}$ cleavage, B = $O-4'$ cleavage, C = $\beta-O$ cleavage, D = C_{α} -oxidation, E = HBT grafting and F = repolymerization. As E and F are expected to follow similar mechanisms, only reaction E is completely shown. Mechanisms are based on model compound studies in literature.^{18,23,63,64} Degradation pathways of $\beta-5'$ and $\beta-\beta'$ linkages are not distinctly shown due to their low abundance.

plausible, and has been suggested more often.²³ Since S-units have a lower redox potential than G-units, due to the presence of an extra methoxyl group, it is expected that *O*-4' cleavage preferentially occurs in β -*O*-4' linkages with a 4'-linked S-unit. Route B in **Fig. 5.7** could, in theory, also occur via one-electron oxidation of C_{α} -oxidized structures and subsequent cleavage. Since we found that a C_{α} -oxidized lignin dimer (veratrone) was inert to the laccase/HBT system (data not shown), we consider the mechanism displayed in **Fig. 5.7** more plausible. Considering that we observed that C_{α} -oxidation and β -*O* cleavage were more predominant than *O*-4' cleavage, our results confirm that HAT is the main oxidation mechanism underlying lignin degradation by laccase/HBT.

Upon cleavage of β -*O*-4' linkages, phenoxyl radicals are expected to be formed.²³ We suggest that these radicals undergo coupling (grafting) to HBT radicals present in solution. This is further evidenced by model compound studies, in which HBT-coupling was observed with phenoxyl radicals, and not with benzylic radicals.^{18,19} In addition to HBT grafting, phenoxyl radicals may also undergo radical coupling to other lignin-derived radicals (repolymerization).^{18,64} Although no NMR based evidence could be obtained for this, SEC results indeed suggested that (re)polymerization of lignin occurred (**Fig. S5.4**).

The insights presented in this study can be used as a starting point for further optimization of lignin degradation by LMS. Our results indicated that the presence of esterified *p*CA decreases the susceptibility of linkages toward degradation by LMS. Therefore, removal of *p*CA esters, either during a pretreatment step or simultaneously with LMS treatment, is expected to increase LMS-induced lignin degradation. A green approach for *p*CA removal could be the addition of feruloyl or coumaroyl esterases.^{65,66}

5.4. Conclusions

By fractionation, purification and comprehensive analysis of laccase/HBT treated milled wheat straw (MWS) and milled corn stover (MCS), we were able to elucidate laccase/HBT induced delignification pathways. We have shown that laccase/HBT treatment successfully degrades lignin in MWS and MCS, via both ether cleavage and C_{α} - C_{β} cleavage. For the first time, we showed that β -*O*-4' ether cleavage predominantly occurs via cleavage of the β -*O* bond, rather than the *O*-4' bond. Furthermore, our findings suggested that *p*CA-esterification decreased the susceptibility of linkage degradation in lignin and that HBT grafts onto lignin. These mechanistic insights contribute to the fundamental understanding of enzymatic lignin degradation and can be used to optimize lignin degradation by LMS or comparable treatments in the future.

5.5. References and notes

1. Mansfield SD, Mooney C and Saddler JN. Substrate and enzyme characteristics that limit cellulose hydrolysis. *Biotechnology Progress* **1999**, *15* (5), 804-816.
2. Christopher LP, Yao B and Ji Y. Lignin biodegradation with laccase-mediator systems. *Frontiers in Energy Research* **2014**, *2*, 12.
3. Munk L, Sitarz AK, Kalyani DC, Mikkelsen JD and Meyer AS. Can laccases catalyze bond cleavage in lignin? *Biotechnology Advances* **2015**, *33* (1), 13-24.
4. Behera S, Arora R, Nandhagopal N and Kumar S. Importance of chemical pretreatment for bioconversion of lignocellulosic biomass. *Renewable and Sustainable Energy Reviews* **2014**, *36*, 91-106.
5. Van Erven G, Nayan N, Sonnenberg ASM, Hendriks WH, Cone JW and Kabel MA. Mechanistic insight in the selective delignification of wheat straw by three white-rot fungal species through quantitative ¹³C-1S py-GC-MS and whole cell wall HSQC NMR. *Biotechnology for Biofuels* **2018**, *11* (1), 262.
6. Mamilla JL, Novak U, Grilc M and Likozar B. Natural deep eutectic solvents (DES) for fractionation of waste lignocellulosic biomass and its cascade conversion to value-added bio-based chemicals. *Biomass and Bioenergy* **2019**, *120*, 417-425.
7. Gall DL, Ralph J, Donohue TJ and Noguera DR. Biochemical transformation of lignin for deriving valued commodities from lignocellulose. *Current Opinion in Biotechnology* **2017**, *45*, 120-126.
8. Martínez ÁT, Ruiz-Duenas FJ, Martínez MJ, del Río JC and Gutierrez A. Enzymatic delignification of plant cell wall: from nature to mill. *Current Opinion in Biotechnology* **2009**, *20* (3), 348-357.
9. Ralph J, Lapierre C and Boerjan W. Lignin structure and its engineering. *Current Opinion in Biotechnology* **2019**, *56*, 240-249.
10. Ralph J, Lundquist K, Brunow G, Lu F, Kim H, Schatz PF, Marita JM, Hatfield RD, Ralph SA and Christensen JH. Lignins: natural polymers from oxidative coupling of 4-hydroxyphenylpropanoids. *Phytochemistry Reviews* **2004**, *3* (1-2), 29-60.
11. Vanholme R, Demedts B, Morreel K, Ralph J and Boerjan W. Lignin biosynthesis and structure. *Plant Physiology* **2010**, *153* (3), 895-905.
12. Lundquist K and Parkäs J. Different types of phenolic units in lignins. *BioResources* **2011**, *6* (2), 920-926.
13. Mate DM and Alcalde M. Laccase: a multi-purpose biocatalyst at the forefront of biotechnology. *Microbial Biotechnology* **2017**, *10* (6), 1457-1467.
14. Baiocco P, Barreca AM, Fabbrini M, Galli C and Gentili P. Promoting laccase activity towards non-phenolic substrates: a mechanistic investigation with some laccase-mediator systems. *Organic & Biomolecular Chemistry* **2003**, *1* (1), 191-197.
15. Fabbrini M, Galli C and Gentili P. Comparing the catalytic efficiency of some mediators of laccase. *Journal of Molecular Catalysis B: Enzymatic* **2002**, *16* (5), 231-240.
16. d'Acunzo F and Galli C. First evidence of catalytic mediation by phenolic compounds in the laccase-induced oxidation of lignin models. *European Journal of Biochemistry* **2003**, *270* (17), 3634-3640.
17. Astolfi P, Brandi P, Galli C, Gentili P, Gerini MF, Greci L and Lanzalunga O. New mediators for the enzyme laccase: mechanistic features and selectivity in the oxidation of non-phenolic substrates. *New Journal of Chemistry* **2005**, *29* (10), 1308-1317.
18. Hilgers RJ, Vincken J-P, Gruppen H and Kabel MA. Laccase/mediator systems: Their reactivity towards phenolic lignin structures. *ACS Sustainable Chemistry & Engineering* **2018**, *6* (2), 2037-2046.
19. Hilgers R, Twentyman-Jones M, van Dam A, Gruppen H, Zuilhof H, Kabel MA and Vincken J-P. The impact of lignin sulfonation on its reactivity with laccase and laccase/HBT. *Catalysis Science & Technology* **2019**, *9* (6), 1535-1542.
20. Kawai S, Asukai M, Ohya N, Okita K, Ito T and Ohashi H. Degradation of a non-phenolic β-O-4 substructure and of polymeric lignin model compounds by laccase of *Coriolus versicolor* in the presence of 1-hydroxybenzotriazole. *FEMS Microbiology Letters* **1999**, *170* (1), 51-57.

21. Kawai S, Umezawa T and Higuchi T. Degradation mechanisms of phenolic β -1 lignin substructure model compounds by laccase of *Coriolus versicolor*. *Archives of Biochemistry and Biophysics* **1988**, 262 (1), 99-110.
22. Kawai S, Nakagawa M and Ohashi H. Aromatic ring cleavage of a non-phenolic β -O-4 lignin model dimer by laccase of *Trametes versicolor* in the presence of 1-hydroxybenzotriazole. *FEBS Letters* **1999**, 446 (2-3), 355-358.
23. Kawai S, Nakagawa M and Ohashi H. Degradation mechanisms of a nonphenolic β -O-4 lignin model dimer by *Trametes versicolor* laccase in the presence of 1-hydroxybenzotriazole. *Enzyme and Microbial Technology* **2002**, 30 (4), 482-489.
24. Potthast A, Rosenau T, Koch H and Fischer K. The reaction of phenolic model compounds in the laccase-mediator system (LMS) investigations by matrix assisted laser desorption ionization time-of-flight mass spectrometry (MALDI-TOF-MS). *Holzforschung* **1999**, 53 (2), 175-180.
25. Srebotnik E and Hammel KE. Degradation of nonphenolic lignin by the laccase/1-hydroxybenzotriazole system. *Journal of Biotechnology* **2000**, 81 (2), 179-188.
26. Bourbonnais R, Paice MG, Freiermuth B, Bodie E and Borneman S. Reactivities of various mediators and laccases with kraft pulp and lignin model compounds. *Applied and Environmental Microbiology* **1997**, 63 (12), 4627-4632.
27. Rico A, Rencoret J, Del Río JC, Martínez AT and Gutiérrez A. In-depth 2D NMR study of lignin modification during pretreatment of Eucalyptus wood with laccase and mediators. *BioEnergy Research* **2015**, 8 (1), 211-230.
28. Rencoret J, Pereira A, Del Río JC, Martínez AT and Gutiérrez A. Laccase-mediator pretreatment of wheat straw degrades lignin and improves saccharification. *BioEnergy Research* **2016**, 9 (3), 917-930.
29. Rico A, Rencoret J, Del Río JC, Martínez AT and Gutiérrez A. Pretreatment with laccase and a phenolic mediator degrades lignin and enhances saccharification of Eucalyptus feedstock. *Biotechnology for Biofuels* **2014**, 7 (1), 6.
30. Camarero S, Ibarra D, Martínez ÁT, Romero J, Gutiérrez A and Del Río JC. Paper pulp delignification using laccase and natural mediators. *Enzyme and Microbial Technology* **2007**, 40 (5), 1264-1271.
31. Du X, Li J, Gellerstedt G, Rencoret J, Del Río JC, Martínez AT and Gutiérrez A. Understanding pulp delignification by laccase-mediator systems through isolation and characterization of lignin-carbohydrate complexes. *Biomacromolecules* **2013**, 14 (9), 3073-3080.
32. Chen Q, Marshall MN, Geib SM, Tien M and Richard TL. Effects of laccase on lignin depolymerization and enzymatic hydrolysis of ensiled corn stover. *Bioresource Technology* **2012**, 117, 186-192.
33. Zheng Z, Li H, Li L and Shao W. Biobleaching of wheat straw pulp with recombinant laccase from the hyperthermophilic *Thermus thermophilus*. *Biotechnology Letters* **2012**, 34 (3), 541-547.
34. Babot ED, Rico A, Rencoret J, Kalum L, Lund H, Romero J, Del Río JC, Martínez ÁT and Gutiérrez A. Towards industrially-feasible delignification and pitch removal by treating paper pulp with *Myceliophthora thermophila* laccase and a phenolic mediator. *Bioresource Technology* **2011**, 102 (12), 6717-6722.
35. Barneto AG, Aracri E, Andreu G and Vidal T. Investigating the structure-effect relationships of various natural phenols used as laccase mediators in the biobleaching of kenaf and sisal pulps. *Bioresource Technology* **2012**, 112, 327-335.
36. Moldes D, Díaz M, Tzanov T and Vidal T. Comparative study of the efficiency of synthetic and natural mediators in laccase-assisted bleaching of Eucalyptus kraft pulp. *Bioresource Technology* **2008**, 99 (17), 7959-7965.
37. Moldes D, Cadena E and Vidal T. Biobleaching of Eucalypt kraft pulp with a two laccase-mediator stages sequence. *Bioresource Technology* **2010**, 101 (18), 6924-6929.
38. Rencoret J, Pereira A, Del Río JC, Martínez AT and Gutiérrez A. Delignification and saccharification enhancement of sugarcane byproducts by a laccase-based pretreatment. *ACS Sustainable Chemistry & Engineering* **2017**, 5 (8), 7145-7154.
39. Rencoret J, Pereira A, Marques G, Del Río JC, Martínez ÁT and Gutiérrez A. A commercial laccase-mediator system to delignify and improve saccharification of the fast-growing *Paulownia fortunei* (Seem.) Hemsl. *Holzforschung* **2018**, 73 (1), 45-54.

40. Gierer J, Imsgard F and Noren I. Studies on the degradation of phenolic lignin units of the β -aryl ether type with oxygen in alkaline media. *Acta Chemica Scandinavica B* **1977**, *31* (7), 561-572.
41. Rosado T, Bernardo P, Koci K, Coelho AV, Robalo MP and Martins LO. Methyl syringate: an efficient phenolic mediator for bacterial and fungal laccases. *Bioresource Technology* **2012**, *124*, 371-378.
42. Van Erven G, De Visser R, Merckx DWH, Strolenberg W, De Gijssel P, Gruppen H and Kabel MA. Quantification of lignin and its structural features in plant biomass using ^{13}C lignin as internal standard for pyrolysis-GC-SIM-MS. *Analytical Chemistry* **2017**, *89* (20), 10907-10916.
43. Van Erven G, Hilgers R, De Waard P, Gladbeek E-J, Van Berkel WJH and Kabel MA. Elucidation of *in situ* ligninolysis mechanisms of the selective white-rot fungus *Ceriporiopsis subvermispora*. *ACS Sustainable Chemistry & Engineering* **2019**, *7* (19), 16757-16764.
44. Van Erven G, De Visser R, De Waard P, Van Berkel WJH and Kabel MA. Uniformly ^{13}C labeled lignin internal standards for quantitative py-GC-MS analysis of grass and wood. *ACS Sustainable Chemistry & Engineering* **2019**, *7* (24), 20070-20076.
45. Jurak E, Punt AM, Arts W, Kabel MA and Gruppen H. Fate of carbohydrates and lignin during composting and mycelium growth of *Agaricus bisporus* on wheat straw based compost. *PLoS One* **2015**, *10* (10), e0138909.
46. Mansfield SD, Kim H, Lu F and Ralph J. Whole plant cell wall characterization using solution-state 2D NMR. *Nature Protocols* **2012**, *7* (9), 1579.
47. Zinovyev G, Sulaeva I, Podzimek S, Rössner D, Kilpeläinen I, Summerskii I, Rosenau T and Potthast A. Getting closer to absolute molar masses of technical lignins. *ChemSusChem* **2018**, *11* (18), 3259-3268.
48. Unpurified WEL fractions were expected to have a very high content of HBT, which is explosive in unhydrated form, and therefore unsuitable for pyrolysis.
49. Martin-Sampedro R, Capanema EA, Hoeger I, Villar JC and Rojas OJ. Lignin changes after steam explosion and laccase-mediator treatment of eucalyptus wood chips. *Journal of Agricultural and Food Chemistry* **2011**, *59* (16), 8761-8769.
50. Kawai S, Umezawa T and Higuchi T. *p*-Benzoquinone monoketals, novel degradation products of β -O-4 lignin model compounds by *Coriolus versicolor* and lignin peroxidase of *Phanerochaete chrysosporium*. *FEBS Letters* **1987**, *210* (1), 61-65.
51. Jestel T, Roth S, Heesel D, Kress A, Fischer R and Spiess AC. Laccase-induced HBT-grafting to milled beech wood reduces unspecific protein adsorption. *Biocatalysis and Biotransformation* **2019**, *37* (1), 66-76.
52. Munk L, Punt AM, Kabel MA and Meyer AS. Laccase catalyzed grafting of N-OH type mediators to lignin via radical-radical coupling. *RSC Advances* **2017**, *7* (6), 3358-3368.
53. Zeng J, Helms GL, Gao X and Chen S. Quantification of wheat straw lignin structure by comprehensive NMR analysis. *Journal of Agricultural and Food Chemistry* **2013**, *61* (46), 10848-10857.
54. Del Río JC, Rencoret J, Prinsen P, Martínez AT, Ralph J and Gutiérrez A. Structural characterization of wheat straw lignin as revealed by analytical pyrolysis, 2D-NMR, and reductive cleavage methods. *Journal of Agricultural and Food Chemistry* **2012**, *60* (23), 5922-5935.
55. Del Río JC, Lino AG, Colodette JL, Lima CF, Gutiérrez A, Martínez ÁT, Lu F, Ralph J and Rencoret J. Differences in the chemical structure of the lignins from sugarcane bagasse and straw. *Biomass and Bioenergy* **2015**, *81*, 322-338.
56. Guo H, Miles-Barrett DM, Neal AR, Zhang T, Li C and Westwood NJ. Unravelling the enigma of lignin OX: can the oxidation of lignin be controlled? *Chemical Science* **2018**, *9* (3), 702-711.
57. Martin AF, Tobimatsu Y, Kusumi R, Matsumoto N, Miyamoto T, Lam PY, Yamamura M, Koshiba T, Sakamoto M and Umezawa T. Altered lignocellulose chemical structure and molecular assembly in cinnamyl alcohol dehydrogenase-deficient rice. *Scientific Reports* **2019**, *9* (1), 1-14.
58. Li Y, Akiyama T, Yokoyama T and Matsumoto Y. NMR assignment for diaryl ether structures (4-O-5 structures) in pine wood lignin. *Biomacromolecules* **2016**, *17* (6), 1921-1929.

59. Yue F, Lu F, Ralph S and Ralph J. Identification of 4-*O*-5-units in softwood lignins via definitive lignin models and NMR. *Biomacromolecules* **2016**, *17* (6), 1909-1920.
60. Ralph SA, Ralph J and Landucci L. NMR database of lignin and cell wall model compounds. **2009**, available at URL www.glbrc.org/databases_and_software/nmrdatabase/.
61. In the py-GC-MS analysis, 4-vinylphenol was used as a marker for the abundance of *p*-coumaric acid. Although also pyrolysis of H-units may contribute to the formation of 4-vinylphenol, this contribution is expected to be minor as the abundance of H-units in the WS and CS fractions was very low ($\leq 5\%$).
62. Sun R, Sun XF, Wang SQ, Zhu W and Wang XY. Ester and ether linkages between hydroxycinnamic acids and lignins from wheat, rice, rye, and barley straws, maize stems, and fast-growing poplar wood. *Industrial Crops and Products* **2002**, *15* (3), 179-188.
63. Ten Have R and Teunissen PJM. Oxidative mechanisms involved in lignin degradation by white-rot fungi. *Chemical Reviews* **2001**, *101* (11), 3397-3414.
64. Ramalingam B, Sana B, Seayad J, Ghadessy FJ and Sullivan MB. Towards understanding of laccase-catalysed oxidative oligomerisation of dimeric lignin model compounds. *RSC Advances* **2017**, *7* (20), 11951-11958.
65. Benoit I, Navarro D, Marnet N, Rakotomanomana N, Lesage-Meessen L, Sigoillot J-C, Asther M and Asther M. Feruloyl esterases as a tool for the release of phenolic compounds from agro-industrial by-products. *Carbohydrate Research* **2006**, *341* (11), 1820-1827.
66. Borneman WS, Ljungdahl LG, Hartley RD and Akin DE. Isolation and characterization of *p*-coumaroyl esterase from the anaerobic fungus *Neocallimastix* strain MC-2. *Applied and Environmental Microbiology* **1991**, *57* (8), 2337-2344.

5.6. Supporting Information

5.6.1. Laccase activity determination (ABTS assay)

The activity of the commercial laccase preparation was determined spectrophotometrically by oxidation of ABTS. Hereto, a 1 mL quartz cuvette was filled with 0.5 mM ABTS in a sodium acetate buffer (pH 5, 100 mM). A solution of laccase was added and the increase in absorbance at 420 nm was measured over time ($\epsilon = 36,000 \text{ M}^{-1} \text{ cm}^{-1}$). The laccase activity was expressed in units (1 U = 1 μmol ABTS oxidized per minute).

5.6.2. Estimation of total laccase activity in laccase/HBT treatments

Incubations at pH 6 were performed both at equal laccase concentration and at equal laccase activity, as compared to pH 4. In order to determine the required laccase concentration at pH 6 to obtain equal laccase activity as compared to pH 4, we determined: (i) the ratio (pH 4 to pH 6) of initial laccase activity toward HBT, and (ii) the ratio (pH 4 to pH 6) of integrated residual laccase activity in incubations with HBT and milled wheat straw (MWS). The product of these two ratios was used to determine the required laccase concentration at pH 6, to obtain a similar overall activity as in the incubation with 50 U of laccase at pH 4.

Determination of laccase activity toward HBT

Relative laccase activity (pH 4 compared to pH 6) toward HBT was determined by using two methods: oxygen consumption and UV/VIS spectrophotometry. The average between the two measurements was used in further calculations.

For the oxygen consumption measurements were performed by using an Oxytherm System (Hansatech Instruments, Pentney, UK). Hereto, 1 mL of a 78 mM HBT solution in 200 mM citrate buffer at pH 4 or 6 was added to the measuring cell, and the sample was allowed to equilibrate at 40 °C under magnetic stirring (75 rpm) for approximately 1 h. Next, 0.12 U laccase was added and the oxygen concentration was monitored over time. The slopes of the oxygen consumption measurements were then corrected using blank measurements (without laccase) and used to estimate the ratio of laccase activity at pH 4 relative to pH 6 (**Table S5.1**).

For UV/VIS spectrophotometry, 1 mL aliquots of the same HBT solution as described above were used at 40 °C. Laccase (0.23 U) was added, and spectra (300-600 nm) were recorded every minute on a Shimadzu UV1800 spectrophotometer equipped with a CPS-240A temperature controller. The absorbance at 420 nm was plotted over time, and the slope was used to estimate the ratio of laccase activity at pH 4 relative to pH 6 (**Table S5.1**).

Determination of integrated residual laccase activity in incubations with HBT and MWS

HBT solutions (250 μL , 78 mM) at either pH 4 or pH 6 in a 200 mM citrate buffer were added to 650 μL Eppendorf tubes. MWS was suspended at a 6% (w/w) concentration and laccase was added at a dose of 33 U g^{-1} MWS. Immediately after enzyme addition, a 10 μL sample was withdrawn and stored at 4 $^{\circ}\text{C}$. Next, the tubes were incubated in a thermomixer (40 $^{\circ}\text{C}$; 1,100 rpm). Samples of 10 μL were taken after 1, 2, 4.5, 7 and 21 h, and stored at 4 $^{\circ}\text{C}$. To determine the laccase activity, samples were diluted with sodium acetate buffer (100 mM, pH 5), vortexed, centrifuged, and the activity of the supernatant was determined by using the ABTS assay (see section 5.6.1).¹ The residual laccase activity (RA, %) was plotted versus time and a first-order exponential decay was fitted to the data according to the equation:

$$\text{RA} = e^{-kt}$$

where k (s^{-1}) is the inactivation rate constant and t (s) is the time. The functions were then integrated to obtain the areas under the curves, which are a measure for the total laccase activity in a 21 h incubation. The ratio between the areas at pH 4 and pH 6 was used to compensate for differences in laccase stability (**Table S5.1**).

Table S5.1. Ratio (pH 4 to pH 6) of laccase activity and of integrated residual laccase activity.

	Ratio pH 4 to pH 6
Activity toward HBT (O_2 consumption)	5.9 ± 0.71
Activity toward HBT (spectrophotometry)	7.4 ± 0.93
Integrated residual activity	0.38 ± 0.05
Overall activity	2.5

Based on the results displayed in **Table S5.1**, incubations at pH 6 were performed with both 50 and 125 U g^{-1} MWS/MCS.

5.6.3. Flash chromatography purification of WECEL and WEL fractions

The Rovabio® Advance treated and pooled WECEL and WEL fractions were injected on a Grace Reveleris Flash chromatography system (Grace, Columbia, MD, USA), equipped with a Reveleris C18 RP 40 g cartridge (particle size 40 μm). Eluents used were water (A) and acetonitrile (B), both containing 1% (v/v) formic acid. The flow rate was 30 mL min^{-1} . UV absorbance at 280 and 310 nm and evaporative light scattering detector (ELSD) were used to monitor the elution of compounds. The following elution program was used: 0–3 min, isocratic at 0% B; 3–6.5 min, linear gradient to 14 % B; 6.5–12.5 min, isocratic at 14% B; 12.5–26 min, linear gradient to 68% B; 26–29.2 min, linear gradient to 100% B; 29.2–37.2 min, isocratic at 100% B; 37.2–39.2 min, linear gradient to 0% B; 39.2–

43.2 min, isocratic at 0% B. The eluent was collected from 16.5–39.2 min, after which it was concentrated under reduced pressure at 30 °C, and lyophilized to obtain purified water extractable lignin (WELpure).

For WECEL purification, a slightly different elution program was used with a flow rate of 40 mL min⁻¹: 0–2.9 min, isocratic at 0% B; 2.9–12.9 min, linear gradient to 20% B; 12.9–20.9 min, linear gradient to 68% B; 20.9–23.4 min, linear gradient to 100% B; 23.1–29.1 min, isocratic at 100% B; 29.1–31.1 min, linear gradient to 0% B; 31.1–34 min, isocratic at 0% B. The eluent was collected from 12.5–31 min, after which it was concentrated under reduced pressure at 30 °C, and lyophilized to obtain purified water extractable cellulolytic enzyme lignin (WECELpure).

5.6.4. Quantitative py-GC-MS with ¹³C-lignin as internal standard

Quantitative pyrolysis-gas chromatography-mass spectrometry (py-GC-MS) was performed by using an EGA/PY-3030D Multi-shot pyrolyzer (Frontier Laboratories, New Ulm, MN, USA) equipped with an AS-1020E Autoshot auto-sampler as described previously.² The pyrolyzer was coupled to a GC-MS system consisting of a Trace GC (Thermo Scientific, Waltham, MA, USA) equipped with a DB-1701 fused-silica capillary column (30 m × 0.25 mm i.d. 0.25 µm film thickness), of which the first meter is employed as pre-column, and an Exactive Orbitrap Mass Spectrometer (Thermo Scientific). Samples were weighed using an XP6 excellence-plus microbalance (Mettler Toledo, Columbus, OH, USA). Sample masses were used roughly according to their estimated lignin content: ~60 µg for CEL, ~40 µg for WELpure, ~40 µg for WECELpure, and ~80 µg for all other samples. To all samples, 10 µL of a ¹³C-labeled wheat straw lignin isolate solution (1 mg mL⁻¹ in CHCl₃:EtOH 50:50 v/v) was added as an internal standard. Samples were then air dried at room temperature prior to analysis. Pyrolysis was performed at 500 °C for 1 min with an interface temperature of 300 °C. Pyrolysis products were injected on the column via split/splitless injection at 250 °C with a split ratio of 1:133 and helium was used as carrier gas with constant flow at 1.5 mL min⁻¹. The GC oven was programmed from 70 °C (2 min) to 270 °C at 5 °C min⁻¹ and held at 270 °C for 15 min. MS detection was used with EI at 70 eV, a source temperature of 275 °C, a resolution of 60,000, AGC target at 10⁶, maximum IT at 'auto' and a scan range of *m/z* 35–550. Fifty one lignin pyrolysis compounds were identified by comparing retention time and mass spectrum with literature (**Table S5.2**).²

Pyrograms were processed by Tracefinder 4.0 software (Thermo Scientific). For each compound, the most abundant ion was selected and automatically integrated using ICIS peak integration with optimized settings per compound. Manual corrections were only performed when irregular peak shapes were observed that led to erroneous peak integration with automated integration. From the processed data, lignin contents and relative abundances of lignin-derived pyrolysis products were calculated as described previously.³ For absolute lignin quantification, all lignin-derived pyrolysis products were

included in the processing. In case pyrolysis data were used to fingerprint structural changes in lignin, two pyrolysis products were excluded from processing: 4-vinylphenol (4-VP) and 4-vinylguaiacol (4-VG). This was mainly done to improve the comparability between the py-GC-MS results and the results from HSQC NMR experiments. The rationale behind this, is that in HSQC NMR analysis, FA and *p*CA can be distinguished from 'core lignin' units, while pyrolysis of hydroxycinnamic acids and lignin interunit linkages both yield vinyl products.^{4,5}

In more detail, for relative quantification of C_α-oxidation and intact interunit linkages in HSQC NMR, only S, S_{ox}, G, G_{ox} and H-units were taken into account. For comparative purposes, the origin of the vinyl products in py-GC-MS based relative quantifications should be dealt with. Although 4-VP can also be formed from pyrolysis of H-units, the abundance of H-units is low compared to that of *p*CA (especially in corn stover). It can therefore be fairly assumed that 4-VP mainly originates from pyrolysis of *p*CA, and that exclusion from 4-VP increases the comparability between HSQC and py-GC-MS results. The formed 4-VG, however, can originate from both FA and G-units, which are both highly abundant in WS and CS lignin. Therefore, neither inclusion nor exclusion of 4-VG would result in a perfect comparability between both techniques. We decided to exclude 4-VG from data comparison. For py-GC-MS based estimation of the *p*CA content, the relative abundance of 4-VP was taken from the total abundance of lignin-derived pyrolysis products (i.e. including 4-VP and 4-VG) and reported separately (**Table S5.18**).

5.6.5. NMR spectroscopy

Sample preparation

NMR spectroscopy of CEL samples was performed in gel-state, based on a previously described protocol.⁶ Hereto, approximately 40 mg CEL was swollen with 500 μ L (for CS) or 650 μ L (for WS) deuterated dimethyl sulfoxide (DMSO-*d*₆) in a 5 mm NMR tube, followed by sonication for 1-5 h to obtain a homogeneous gel. WECelpure samples (15-60 mg) were dissolved in 450 μ L DMSO-*d*₆, vortexed, and transferred to a 5 mm NMR tube. For WELpure samples, solutions of 15-45 mg in 200 μ L DMSO-*d*₆ were prepared, vortexed, and transferred to a 5 mm Shigemi NMR microtube.

HSQC NMR analysis

HSQC experiments were performed based on previously reported methods.⁶ Spectra were recorded at 25 °C on a Bruker AVANCE III 600 MHz NMR spectrometer (Bruker BioSpin, Rheinstetten, Germany) equipped with a 5 mm cryoprobe. Spectra were recorded using a standard Bruker pulse sequence 'hsqcetgpsisp2.2'. The spectral widths were 0-12 ppm (7,200 Hz) for the ¹H dimension and 0-200 ppm (30,000 Hz) for the ¹³C dimension. Sixteen scans were acquired with a relaxation time of 1 s and a FID size of 2018 in the ¹H dimension, and 400 the ¹³C dimension. For ¹J_{CH} 145 Hz was used.

Data was processed with Bruker TopSpin version 4.0.5. DMSO-*d*₆ (δC 39.5 ppm; δH 2.49 ppm) was used to calibrate the chemical shifts. Processing was performed by Gaussian apodization, and a squared cosine function in the ¹H and ¹³C dimensions, respectively.

Table S5.2. Identity and structural classification of lignin-derived pyrolysis products by ^{13}C -IS py-GC-MS.

#	Compound	Rt (min)	Struct. feature	Side-chain length	Mw ^{12}C (Da)	Quan ion ^{12}C [M-e ⁻]	Mw ^{13}C (Da)	Quan ion ^{13}C [M-e ⁻]
1	phenol	9.79	H, unsub.	—	94	94.041320	100	100.06145
2	guaiacol	10.03	G, unsub.	—	124	124.05188	131	115.04853
3	2-methylphenol	11.03	H, methyl	1	108	108.05698	115	115.08045
4	4-methylphenol (+3-MP)	12.00	H, methyl	1	108	107.04914	115	114.07263
5	4-methylguaiacol	12.71	G, methyl	1	138	138.06753	146	146.09437
6	2,4-imethylphenol	13.18	H, methyl	1	122	107.04914	130	114.07263
7	4-ethylphenol	14.25	H, misc.	2	122	107.04914	130	114.07263
8	4-ethylguaiacol	14.83	G, misc.	2	152	137.05971	161	145.08654
9	4-vinylguaiacol ^a	16.29	G, vinyl	2	150	150.06753	159	159.09754
10	4-vinylphenol ^a	16.46	H, vinyl	2	120	120.05697	128	128.08381
11	eugenol	16.89	G, misc.	3	164	164.08318	174	174.11673
12	4-propylguaiacol	16.99	G, misc.	3	166	137.05971	175	145.08654
13	syringol	17.64	S, unsub.	—	154	154.06245	162	162.08928
14	<i>cis</i> -isoeugenol	18.25	G, misc.	3	164	164.08318	174	174.11673
15	4-propenylphenol	19.24	H, misc.	3	134	133.06479	143	142.09498
16	<i>trans</i> -isoeugenol	19.50	G, misc.	3	164	164.08318	174	174.11673
17	4-methylsyringol	19.86	S, methyl	3	168	168.07810	177	177.10829
18	vanillin	19.99	G, C σ -O	3	152	151.03897	160	159.06581
19	4-propyneguaiacol	20.23	G, misc.	3	162	162.06753	172	172.10108
20	4-alleneguaiacol	20.49	G, misc.	3	162	162.06753	172	172.10108
21	homovanillin	21.44	G, C β -O	2	166	137.05971	175	145.08654
22	4-ethylsyringol	21.58	S, misc.	2	182	167.07022	192	176.10046
23	vanillic acid methyl ester	21.82	G, C σ -O	1	182	182.05736	191	191.08766
24	acetovanillone	21.89	G, C σ -O	2	166	151.03897	175	159.06581
25	4-hydroxy-benzaldehyde	22.76	H, C σ -O	1	122	121.02848	129	128.05189
26	4-vinylsyringol	22.90	S, vinyl	2	180	180.07810	190	190.11164
27	guaiacylacetone	23.10	G, C β -O	3	180	137.05971	190	145.08654
28	4-allylsyringol	23.31	S, misc.	3	194	194.09373	205	205.13065
29	propiovanillone	23.79	G, C σ -O	3	180	151.03897	190	159.06581
30	guaiacyl vinyl ketone	24.09	G, C σ -O	3	178	151.03897	188	159.06581
31	guaiacyl diketone	24.32	G, C σ -O, C β -O	3	194	151.03897	204	159.06581
32	<i>cis</i> -4-propenyl-syringol	24.43	S, misc.	3	194	194.09373	205	205.13065
33	4-propynesyringol	25.06	S, misc.	3	192	192.07810	203	203.11500
34	4-allenesyringol	25.27	S, misc.	3	192	192.07810	203	203.11500
35	<i>trans</i> -4-propenylsyringol	25.72	S, misc.	3	194	194.09373	205	205.13065
36	dihydroconiferyl alcohol	25.81	S, C γ -O	3	182	137.05971	192	145.08654

Table S5.2 continued.

#	Compound	Rt (min)	Struct. feature	Side-chain length	Mw ¹² C (Da)	Quan ion ¹² C [M-e ⁻]	Mw ¹³ C (Da)	Quan ion ¹³ C [M-e ⁻]
37	syringaldehyde	26.34	S, C _α -O	1	182	182.05736	191	191.08755
38	<i>cis</i> -coniferyl-alcohol	26.42	G, C _γ -O	3	180	137.05971	190	145.08654
39	Homosyring-aldehyde	27.32	S, C _β -O	2	196	167.07027	206	176.10046
40	syringic acid methyl ester	27.66	S, C _α -O	1	212	212.06793	222	222.10147
41	acetosyringone	27.76	S, C _α -O	2	196	181.04954	206	190.07973
42	<i>trans</i> -coniferyl alcohol	28.11	G, C _γ -O	3	180	137.05971	190	145.08654
43	<i>trans</i> -conifer-aldehyde	28.50	G, C _γ -O	3	178	147.04406	188	156.07425
44	syringylacetone	28.68	S, C _β -O	3	210	167.07027	221	176.10046
45	propiosyringone	29.29	S, C _α -O	3	210	181.04954	221	190.07973
46	syringyl diketone	29.43	S, C _α -O, C _β -O	3	224	181.04954	235	190.07973
47	syringyl vinyl ketone	29.57	S, C _α -O	3	208	181.04954	219	190.07973
48	dihydrosinapyl alcohol	31.13	G, C _γ -O	3	212	168.07841	223	177.10829
49	<i>cis</i> -sinapyl alcohol	31.63	S, C _γ -O	3	210	167.07027	221	176.10046
50	<i>trans</i> -sinapyl alcohol	33.31	S, C _γ -O	3	210	167.07027	221	176.10046
51	<i>trans</i> -sinap-aldehyde	33.54	S, C _γ -O	3	208	208.07301	219	219.10994

^a 4-vinylphenol and 4-vinylguaiacol were excluded from all calculations. The relative abundance of 4-vinylphenol is reported separately in Table S5.18.

For the different sample fractions slightly different values for LB and GB were used, WELpure, and WECELPure: LB = -0.2 and GB = 0.001; WS-CEL LB = -0.20 and GB = 0.0005; CS-CEL LB = -0.30 and GB = 0.0005. LPfr linear prediction in F1 of 32 points was performed. Prior to Fourier transformation, the ¹³C dimension was zero filled up to 1024 points. HSQC correlations were assigned in accordance to literature (**Table S5.3**).⁷⁻¹¹ Semi-quantitative volume integration was performed as previously described by Del Río et al.,⁸ on a single zoom level within each sample.

The abundances of β-O-4' substructures and the cleavage products (DHPV, DHPs, HPV, HPS) were determined using their C_β-H_β correlations. For phenylcoumaran (B) and resinol (C) substructures C_α-H_α correlations were used. The signals of HPV+HPS (L) and resinol (C) were logically halved. S_{2,6}, G₂, and H_{2,6} signals were used for S, G, and H units, respectively, where S and H integrals were halved as well. Abundances of oxidized analogues were estimated in a similar manner. Tricin, pCA, and FA were determined from their respective T_{2',6'}, pCA_{2,6}, and FA₂ signals. H_{2,6} integrals were corrected for the overlapping phenylalanine cross peak (PHE_{3,5}) by subtraction of the isolated PHE_{2,6} cross-peak integral.¹² Amounts were calculated relative to the total aromatic lignin subunits (H + G + G_{ox} + S + S_{ox} = 100).

HMBC experiments

HMBC experiments were performed with the following WS fractions: WECEL_{pure} (pH 4, control), WECEL_{pure} (pH 4, 50 U g⁻¹) and WEL_{pure} (pH 6, 125 U g⁻¹). Hereto, 20, 32 and 49 mg of the fractions, respectively, were dissolved in 200 µL DMSO-*d*₆, vortexed, and transferred into Shigemi NMR microtubes. Experiments were performed similar to the HSQC experiments, using the standard Bruker pulse program 'hmbcgp1pndqf'. Sixteen dummy scans and 88 scans were acquired with an evolution period of 53 ms for long range coupling. The FID size was 8192 in the ¹H dimension, and 400 the ¹³C dimension. Processing used Gaussian apodization (LB=-5, GB=0.8), and a squared cosine function (SSB=1) in the ¹H and ¹³C, respectively.

Table S5.3 Assignments of the lignin ¹H/¹³C correlation signals in HSQC NMR spectra. Assignments are based on literature.⁷⁻¹² t = tentative annotation.

Label	δ _C /δ _H (ppm)	Assignment
E _β	40.3/3.08	C _β -H _β of HPV and HPS, i.e. β- <i>O</i> cleaved β- <i>O</i> -4' linkage
F-OCH ₃	51.6/3.60	C-H in methoxyl groups of cyclohexadienone ketals (t)
C _β	53.0/3.43	C _β -H _β in resinol substructures
B _β	53.6/3.05	C _β -H _β in phenylcoumaran substructures
-OCH ₃	55.6/3.73	C-H in methoxyl groups
E _γ	56.9/3.75	C _γ -H _γ in HPV and HPS, i.e. β- <i>O</i> cleaved β- <i>O</i> -4' linkage
A _γ	59.6/3.4 and 3.7	C _γ -H _γ in β- <i>O</i> -4' substructures
J _γ	61.4/4.09	C _γ -H _γ in cinnamyl alcohol end groups
A' _γ /A'' _γ	62.3/4.02	C _γ -H _γ in C _α -oxidized β- <i>O</i> -4' substructures
B _γ	62.6/3.67	C _γ -H _γ in phenylcoumaran substructures
D _γ	64.0/3.64	C _γ -H _γ in DHPV and DHPS, i.e. <i>O</i> -4' cleaved β- <i>O</i> -4'
A _{γ(ac)}	64.2/4.1 and 4.3	C _γ -H _γ in acylated β- <i>O</i> -4' substructures
A _α (G)	70.9/4.71	C _α -H _α in β- <i>O</i> -4' substructures linked to a G-unit
C _γ	71.0/3.79 and 4.16	C _γ -H _γ in resinol substructures
A _α (S)	71.8/4.81	C _α -H _α in β- <i>O</i> -4' substructures linked to a S-unit
D _β	73.8/4.98	C _β -H _β of DHPV and DHPS, i.e. <i>O</i> -4' cleaved β- <i>O</i> -4'
A'' _β (G)	81.2/5.88	C _β -H _β in C _α -oxidized β- <i>O</i> -4' substructures linked to a
A' _β (S)	83.2/5.18	C _β -H _β in C _α -oxidized β- <i>O</i> -4' substructures linked to a S-
A'' _β (S)	83.2/5.57	C _β -H _β in C _α -oxidized β- <i>O</i> -4' substructures linked to a
A _β (H)	83./4.49	C _β -H _β in β- <i>O</i> -4' substructures linked to a H-unit
A _β (G)	83.5/4.27	C _β -H _β in β- <i>O</i> -4' substructures linked to a G-unit
C _α	84.9/4.64	C _α -H _α in resinol substructures
A _β (S _{erythro})	85.9/4.09	C _β -H _β in β- <i>O</i> -4' substructures linked to an S _{erythro} -unit
A _β (T)	86.2/4.36; 86.7/4.26	C _β -H _β in β- <i>O</i> -4' substructures linked to a T-unit*
A _β (S _{threo})	86.9/3.97	C _β -H _β in β- <i>O</i> -4' substructures linked to an S _{threo} -unit
B _α	86.9/5.43; 87.6/5.54	C _α -H _α in phenylcoumaran substructures
T ₈	94.1/6.57	C ₈ -H ₈ in triclin
T ₆	98.8/6.21	C ₆ -H ₆ in triclin
S _{2,6}	103.9/6.69	C ₂ -H ₂ and C ₆ -H ₆ in S-unit

Table S5.3 Continued.

Label	δ_C/δ_H (ppm)	Assignment
T _{2',6'}	104.0/7.31	C _{2'} -H _{2'} and C _{6'} -H _{6'} in triclin
T ₃	104.6/7.04	C ₃ -H ₃ in triclin
Sox _{2,6} (carbonyl)	106.4/7.30	C ₂ -H ₂ and C ₆ -H ₆ in C _α -oxidized (C _α =O) S-unit
Sox _{2,6} (acid)	106.5/7.19	C ₂ -H ₂ and C ₆ -H ₆ in C _α -oxidized (C _α OOH) S-unit
G ₂	110.8/6.96	C ₂ -H ₂ in G-unit
FA ₂	110.9/7.34	C ₂ -H ₂ in ferulate
Gox ₂	111.4/7.51; 112.4/7.45	C ₂ -H ₂ in C _α -oxidized G-unit
H _{3,5} /FA ₅	114.6/6.70	C ₃ -H ₃ and C ₅ -H ₅ in H-unit, C ₅ -H ₅ in FA
G ₅ /G ₆	114.9/6.76, 118.7/6.81	C ₅ -H ₅ and C ₆ -H ₆ in G-unit, C ₃ -H ₃
Gox ₅	115.0/6.80	C ₅ -H ₅ in C _α -oxidized G-unit
<i>p</i> CA _{3,5}	115.0/6.75	C ₅ -H ₅ of <i>p</i> CA
FA _β / <i>p</i> CA _β	115.3/6.33	C _β -H _β in ferulate/ <i>p</i> -coumarate
FA ₆	122.5/7.09	C ₆ -H ₆ in ferulate
Gox ₆	122.7/7.51	C ₆ -H ₆ in C _α -oxidized G-unit
Phe ₄	126.3/7.18	C ₄ -H ₄ in phenylalanine
H _{2,6} /Phe _{3,5}	127.7/7.18	C ₂ -H ₂ and C ₆ -H ₆ in H-units, C ₃ -H ₃ and C ₅ -H ₅ in
Phe _{2,6}	129.0/7.21	C ₂ -H ₂ and C ₆ -H ₆ in phenylalanine
Tyr _{2,6}	129.8/7.00	C ₆ -H ₆ in C _α -oxidized G-unit
PHE _{2,6}	128.0/7.21	C ₂ -H ₂ and C ₆ -H ₆ in phenylalanine
<i>p</i> CA _{2,6}	130.1/7.50	C ₂ -H ₂ and C ₆ -H ₆ in <i>p</i> -coumarate
FA _α / <i>p</i> CA _α	144.2/7.49	C _α -H _α in ferulate/ <i>p</i> -coumarate

* Or electron-withdrawing moieties other than triclin.

5.6.6. RP-UHPLC-PDA-MS

High resolution RP-UHPLC-PDA-MS analysis was performed as described in a previous study,¹ using water (A) and acetonitrile (B) as eluents, both containing 0.1% formic acid. An adapted elution gradient was used: From 0-1.5 min at 5% B (isocratic), 1.5-35 min from 5 to 60% B (linear gradient), 35 to 41.2 min from 60 to 100% B (linear gradient), 41.2-45.7 min at 100% B (isocratic), 45.7-46.2 min from 100 to 5% B (linear gradient) and 46.2-50 min at 5% B (isocratic). The capillary temperature was 254 °C; the probe heater temperature was 408 °C; S-lens RF level was 50 and the source voltages were 3.5 and 2.5 kV in positive and negative ionization mode, respectively. Nitrogen was used as sheath gas (46.6 arbitrary units) and auxiliary gas (10.8 arbitrary units). All other settings were the same as described in Hilgers et al.¹

Table S5.4 Recoveries (%) of residues of wheat straw and corn stover during extraction, ball milling and washing relative to the starting material (dry matter) of each step. N.D. = Not determined.

Step	Wheat straw	Corn stover
Soxhlet extraction	98	N.D.
Ball-milling	92	93
Washing (water)	80	84

Table S5.5 Klason lignin determination of MWS and its RES fractions after control and laccase/HBT incubations (24h) at pH 4. Acid-soluble lignin could not be determined, due to the interfering UV absorption of HBT and its degradation products.

	MWS	Control	Laccase/HBT
Acid-insoluble lignin (AIL) (%) ^a	21.0 ± 0.6	20.1 ± 0.7	15.0 ± 0.4
Klason lignin (mg) ^a	-	292 ± 10	216 ± 7
Ash (% of AIL)	14.7 ± 1.0	16.3 ± 1.8	16.3 ± 1.5
Protein (% of AIL) ^b	3.2 ± 0.0	3.7 ± 0.1	8.1 ± 1.0
Delignification (%)		7.4	31.7

^a Corrected for ash and protein content.^b As determined by using the Dumas method with N-to-protein ratio 6.25, assuming that all nitrogen originates from protein

5.6.7. Effects of laccase/HBT treatment on lignin quantification by using Klason and py-GC-MS methodologies

The most widely applied method for lignin quantification is the Klason lignin determination method, which relies on gravimetric analysis of samples after a hydrolytic treatment with sulfuric acid (including correction for ash and protein content). Although this method gives a fairly accurate estimation of the lignin content of untreated biomass, the presence of HBT, either in free form or grafted, may heavily interfere with the lignin determination. In our case, HBT and its degradation product BT were, despite extensive washing, still present in the residue (see **Table S5.6**). During the Klason method, free HBT and BT are expected to end up in the acid-soluble fraction. Since these products show absorbance at 205 nm, no reliable acid-soluble lignin content could be determined in this study. For grafted HBT it is unclear how it influences the Klason lignin determination. If grafted HBT is cleaved off during the sulfuric acid treatment, it will also end up in the acid-soluble fraction, but if it 'survives' the sulfuric acid treatment, it will be measured as acid-insoluble lignin, and thereby result in an overestimation of the lignin content. The presence of grafted HBT will also interfere with the protein correction, which is based on nitrogen content.

To overcome the major drawback of the Klason method (i.e. poor selectivity for lignin), recently, a py-GC-MS based lignin quantification method was developed.² In this method, lignin-derived pyrolysis products are measured exclusively, and quantification is performed using a ¹³C-labeled wheat straw lignin isolate as internal standard. The method

has been shown to accurately quantify lignin in several grasses, amongst which wheat straw and corn stover. Nevertheless, it is possible that reactions such as (re)polymerization and grafting resulted in substructures that are considerably more resistant against pyrolysis than those originally present in the substrate and internal standard.^{13,14} These substructures may, therefore, have accumulated in the pyrolysis residue or may have been released as (dimeric) products that were not quantified in the used method. Consequently, the formation of such substructures likely resulted in an underestimation of the lignin content of the laccase/HBT treated samples, and thus in an overestimation of delignification. Although we cannot prove that py-GC-MS is a more accurate quantification method for laccase/HBT samples, we chose to use this method for quantification of lignin since it also provides useful information on the lignin structure and it can also be used on soluble fractions.

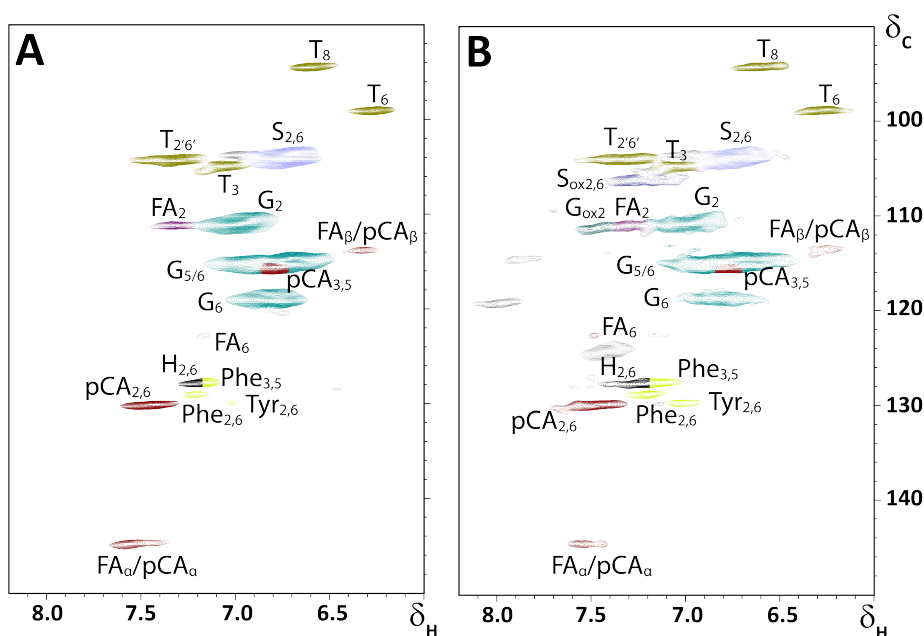


Fig. S5.1 Aromatic regions of the HSQC spectra obtained from CEL fractions of MWS treated with laccase/HBT at pH 4 (B) and the corresponding control (A). HSQC analyses of other CEL fractions showed the same peaks with different intensities. Only processed data from these spectra are shown (in other Figures and Tables). Example spectra of WECEL_{pure} and WEL_{pure} fractions are shown in Fig. 5.5.

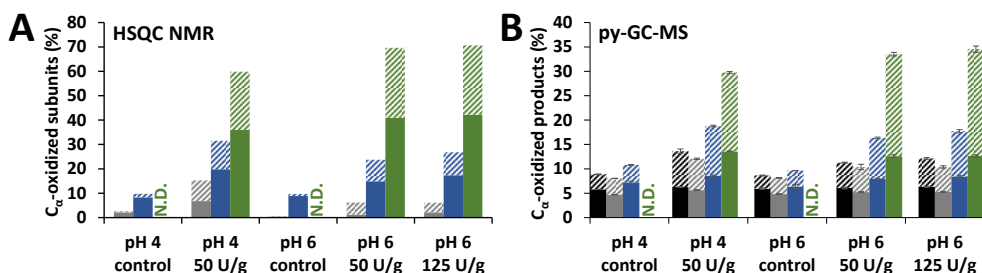


Fig. S5.2 Relative abundance of C_{α} -oxidized structures as determined by HSQC NMR (A) and estimated based on py-GC-MS (B) in RES (black), CEL (grey), WECEL_{pure} (blue) and WEL_{pure} (green) fractions of laccase/HBT treated MCS and controls. Solid and striped bars correspond to G and S units, respectively. Because of their low abundance, H-units are not included. Error bars in B represent the standard deviation of two treatment duplicates and two analytical duplicates. N.D. = Not determined.

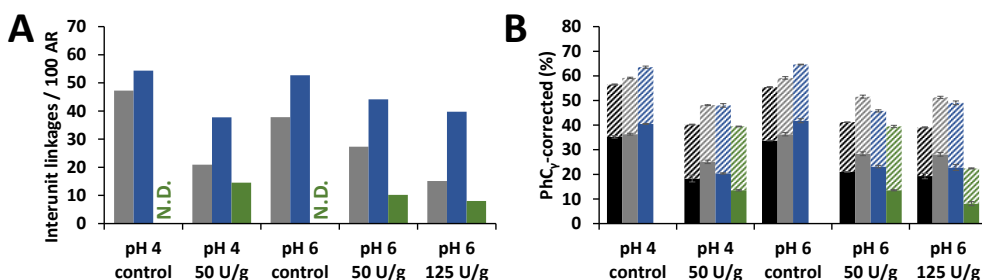


Fig. S5.3 HSQC NMR based (A) and py-GC-MS based (B) estimation of intact interunit linkages in RES (black), CEL (grey), WECEL_{pure} (blue) and WEL_{pure} (green) fractions of laccase/HBT treated MCS and controls. In B, solid and striped bars refer to G and S units, respectively. Error bars in B represent the standard deviation of two treatment duplicates and two analytical duplicates. N.D. = Not determined.

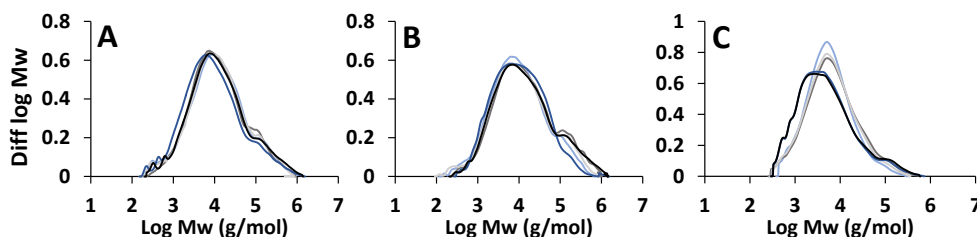


Fig. S5.4 Molecular weight distributions of WS CEL (A) CS CEL (B) and CS WECEL_{pure} fractions as determined by using SEC-MALS_(1R). pH 4 control = dark blue; pH 4 - 50U = light blue; pH 6 control = black; pH 6 - 50U = dark grey; pH 6 - 125U = light grey.

Table S5.6 Summarized RP-UHPLC-MS data of WECEL_{pure} samples of laccase/HBT treated samples (LMS) and controls. Several compounds were tentatively annotated as lignin-HBT adducts, based on their molecular formula (shown in bold). These structures were absent in control incubations and in the control containing only laccase and HBT.

Rt (min)	Molecular formula	Ion	Observed/ calculated mass	Mass error (ppm)	Tentative annotation	Detected in
3.84	C ₆ H ₅ N ₃ O	[M+H] ⁺	135.04333/135.04326	0.53	HBT	LMS
6.41	C ₆ H ₅ N ₃	[M+H] ⁺	119.04841/119.04835	0.55	Benzotriazole	LMS
8.33	C ₉ H ₈ O ₃	[M-H] ⁻	164.04751/164.04735	1.03	<i>p</i> -coumaric acid	Control & LMS
9.25	C₁₃H₁₁N₃O₄	[M+H] ⁺	273.07496/273.07496	0.03	Lignin-HBT adduct	LMS
9.38	C₁₉H₁₉N₃O₇	[M+H] ⁺	401.12263/401.12230	0.83	Lignin-HBT adduct	LMS
9.76	C ₁₀ H ₁₀ O ₄	[M-H] ⁻	194.05801/194.05791	0.54	Ferulic acid	Control & LMS
11.00	C ₂₀ H ₂₂ O ₈	[M+Na] ⁺	390.13175/390.13147	0.68	<i>Unknown</i>	Control & LMS
11.32	C₁₄H₁₃N₃O₄	[M+H] ⁺	287.09065/287.09061	0.17	Lignin-HBT adduct	LMS
13.78	C ₂₀ H ₂₀ O ₈	[M+Na] ⁺	388.11610/388.11582	0.68	<i>Unknown</i>	Control & LMS
13.92	C ₂₁ H ₂₂ O ₉	[M+Na] ⁺	418.12650/418.12639	0.26	<i>Unknown</i>	Control & LMS
14.01	C₁₉H₁₉N₃O₆	[M+H] ⁺	385.12752/385.12739	0.36	Lignin-HBT adduct	LMS
15.31	C₁₃H₁₁N₃O₃	[M+H] ⁺	257.08018/257.08004	0.55	Lignin-HBT adduct	LMS
15.86	C ₁₉ H ₁₈ O ₆	[M+H] ⁺	342.11043/342.11034	0.28	<i>Unknown</i>	Control & LMS
17.01	C ₂₀ H ₁₈ O ₁₀	[M+H] ⁺	418.09022/418.09000	0.54	<i>Unknown</i>	Control & LMS
18.54	C ₁₇ H ₁₄ O ₇	[M+H] ⁺	330.07399/330.07396	0.12	Tricin	Control & LMS
21.62	C ₂₂ H ₂₂ O ₆	[M+Na] ⁺	382.14158/382.14164	-0.15	<i>Unknown</i>	LMS

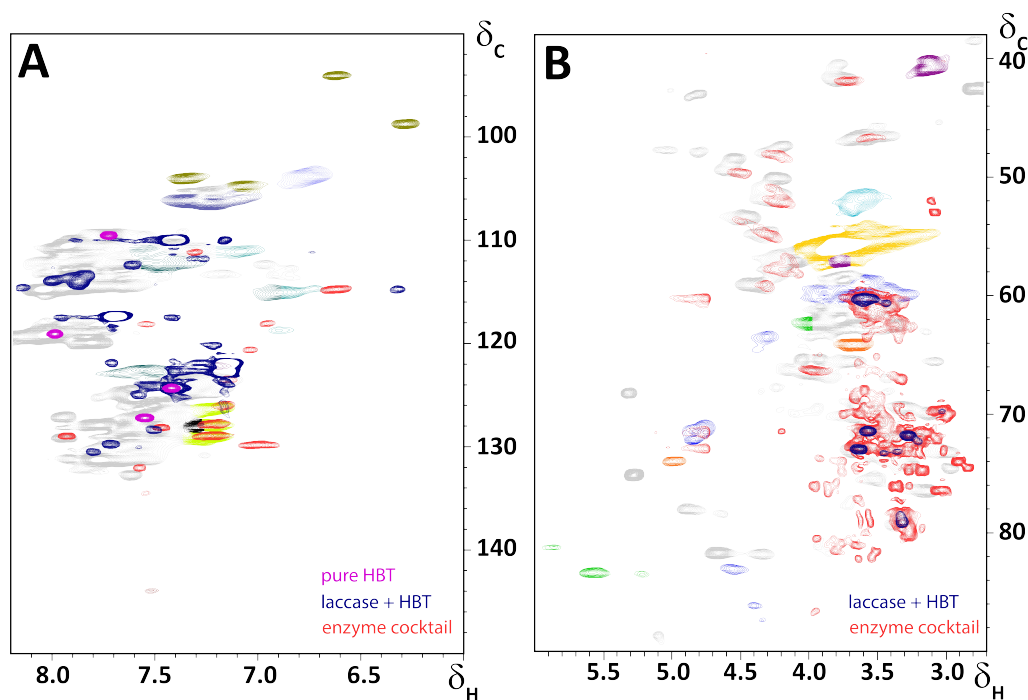


Fig. S5.5 Overlay of aromatic (A) and aliphatic (B) regions of the HSQC spectra obtained from the WEL_{pure} fraction of laccase/HBT treated MWS (pH 4), the Rovabio Advance enzyme cocktail, pure HBT, and an incubation containing only laccase and HBT. Colors and annotations of the WEL_{pure} fraction are as displayed in Fig 5.5 and Table S5.3. Correlations from the Rovabio enzyme cocktail are shown in red, those of pure HBT and the laccase+HBT mixture are shown in pink and navy, respectively.

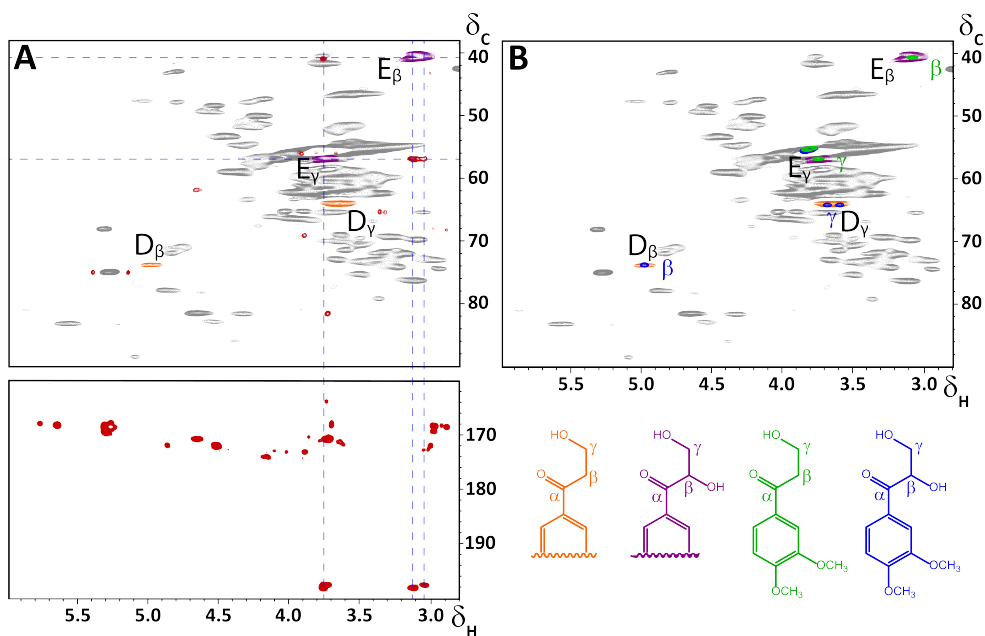


Fig. S5.6 NMR spectra used for the annotation of ether cleavage structures D (yellow) and E (purple): diagnostic HSQC and HMBC correlations in WEL_{pure} fraction of laccase/HBT treated MWS (pH 6, 125 U) between α , β and γ positions of E (A), and overlapping HSQC signals of D and E with purified 1-(3,4-dimethoxyphenyl)-3-hydroxypropan-1-one (green) and 1-(3,4-dimethoxyphenyl)-2,3-dihydroxypropan-1-one (blue), respectively. Due to low intensity, diagnostic HMBC correlations of structure D are not visible in (A).

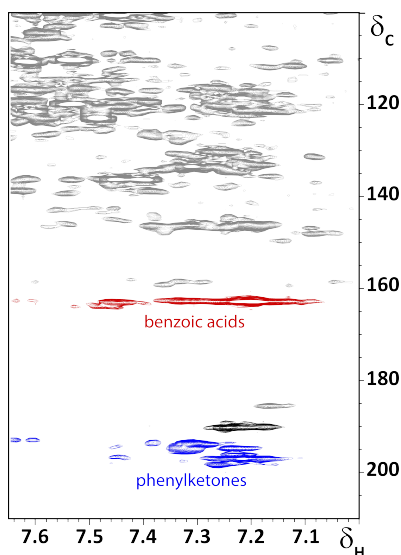


Fig. S5.7 HMBC spectrum of WEL_{pure} fraction of laccase/HBT treated MWS at pH 4. The spectrum is identical to the spectrum in Fig. 5.6C, but zoomed in (3×). The spectrum shows that a large variety of phenylketones are present, mainly corresponding to S-units. The black peak most likely corresponds to an aldehyde.

Table S5.7 Structural features of lignin in WEL_{pure} fractions after laccase/HBT and control treatments as measured by HSQC NMR.

Laccase (U g ⁻¹)	Wheat straw				Corn stover			
	pH 4		pH 6		pH 4		pH 6	
	50	50	125	125	50	50	50	125
Lignin subunits (%)								
H	0	0	0	0	0	0	0	0
G	14	15	11	14	14	14	14	12
G _{ox}	41	40	43	36	36	41	42	
S	16	15	14	29	17	17	17	
S _{ox}	30	30	32	21	29	28		
S/G	0.84	0.83	0.86	1.02	0.83	0.84		
Hydroxycinnamates^a								
pCA	0	0	0	0	0	0	0	0
FA	0	0	0	0	0	0	0	0
Flavonoids^a								
Tricin	8	1	2	6	1	1		
Interunit linkages^{a,b}								
β-O-4' (A)	7.5 (49)	7.0 (63)	5.1 (37)	12.1 (84)	8.6 (84)	3.7 (46)		
β-O-4' ox (A'/A'')	7.9 (51)	4.1 (37)	8.6 (63)	2.4 (16)	1.6 (16)	4.4 (56)		
β-5' (B)	0 (0)	0 (0)	0 (0)	0 (0)	0 (0)	0 (0)		
β-β' (C)	0 (0)	0 (0)	0 (0)	0 (0)	0 (0)	0 (0)		
Total (100%)	15.4	11.1	13.7	14.5	10.2	8.0		
Cleavage products^a								
DHPV/DHPS (D)	5.1	2.2	3.6	1.6	1.1	1.4		
HPV/HPS (E)	14.6	18.7	24.7	14.5	13.6	22.5		

^a Amount of substructures per 100 aromatic subunits (S+S_{ox}+G+G_{ox}+H). ^b numbers between brackets refer to relative abundances of linkages.

Table S5.8 Lignin content and relative abundances of structural features in MWS/MCS as determined by quantitative py-GC-MS.

Lignin % (w/w) ^a	MWS	MCS
Lignin subunits (%)^b		
H	18.3 ± 0.2	22.7 ± 0.1
G	3.6 ± 0.1	10.3 ± 0.2
S	56.4 ± 0.4	51.7 ± 0.6
	40.0 ± 0.5	37.9 ± 0.4
S/G	0.7 ± 0.0	0.7 ± 0.0
Structural features (%)^b		
Unsubstituted	10.1 ± 0.7	18.0 ± 0.2
Methyl	5.5 ± 0.4	10.2 ± 0.7
Ca-O	6.3 ± 0.3	11.2 ± 0.2
Ca-O, G	3.4 ± 0.2	6.5 ± 0.1
Ca-O, S	2.8 ± 0.1	3.3 ± 0.1
Diketones	0.8 ± 0.0	0.7 ± 0.0
Vinyl ketones	0.2 ± 0.0	0.2 ± 0.0
Cβ-O ^c	1.8 ± 0.0	2.1 ± 0.0
Cy-O	64.2 ± 0.4	38.3 ± 1.5
Misc	6.1 ± 0.4	11.2 ± 0.9
Vinyl	6.0 ± 0.2	8.9 ± 0.3
PhCy ^d	71.1 ± 0.0	50.5 ± 0.7
PhCy-corrected ^e	70.0 ± 0.0	49.5 ± 0.7
PhCy-corrected, G	42.4 ± 0.0	31.2 ± 0.7
PhCy-corrected, S	27.5 ± 0.0	18.1 ± 0.1

^a 4-vinylphenol and 4-vinylguaiacol included in processing. ^b 4-vinylphenol and 4-vinylguaiacol not included in processing. ^c Excluding diketones. ^d phenols with intact 3-carbon (α, β, γ) side chain. ^e phenols with intact 3-carbon (α, β, γ) side chain minus diketones and vinylketones.

Table S5.9 Lignin content, recovery and relative abundances of structural features in WS-RES as determined by quantitative py-GC-MS.

Laccase (U g ⁻¹)	pH 4			pH 6		
	0	50		0	50	125
Lignin % (w/w) ^a	18.6±0.8	9.4±0.8		18.0±0.5	10.8±0.8	10.3±0.6
Lignin (mg) ^a	270.5±11.5	134.1±11.1		261.2±7.1	152.9±11.6	145.4±8.6
Lignin recovery vs MWS (%) ^a	98.2±4.3	48.8±4.1		94.8±2.7	55.6±4.2	52.9±3.2
Lignin subunits (%) ^b						
H	3.5 ± 0.1	7.6 ± 0.2		3.9 ± 0.1	7.2 ± 0.1	7.4 ± 0.1
G	55.8 ± 0.3	44.4 ± 0.5		56.7 ± 0.3	48.3 ± 0.6	48.4 ± 0.3
S	40.7 ± 0.4	48.0 ± 0.4		39.4 ± 0.3	44.5 ± 0.5	44.2 ± 0.2
S/G	0.7 ± 0.0	1.1 ± 0.0		0.7 ± 0.0	0.9 ± 0.0	0.9 ± 0.0
Structural moieties (%) ^b						
Unsubstituted	11.0 ± 0.9	20.8 ± 1.1		10.6 ± 0.2	17.6 ± 0.5	18.3 ± 0.4
Methyl	5.2 ± 0.5	6.9 ± 0.3		5.5 ± 0.1	8.0 ± 0.1	8.3 ± 0.1
Cα-O	5.7 ± 0.2	16.8 ± 1.1		6.0 ± 0.1	12.4 ± 0.3	12.9 ± 0.5
Cα-O, G	2.9 ± 0.2	8.0 ± 0.5		3.2 ± 0.0	6.0 ± 0.2	6.3 ± 0.2
Cα-O, S	2.6 ± 0.0	8.5 ± 0.6		2.6 ± 0.0	6.1 ± 0.1	6.3 ± 0.3
Diketones	0.5 ± 0.0	4.5 ± 0.5		0.5 ± 0.0	2.1 ± 0.1	2.3 ± 0.2
Diketones, G	0.2 ± 0.0	2.2 ± 0.2		0.2 ± 0.0	0.9 ± 0.0	1.1 ± 0.1
Diketones, S	0.3 ± 0.0	2.4 ± 0.3		0.2 ± 0.0	1.2 ± 0.1	1.3 ± 0.1
Vinyl ketones	0.2 ± 0.0	0.7 ± 0.0		0.2 ± 0.0	0.4 ± 0.0	0.5 ± 0.0
Vinyl ketones, G	0.2 ± 0.0	0.6 ± 0.0		0.2 ± 0.0	0.4 ± 0.0	0.4 ± 0.0
Vinyl ketones, S	0.0 ± 0.0	0.1 ± 0.0		0.2 ± 0.0	0.1 ± 0.0	0.1 ± 0.0
Cβ-O ^c	1.8 ± 0.1	2.6 ± 0.1		1.8 ± 0.0	2.6 ± 0.0	2.6 ± 0.1
Cγ-O	64.7 ± 0.7	40.3 ± 1.6		64.9 ± 0.4	45.3 ± 0.3	43.7 ± 0.6
Miscellaneous	5.8 ± 0.5	5.8 ± 0.4		5.7 ± 0.2	7.3 ± 0.2	7.6 ± 0.3
Vinyl	5.8 ± 0.1	6.8 ± 0.1		5.5 ± 0.1	6.8 ± 0.1	6.7 ± 0.1
PhCγ ^d	72.0 ± 0.6	53.1 ± 1.3		71.9 ± 0.3	56.3 ± 0.5	55.2 ± 0.6
PhCγ-corrected ^e	71.3 ± 0.6	47.9 ± 1.8		71.3 ± 0.3	53.7 ± 0.5	52.4 ± 0.7
PhCγ-corrected, G	43.0 ± 0.5	22.6 ± 1.3		43.8 ± 0.2	29.1 ± 0.7	28.4 ± 0.6
PhCγ-corrected, S	28.2 ± 0.3	25.1 ± 0.5		27.4 ± 0.3	24.4 ± 0.3	23.9 ± 0.2

^a 4-vinylphenol and 4-vinylguaiacol included in processing. ^b 4-vinylphenol and 4-vinylguaiacol not included in processing. ^c excluding diketones. ^d phenols with intact 3-carbon (α, β, γ) side chain. ^e phenols with intact 3-carbon (α, β, γ) side chain minus diketones and vinylketones.

Table S5.10 Lignin content, recovery and relative abundances of structural features in CS-RES as determined by quantitative py-GC-MS.

	pH 4			pH 6		
	0	50		0	50	125
Laccase (U g⁻¹)						
Lignin % (w/w)^a						
Lignin (mg)^a	24.8±1.0	14.8±0.7		24.4±0.6	15.9±1.0	13.8±1.3
Lignin recovery vs MCS (%)^a	348.6±13.7	207.9±9.4		340.6±8.4	222.2±13.9	192.2±17.9
Lignin subunits (%)^b	102.3±4.1	60.9±2.8		99.9±2.6	65.2±4.1	56.3±5.3
H	9.2 ± 0.4	16.2 ± 0.8		10.3 ± 0.1	16.9 ± 0.4	17.4 ± 0.3
G	52.7 ± 0.3	37.5 ± 1.5		51.7 ± 0.1	40.9 ± 0.1	39.8 ± 1.0
S	38.1 ± 0.2	46.4 ± 0.8		38.0 ± 0.1	42.3 ± 0.4	42.7 ± 0.7
S/G	0.7 ± 0.0	1.2 ± 0.1		0.7 ± 0.0	1.0 ± 0.0	1.1 ± 0.0
Structural moieties (%)^b						
Unsubstituted	17.2 ± 0.3	25.9 ± 0.8		18.2 ± 0.4	25.7 ± 0.3	26.5 ± 1.1
Methyl	7.0 ± 0.4	8.7 ± 0.1		7.3 ± 0.2	10.2 ± 0.2	10.8 ± 0.1
Cα-O	10.2 ± 0.1	15.4 ± 0.5		10.0 ± 0.2	12.8 ± 0.3	13.6 ± 0.1
Cα-O, G	5.8 ± 0.0	6.3 ± 0.1		5.9 ± 0.1	6.1 ± 0.2	6.3 ± 0.1
Cα-O, S	3.1 ± 0.1	7.4 ± 0.4		2.7 ± 0.1	5.2 ± 0.1	5.8 ± 0.2
Diketones	0.7 ± 0.0	3.0 ± 0.3		0.5 ± 0.0	1.5 ± 0.0	1.8 ± 0.1
Diketones, G	0.2 ± 0.0	0.8 ± 0.1		0.2 ± 0.0	0.4 ± 0.0	0.5 ± 0.0
Diketones, S	0.5 ± 0.0	2.2 ± 0.2		0.4 ± 0.0	1.1 ± 0.0	1.3 ± 0.0
Vinyl ketones	0.2 ± 0.0	0.4 ± 0.0		0.2 ± 0.0	0.2 ± 0.0	0.3 ± 0.0
Vinyl ketones, G	0.1 ± 0.0	0.3 ± 0.0		0.1 ± 0.0	0.2 ± 0.0	0.2 ± 0.0
Vinyl ketones, S	0.1 ± 0.0	0.1 ± 0.0		0.1 ± 0.0	0.1 ± 0.0	0.1 ± 0.0
Cβ-O ^c	2.1 ± 0.0	2.6 ± 0.0		1.7 ± 0.0	2.3 ± 0.0	2.3 ± 0.1
Cγ-O	47.6 ± 0.9	31.1 ± 1.3		48.1 ± 0.2	32.7 ± 0.6	30.3 ± 1.3
Miscellaneous	8.4 ± 0.3	8.1 ± 0.1		7.3 ± 0.2	8.3 ± 0.4	8.6 ± 0.1
Vinyl	7.4 ± 0.1	8.2 ± 0.1		7.4 ± 0.1	8.1 ± 0.1	7.9 ± 0.2
PhCγ ^d	57.6 ± 0.7	43.9 ± 1.0		56.3 ± 0.1	43.2 ± 0.4	41.4 ± 1.2
PhCγ-corrected ^e	56.7 ± 0.7	40.5 ± 1.4		55.6 ± 0.1	41.4 ± 0.4	39.3 ± 1.3
PhCγ-corrected, G	35.2 ± 0.5	18.3 ± 1.4		33.7 ± 0.1	21.0 ± 0.2	19.3 ± 1.1
PhCγ-corrected, S	21.3 ± 0.2	21.9 ± 0.1		21.8 ± 0.1	20.2 ± 0.4	19.8 ± 0.2

^a 4-vinylphenol and 4-vinylguaiacol included in processing. ^b 4-vinylphenol and 4-vinylguaiacol not included in processing. ^c excluding diketones. ^d phenols with intact 3-carbon (α, β, γ) side chain. ^e phenols with intact 3-carbon (α, β, γ) side chain minus diketones and vinylketones.

Table S5.1.1 Lignin content, recovery and relative abundances of structural features in WS-CEL as determined by quantitative py-GC-MS.

Laccase (U g ⁻¹)	pH 4			pH 6		
	0	50	0	50	125	
Lignin % (w/w)^a	39.4 ± 5.1	23.0 ± 1.6	48.4 ± 4.0	28.7 ± 1.1	26.6 ± 0.9	
Lignin (mg)^a	81.9 ± 12.0	26.2 ± 1.9	103.0 ± 8.7	38.9 ± 1.5	33.7 ± 3.7	
Lignin recovery vs MWS (%)^{a,b}	66.5 ± 9.8	21.0 ± 1.5	83.2 ± 7.1	30.9 ± 1.2	26.7 ± 2.9	
vs WS-RES (%)^{a,b}	67.7 ± 10.3	43.0 ± 4.7	87.7 ± 7.8	55.6 ± 4.7	50.4 ± 6.2	
Lignin subunits (%)^c						
H	3.1 ± 0.4	4.6 ± 0.3	3.0 ± 0.2	3.8 ± 0.1	3.8 ± 0.1	
G	54.7 ± 0.2	48.7 ± 0.6	54.3 ± 0.4	50.5 ± 0.5	50.7 ± 0.5	
S	42.2 ± 0.3	46.6 ± 0.4	42.8 ± 0.3	45.7 ± 0.5	45.5 ± 0.3	
S/G	0.8 ± 0.0	1.0 ± 0.0	0.8 ± 0.0	0.9 ± 0.0	0.9 ± 0.0	
Structural moieties (%)^c						
Unsubstituted	8.5 ± 0.2	12.9 ± 0.8	8.9 ± 0.6	10.7 ± 0.6	10.7 ± 0.3	
Methyl	5.3 ± 0.5	5.6 ± 0.2	5.0 ± 0.4	5.4 ± 0.2	5.4 ± 0.2	
C α -O	5.5 ± 0.2	10.4 ± 0.1	5.4 ± 0.1	7.4 ± 0.1	7.3 ± 0.1	
C α -O, G	2.6 ± 0.1	4.9 ± 0.1	2.5 ± 0.1	3.4 ± 0.1	3.4 ± 0.1	
C α -O, S	2.7 ± 0.1	5.2 ± 0.1	2.7 ± 0.1	3.8 ± 0.0	3.8 ± 0.0	
Diketones	0.5 ± 0.0	2.1 ± 0.0	0.5 ± 0.0	1.1 ± 0.0	1.1 ± 0.0	
Diketones, G	0.2 ± 0.0	1.0 ± 0.0	0.2 ± 0.0	0.5 ± 0.0	0.5 ± 0.0	
Diketones, S	0.3 ± 0.0	1.1 ± 0.0	0.3 ± 0.0	0.6 ± 0.0	0.6 ± 0.0	
Vinyl ketones	0.3 ± 0.0	0.5 ± 0.0	0.2 ± 0.0	0.3 ± 0.0	0.3 ± 0.0	
Vinyl ketones, G	0.2 ± 0.0	0.4 ± 0.0	0.2 ± 0.0	0.3 ± 0.0	0.3 ± 0.0	
Vinyl ketones, S	0.0 ± 0.0	0.1 ± 0.0	0.0 ± 0.0	0.1 ± 0.0	0.1 ± 0.0	
C β -O ^d	1.6 ± 0.0	2.1 ± 0.1	1.6 ± 0.0	1.8 ± 0.1	1.8 ± 0.0	
C γ -O	67.4 ± 1.6	56.8 ± 1.4	67.4 ± 1.9	62.2 ± 0.5	62.4 ± 0.5	
Miscellaneous	6.5 ± 0.6	5.8 ± 0.3	6.4 ± 0.6	6.1 ± 0.2	6.0 ± 0.2	
Vinyl	5.2 ± 0.1	6.5 ± 0.3	5.4 ± 0.3	6.3 ± 0.2	6.3 ± 0.2	
PhC γ ^e	75.1 ± 1.0	66.6 ± 1.1	75.1 ± 1.4	70.7 ± 0.5	70.9 ± 0.4	
PhC γ -corrected ^f	74.4 ± 1.0	64.0 ± 1.1	74.4 ± 1.4	69.3 ± 0.5	69.4 ± 0.3	
PhC γ -corrected, G	43.7 ± 0.5	33.8 ± 0.8	43.3 ± 0.9	38.0 ± 0.6	38.2 ± 0.5	
PhC γ -corrected, S	30.5 ± 0.6	30.0 ± 0.4	31.0 ± 0.7	31.2 ± 0.3	31.1 ± 0.4	

^a 4-vinylphenol and 4-vinylguaiacol included in processing. ^b note that CEL was prepared from ~650 mg of RES. ^c 4-vinylphenol and 4-vinylguaiacol not included in processing. ^d excluding diketones. ^e phenols with intact 3-carbon (α , β , γ) side chain. ^f phenols with intact 3-carbon (α , β , γ) side chain minus diketones and vinylketones.

Table S5.1.2 Lignin content, recovery and relative abundances of structural features in CS-CEL as determined by quantitative py-GC-MS.

Laccase (U g ⁻¹)	pH 4			pH 6		
	0	50		0	50	125
Lignin % (w/w)^a						
Lignin (mg) ^a	49.5 ± 1.9	32.6 ± 1.9		51.6 ± 4.4	32.9 ± 4.1	31.1 ± 2.0
Lignin recovery vs MCS (%) ^{a,b}	75.9 ± 3.2	36.9 ± 3.0		80.7 ± 7.4	48.1 ± 6.1	42.4 ± 2.9
vs CS-RES ^{a,b}	56.8 ± 2.4	27.6 ± 2.2		60.0 ± 5.5	35.8 ± 4.5	31.4 ± 2.1
	55.5 ± 3.2	45.4 ± 4.2		60.1 ± 5.7	54.9 ± 7.7	55.8 ± 6.4
Lignin subunits (%)^c						
H	8.9 ± 0.2	12.3 ± 0.4		9.1 ± 0.3	11.5 ± 0.1	11.5 ± 0.3
G	50.6 ± 0.2	41.7 ± 0.7		50.6 ± 0.3	44.4 ± 1.0	44.4 ± 0.6
S	40.4 ± 0.0	46.0 ± 0.8		40.3 ± 0.1	44.1 ± 0.9	44.1 ± 0.4
S/G	0.8 ± 0.0	1.1 ± 0.0		0.8 ± 0.0	1.0 ± 0.0	1.0 ± 0.0
Structural moieties (%)^c						
Unsubstituted	14.5 ± 0.4	20.2 ± 0.4		14.4 ± 0.6	18.8 ± 0.1	18.9 ± 0.5
Methyl	7.3 ± 0.1	8.1 ± 0.2		7.3 ± 0.3	7.8 ± 0.1	8.0 ± 0.2
Cα-O	9.4 ± 0.0	13.5 ± 0.2		9.5 ± 0.1	11.7 ± 0.6	11.7 ± 0.3
Cα-O, G	4.7 ± 0.0	5.6 ± 0.1		4.8 ± 0.0	5.2 ± 0.1	5.3 ± 0.1
Cα-O, S	3.4 ± 0.0	6.4 ± 0.1		3.3 ± 0.1	5.2 ± 0.5	5.1 ± 0.2
Diketones	0.7 ± 0.0	2.3 ± 0.1		0.7 ± 0.0	1.5 ± 0.2	1.5 ± 0.1
Diketones, G	0.2 ± 0.0	0.5 ± 0.1		0.2 ± 0.0	0.3 ± 0.0	0.3 ± 0.0
Diketones, S	0.5 ± 0.0	1.7 ± 0.1		0.5 ± 0.0	1.1 ± 0.2	1.1 ± 0.1
Vinyl ketones	0.3 ± 0.0	0.4 ± 0.0		0.3 ± 0.0	0.3 ± 0.0	0.3 ± 0.0
Vinyl ketones, G	0.2 ± 0.0	0.3 ± 0.0		0.2 ± 0.0	0.2 ± 0.0	0.2 ± 0.0
Vinyl ketones, S	0.1 ± 0.0	0.2 ± 0.0		0.1 ± 0.0	0.1 ± 0.0	0.1 ± 0.0
Cβ-O ^d	1.9 ± 0.0	2.4 ± 0.0		1.9 ± 0.0	2.3 ± 0.0	2.3 ± 0.0
Cγ-O	49.8 ± 0.7	39.0 ± 0.6		49.9 ± 1.3	42.8 ± 0.3	42.4 ± 1.1
Miscellaneous	9.0 ± 0.1	8.0 ± 0.1		8.8 ± 0.2	7.9 ± 0.3	8.0 ± 0.1
Vinyl	8.0 ± 0.1	8.8 ± 0.1		8.2 ± 0.2	8.7 ± 0.3	8.7 ± 0.1
PhCy ^e	60.3 ± 0.6	51.0 ± 0.5		60.3 ± 1.2	53.6 ± 0.3	53.3 ± 1.0
PhCy-corrected ^f	59.4 ± 0.6	48.3 ± 0.6		59.4 ± 1.2	51.8 ± 0.3	51.5 ± 1.1
PhCy-corrected, G	36.3 ± 0.4	25.1 ± 0.7		36.3 ± 0.7	28.4 ± 0.8	28.1 ± 0.8
PhCy-corrected, S	22.9 ± 0.3	23.0 ± 0.2		22.9 ± 0.5	23.2 ± 0.6	23.1 ± 0.4

^a 4-vinylphenol and 4-vinylguaiacol included in processing. ^b note that CEL was prepared from ~550 mg of RES. ^c 4-vinylphenol and 4-vinylguaiacol not included in processing. ^d excluding diketones. ^e phenols with intact 3-carbon (α, β, γ) side chain. ^f phenols with intact 3-carbon (α, β, γ) side chain minus diketones and vinylketones.

Table S5.13 Lignin content, recovery and relative abundances of structural features in WS-WECEL as determined by quantitative py-GC-MS.

Laccase (U g ⁻¹)	pH 4		pH 6	
	0	50	0	125
Lignin % (w/w) ^a	6.5 ± 0.7	6.5 ± 0.5	7.3 ± 0.2	6.5 ± 0.3
Lignin (mg) ^a	41.6 ± 4.7	46.4 ± 3.8	46.2 ± 1.8	45.8 ± 2.9
Lignin recovery vs MWS (%) ^{a,b}	33.8 ± 3.8	37.2 ± 3.1	37.3 ± 1.5	36.2 ± 2.3
vs WS-RES ^{a,b}	34.4 ± 4.2	76.2 ± 8.9	39.4 ± 1.9	68.5 ± 5.9
Lignin subunits (%) ^c				
H	9.1 ± 0.0	9.8 ± 0.4	8.7 ± 0.0	9.1 ± 0.3
G	58.6 ± 0.0	48.6 ± 0.5	58.5 ± 0.5	50.8 ± 0.8
S	32.3 ± 0.1	41.6 ± 0.6	32.8 ± 0.5	39.9 ± 1.1
S/G	0.6 ± 0.0	0.9 ± 0.0	0.6 ± 0.0	0.8 ± 0.0
Structural moieties (%) ^c				
Unsubstituted	16.3 ± 0.2	24.2 ± 0.9	15.1 ± 0.2	22.7 ± 1.3
Methyl	7.9 ± 0.1	8.8 ± 0.1	7.9 ± 0.1	9.3 ± 0.3
Cα-O	6.8 ± 0.2	20.4 ± 0.1	6.5 ± 0.0	16.1 ± 0.4
Cα-O, G	4.1 ± 0.2	10.5 ± 0.2	3.8 ± 0.0	8.4 ± 0.3
Cα-O, S	2.5 ± 0.1	9.5 ± 0.1	2.4 ± 0.0	7.1 ± 0.1
Diketones	0.5 ± 0.1	4.1 ± 0.1	0.4 ± 0.0	2.2 ± 0.1
Diketones, G	0.3 ± 0.1	2.0 ± 0.1	0.2 ± 0.0	1.4 ± 0.1
Diketones, S	0.3 ± 0.1	2.2 ± 0.0	0.2 ± 0.0	1.1 ± 0.1
Vinyl ketones	0.2 ± 0.0	1.0 ± 0.1	0.2 ± 0.0	0.6 ± 0.0
Vinyl ketones, G	0.2 ± 0.0	0.8 ± 0.1	0.2 ± 0.0	0.5 ± 0.0
Vinyl ketones, S	0.0 ± 0.0	0.1 ± 0.0	0.0 ± 0.0	0.1 ± 0.0
Cβ-O ^d	1.4 ± 0.0	2.5 ± 0.0	1.4 ± 0.0	2.4 ± 0.1
Cγ-O	58.6 ± 0.4	34.3 ± 0.8	60.1 ± 0.2	38.8 ± 2.0
Miscellaneous	5.4 ± 0.0	5.8 ± 0.0	5.3 ± 0.0	6.6 ± 0.2
Vinyl	3.6 ± 0.0	4.1 ± 0.2	3.7 ± 0.1	4.1 ± 0.1
PhCγ ^e	64.6 ± 0.3	46.6 ± 0.8	66.0 ± 0.2	49.8 ± 1.9
PhCγ-corrected ^f	63.8 ± 0.4	41.5 ± 0.9	65.4 ± 0.2	46.4 ± 1.9
PhCγ-corrected, G	41.9 ± 0.2	21.6 ± 0.4	42.7 ± 0.3	26.2 ± 0.5
PhCγ-corrected, S	21.9 ± 0.2	19.8 ± 0.7	22.5 ± 0.5	20.1 ± 1.6

^a 4-vinylphenol and 4-vinylguaiacol included in processing. ^b note that WECEL was prepared from ~650 mg of RES. ^c 4-vinylphenol and 4-vinylguaiacol not included in processing. ^d excluding diketones. ^e phenols with intact 3-carbon (α, β, γ) side chain. ^f phenols with intact 3-carbon (α, β, γ) side chain minus diketones and vinylketones.

Table S5.1.4 Lignin content, recovery and relative abundances of structural features in CS-WECEL as determined by quantitative py-GC-MS.

Laccase (U g ⁻¹)	pH 4		pH 6	
	0	50	0	125
Lignin % (w/w) ^a	10.6 ± 0.3	6.4 ± 0.4	9.7 ± 0.6	5.3 ± 0.3
Lignin (mg) ^a	58.6 ± 2.7	36.8 ± 2.1	55.6 ± 4.3	35.2 ± 3.9
Lignin recovery vs MCS (%) ^{a,b}	43.8 ± 2.0	27.6 ± 1.6	41.8 ± 3.3	26.2 ± 2.9
vs CS-RES ^{a,b}	42.9 ± 2.6	45.3 ± 3.3	41.4 ± 3.4	46.3 ± 6.7
Lignin subunits (%) ^c				
H	16.3 ± 1.8	24.3 ± 1.0	21.1 ± 3.8	25.1 ± 5.4
G	57.4 ± 0.4	39.0 ± 0.2	54.9 ± 2.4	37.8 ± 2.5
S	26.3 ± 1.4	36.7 ± 0.8	24.1 ± 1.4	37.1 ± 2.9
S/G	0.5 ± 0.0	0.9 ± 0.0	0.4 ± 0.0	1.0 ± 0.0
Structural moieties (%) ^c				
Unsubstituted	22.5 ± 2.9	35.5 ± 0.0	24.3 ± 3.0	26.7 ± 4.0
Methyl	11.6 ± 1.0	12.4 ± 0.5	12.5 ± 1.3	11.7 ± 0.0
Cα-O	11.5 ± 0.0	18.9 ± 0.5	11.1 ± 0.5	16.6 ± 1.2
Cα-O, G	7.6 ± 0.0	8.4 ± 0.2	7.5 ± 0.3	7.4 ± 0.5
Cα-O, S	2.5 ± 0.1	8.0 ± 0.2	2.4 ± 0.1	7.4 ± 0.5
Diketones	0.6 ± 0.0	3.0 ± 0.1	0.6 ± 0.0	2.2 ± 0.2
Diketones, G	0.2 ± 0.0	1.1 ± 0.1	0.2 ± 0.0	0.7 ± 0.1
Diketones, S	0.6 ± 0.0	1.9 ± 0.0	0.3 ± 0.0	1.6 ± 0.1
Vinyl ketones	0.2 ± 0.0	0.5 ± 0.0	0.2 ± 0.0	0.5 ± 0.0
Vinyl ketones, G	0.1 ± 0.0	0.4 ± 0.0	0.2 ± 0.0	0.4 ± 0.0
Vinyl ketones, S	0.0 ± 0.0	0.1 ± 0.0	0.0 ± 0.0	0.1 ± 0.0
Cβ-O ^d	1.2 ± 0.0	2.0 ± 0.2	1.2 ± 0.1	1.9 ± 0.2
Cγ-O	43.1 ± 3.6	20.2 ± 0.2	37.2 ± 1.0	28.6 ± 0.1
Miscellaneous	6.4 ± 0.0	6.9 ± 0.1	10.1 ± 4.4	10.4 ± 5.8
Vinyl	3.7 ± 0.3	4.0 ± 0.2	3.5 ± 0.4	4.1 ± 0.5
PhCγ ^e	49.3 ± 3.9	30.7 ± 0.1	43.4 ± 0.5	37.7 ± 0.6
PhCγ-corrected ^f	48.6 ± 3.9	27.2 ± 0.0	42.6 ± 0.5	34.9 ± 0.4
PhCγ-corrected, G	33.7 ± 2.3	13.7 ± 0.1	30.1 ± 0.4	17.3 ± 0.2
PhCγ-corrected, S	14.7 ± 1.5	13.3 ± 0.1	12.4 ± 0.1	17.5 ± 0.2

^a 4-vinylphenol and 4-vinylguaiacol included in processing. ^b note that WECEL was prepared from ~550 mg of RES. ^c 4-vinylphenol and 4-vinylguaiacol not included in processing. ^d excluding diketones. ^e phenols with intact 3-carbon (α, β, γ) side chain. ^f phenols with intact 3-carbon (α, β, γ) side chain minus diketones and vinylketones.

Table S5.15 Lignin content, recovery and relative abundances of structural features in WS-WECEL_{pure} as determined by quantitative py-GC-MS.

Laccase (U g ⁻¹)	pH 4		pH 6	
	0	50	0	125
Lignin % (w/w) ^{a,b}	111.6 ± 3.8	50.4 ± 0.4	113.1 ^g ± 6.2	55.0 ± 1.6
Lignin (mg) ^{a,b}	30.5 ± 1.0	47.1 ± 0.4	46.6 ± 2.5	35.9 ± 1.1
Lignin recovery vs MWS (%) ^{a,b,c}	24.8 ± 0.9	37.8 ± 0.5	37.6 ± 2.1	28.4 ± 0.9
vs WS-WECEL _{ab,c}	84.2 ± 9.9	123.0 ^g ± 10.1	115.1 ^g ± 7.7	95.9 ± 6.6
Lignin subunits (%) ^d				
H	2.1 ± 0.0	4.6 ± 0.1	2.6 ± 0.2	3.6 ± 0.1
G	57.4 ± 0.3	43.8 ± 0.1	58.6 ± 0.5	46.3 ± 0.4
S	40.5 ± 0.3	51.6 ± 0.0	38.7 ± 0.3	50.1 ± 0.5
S/G	0.7 ± 0.0	1.2 ± 0.0	0.7 ± 0.0	1.1 ± 0.0
Structural moieties (%) ^d				
Unsubstituted	7.4 ± 0.1	19.0 ± 1.3	7.8 ± 0.1	12.6 ± 0.3
Methyl	3.3 ± 0.0	5.0 ± 0.4	3.5 ± 0.2	5.2 ± 0.7
CaO	5.8 ± 0.1	20.4 ± 0.2	5.9 ± 0.2	18.4 ± 0.2
CaO, G	3.3 ± 0.0	8.9 ± 0.0	3.5 ± 0.2	8.4 ± 0.1
CaO, S	2.4 ± 0.1	11.0 ± 0.2	2.2 ± 0.1	9.7 ± 0.2
Diketones	0.4 ± 0.0	3.9 ± 0.1	0.4 ± 0.0	3.1 ± 0.1
Diketones, G	0.2 ± 0.0	1.8 ± 0.1	0.2 ± 0.0	1.3 ± 0.0
Diketones, S	0.2 ± 0.0	2.2 ± 0.1	0.2 ± 0.0	1.7 ± 0.0
Vinyl ketones	0.2 ± 0.0	0.9 ± 0.0	0.2 ± 0.0	0.7 ± 0.1
Vinyl ketones, G	0.1 ± 0.0	0.8 ± 0.1	0.1 ± 0.0	0.6 ± 0.0
Vinyl ketones, S	0.0 ± 0.0	0.1 ± 0.0	0.0 ± 0.0	0.1 ± 0.0
CβO ^e	1.4 ± 0.0	2.1 ± 0.0	1.4 ± 0.0	2.1 ± 0.1
CγO	75.0 ± 0.2	42.0 ± 2.3	73.9 ± 0.2	51.1 ± 0.6
Miscellaneous	3.8 ± 0.0	5.3 ± 0.3	4.2 ± 0.2	5.1 ± 0.2
Vinyl	3.3 ± 0.0	6.1 ± 0.1	3.2 ± 0.0	5.5 ± 0.1
PhCγ ^f	79.6 ± 0.1	54.2 ± 1.8	78.7 ± 0.2	61.0 ± 0.2
PhCγ-corrected ^g	79.1 ± 0.1	49.4 ± 1.9	78.1 ± 0.2	57.2 ± 0.4
PhCγ-corrected, G	46.6 ± 0.1	21.9 ± 1.1	47.1 ± 0.2	27.5 ± 0.1
PhCγ-corrected, S	32.4 ± 0.2	27.4 ± 0.8	30.9 ± 0.3	29.6 ± 0.3

^a 4-vinylphenol and 4-vinylguaiacol included in processing. ^b these numbers are expected to be an overestimation due to the high abundance of free ferulic acid (released upon XLA treatment), which is known to be pyrolyzed with high efficiency.¹⁵ ^c note that WECEL_{pure} was prepared from 550-600 mg WECEL. ^d 4-vinylphenol and 4-vinylguaiacol not included in processing. ^e excluding diketones. ^f phenols with intact 3-carbon (α, β, γ) side chain. ^g phenols with intact 3-carbon (α, β, γ) side chain minus diketones and vinylketones.

Table S5.16 Lignin content, recovery and relative abundances of structural features in CS-WECEL_{pure} as determined by quantitative py-GC-MS.

Laccase (U g ⁻¹)	pH 4			pH 6		
	0	50		0	50	125
Lignin % (w/w)^{a,b}	118.1 ± 8.8	56.4 ± 1.1		121.0 ± 6.1	59.4 ± 3.5	62.4 ± 0.6
Lignin (mg)^{a,b}	68.6 ± 5.1	21.3 ± 0.4		63.5 ± 3.2	22.9 ± 1.4	26.1 ± 0.3
Lignin recovery vs MCS (%)^{a,b,c}	51.4 ± 3.9	15.9 ± 0.3		47.7 ± 2.4	17.1 ± 1.0	19.4 ± 0.2
vs CS-WECEL^{a,b,c}	137.9 ± 12.1	71.9 ± 4.3		137.7 ± 12.7	76.7 ± 8.5	92.0 ± 10.3
Lignin subunits (%)^d						
H	5.5 ± 0.1	10.6 ± 0.4		5.5 ± 0.3	10.1 ± 0.2	9.7 ± 0.3
G	59.1 ± 0.5	39.2 ± 0.0		59.0 ± 0.2	44.7 ± 0.3	42.5 ± 0.5
S	35.5 ± 0.6	50.2 ± 0.4		35.5 ± 0.1	45.2 ± 0.4	47.8 ± 0.2
S/G	0.6 ± 0.0	1.3 ± 0.0		0.6 ± 0.0	1.0 ± 0.0	1.1 ± 0.0
Structural moieties (%)^d						
Unsubstituted	12.6 ± 0.2	16.9 ± 0.5		12.7 ± 0.2	19.5 ± 0.4	17.0 ± 0.9
Methyl	5.8 ± 0.2	6.1 ± 0.1		5.5 ± 0.5	8.0 ± 0.5	6.4 ± 0.3
Cα-O	11.7 ± 0.2	21.8 ± 0.3		10.6 ± 0.4	18.1 ± 0.4	20.0 ± 0.5
Cα-O, G	7.2 ± 0.2	8.6 ± 0.1		6.4 ± 0.4	7.9 ± 0.1	8.5 ± 0.1
Cα-O, S	3.6 ± 0.0	10.2 ± 0.2		3.3 ± 0.0	8.4 ± 0.2	9.2 ± 0.3
Diketones	0.8 ± 0.0	2.8 ± 0.1		0.7 ± 0.0	2.2 ± 0.1	2.5 ± 0.1
Diketones, G	0.3 ± 0.0	0.7 ± 0.1		0.2 ± 0.0	0.6 ± 0.0	0.6 ± 0.0
Diketones, S	0.5 ± 0.0	2.1 ± 0.0		0.5 ± 0.0	1.6 ± 0.0	1.8 ± 0.1
Vinyl ketones	0.2 ± 0.0	0.6 ± 0.0		0.2 ± 0.0	0.5 ± 0.0	0.5 ± 0.0
Vinyl ketones, G	0.2 ± 0.0	0.5 ± 0.0		0.2 ± 0.0	0.4 ± 0.0	0.4 ± 0.0
Vinyl ketones, S	0.0 ± 0.0	0.1 ± 0.0		0.0 ± 0.0	0.1 ± 0.0	0.1 ± 0.0
Cβ-O ^e	1.8 ± 0.0	2.1 ± 0.0		1.8 ± 0.0	2.5 ± 0.0	2.3 ± 0.1
Cγ-O	57.9 ± 0.5	41.2 ± 1.1		58.8 ± 0.9	38.0 ± 1.0	42.3 ± 2.2
Miscellaneous	5.7 ± 0.0	6.2 ± 0.3		5.8 ± 0.2	7.5 ± 0.1	6.3 ± 0.3
Vinyl	4.4 ± 0.1	5.8 ± 0.1		4.8 ± 0.1	6.4 ± 0.1	5.8 ± 0.2
PhCγ ^f	64.7 ± 0.5	51.6 ± 1.0		65.6 ± 0.7	48.7 ± 0.9	52.3 ± 1.8
PhCγ-corrected ^g	63.7 ± 0.5	48.2 ± 1.0		64.7 ± 0.7	46.0 ± 0.9	49.3 ± 2.0
PhCγ-corrected, G	40.5 ± 0.2	20.3 ± 0.3		41.8 ± 0.8	23.1 ± 0.5	22.8 ± 1.2
PhCγ-corrected, S	23.0 ± 0.5	27.6 ± 0.7		22.8 ± 0.1	22.6 ± 0.4	26.3 ± 0.7

^a 4-vinylphenol and 4-vinylguaiacol included in processing. ^b these numbers are expected to be an overestimation due to the high abundance of free ferulic acid (released upon XLA treatment), which is known to be pyrolyzed with high efficiency. ^c note that WECEL_{pure} was prepared from 450-550 mg WECEL. ^d 4-vinylphenol and 4-vinylguaiacol not included in processing. ^e excluding diketones. ^f phenols with intact 3-carbon (α, β, γ) side chain. ^g phenols with intact 3-carbon (α, β, γ) side chain minus diketones and vinylketones.

Table S5.1.7 Lignin content, recovery and relative abundances of structural features in WS/CS WEL_{pure} as determined by quantitative py-GC-MS.

Laccase (U g ⁻¹)	Wheat straw			Corn stover		
	pH 4 50	pH 6 50	pH 6 125	pH 4 50	pH 6 50	pH 6 125
Lignin % (w/w) ^a	23.2 ± 1.9	6.6 ± 0.4	15.4 ± 0.6	20.9 ± 3.2	9.1 ± 0.3	12.7 ± 0.3
Lignin (mg) ^{a,b}	6.9 ± 0.6	4.6 ± 0.3	5.7 ± 0.2	3.6 ± 0.6	2.6 ± 0.1	2.9 ± 0.1
Lignin recovery vs MWIS/MCS (%) ^{b,c,d}	5.0 ± 0.4	3.4 ± 0.2	4.2 ± 0.2	2.1 ± 0.3	1.5 ± 0.0	1.7 ± 0.0
vs WS/CS-WEL (%) ^{b,c,d}	9.7 ± 1.8	7.6 ± 1.6	8.8 ± 1.3	5.4 ± 1.1	4.4 ± 1.0	4.0 ± 1.0
Lignin subunits (%) ^d						
H	5.4 ± 0.0	9.7 ± 0.2	5.4 ± 0.1	12.2 ± 0.0	15.6 ± 0.5	13.4 ± 1.5
G	43.8 ± 0.3	40.5 ± 0.0	42.9 ± 0.3	33.9 ± 0.3	32.9 ± 0.0	31.7 ± 0.9
S	50.8 ± 0.3	49.9 ± 0.2	51.7 ± 0.4	53.9 ± 0.3	51.5 ± 0.5	54.9 ± 0.9
S/G	1.2 ± 0.0	1.2 ± 0.0	1.2 ± 0.0	1.6 ± 0.0	1.6 ± 0.0	1.7 ± 0.0
Structural moieties (%) ^d						
Unsubstituted	16.2 ± 1.9	21.9 ± 0.2	17.5 ± 0.5	18.5 ± 0.1	31.2 ± 1.3	22.9 ± 0.9
Methyl	3.0 ± 0.1	3.4 ± 0.1	3.0 ± 0.1	4.3 ± 0.0	6.1 ± 0.2	4.7 ± 0.4
Cα-O	33.5 ± 1.1	37.1 ± 0.0	34.4 ± 0.5	32.2 ± 0.2	35.6 ± 0.6	36.5 ± 0.8
Cα-O, G	15.8 ± 0.4	15.8 ± 0.4	15.4 ± 0.3	13.6 ± 0.1	12.6 ± 0.3	12.6 ± 0.2
Cα-O, S	17.2 ± 0.6	18.1 ± 0.2	18.4 ± 0.3	16.2 ± 0.2	20.9 ± 0.4	21.9 ± 0.7
Diketones	8.3 ± 0.6	7.3 ± 0.5	6.8 ± 0.2	5.2 ± 0.2	7.2 ± 0.5	7.1 ± 0.2
Diketones, G	3.6 ± 0.3	3.5 ± 0.1	2.8 ± 0.2	1.5 ± 0.2	2.2 ± 0.2	2.2 ± 0.2
Diketones, S	4.7 ± 0.3	3.9 ± 0.3	3.9 ± 0.1	3.7 ± 0.1	5.0 ± 0.2	5.0 ± 0.2
Vinyl ketones	2.6 ± 0.0	2.3 ± 0.4	2.6 ± 0.1	1.3 ± 0.0	1.7 ± 0.1	2.1 ± 0.0
Vinyl ketones, G	2.1 ± 0.0	1.8 ± 0.0	2.1 ± 0.0	1.0 ± 0.0	1.2 ± 0.0	1.5 ± 0.0
Vinyl ketones, S	0.6 ± 0.0	0.4 ± 0.1	0.4 ± 0.0	0.4 ± 0.0	0.5 ± 0.0	0.6 ± 0.0
Cβ-O ^e	1.6 ± 0.0	2.0 ± 0.0	1.7 ± 0.0	1.8 ± 0.0	2.3 ± 0.0	2.1 ± 0.0
Cγ-O	40.3 ± 1.2	30.5 ± 0.2	37.8 ± 0.8	34.9 ± 0.3	17.5 ± 0.8	25.9 ± 1.0
Miscellaneous	2.2 ± 0.1	2.2 ± 0.0	2.4 ± 0.1	3.2 ± 0.0	3.2 ± 0.0	3.2 ± 0.0
Vinyl	3.2 ± 0.1	2.8 ± 0.0	3.2 ± 0.1	5.2 ± 0.1	4.1 ± 0.1	4.7 ± 0.1
PhCγ ^f	55.0 ± 1.7	43.8 ± 0.1	51.2 ± 0.7	46.1 ± 0.5	31.4 ± 1.3	40.2 ± 0.9
PhCγ-corrected ^g	44.1 ± 1.1	34.2 ± 0.2	41.9 ± 0.9	39.5 ± 0.2	22.5 ± 0.8	31.0 ± 1.1
PhCγ-corrected, G	20.2 ± 0.8	14.6 ± 0.4	19.2 ± 0.5	13.5 ± 0.3	8.1 ± 0.3	11.2 ± 0.9
PhCγ-corrected, S	23.8 ± 0.4	19.5 ± 0.6	22.7 ± 0.4	25.9 ± 0.2	14.3 ± 0.5	19.8 ± 0.2

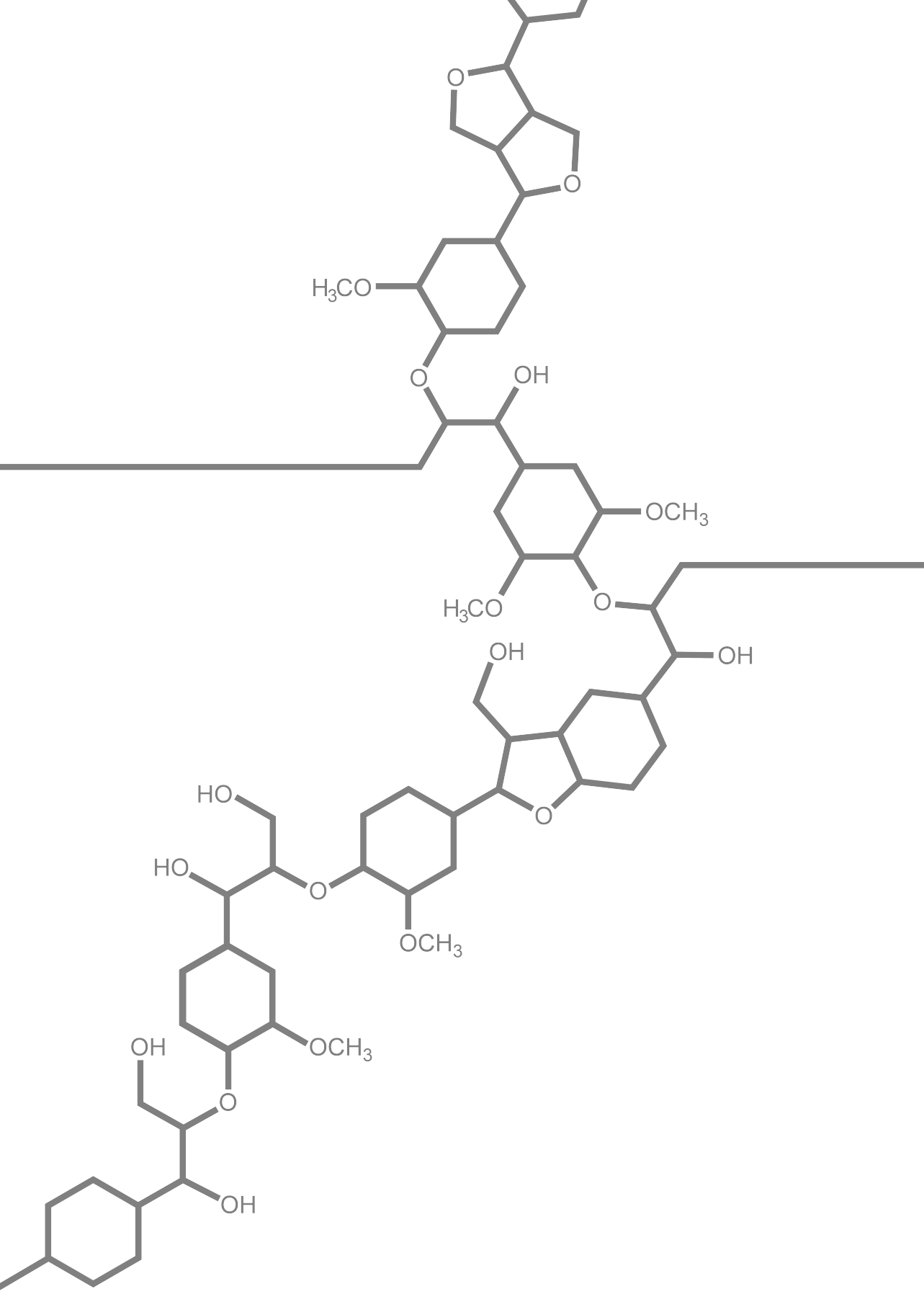
^a 4-vinylphenol and 4-vinylguaiacol included in processing. ^b note that WEL_{pure} was purified from ~50% of the obtained WEL. ^c the amount of lignin in WEL was calculated by subtracting the amount of lignin in PWS/PCS with that in WS/CS-RES. ^d 4-vinylphenol and 4-vinylguaiacol not included in processing. ^e excluding diketones. ^f phenols with intact 3-carbon (α, β, γ) side chain. ^g phenols with intact 3-carbon (α, β, γ) side chain minus diketones and vinylketones.

Table S5.18 ^{13}C -IS py-GC-MS relative abundance of 4-vinylphenol in fractions of laccase/HBT treated MWS and MCS and controls.

Laccase (U g^{-1})	pH 4		pH 6		
	0	50	0	50	125
Wheat straw					
RES			8.1 ± 0.9	8.2 ± 0.9	8.1 ± 0.7
CEL	8.7 ± 0.8	8.9 ± 0.9	9.4 ± 1.1	10.0 ± 1.1	10.1 ± 0.9
WECEL _{pure}	8.7 ± 0.8	10.6 ± 1.1	7.6 ± 0.6	9.4 ± 0.8	9.8 ± 0.8
WEL _{pure}	6.5 ± 0.5	8.5 ± 0.7	-	1.0 ± 0.1	1.2 ± 0.1
Corn stover					
RES	-	1.0 ± 0.1	31.7 ± 3.4	36.9 ± 2.9	35.4 ± 3.0
CEL	30.6 ± 2.7	39.3 ± 3.5	40.0 ± 3.3	41.3 ± 3.9	41.0 ± 3.8
WECEL _{pure}	38.5 ± 3.4	44.1 ± 3.8	18.4 ± 1.5	35.9 ± 3.0	31.5 ± 2.5
WEL _{pure}	16.8 ± 1.4	38.6 ± 3.1	-	4.6 ± 0.4	5.0 ± 0.4
	-	8.7 ± 0.7	-		

References Supporting Information

- Hilgers R, Vincken J-P, Gruppen H and Kabel MA. Laccase/mediator systems: Their reactivity towards phenolic lignin structures. *ACS Sustainable Chemistry & Engineering* **2018**, 6 (2), 2037-2046.
- Van Erven G, De Visser R, Merckx DWH, Strolenberg W, De Gijssel P, Gruppen H and Kabel MA. Quantification of lignin and its structural features in plant biomass using ^{13}C lignin as internal standard for pyrolysis-GC-SIM-MS. *Analytical Chemistry* **2017**, 89 (20), 10907-10916.
- Van Erven G, Nayan N, Sonnenberg ASM, Hendriks WH, Cone JW and Kabel MA. Mechanistic insight in the selective delignification of wheat straw by three white-rot fungal species through quantitative ^{13}C -IS py-GC-MS and whole cell wall HSQC NMR. *Biotechnology for Biofuels* **2018**, 11 (1), 262.
- Del Río JC, Martin F and Gonzalez-Vila FJ. Thermally assisted hydrolysis and alkylation as a novel pyrolytic approach for the structural characterization of natural biopolymers and geomacromolecules. *TrAC Trends in Analytical Chemistry* **1996**, 15 (2), 70-79.
- Del Río JC, Gutiérrez A, Rodríguez IM, Ibarra D and Martínez AT. Composition of non-woody plant lignins and cinnamic acids by Py-GC/MS, Py/TMAH and FT-IR. *Journal of Analytical and Applied Pyrolysis* **2007**, 79 (1-2), 39-46.
- Mansfield SD, Kim H, Lu F and Ralph J. Whole plant cell wall characterization using solution-state 2D NMR. *Nature Protocols* **2012**, 7 (9), 1579.
- Guo H, Miles-Barrett DM, Neal AR, Zhang T, Li C and Westwood NJ. Unravelling the enigma of lignin OX: can the oxidation of lignin be controlled? *Chemical Science* **2018**, 9 (3), 702-711.
- Del Río JC, Rencoret J, Prinsen P, Martínez AT, Ralph J and Gutiérrez A. Structural characterization of wheat straw lignin as revealed by analytical pyrolysis, 2D-NMR, and reductive cleavage methods. *Journal of Agricultural and Food Chemistry* **2012**, 60 (23), 5922-5935.
- Del Río JC, Lino AG, Colodette JL, Lima CF, Gutiérrez A, Martínez AT, Lu F, Ralph J and Rencoret J. Differences in the chemical structure of the lignins from sugarcane bagasse and straw. *Biomass and Bioenergy* **2015**, 81, 322-338.
- Zeng J, Helms GL, Gao X and Chen S. Quantification of wheat straw lignin structure by comprehensive NMR analysis. *Journal of Agricultural and Food Chemistry* **2013**, 61 (46), 10848-10857.
- Van Erven G, Hilgers RJ, De Waard P, Gladbeek E-J, Van Berkel WJH and Kabel MA. Elucidation of *in situ* ligninolysis mechanisms of the selective white-rot fungus *Ceriporiopsis subvermispora*. *ACS Sustainable Chemistry & Engineering* **2019**, 7 (19), 16757-16764.
- Kim H, Padmakshan D, Li Y, Rencoret J, Hatfield RD and Ralph J. Characterization and elimination of undesirable protein residues in plant cell wall materials for enhancing lignin analysis by solution-state nuclear magnetic resonance spectroscopy. *Biomacromolecules* **2017**, 18 (12), 4184-4195.
- Kawamoto H. Lignin pyrolysis reactions. *Journal of Wood Science* **2017**, 63 (2), 117-132.
- Kawamoto H, Horigoshi S and Saka S. Pyrolysis reactions of various lignin model dimers. *Journal of Wood Science* **2007**, 53 (2), 168-174.
- Ralph J and Hatfield RD. Pyrolysis-GC-MS characterization of forage materials. *Journal of Agricultural and Food Chemistry* **1991**, 39 (8), 1426-1437.



Facile enzymatic C_γ-acylation of lignin model compounds

Simple β -O-4' linked dimeric model compounds are often targeted as substrate to mimic the reactivity of lignin in enzymatic or chemical treatments. These models mimic the structure and reactivity of regular β -O-4' linkages in lignin, but are less suitable to predict the reactivity of acylated β -O-4' substructures, which are abundant in various types of lignin. Here, we present a one-step lipase-catalyzed acylation of a commercially available lignin model compound with *p*-coumaric acid, *p*-hydroxybenzoic acid, cinnamic acid and acetic acid as acyl donors. This facile procedure allows to obtain new and relevant lignin model compounds at milligram scale, with simple purification of products and unreacted substrate.

Based on: Roelant Hilgers, Jean-Paul Vincken and Mirjam A. Kabel. Facile enzymatic C_γ-acylation of lignin model compounds. *Catalysis Communications* **2020**, 136: 105919.

6.1 Introduction

Lignin is an aromatic polymer that occurs in the cell wall of plants. Its selective removal, and degradation, is one of the major challenges in biorefinery and (bio-)catalysis, and consequently, it receives a lot of attention in the scientific literature. The main building blocks of lignin are sinapyl alcohol, coniferyl alcohol and *p*-coumaroyl alcohol, which couple oxidatively to form a heterogeneous polymer consisting of syringyl (S), guaiacyl (G) and *p*-hydroxycoumaroyl (H) units. Upon polymerization, several C-O and C-C inter-unit linkages are formed, of which the β -O-4' linkage is the most abundant one in all types of native lignin (**Fig. 6.1**).¹

The exact structure of lignin depends on multiple factors, but in general three classes are distinguished: softwood, hardwood and grass lignin. They differ in their S/G/H ratio, but also in their degree and type of acylation at the C_V-position. Whereas C_V-acylation is absent in softwood, grass lignins can be extensively C_V-acetylated and C_V-coumaroylated (**Fig. 6.1A**).² Similarly, several hardwood lignins (i.e. those from willow, poplar, aspen and palms) contain C_V-esterified acetyl and *p*-hydroxybenzoyl groups (**Fig. 6.1B**).²

Most fundamental insights on the reactions of lignin (e.g. during degradative treatments) have been obtained by studying the reactivity of low-molecular-weight lignin model compounds, as recently reviewed by, amongst others, Vangeel et al. and Liu et al.^{3,4} Hereto, mostly simple β -O-4' linked dimers have been used, such as veratrylglycerol- β -guaiacyl ether (VBG; **Fig. 6.2**).⁵⁻⁷ Although structures like VBG are suitable to mimic the reactivity of regular β -O-4' bonds in lignin, their reactivity cannot directly be extrapolated to other lignin structural elements, such as the above-mentioned C_V-acylated substructures in grass and hardwood lignins. Consequently, little is known on how acylation of the C_V-position influences the reactivity of β -O-4' bonds in lignin. To overcome this gap, C_V-coumaroylated, C_V-*p*-hydroxybenzoylated and C_V-acetylated lignin model compounds are required.

Synthesis of C_V-coumaroylated and C_V-hydroxybenzoylated models has been described in literature, but the synthesis of both models entails a relatively complex multistep chemical synthesis starting from monomeric building blocks (**Fig. 6.2A**).^{8,9} In addition, thus far, only phenolic model compounds were synthesized (i.e. models bearing a hydroxyl group on the aromatic ring), which often do not reflect the reactivity of the more recalcitrant non-phenolic lignin structures, accounting for up to 90% of the native polymer.¹ Obviously, a more simple procedure for the synthesis of acylated lignin models is preferable. Recently, a relatively simple procedure was described for C_V-acetylation of VBG, a non-phenolic lignin model compound, which entails ball milling of the lignin model in presence of a suitable acetyl donor and an immobilized lipase.¹⁰ Although successful, the method was only shown to work with liquid esters as acetyl donors. Acylation with small linear acyl groups was also reported, but more complex acylations with *p*-coumaroyl or *p*-hydroxybenzoyl groups were not yet investigated (**Fig. 6.2A**).¹⁰

Here, we present a facile one-step enzymatic synthesis of C_V-coumaroylated, C_V-hydroxybenzoylated and C_V-acetylated lignin models, using an immobilized lipase from

Candida antarctica (CALB) as catalyst and *p*-coumaric acid (*p*CA), *p*-hydroxybenzoic acid (pHBA) or acetic acid (HOAc) as acyl donors. For screening purposes, and to provide a non-phenolic analogue of the VBG-*p*CA ester, acylation was also performed using cinnamic acid (CinA) as acyl donor (**Fig. 6.2B**). This facile procedure opens up possibilities to study the reactivity of acylated lignin substructures in more detail.

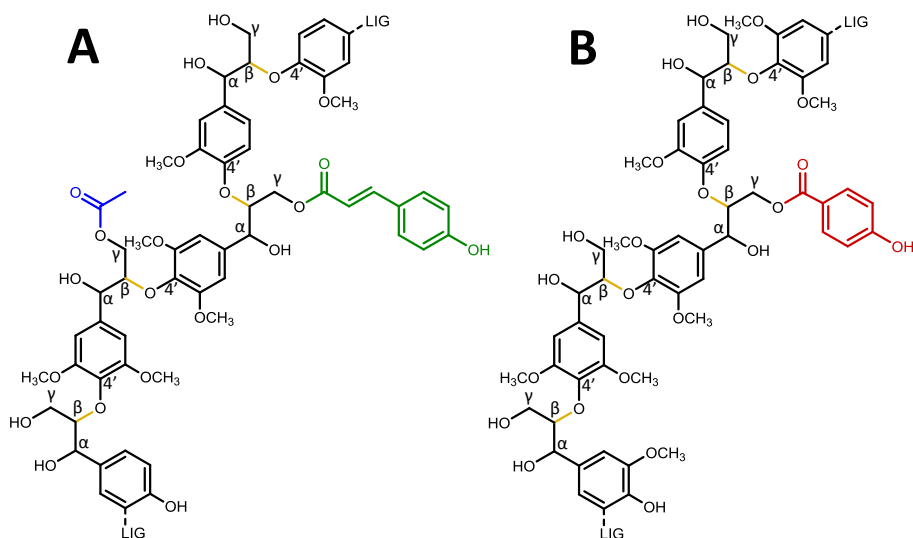


Fig. 6.1 Highly simplified example structures of grass lignin (A) and hardwood lignin (B), illustrating β -O-4' bonds (yellow), *p*-coumaroyl groups (green), acetyl groups (blue) and *p*-hydroxybenzoate groups (red). LIG = lignin polymer.

6.2 Materials & Methods

6.2.1 Materials

Veratrylglycerol- β -guaiacyl ether (VBG; 1-(3,4-dimethoxyphenyl)-2-(2-methoxyphenoxy)-propane-1,3-diol) was obtained from ABCR (Karlsruhe, Germany) and immobilized CALB (Novozym 435) was a kind gift of Novozymes (Bagsværd, Denmark). All other chemicals were purchased from Sigma Aldrich (St. Louis, MO, USA). Water was prepared by using a Milli-Q water purification system (Merck Millipore, Billerica, MA, USA).

6.2.2 Screening of different solvents for VBG acylation

In order to determine the optimal solvent for C_V-acylation of VBG, esterification of VBG with CinA was performed in different solvents. Hereto, mixtures of VBG (30 mM) and CinA (30 mM) were prepared in acetone, acetonitrile, *t*-butanol, toluene and *t*-butanol/toluene 1:1 (v/v), all dried with 3 Å molecular sieves. Total reaction volumes of 200 μ L were incubated with \sim 10 mg CALB in 1.5 mL glass vials at 55 °C under 600 rpm shaking in a thermomixer. After two days of incubation, samples were diluted 200 times in methanol, centrifuged

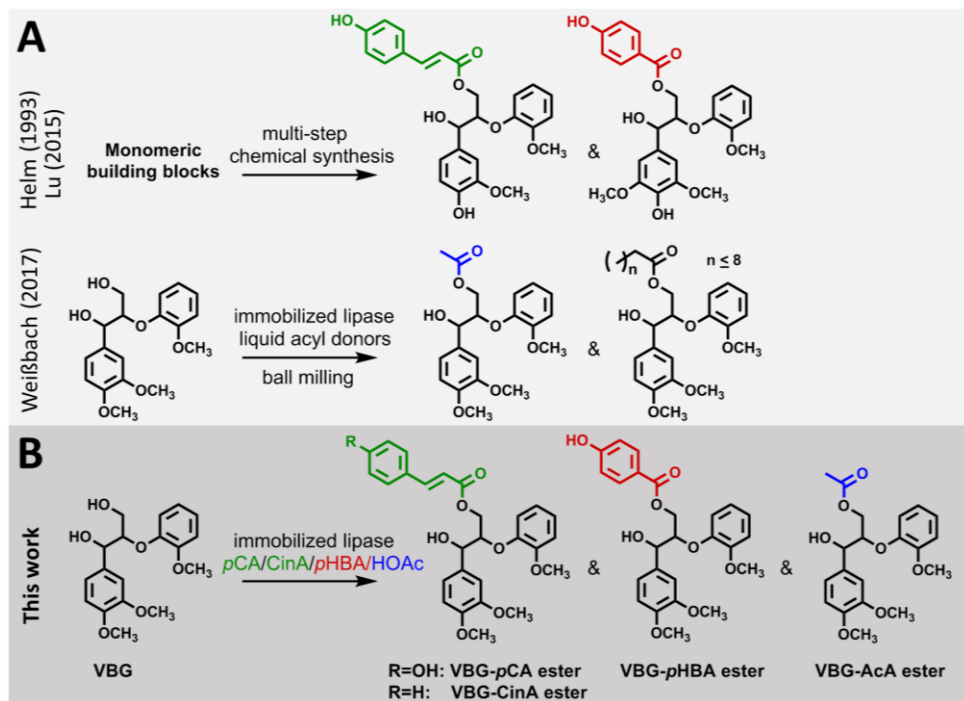


Fig. 6.2 Syntheses of acylated lignin model compounds reported in literature (A) and those described in this study (B).

(12500g, 5 min, 20 °C) and analyzed using RP-UHPLC-PDA-MS. The molar ratio VBG:VBG-CinA ester was then determined from the ratio of their UV peaks (280 nm) and calibration curves of VBG and purified VBG-CinA ester (see Supporting Information for purification details and calibration curves).

6.2.3 Acylation of lignin model compounds

Acylation of VBG were performed in *t*-butanol:toluene 1:1 (v/v) dried with 3 Å molecular sieves, unless stated otherwise. Cinnamic acid (CinA), *p*-coumaric acid (*p*CA), *p*-hydroxybenzoic acid (*p*HBA) and acetic acid (HOAc) were employed as acyl donors. Stock solutions were prepared of VBG (60 mM) and acyl donors (60 mM). The stock solutions were mixed in 1.5 mL glass vials in a 1:1 ratio to obtain a total reaction volume of 500 µL. For acetylation in pure HOAc, VBG was directly dissolved in 500 µL HOAc at a concentration of 30 mM. To all incubations, ~30 mg CALB and ~10 mg molecular sieves (3 Å) were added. The vials were incubated at 45, 55 and 65 °C in thermomixers under 600 rpm shaking. After four or six days the samples were removed and stored at 4 °C prior to analysis. After samples for analysis were withdrawn, the three reaction mixtures (i.e. those incubated at the three different temperatures) were pooled in case *p*CA or CinA was used as acyl donor. From the resulting pooled samples, VBG-*p*CA ester and

VBG-CinA ester were purified (see Supporting Information for details). In the case of acyl donor *p*HBA, only the incubation performed at 65 °C was purified.

6.2.4 Analytical methods

From all incubations, 1 μ L aliquots were collected and diluted 200 times in methanol. Samples were then centrifuged (12500 *g*, 5 min, 20 °C) and analyzed by using RP-UHPLC-PDA-MS. Hereto, reaction products were separated by using a Vanquish UHPLC system (Thermo Scientific, San Jose, CA, USA), equipped with a pump, degasser, autosampler and photodiode array (PDA) detector. Samples (1 μ L) were injected onto an Acquity UPLC BEH C18 column (150 \times 2.1 mm, particle size 1.7 μ m) with a VanGuard guard column (5 \times 2.1 mm) of the same material (Waters, Milford, MA, USA). The flow rate was 400 μ L min⁻¹ and the column temperature was 45 °C. Water (A) and acetonitrile (B) were used as eluents, both acidified with 1% formic acid. The following elution profile was used: 0-1.5 min at 5% B (isocratic), 1.5-3 min from 5 to 20% (linear gradient), 3-28 min from 20 to 75% (linear gradient), 28-28.8 min from 75 to 100%, 28.8-33.3 min at 100% (isocratic), 33.3-34 min from 100 to 5% (linear gradient) and 34-38 min at 5% (isocratic). The PDA detector was set to record wavelengths between 190 and 700 nm. After purification, the obtained VBG-*p*CA and VBG-CinA esters were analyzed at various concentrations using the same method, to check their purity and to determine their molar extinction coefficient (λ = 280 nm) relative to that of VBG. The resulting factor was used to calculate the molar ratio VBG:VBG-*p*CA ester and VBG:VBG-CinA ester in the incubated (non-purified) samples. The molar ratios VBG:ester in incubations with *p*HBA and HOAc were estimated by assuming an equal molar extinction coefficient for VBG and the corresponding esters. Although it is unlikely that VBG and VBG-*p*HBA ester have exactly the same extinction coefficients, the calculated molar ratios were in good agreement with gravimetrically determined yields.

High resolution mass spectrometric data were recorded on a Q Exactive Focus hybrid quadrupole-orbitrap mass spectrometer (Thermo Scientific) equipped with a heated ESI probe coupled to the UHPLC system. In order to obtain CID fragmentation patterns, the analysis was repeated using a Velos Pro ion-trap mass spectrometer (Thermo Scientific) coupled to the UHPLC system. For a detailed description of the methods see the Supporting Information.

In addition to UHPLC-MS analysis, the purified VBG-*p*CA, VBG-CinA and VBG-*p*HBA esters were analyzed by using 2D NMR, to confirm that acylation occurred at the C_γ-position (see Supporting Information).

6.3 Results & Discussion

6.3.1 Screening of solvents for VBG acylation

In order to determine the best conditions for CALB-catalyzed C_γ-acylation of VBG, we first performed a screening of different solvents. For this experiment, CinA was picked as an

acyl donor. Although cinnamoyl-groups do not occur in lignin, CinA has been reported to be a reasonably good acyl donor for CALB-catalyzed acylations of a variety of (non-lignin) compounds, and was therefore considered to be a good acyl donor for a first screening experiment.¹¹⁻¹⁴ Acetonitrile, acetone, *t*-butanol, toluene and *t*-butanol/toluene were employed as comparative solvents. In all solvents a product was formed that corresponded to C₂₇H₂₈O₈. Based on accurate mass and MS² fragmentation pattern, this product was annotated as the VBG-CinA ester (**Table 6.2** and **Fig. S6.2**). The results indicated that the highest conversion was obtained in toluene, followed by *t*-butanol/toluene (**Table 6.1**). Although incubation in toluene resulted in the highest product/substrate ratio, *p*CA and *p*HBA were poorly soluble in pure toluene. Therefore, *t*-butanol/toluene was selected as the solvent for further incubations.

Table 6.1 Molecular ratios of VBG and VBG-CinA ester after 2 days of incubation with CALB at 55 °C.

Solvent	Molar ratio (%) VBG:VBG-CinA ester
Acetonitrile	97:3
Acetone	97:3
<i>t</i> -Butanol	95:5
<i>t</i> -Butanol/toluene (1:1)	87:13
Toluene	19:81

6.3.2 CALB-catalyzed cinnamoylation of VBG

Enzymatic C_V-acylation of VBG with CinA was performed for four days at 45, 55 and 65 °C. In all cases, this resulted in the formation of one major product corresponding to C₂₇H₂₈O₇ (**Fig. 6.3A** and **Table 6.2**). The highest conversion was obtained at 55 °C, although the difference with other temperatures was minor (**Table 6.3**). The product was then purified using Flash chromatography, which resulted in 14.2 mg of the VBG-CinA ester. In order to prove that acylation occurred on the C_V-position and not on the C₆-position, the purified VBG-CinA ester was analyzed by using 2D-NMR, which indeed confirmed acylation at C_V (**Fig. S6.3**). Overall, this showed that incubation with CALB in combination with a simple Flash chromatography purification forms a facile and effective procedure for the production of C_V-acylated lignin models.

6.3.3 CALB-catalyzed *p*-coumaroylation and acetylation of VBG

In order to form C_V-acylated lignin models that more accurately resemble the structure of grass lignins, incubations with CALB were performed with *p*CA and HOAc as acyl donors. After VBG incubation for six days with *p*CA and CALB, a few new peaks were observed in the UHPLC-UV chromatogram, the most abundant of which corresponded to C₂₇H₂₈O₈ (**Fig. 6.3B** and **Table 6.2**). Based on accurate mass, fragmentation pattern and 2D NMR, this product was annotated as the desired VBG-*p*CA ester (**Table 6.2**, **Fig. S6.2** and **Fig. S6.4**). Similarly as in the case of cinnamoylation, the highest extent of

p-coumaroylation was obtained at 55 °C (**Table 6.3**). Despite the modest conversion, a simple Flash chromatography purification resulted in 2.0 mg of the pure VBG-*p*CA ester (**Table 6.3**). In addition, due to the very limited formation of side-products, most of the unreacted VBG (11.2 mg) was recovered after Flash chromatography. It should be noted that during the incubation, *p*CA underwent slight isomerization to its *cis*-form, which also resulted in the formation of a VBG-*cis-p*CA ester. As Flash chromatography did not baseline-separate the isomers, traces (~5% based on UV₂₈₀ peak area) of the VBG-*cis-p*CA ester were still present in the purified product (**Fig. S6.4**).

We attempted to increase the yield of the VBG-*p*CA ester by increasing the *p*CA concentration to a VBG:*p*CA molar ratio 1:3 and by performing the reaction in pure toluene (with *p*CA partly dissolved), but this mainly resulted in the formation of more side-products (data not shown). In addition, we repeated the incubations with 4-acetoxycinnamic acid instead of *p*CA as acyl donor. As the former molecule lacks an electron-donating *p*-hydroxyl group, it could be expected to be more reactive in lipase-catalyzed esterification.¹⁴ The resulting ester could then be converted to the VBG-*p*CA ester via a mild deacetylation step.

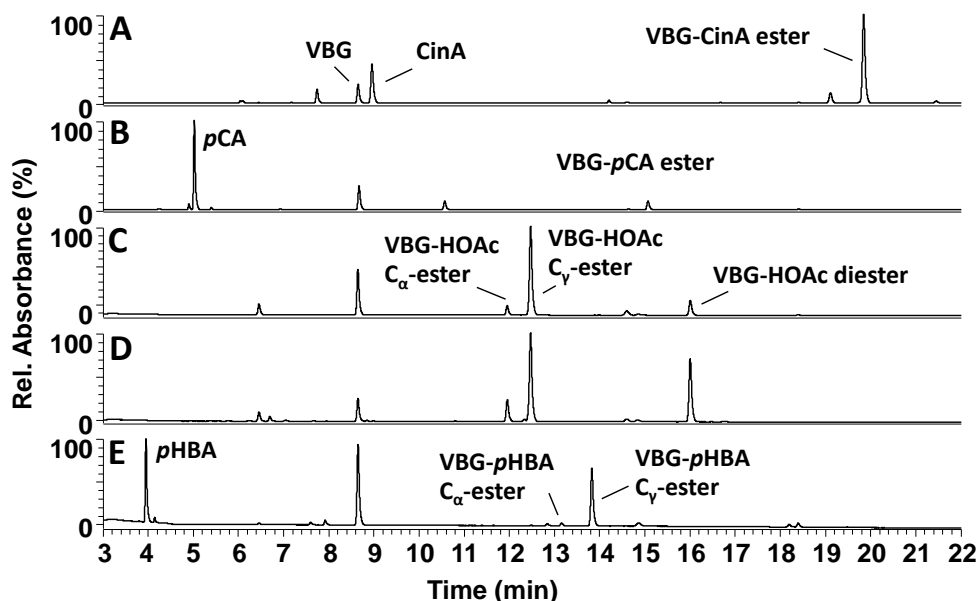


Fig. 6.3 RP-UHPLC-UV₂₈₀ chromatograms of VBG incubated with CALB and CinA (A), *p*CA (B), HOAc (C&D) and *p*HBA (E) at 55 °C (A-D) or 65 °C (E) for 6 (A, B and E) and 4 days (C&D). Incubation D was performed in pure acetic acid (i.e. solvent-free). Mass spectrometric data corresponding to the annotated peaks is displayed in Table 6.2. Mass spectrometric data corresponding to side-products can be found in Table S6.1.

Table 6.2 RP-UHPLC-MS data of substrates and products of VBG incubations with CALB and several acyl donors. The MS² fragments are given with their relative abundance (%) in parentheses. Proposed fragmentation patterns and a table including data of by-products can be found in the Supporting Information. N.D. = Not detected.

Acyl donor	Rt (min)	Tent. annot.	Mol. formula	Ion	Observed/ calculated mass	Mass error (ppm)	MS ²	λ_{max} (nm)
CinA	8.65	VBG	C ₁₈ H ₂₂ O ₆	[M+Na] ⁺	334.14161/ 334.14164	-0.10	309 (100), 339 (24), 342 (23), 215 (4), 233 (4)	278
	8.96	CinA	C ₉ H ₈ O ₂	[M-H] ⁻	148.05260/ 148.05243	1.15	103 (100)	278
	19.85	VBG-CinA ester	C ₂₇ H ₂₈ O ₇	[M+Na] ⁺	464.18317/ 464.18350	-0.71	363 (100), 469 (40), 472 (38), 215 (28), 321 (23), 339 (18), 197 (16)	278
pCA	5.00	trans-pCA	C ₉ H ₈ O ₃	[M-H] ⁻	164.04735/ 164.04735	0.05	119 (100)	310
	5.39	cis-pCA	C ₉ H ₈ O ₃	[M-H] ⁻	164.04742/ 164.04735	0.45	119 (100)	298
	8.65	VBG	C ₁₈ H ₂₂ O ₆	[M+Na] ⁺	334.14159/ 334.14164	-0.15	309 (100), 339 (24), 342 (23), 215 (4), 233 (4)	278
	15.07	VBG-trans- pCA ester	C ₂₇ H ₂₈ O ₈	[M+Na] ⁺	480.17817/ 480.17842	-0.52	379 (100), 488 (25), 485 (22), 215 (18), 339 (11), 321 (11), 309 (8)	286, 314
	15.74	VBG-cis-pCA ester	C ₂₇ H ₂₈ O ₈	[M+Na] ⁺	480.17844/ 480.17842	0.05	379 (100), 488 (25), 485 (22), 215 (18), 339 (11), 321 (11), 309 (8)	282, 310
HOAc	8.65	VBG	C ₁₈ H ₂₂ O ₆	[M+Na] ⁺	334.14161/ 334.14164	-0.09	309 (100), 339 (24), 342 (23), 215 (4), 233 (4)	278
	11.95	VBG-HOAc Co-ester	C ₂₀ H ₂₄ O ₇	[M+Na] ⁺	376.15211/ 376.15221	-0.26	309 (100), 339 (6)	278
	12.47	VBG-HOAc Cy-ester	C ₂₀ H ₂₄ O ₇	[M+Na] ⁺	376.15205/ 376.15221	-0.42	275 (100), 384 (93), 381 (56), 309 (45), 215 (38), 321 (35), 299 (34) 339 (22), 147 (22)	278
	16.00	VBG-HOAc diester	C ₂₂ H ₂₆ O ₈	[M+Na] ⁺	418.16260/ 418.16277	-0.41	299 (100), 381 (43)	278
	3.97	pHBA	C ₇ H ₆ O ₃	[M-H] ⁻	138.03161/ 138.03170	-0.58	93 (100)	254
pHBA	8.65	VBG	C ₁₈ H ₂₂ O ₆	[M+Na] ⁺	334.14143/ 334.14164	-0.59	309 (100), 339 (24), 342 (23), 215 (4), 233 (4)	278
	13.06	VBG-pHBA Co-ester	C ₂₅ H ₂₆ O ₈	[M+Na] ⁺	454.16264/ 454.16277	-0.27	309 (100), 339 (10)	N.D.
	13.85	VBG-pHBA Cy-ester	C ₂₅ H ₂₆ O ₈	[M+Na] ⁺	454.16270/ 454.16277	-0.14	353 (100), 462 (44), 215 (30), 459 (27), 321 (18), 339 (17), 290 (15)	258

Although incubation with 4-acetoxycinnamic acid resulted in a much higher conversion of VBG, mainly acetylated VBG was formed, showing that CALB catalyzed transesterification at the acetoxo group of 4-acetoxycinnamic acid rather than esterification at the carboxylic acid group (see **Fig. S6.6** for a schematic overview of the desired and the observed reaction).

Incubation of VBG with HOAc was performed both in *t*-butanol:toluene 1:1 and in pure HOAc. In both incubations, multiple products were formed (**Fig. 6.3C/D**). Two products were detected corresponding to molecular formula C₂₀H₂₄O₇ (**Table 6.2**). Based on comparison of their highly different MS² fragmentation patterns with that of the VBG-CinA and VBG-*p*CA ester, we tentatively annotated the major product as the VBG-HOAc C_γ-ester and the minor one as the VBG-HOAc C_α-ester (**Table 6.2** and **Fig. S6.2**). Additional evidence for regio-isomerism comes from the fact that also a diester (C₂₂H₂₆O₈) of VBG was detected (**Fig. 6.3C/D**, **Table 6.1** and **Fig. S6.2**), suggesting that acetylation by CALB can occur at both alcohol groups. Although the overall conversion of VBG was higher in incubations with pure HOAc (except for the incubation at 45 °C), the higher conversion mainly resulted in an increased formation of the diester. Therefore, incubation in *t*-butanol-toluene was better for a maximum yield of the desired C_γ-acetylated VBG.

Table 6.3 Summarized results of the incubations of VBG with CALB and several acyl donors. The underlined numbers in the column 'molar ratio' refer to the desired product (i.e. C_γ-esters of VBG).

Acyl donor	Incubation time (days)	T (°C)	Molar ratio (%) VBG:product(s)	Yield after purification (%)
CinA	6	45	30:70	69 ^a
		55	26:74	
		65	33:67	
<i>p</i> CA	6	45	95:5	9 ^a
		55	87:13	
		65	91:9	
HOAc	4	45	28:6:57:9 ^{b,c}	N.D.
		55	29:5:57:9	
		65	23:8:51:18	
HOAc ^d	4	45	50:9:36:5	N.D.
		55	11:11:47:31	
		65	8:10:45:37	
<i>p</i> HBA	6	45	Traces of ester	30 ^e
		55	Traces of ester	
		65	64:36 ^c	

^aYields of pooled incubations (45, 55 and 65 °C) ^bRatio VBG:C_α-ester:C_γ-ester:diester. ^cMolar ratio estimated (see experimental section). ^dThis incubation was performed in pure HOAc (i.e. no organic solvent was used). ^eYield of (non-pooled) incubation at 65 °C. N.D. = Not determined. Molar ratios were calculated as explained in the Supporting Information (see Fig. S6.1).

6.3.4 CALB-catalyzed *p*-hydroxybenzoylation of VBG

In order to form VBG-*p*HBA ester, a relevant model compound for several hardwood lignins, *p*HBA was employed as acyl donor. At 45 and 55 °C, acylation occurred in trace amounts (data not shown). The limited reactivity of hydroxybenzoic acids towards esterification by CALB has been reported multiple times in literature, and is suggested to be related to the same electron-donating effect of the *p*-hydroxyl group as described for *p*CA.^{12,15-19} Remarkably, after incubation at 65 °C, a prominent peak corresponding to C₂₅H₂₆O₈ was observed in the UHPLC-UV₂₈₀ chromatogram (**Fig. 6.3E** and **Table 6.2**). Based on its molecular formula, fragmentation pattern and 2D NMR it was annotated as the VBG-*p*HBA C_γ-ester (**Table 6.2**, **Fig. S6.2** and **Fig. S6.5**). In addition, a small peak corresponding to the same molecular formula was detected. As the fragmentation pattern of the compound was highly different from that of the major product, the minor product was tentatively annotated as VBG-*p*HBA C_α-ester (**Fig. 6.3E**, **Table 6.2** and **Fig. S6.2**). Although the formation of a C_α-ester was unwanted, this only accounted for ~4% of the total ester formation (based on UV₂₈₀ peak area). After purification, the desired VBG-*p*HBA C_γ-ester was obtained with a yield of 30% (**Table 6.3**), and the C_α-ester was only present in trace amounts (<1%). It should be noted that a repetition of the incubation with *p*HBA at 65 °C resulted in a lower conversion than initially found (VBG:VBG-*p*HBA ester ratio 97:3). The reason behind this remains unknown. Increasing the incubation temperature to 75 °C did not improve the conversion (data not shown).

All incubations described above were also performed in the absence of CALB, which showed no acylation of VBG. This indicated that all acylations described above were truly catalyzed by the enzyme. Although the product yields were strongly dependent on the acyl donor, all desired products were obtained at mg scale, which is sufficient to perform multiple model compound experiments followed by UHPLC-MS or GC-MS analysis.^{6,20-22}

6.4 Conclusions

In summary, C_γ-acylation of the commercially available lignin model compound VBG was performed in *t*-butanol/toluene by using CALB as a catalyst. This way, new lignin models were obtained that resemble specific structural motifs of grass and hardwood lignins. A one-step incubation and simple purification allowed to obtain the acylated products at mg scale, while unreacted substrate could be recovered. The procedure provides a facile and effective alternative for multi-step chemical synthesis.

6.5 References

1. Munk L, Sitarz AK, Kalyani DC, Mikkelsen JD and Meyer AS. Can laccases catalyze bond cleavage in lignin? *Biotechnology Advances* **2015**, *33* (1), 13-24.
2. Ralph J, Lapierre C and Boerjan W. Lignin structure and its engineering. *Current Opinion in Biotechnology* **2019**, *56*, 240-249.
3. Vangeel T, Schutyser W, Renders T and Sels BF. Perspective on lignin oxidation: advances, challenges, and future directions. *Topics in Current Chemistry* **2018**, *376* (4), 30.
4. Liu C, Wu S, Zhang H and Xiao R. Catalytic oxidation of lignin to valuable biomass-based platform chemicals: a review. *Fuel Processing Technology* **2019**, *191*, 181-201.
5. Kim KH, Dutta T, Walter ED, Isern NG, Cort JR, Simmons BA and Singh S. Chemoselective methylation of phenolic hydroxyl group prevents quinone methide formation and repolymerization during lignin depolymerization. *ACS Sustainable Chemistry & Engineering* **2017**, *5* (5), 3913-3919.
6. Hilgers R, Twentymann-Jones M, van Dam A, Gruppen H, Zuilhof H, Kabel MA and Vincken J-P. The impact of lignin sulfonation on its reactivity with laccase and laccase/HBT. *Catalysis Science & Technology* **2019**, *9* (6), 1535-1542.
7. Zeng J, Mills MJL, Simmons BA, Kent MS and Sale KL. Understanding factors controlling depolymerization and polymerization in catalytic degradation of β -ether linked model lignin compounds by versatile peroxidase. *Green Chemistry* **2017**, *19* (9), 2145-2154.
8. Helm RF and Ralph J. Lignin-hydroxycinnamoyl model compounds related to forage cell wall structure. 2. Ester-linked structures. *Journal of Agricultural and Food Chemistry* **1993**, *41* (4), 570-576.
9. Lu F, Karlen SD, Regner M, Kim H, Ralph SA, Sun R-C, Kuroda K-I, Augustin MA, Mawson R and Sabarez H. Naturally *p*-hydroxybenzoylated lignins in palms. *BioEnergy Research* **2015**, *8* (3), 934-952.
10. Weißbach U, Dabral S, Konnert L, Bolm C and Hernández JG. Selective enzymatic esterification of lignin model compounds in the ball mill. *Beilstein Journal of Organic Chemistry* **2017**, *13* (1), 1788-1795.
11. Enaud E, Humeau C, Piffaut B and Girardin M. Enzymatic synthesis of new aromatic esters of phloridzin. *Journal of Molecular Catalysis B: Enzymatic* **2004**, *27* (1), 1-6.
12. Jakovetić SM, Jugović BZ, Gvozdenović MM, Bezbradica DI, Antov MG, Mijin DŽ and Knežević-Jugović ZD. Synthesis of aliphatic esters of cinnamic acid as potential lipophilic antioxidants catalyzed by lipase B from *Candida antarctica*. *Applied Biochemistry and Biotechnology* **2013**, *170* (7), 1560-1573.
13. Tanasković SJ, Jokić B, Grbavčić S, Drvenica I, Prlainović N, Luković N and Knežević-Jugović Z. Immobilization of *Candida antarctica* lipase B on kaolin and its application in synthesis of lipophilic antioxidants. *Applied Clay Science* **2017**, *135*, 103-111.
14. Cassani J, Luna H, Navarro A and Castillo E. Comparative esterification of phenylpropanoids versus hydrophenylpropanoids acids catalyzed by lipase in organic solvent media. *Electronic Journal of Biotechnology* **2007**, *10* (4), 508-513.
15. Buisman GJH, Van Helteren CTW, Kramer GFH, Veldsink JW, Derksen JTP and Cuperus FP. Enzymatic esterifications of functionalized phenols for the synthesis of lipophilic antioxidants. *Biotechnology Letters* **1998**, *20* (2), 131-136.
16. Stamatis H, Sereti V and Kolisis FN. Studies on the enzymatic synthesis of lipophilic derivatives of natural antioxidants. *Journal of the American Oil Chemists' Society* **1999**, *76* (12), 1505.
17. Bitencourt TB and da Graça Nascimento M. Chemo-enzymatic synthesis of N-alkyloxaziridines mediated by lipases and urea-hydrogen peroxide. *Green Chemistry* **2009**, *11* (2), 209-214.
18. Otto RT, Scheib H, Bornscheuer UT, Pleiss J, Syltatk C and Schmid RD. Substrate specificity of lipase B from *Candida antarctica* in the synthesis of arylaliphatic glycolipids. *Journal of Molecular Catalysis B: Enzymatic* **2000**, *8* (4-6), 201-211.
19. Ardhaoui M, Falcimaigne A, Engasser J, Moussou P, Pauly G and Ghoul M. Enzymatic synthesis of new aromatic and aliphatic esters of flavonoids using *Candida antarctica* lipase as biocatalyst. *Biocatalysis and Biotransformation* **2004**, *22* (4), 253-259.

20. Hilgers RJ, Vincken J-P, Gruppen H and Kabel MA. Laccase/mediator systems: Their reactivity towards phenolic lignin structures. *ACS Sustainable Chemistry & Engineering* **2018**, *6* (2), 2037-2046.
21. Kawai S, Iwatsuki M, Nakagawa M, Inagaki M, Hamabe A and Ohashi H. An alternative β -ether cleavage pathway for a non-phenolic β -O-4 lignin model dimer catalyzed by a laccase-mediator system. *Enzyme and Microbial Technology* **2004**, *35* (2-3), 154-160.
22. Kawai S, Nakagawa M and Ohashi H. Degradation mechanisms of a nonphenolic β -O-4 lignin model dimer by *Trametes versicolor* laccase in the presence of 1-hydroxybenzotriazole. *Enzyme and Microbial Technology* **2002**, *30* (4), 482-489.

6.6 Supporting Information

6.6.1 Electrospray Ionization – Fourier Transform Mass Spectrometry

High-resolution mass spectra were recorded on a Q Exactive Focus hybrid quadrupole-orbitrap mass spectrometer (Thermo Scientific), equipped with a heated ESI probe, coupled to the UHPLC system. Two-thirds of the flow was directed toward the MS. Full MS data were recorded in both negative and positive ionization mode over a range of m/z 120-1,500 at a resolution of 70,000. The mass spectrometer was calibrated in both positive and negative mode using Tune 2.8 software (Thermo Scientific) by direct infusion of Pierce LTQ ESI positive and negative ion calibration solutions (Thermo Scientific). Nitrogen was used as sheath gas (46.7 arbitrary units) and auxiliary gas (10.8 arbitrary units). The capillary temperature was 254 °C; the probe heater temperature was 408 °C; the source voltage was 2.5 kV in negative mode and 3.5 kV in positive mode; and the S-lens RF level was 50. Data processing was performed using Xcalibur 2.2 (Thermo Scientific) and Compound Discoverer 2.0 (Thermo Scientific).

6.6.2 Electrospray Ionization – Ion Trap Mass Spectrometry

Mass spectra were recorded on a Velos Pro ion-trap mass spectrometer (Thermo Scientific), equipped with a heated ESI probe coupled to the UHPLC system. Data were collected in both positive and negative ionization mode (m/z 120-2000), and data-dependent MS² analysis was performed using collision-induced dissociation with a normalized collision energy of 35%. Gas flows, temperatures and voltages were identical to those described for Fourier Transform Mass Spectrometry. The S-lens RF level was 65.30. Data processing was performed using Xcalibur 2.2 (Thermo Scientific).

6.6.3 Purification of acylated model compounds

The obtained VBG-*p*CA, VBG-CinA and VBG-*p*HBA esters were purified by using Flash chromatography. Hereto, the (pooled) reaction mixtures were lyophilized and re-dissolved in 1 mL methanol. The reaction mixtures were then purified by using a Reveleris Flash system (Grace Davison Discovery Sciences, Columbia, MD, USA), equipped with a 4 g Reveleris RP Flash cartridge, ELSD detector and UV detector. The eluents used were water (eluent A) and ACN (eluent B), both containing 1% (v/v) formic acid. After activation of the cartridge with eluent B, and washing with 5 column volumes of eluent A, the samples were injected. The following elution profiles were used: for VBG-*p*CA and VBG-CinA, 0-1 min at 5% B (isocratic), 1-2 min from 5 to 20% B (linear gradient), 2-16 min from 20 to 52% B (linear gradient), 16-16.5 min from 52 to 100% B (linear gradient), 16.5-17.7 min at 100% B (isocratic); for VBG-*p*HBA: 0-1 min at 5% B (isocratic), 1-2 min from 5 to 20% B (linear gradient), 2-16 min from 20 to 45% B (linear gradient), 16-16.5 min from 45 to 100% B (linear gradient), 16.5-17.7 min at 100% B (isocratic). The

flowrate was 18 mL min⁻¹ and fractions of 6 mL were collected. The resulting fractions were diluted 10 times with methanol and analyzed by using RP-UHPLC-PDA-MS. Fractions that contained the desired esters and that were free of other products were pooled. From the incubation containing VBG and *p*CA, also unreacted VBG was recovered after purification. Remaining ACN was evaporated under reduced pressure, after which the solutions were lyophilized. The ester yields and VBG recovery were then determined gravimetrically.

6.6.4 2D NMR analysis of the purified VBG-*p*CA ester

In order to prove that acylation of VBG occurred on the C_V-position, 2D NMR experiments were conducted (both HSQC and HMBC). Hereto, approximately 1 mg of purified VBG-*p*CA ester was dissolved in 250 μ L DMSO-*d*₆. The NMR experiments were recorded at 25 °C by using hsqcetgpsisp2.2 and hmbcgpndqf pulse sequences on a Bruker Avance III 600 MHz (VBG-*p*CA ester) or Bruker Avance HD 700 MHz (VBG-CinA and VBG-*p*HBA ester) NMR spectrometer (Bruker BioSpin, Rheinstetten, Germany) equipped with a 5 mm cryo-probe. The internal temperature of the probe was set at 298 K. The solvent peak (DMSO-*d*₆) was used as an internal reference (δ_c 39.5 ppm; δ_H 2.49 ppm).

6.6.5 Oxygen consumption

Oxygen consumption was measured with an Oxytherm System (Hansatech Kings Lynn, UK). Lignin model compounds and mediators were used as substrates at 0.4 mM in a sodium acetate buffer (50 mM) at pH 4. Also in incubations containing both a model compound and a mediator, the individual concentrations were 0.4 mM. After equilibration, laccase was added to obtain an activity of 1 U mL⁻¹. Here, a higher laccase activity was used than in the incubations described in the article, in order to obtain a more clear decrease in O₂ concentration within the short time frame of the measurement. Incubations were performed in a total volume of 1 mL at 25 °C. Data were acquired by using Oxygraph Plus software (Hansatech).

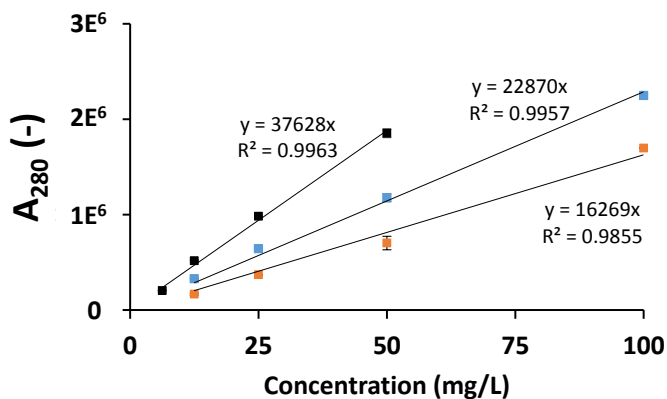


Fig. S6.1 UHPLC-UV₂₈₀ calibration curves of VBG (orange), VBG-CinA (blue) and VBG-pCA (black).

The slopes from these calibration curves were used to calculate the molar ratio product:VBG, according to the following formula:

$$\% \text{ product} = \frac{\frac{A_{\text{product}} / (\text{slope}_{\text{product}} * Mw_{\text{product}})}{A_{\text{VBG-ester}}}}{\frac{A_{\text{VBG-ester}}}{\text{slope}_{\text{product}} * Mw_{\text{product}}} + \frac{A_{\text{VBG}}}{\text{slope}_{\text{VBG}} * Mw_{\text{VBG}}}}$$

Where A is the UV₂₈₀ peak area obtained from RP-UHPLC-PDA-MS analysis of the reaction mixtures and Mw is the molecular weight. % VBG = 100 - % product.

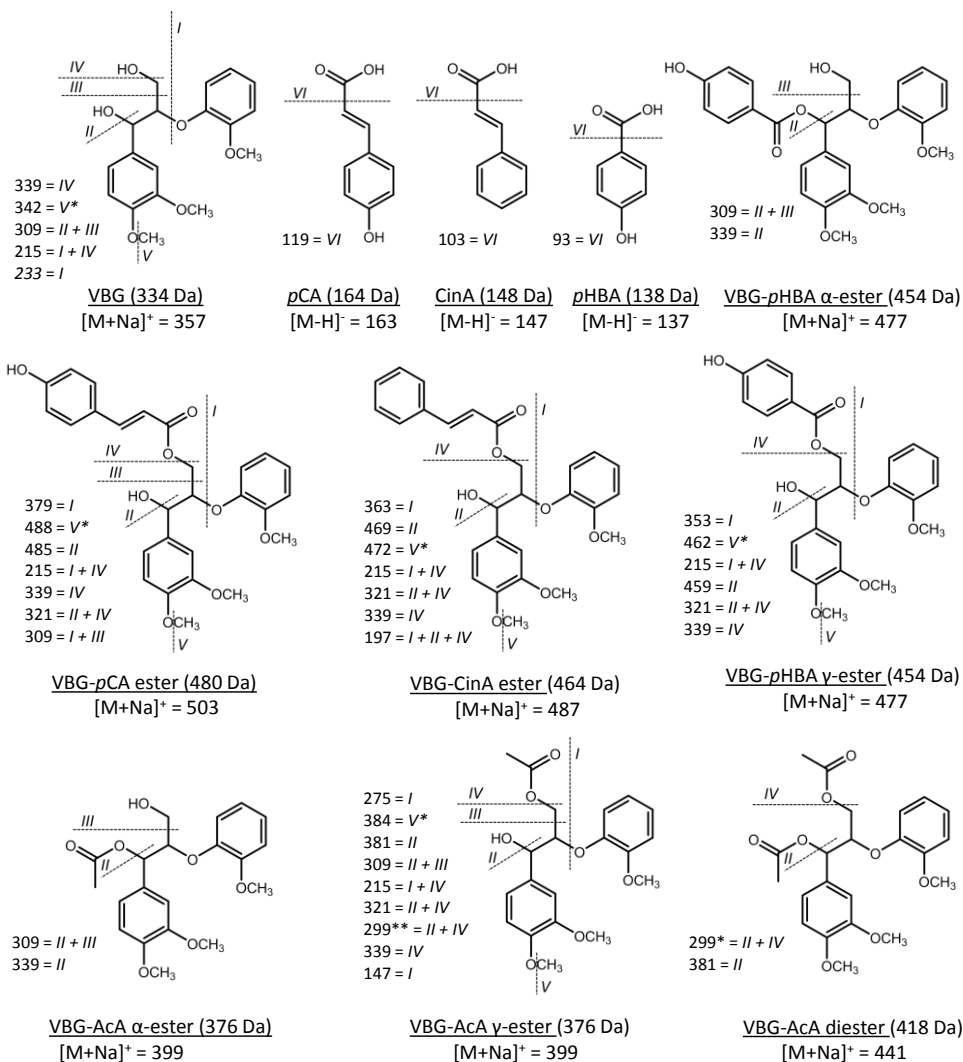


Fig. S6.2 Proposed structures and fragmentation patterns of the substrates and products reported in Table 6.1. *These fragmentations are suggested to form radical fragments. ** This fragmentation is suggested to involve loss of the Na⁺ ion. Since fragmentation of *cis/trans* isomers were identical, only the *trans*-isomers of pCA and VBG-pCA ester are shown. It should be noted that fragmentation V could also correspond to fragmentation of one of the other methoxyl groups.

Table S6.1 RP-UHPLC-MS data of substrates annotated and unknown products of VBG incubations with CAL-B lipase and several acyl donors. The MS² fragments are given with their relative abundance (%) in parentheses.

Acyl donor	Rt (min)	Tent. annot.	Mol. formula	Ion	Observed / calculated mass	Mass error (ppm)	MS ²
<i>p</i> CA	4.90	<i>unknown</i>	C ₁₂ H ₁₄ O ₅	[M-H] ⁻	238.08417/ 238.08413	0.18	119 (100), 163 (69), 145 (44)
	5.00	<i>trans-p</i> CA	C ₉ H ₈ O ₃	[M-H] ⁻	164.04735/ 164.04735	0.05	119 (100)
	5.39	<i>cis-p</i> CA	C ₉ H ₈ O ₃	[M-H] ⁻	164.04742/ 164.04735	0.45	119 (100)
	6.90	<i>unknown</i>	C ₂₄ H ₂₆ O ₁₀	[M+Na] ⁺	474.15275/ 474.15260	0.31	N.D.
	8.65	VBG	C ₁₈ H ₂₂ O ₆	[M+Na] ⁺	334.14159/ 334.14164	-0.15	309 (100), 339 (24), 342 (23), 215 (4), 233 (4)
	10.56	<i>unknown</i>	C ₂₁ H ₂₀ O ₇	[M-H] ⁻	384.12089/ 384.12091	-0.20	163 (100), 219 (30), (13)
	15.07	VBG- <i>trans-p</i> CA ester	C ₂₇ H ₂₈ O ₈	[M+Na] ⁺	480.17817/ 480.17842	-0.52	379 (100), 488 (25), 485 (22), 215 (18)
	15.74	VBG- <i>cis-p</i> CA ester	C ₂₇ H ₂₈ O ₈	[M+Na] ⁺	480.17844/ 480.17842	0.05	379 (100), 488 (25), 485 (22), 215 (18)
CinA	6.06	<i>unknown</i>	C ₁₅ H ₂₀ O ₇	[M+Na] ⁺	312.12107/ 312.12091	0.51	317 (100), 187 (70), 171 (14)
	7.72	<i>unknown</i>	C ₁₂ H ₁₄ O ₄	[M+H] ⁺	222.08936/ 222.08921	0.67	131 (100), 205 (48), 183 (11)
	8.65	VBG	C ₁₈ H ₂₂ O ₆	[M+Na] ⁺	334.14161/ 334.14164	-0.10	309 (100), 339 (24), 342 (23), 215 (4), 233 (4)
	8.96	CinA	C ₉ H ₈ O ₂	[M-H] ⁻	148.05260/ 148.05243	1.15	103 (100)
	14.20	<i>unknown</i>	C ₂₄ H ₂₆ O ₈	[M+Na] ⁺	442.16318/ 442.16277	0.93	447 (100), 317 (68), 243 (11), 299 (8)
	19.12	<i>unknown</i>	C ₂₁ H ₂₀ O ₅	[M+Na] ⁺	352.13099/ 352.13108	-0.26	205 (100), 227 (34), 171 (18), 131 (13)
	19.85	VBG-CinA ester	C ₂₇ H ₂₈ O ₇	[M+Na] ⁺	464.18317/ 464.18350	-0.71	363 (100), 472 (48), 469 (40), 215 (37), 321 (21)
<i>p</i> HBA	3.97	<i>p</i> HBA	C ₇ H ₆ O ₃	[M-H] ⁻	138.03161/ 138.03170	-0.58	93 (100)
	5.60	<i>unknown</i>	C ₁₇ H ₁₆ O ₇	[M-H] ⁻	332.08925/ 332.08961	-1.05	137 (100), 193 (39)
	5.92	<i>unknown</i>	C ₁₇ H ₁₆ O ₇	[M-H] ⁻	332.08931/ 332.08961	-0.87	137 (100), 211 (24), 193 (10)

Table S6.1 Continued.

Acyl donor	Rt (min)	Tent. annot.	Mol. formula	Ion	Observed / calculated mass	Mass error (ppm)	MS ²
	8.65	VBG	C ₁₈ H ₂₂ O ₆	[M+Na] ⁺	334.14143/ 334.14164	-0.59	309 (100), 339 (24), 342 (23), 215 (4), 233 (4)
	12.79	<i>unknown</i>	C ₂₄ H ₂₀ O ₉	[M-H] ⁻	452.11048/ 452.11074	-0.53	313 (100)
	13.06	VBG- <i>p</i> HBA Ca-ester	C ₂₅ H ₂₆ O ₈	[M+Na] ⁺	454.16264/ 454.16277	-0.27	309 (100), 339 (10)
	13.85	VBG- <i>p</i> HBA Cy-ester	C ₂₅ H ₂₆ O ₈	[M+Na] ⁺	454.16270/ 454.16277	-0.14	353 (100), 462 (44), 215 (30), 459 (27), 321 (18), 339 (17), 290 (15)
AcA	6.45	<i>unknown</i>	C ₉ H ₁₄ O ₆	[M+Na] ⁺	218.07902/ 218.07904	-0.09	181 (100)
	8.65	VBG	C ₁₈ H ₂₂ O ₆	[M+Na] ⁺	334.14161/ 334.14164	-0.09	309 (100), 339 (24), 342 (23), 215 (4), 233 (4)
	11.95	VBG-AcA Ca-ester	C ₂₀ H ₂₄ O ₇	[M+Na] ⁺	376.15211/ 376.15221	-0.26	309 (100), 339 (6)
	12.47	VBG-AcA Cy-ester	C ₂₀ H ₂₄ O ₇	[M+Na] ⁺	376.15205/ 376.15221	-0.42	275 (100), 384 (93), 381 (56), 309 (45), 215 (38), 321 (35), 299 (34) 339 (22), 147 (22), 299 (100), 381 (43)
	16.00	VBG-AcA diester	C ₂₂ H ₂₆ O ₈	[M+Na] ⁺	418.16260/ 418.16277	-0.41	

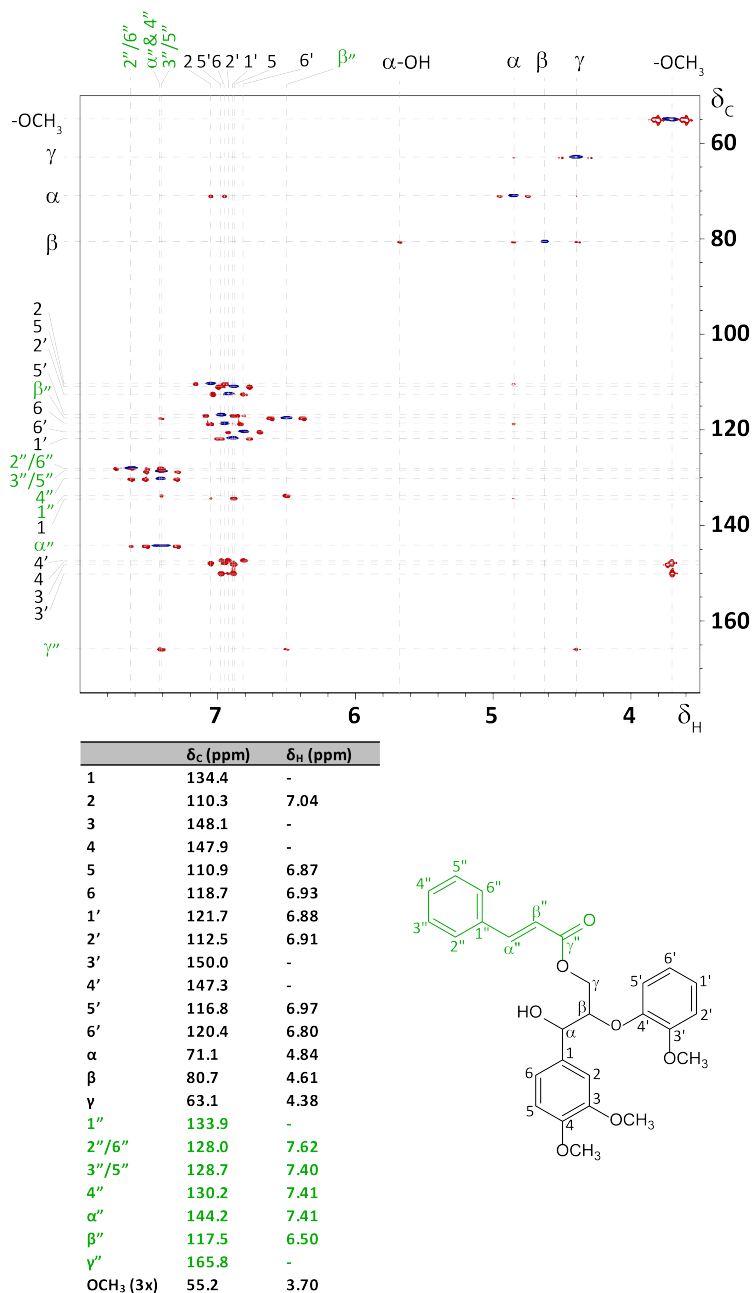


Fig. S6.3 HSQC (blue) and HMBC (red) spectrum of the purified VBG-CinA ester. Exact chemical shifts and annotations are shown in the table. Annotations in black correspond to the VBG moiety and those in green correspond to the CinA moiety.

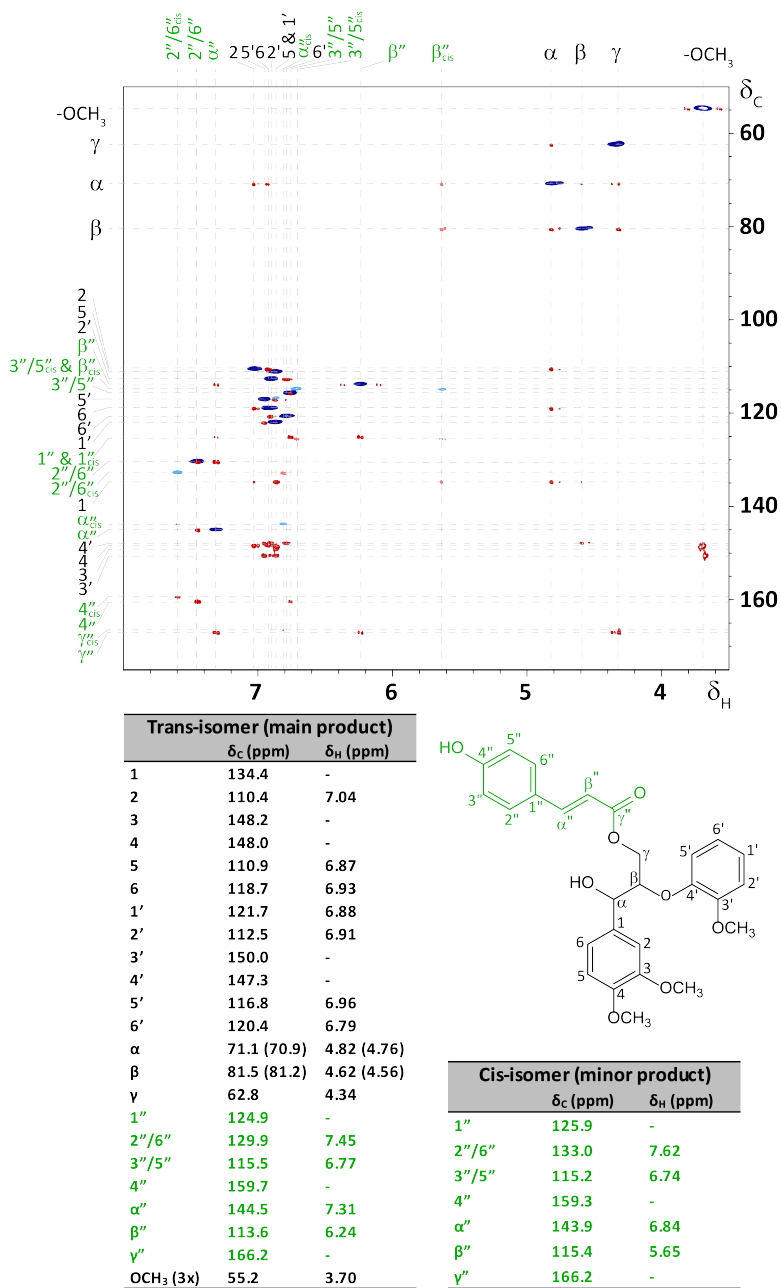
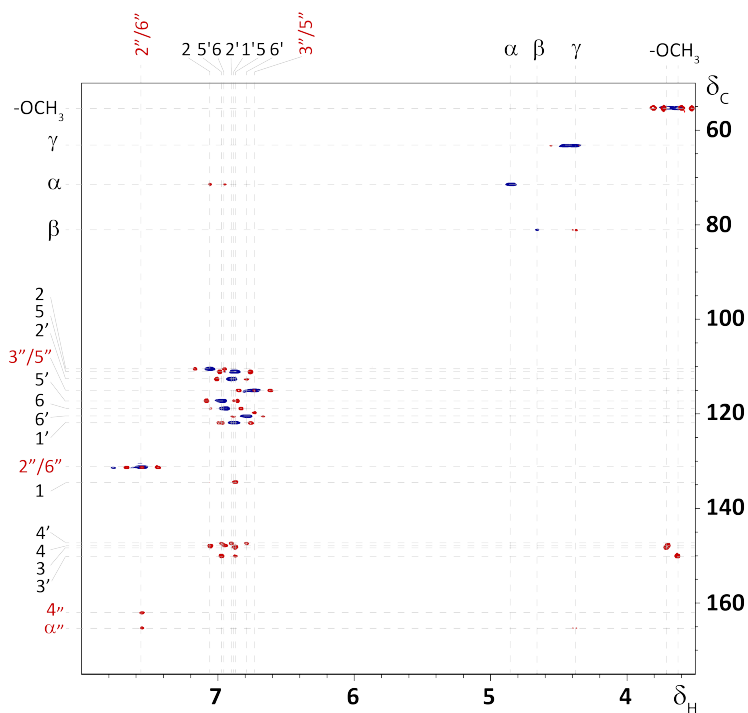


Fig. S6.4 HSQC (blue) and HMBC (red) spectrum of the purified VBG-*p*CA ester. Exact chemical shifts and annotations are shown in the tables. Annotations in black correspond to the VBG moiety and those in green correspond to the *p*CA moiety. In addition to the expected VBG-trans-*p*CA ester, trace peaks corresponding to a VBG-cis-*p*CA ester were detected. Peaks specifically belonging to the cis-isomer are shown in light blue and red. Other signals of the cis-isomer overlap with those of the trans-isomer. Annotation of trans and cis-isomers was performed based on published NMR data of trans and cis-coumaroyl-esters.^{1,2}



	δ_C (ppm)	δ_H (ppm)
1	134.4	-
2	110.4	7.06
3	148.1	-
4	147.8	-
5	110.9	6.87
6	118.7	6.95
1'	121.7	6.88
2'	112.5	6.90
3'	150.0	-
4'	147.2	-
5'	117.1	6.97
6'	120.4	6.79
α	71.4	4.85
β	81.0	4.66
γ	63.2	4.39/4.45
2''/6''	131.1	7.56
3''/5''	114.8	6.73
4''	161.9	-
α''	165.1	-
OCH ₃ (3x)	55.2	3.67

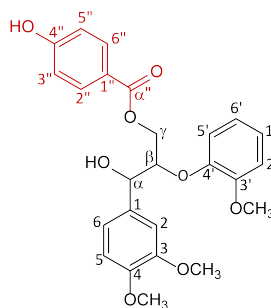


Fig. S6.5 HSQC (blue) and HMBC (red) spectrum of the purified VBG-*p*HBA ester. Exact chemical shifts and annotations are shown in the table. Annotations in black correspond to the VBG moiety and those in red correspond to the *p*HBA moiety.

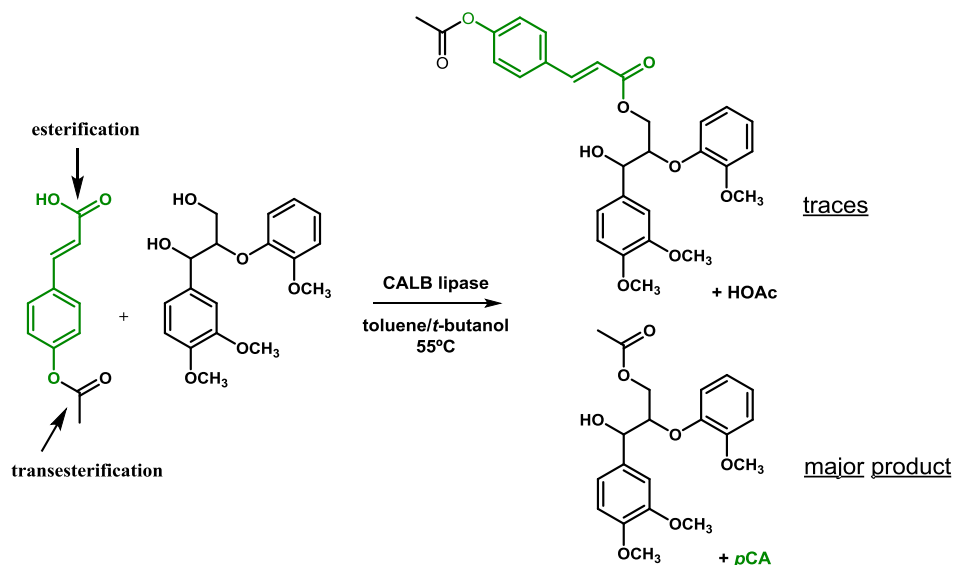
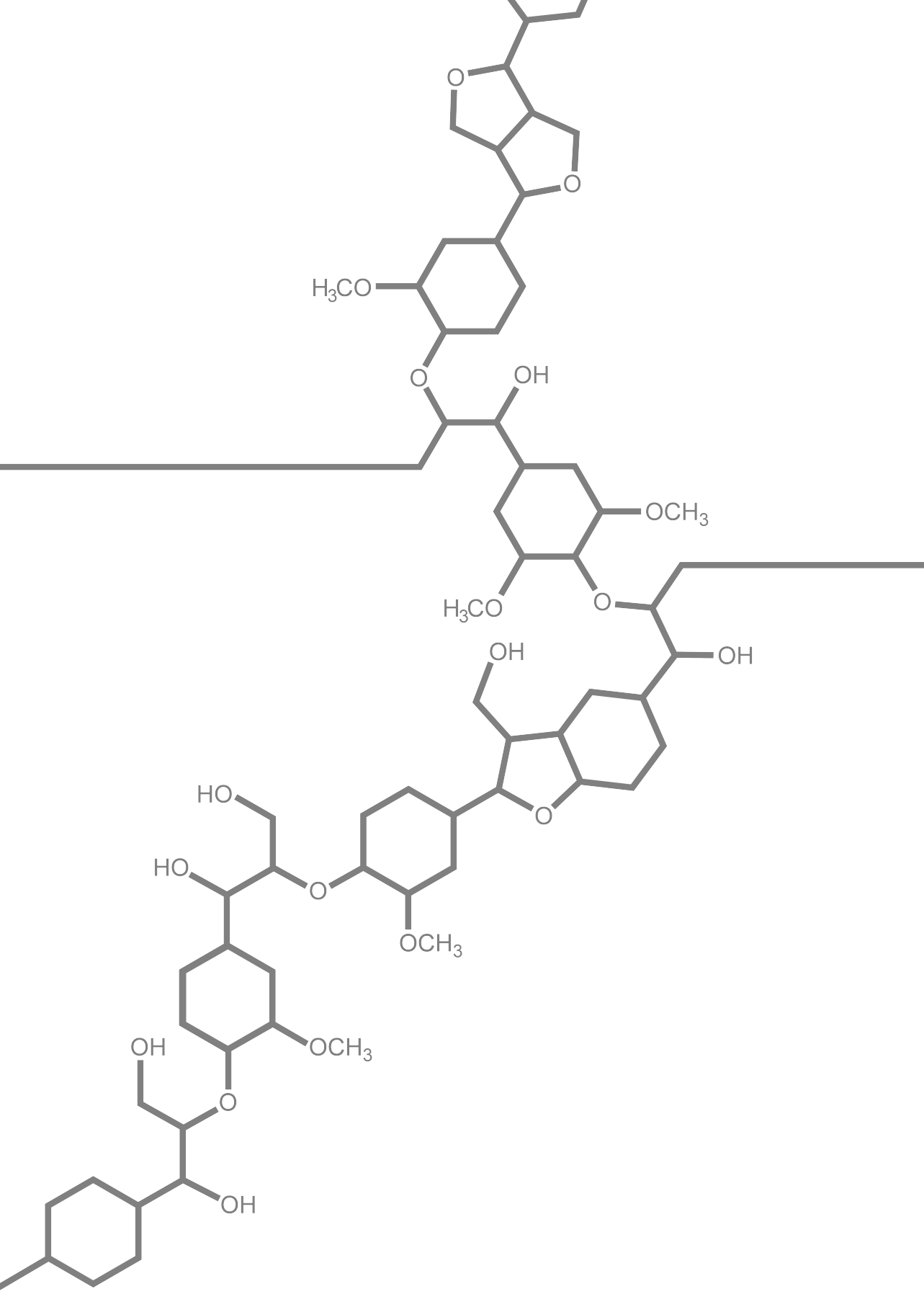


Fig. S6.6 Schematic overview of the incubation of VBG with 4-acetoxycinnamic acid and CALB lipase, showing the formation of the desired esterification reaction at the carboxyl group (top) and the undesired transesterification reaction at the acetoxy group (bottom).

References Supporting Information

1. Hosokawa K, Fukunaga Y, Fukushi E and Kawabata J. Seven acylated anthocyanins in the blue flowers of *Hyacinthus orientalis*. *Phytochemistry* **1995**, 38 (5), 1293-1298.
2. Bero J, Hérent M-F, Schmeda-Hirschmann G, Frédérick M and Quetin-Leclercq J. *In vivo* antimalarial activity of *Keetia leucantha* twigs extracts and in vitro antiplasmodial effect of their constituents. *Journal of Ethnopharmacology* **2013**, 149 (1), 176-18



On the reactivity of *p*-coumaroyl groups in lignin upon laccase and laccase/HBT treatments

Laccase/mediator systems (LMS) are potential green tools for oxidative degradation and modification of lignin. Although LMS convert both phenolic and non-phenolic lignin structures, phenolic structures are more prone to react. Remarkably, in a previous study on laccase/HBT treatment of grasses, we observed accumulation of *p*-coumaroyl moieties in residual lignin, even though such groups are free-phenolic structures. To provide more insights into this apparent paradox, here, we studied the reactivity of *p*-coumaroyl groups in lignin and model compounds, by using HSQC NMR and RP-UHPLC-PDA-MSⁿ, respectively. It was found that a *p*-coumaroylated model compound (VBG-*p*CA), in contrast to its non-acylated analogue, was rapidly converted by laccase and laccase/HBT, resulting in oxidative coupling and HBT-mediated degradation, respectively. The high reactivity of VBG-*p*CA was related to the phenolic character of the *p*-coumaroyl group. Upon laccase/HBT treatment of two grass lignin isolates, *p*-coumaroyl groups accumulated in residual lignin, indicating that *p*-coumaroyl groups in polymeric lignin display different reactivity than those in model compounds. Based on additional experiments, we propose that *p*-coumaroyl groups in lignin polymers can be oxidized by laccase/HBT, but undergo HSQC-undetectable radical coupling or redox reactions rather than degradation.

Based on: Roelant Hilgers, Mirjam A. Kabel and Jean-Paul Vincken. On the reactivity of *p*-coumaroyl groups in lignin upon laccase and laccase/HBT treatments. *ACS Sustainable Chemistry & Engineering* **2020**, 8 (23), 8723-8731.

7.1 Introduction

Lignocellulosic biomass is a promising resource for the sustainable production of biofuels and biochemicals. Efficient conversion of lignocellulosic biomass, however, is challenging, due to its recalcitrant structure. A major factor limiting efficient conversion is the presence of lignin, a complex aromatic heteropolymer.¹ Over the past years, laccase (EC 1.10.3.2) and laccase/mediator systems have gained extensive attention as potential green tools for lignin degradation. However, despite the insights from various mechanistic studies,²⁻⁵ the reactivity of lignin in laccase and LMS incubations is still not fully understood.

Lignin consists, depending on its botanical origin, of syringyl (S), guaiacyl (G) and *p*-hydroxyphenyl (H) subunits. These subunits form a polymer through various C-O and C-C linkages, of which the β -O-4' linkage is the most abundant one.^{6,7} The botanical origin of lignin does not only affect the S/G/H ratio, but also the extent and type of C_V-acylation. Whereas no C_V-acylation occurs in softwood lignin, several hardwood lignins (i.e. those from willow, aspen, poplar and palms) are C_V-acylated by *p*-hydroxybenzoyl and acetyl groups,⁷⁻⁹ and grass lignins can be extensively *p*-coumaroylated and acetylated at the C_V-OH group.^{7,10,11}

Laccases are oxidases that catalyze one-electron oxidation of aromatic substrates. Their redox potential (<800 mV vs. NHE)² is, however, too low to oxidize the non-phenolic substructures of lignin, which account for up to 90% of the lignin polymer.¹² To overcome this recalcitrance, a mediator, such as 1-hydroxybenzotriazole (HBT) can be added to form a laccase/mediator system (LMS). In such a LMS, laccase oxidizes the mediator, which, in turn, oxidizes the non-phenolic lignin substructure. In the case of a laccase/HBT system, the latter step is generally suggested to occur via hydrogen atom transfer (HAT), resulting in benzylic radicals.^{5,13} These radicals can, subsequently, react further via multiple pathways. The final outcome of these radical reactions is dependent on the local structures neighboring the benzylic radical, as well as on the reaction conditions.^{4,13} In various biomass substrates, LMS treatments have been shown to induce oxidation and degradation of lignin interunit linkages, resulting in delignification (up to 50%) of the biomass.¹⁴⁻¹⁶

Recently, we observed that, upon laccase/HBT treatment of milled corn stover and wheat straw, *p*-coumaroylated substructures accumulated in the residue, suggesting that these substructures are more recalcitrant toward LMS-catalyzed degradation than non-acylated substructures.¹⁶ This observation is remarkable, as the *p*-coumaroyl moieties in lignin are generally suggested to occur as free-phenolic groups (i.e. unetherified at the phenolic OH-group),^{10,17,18} which are expected to be more easily oxidized than non-phenolic (etherified) lignin structures.¹⁹⁻²¹ So far, the reason behind this apparent discrepancy remains unknown. In fact, very little is known at all on the reactivity of *p*-coumaroyl moieties in lignin upon oxidative treatments.

As an enhanced understanding of the reactivity of *p*-coumaroyl groups in lignin is expected to be helpful in further optimization of LMS-based lignin conversion, we

investigated the reactivity of *p*-coumaroyl groups in detail. Hereto, we studied the reactions of a *p*-coumaroylated lignin model compound (VBG-*p*CA, **Fig. 7.1**) in laccase and laccase/HBT treatments, and compared this to the reactivity of a cinnamoylated model compound (lacking the phenolic hydroxyl group) and a non-acylated model compound (VBG-CinA and VBG, respectively, **Fig. 7.1**) by using RP-UHPLC-PDA-MSⁿ. In addition, to investigate whether the reactivity of *p*-coumaroyl moieties in polymeric lignin was comparable to those in the model compound, we used 2D HSQC NMR to study the structure of lignin isolates from corn stover and wheat straw, before and after laccase/HBT treatment.

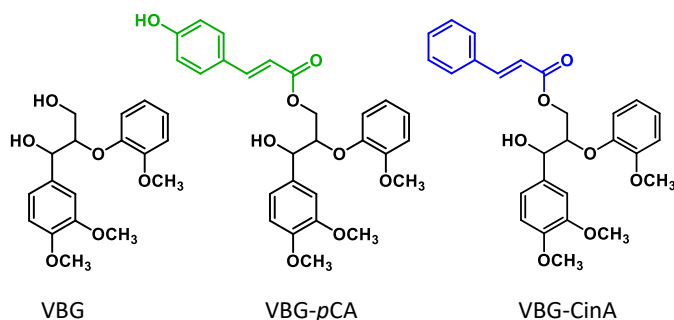


Fig. 7.1 Molecular structures of the model compounds VBG, VBG-*p*CA and VBG-CinA used in this study.

7.2 Materials & Methods

7.2.1 Materials

Acylated lignin model compounds were enzymatically synthesized by using a previously reported method.²² Veratrylglycerol- β -guaiacyl ether (VBG) was purchased from ABCR chemicals (Karlsruhe, Germany), and guaiacylglycerol- β -guaiacyl ether (GBG) was obtained from TCI chemicals (Tokyo, Japan). Laccase from *Trametes versicolor* was obtained from Sigma Aldrich (St. Louis, MO, USA), and was partially purified as described earlier.²³ The activity of both enzymes was determined spectrophotometrically by oxidation of ABTS (1 U = 1 μ mol ABTS oxidized per minute at pH 5). Wheat straw lignin isolate (WSL) and corn stover lignin isolate (CSL) were obtained from previous studies and had lignin contents of 85% and 90% (w/w), respectively (*unpublished data*). All other chemicals were obtained from Sigma Aldrich and were of analytical grade. Water was prepared by using a Milli-Q water purification system (Merck Millipore, Billerica, MA).

7.2.2 Incubation of lignin models with laccase and laccase/HBT

Stock solutions were prepared by dissolving model compounds at a concentration of 1 mM in citrate/phosphate buffer (pH 4, 20/40 mM) containing 25% (v/v) methanol.

Addition of methanol was necessary to ensure complete solubilization of the acylated model compounds. Stock solutions of HBT (10 mM) and laccase (25 U mL⁻¹) were prepared in the same buffer. The stock solutions were then mixed to obtain final substrate and HBT concentrations of 80 μ M and 400 μ M, respectively, and a laccase activity of 2 U mL⁻¹. After 1 and 24 h, 40 μ L aliquots of the samples were transferred to a clean tube, and immediately cooled in ice-water to stop the enzymatic activity. Control incubations containing only model compounds or only model compounds with HBT were performed similarly. In these cases, only a sample incubated for 24 h was analyzed. After cooling for 10 min in ice water, samples were centrifuged (10,000 $\times g$, 5 min, 4 °C) and immediately transferred to the autosampler of the UHPLC system (at 4 °C) prior to RP-UHPLC-PDA-MS analysis.

7.2.3 Incubation of lignin models with laccase-free oxidized VBG-*p*CA

Non-acylated lignin model compounds were dissolved at 1 mM in citrate/phosphate buffer (pH 4, 20/40 mM) containing 25% (v/v) methanol, and 60 μ L of these solutions were transferred to 2 mL reaction tubes. Amicon® Ultra-0.5 centrifugal filters (Merck Millipore) with a normalized molecular weight limit of 10 kDa were placed on top of these solutions, and were loaded with 130 μ L buffer and 20 μ L VBG-*p*CA solution (1 mM). Subsequently, 20 μ L laccase solution was added to obtain a final activity of 6 U mL⁻¹. The tubes were then immediately centrifuged (10,000 $\times g$, 40 °C) until >90% of the liquid had passed through the filter (approximately 30 min). As controls, identical incubations were performed in which laccase was replaced with buffer. The filtrates were collected and analyzed by using RP-UHPLC-PDA-MSⁿ.

7.2.4 Incubation of lignin isolates with laccase/HBT

Laccase/HBT treatment of CSL and WSL was performed based on a previously described protocol.¹⁶ Hereto, approximately 12 mg of WSL and CSL were suspended in 240 μ L of a 200 mM citrate buffer at pH 4, containing 100 mM HBT. To this suspension, 60 μ L of a laccase stock solution (10 U mL⁻¹) was added to obtain a final HBT concentration of 80 mM and a laccase activity of 50 U g⁻¹ lignin isolate. In addition, control samples were prepared by suspending 12 mg of WSL and CSL in 300 μ L of buffer. All samples were incubated at 40 °C in a thermomixer at 650 rpm shaking. After 24 h, the samples were removed from the thermomixer, and washed 5 times with 1 mL of MQ water. The residues were frozen in liquid nitrogen and lyophilized prior to NMR spectroscopy.

7.2.5 Saponification of lignin isolates

For mild saponification of the laccase/HBT treated and untreated CSL and WSL, approximately 10 mg of sample was incubated with 0.5 mL 1 M NaOH at 30 °C for 24 h under 300 rpm shaking.²⁴ Subsequently, the samples were acidified by adding 6 M acetic acid to reach a pH of approximately 6 (as indicated by pH paper). After centrifugation

(10,000 × *g*, 5 min, 20 °C), the supernatants were collected and stored at 4 °C. Prior to RP-UHPLC-PDA-MS analysis, the supernatants were diluted 20 times in MQ water. The residue was washed 4 times with 1 mL MQ water, frozen in liquid nitrogen and lyophilized prior to NMR spectroscopy.

7.2.6 RP-UHPLC-PDA-ESI-MSⁿ

RP-UHPLC-PDA-ESI-MSⁿ analysis was performed by using a Thermo Vanquish UHPLC system (Thermo Scientific, San Jose, CA, USA), equipped with a pump, degasser, autosampler, coupled to a PDA detector and either a Thermo LTQ Velos Pro ion-trap mass spectrometer or a Thermo Q Exactive Focus hybrid quadrupole-orbitrap mass spectrometer. Samples (1 µL) were injected onto an Acquity UPLC BEH C18 column (150 × 2.1 mm, particle size 1.7 µm) with a VanGuard guard column (5 × 2.1 mm) of the same material (Waters, Milford, MA, USA). The flow rate was 400 µL min⁻¹ and the column temperature was 45 °C. Water (A) and acetonitrile (B) were used as eluents, both acidified with 1% formic acid.

For model compound incubations, the following solvent gradient was used: 0–1.5 min at 5% B (isocratic), 1.5–3 min from 5 to 20% (linear gradient), 3–28 min from 20 to 75% (linear gradient), 28–28.8 min from 75 to 100%, 28.8–33.3 min at 100% (isocratic), 33.3–34 min from 100 to 5% (linear gradient) and 34–38 min at 5% (isocratic). All other settings were identical to a previously reported study.²² Quantification was performed based on the UV peak areas at 280 nm. For quantification of VBG, VBG-*p*CA and VBG-CinA, calibration curves (20–80 µM) were recorded in duplicate. In the case of VBG-*p*CA, we assumed that *trans-cis* isomerization did not affect the extinction coefficient at 280 nm. This was verified by injecting equal concentrations of freshly prepared *trans*-VBG-*p*CA and light-exposed partly isomerized VBG-*p*CA, which showed <1% difference in UV₂₈₀ peak area. Yields of the reaction products CLP and VBG_{ox} were calculated based on previously determined relative extinction coefficients.¹³ As no standards were available for other reaction products, their yields were estimated by assuming a molar extinction coefficient equal to that of the substrate.

For supernatants of saponified lignin isolates, the same procedure was used, with the only adaptation being the eluent profile: 0–1.5 min at 5% B (isocratic), 1.5–28 min from 5 to 35% (linear gradient), 28–28.8 min from 35 to 100% (linear gradient), 28.8–33.3 min at 100% (isocratic), 33.3–34 min from 100 to 5% (linear gradient) and 34–38 min at 5% (isocratic). Quantification of released *p*CA was performed based on UV peak area (280 nm) and a calibration curve of *p*CA (10–200 µg/mL, in duplicate).

7.2.7 2D NMR analysis

Structural characterization of laccase/HBT treated WSL and CSL and controls was performed by using 2D HSQC NMR spectroscopy, based on a previously reported method.²⁵ Hereto, the lyophilized samples were dissolved in 250 µL DMSO-*d*₆ and transferred to a 5 mm Shigemi microtube. Spectra were recorded at 25 °C on a Bruker

Avance HD 700 MHz NMR spectrometer equipped with a 5 mm BBI probe. Spectra were recorded using a standard Bruker pulse sequence 'hsqcetgpsisp2.2'. The spectral widths were 12 ppm for the ^1H dimension and 200 ppm for the ^{13}C dimension. Thirty-two scans were acquired with an acquisition time of 0.14 s and an interscan delay of 0.86 s. The FID size was of 2048 in the ^1H dimension, and 400 the ^{13}C dimension. For $^1J_{\text{CH}}$ 145 Hz was used. Settings for HSQC NMR analysis of saponified WSL and CSL were identical, with the only adaptation that 96 scans were acquired. Data was processed with Bruker TopSpin version 4.0.5. The central solvent peak (δC 39.5 ppm; δH 2.49 ppm) was used as an internal reference. HSQC correlations were assigned in accordance to literature.^{10,11,26-28} Semi-quantitative volume integration was performed as previously described by Del Río et al.,¹⁰ on a single zoom level within each sample. The abundances of

$p\text{CA}$, S-units and H-units were determined using their $\text{C}_{2,6}\text{-H}_{2,6}$ correlations, of which the integrals were logically halved. For ferulic acid and G-units, the $\text{C}_2\text{-H}_2$ correlation was used.

7.3 Results & Discussion

7.3.1 Reactivity of acylated and non-acylated model compounds with laccase and laccase/HBT

VBG, VBG- $p\text{CA}$ and VBG-CinA were incubated with laccase in presence or absence of HBT to investigate whether and how acylation of VBG influences its reactivity.

When unacylated VBG was incubated with laccase alone, no conversion was observed, as expected based on its non-phenolic structure (**Fig. 7.2A, Fig. 7.3, Table 7.1 and 7.2**).^{21,29} In case the laccase/HBT system was used, a slight conversion of 4% was observed after 24 h. This conversion is low in comparison to a previous study, and is likely caused by the presence of MeOH as co-solvent in the current study, which decreases laccase activity.^{21,30} The conversion mainly resulted in the formation of its C_α -oxidized analogue (VBG_{ox}), and trace amounts of a cleavage product (CLP), as was also found in previous studies (**Fig. 7.2A, Fig. 7.3, Table 7.1 and 7.2**).^{13,21}

In the case of VBG- $p\text{CA}$, several conversions were observed. First of all, *trans-cis* isomerization was shown to occur (**Fig. 7.2B, Table 7.1**). Isomerization also occurred in absence of laccase, and has been reported more often upon exposure of $p\text{CA}$ derivatives to light.^{31,32} Moreover, in contrast to VBG, VBG- $p\text{CA}$ was readily oxidized by laccase alone, with 39% and 82% substrate conversion after 1 and 24 h, respectively (**Fig. 7.2B, Table 7.1 and 7.2**). This conversion resulted in the formation of multiple products with molecular formula $\text{C}_{54}\text{H}_{54}\text{O}_{16}$, which were annotated as VBG- $p\text{CA}$ dimers. In addition, after 24 h, a small amount of VBG- $p\text{CA}$ trimers and (unacylated) VBG was formed (**Fig. 7.2B, Fig. 7.3, Table 7.1 and 7.2**). Hence, laccase is able to oxidize VBG- $p\text{CA}$ in the absence of a mediator, and this mainly results in oxidative coupling, as previously also observed with other phenolic lignin substructures.^{23,33} The fact that

multiple VBG-*p*CA dimers were formed, is most likely related to *trans-cis* isomerization, but possibly also due to the formation of various new C-C or C-O linkages. The exact structures of the formed bonds (e.g. 5-5', β -5' and 4-*O*-5') were not further investigated.

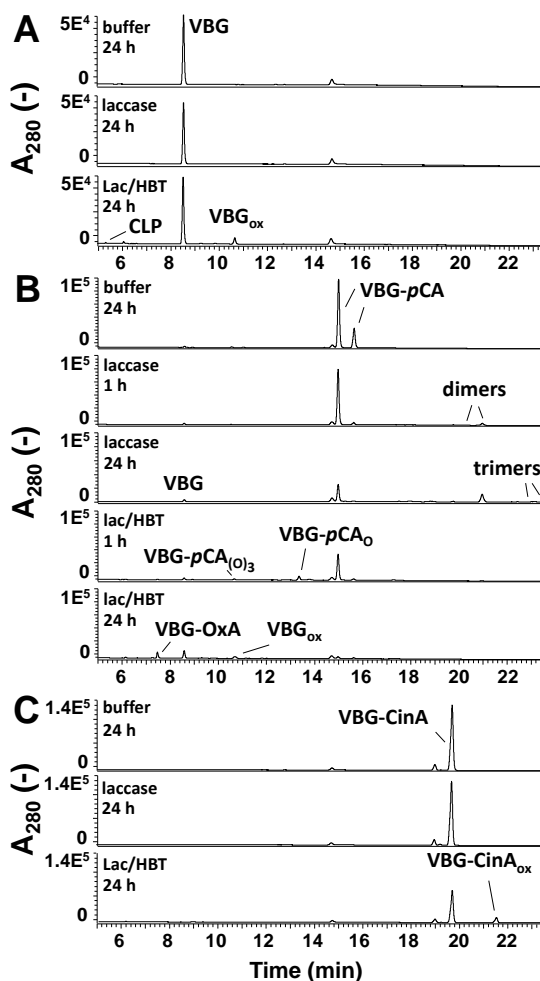


Fig. 7.2 RP-UHPLC-UV₂₈₀ chromatograms of VBG (A) VBG-*p*CA (B) and VBG-CinA (C) after incubation with buffer, laccase or laccase/HBT for 1 or 24 h. HBT and BT (see Table 7.1) eluted within 5 min, and are therefore not visible in the figure. The second VBG-*p*CA peak corresponds to the *cis*-isomer of VBG-*p*CA and was formed spontaneously upon exposure to light.

When VBG-*p*CA was incubated with the laccase/HBT system, a faster conversion was observed than in the incubation with laccase alone, as indicated by substrate conversions of 71 and 97% after 1 and 24 h, respectively (**Table 7.2**). In addition, a completely different product profile was obtained. VBG-*p*CA dimers were absent at all incubation times. Instead, after 1 h, reaction products corresponding to C₂₇H₂₈O₉ (VBG-*p*CA₀) and

$C_{27}H_{28}O_{11}$ (VBG- pCA_{O3}) were detected, as well as trace amounts of $C_{27}H_{28}O_{10}$ (VBG- pCA_{O2}), indicating that hydroxylation of VBG- pCA occurred (**Fig. 7.2B** and **Table 7.1**). After 24 h, the abundance of hydroxylated VBG- pCA products had decreased, which coincided with the formation of relatively large amounts of VBG and VBG_{ox} (**Fig. 7.2B**, **Fig. 7.3**, **Table 7.1** and **7.2**). In addition, a compound corresponding to $C_{20}H_{22}O_9$ and small amounts of $C_{20}H_{20}O_9$ were detected, which were tentatively annotated as a VBG-oxalate ester (VBG-OxA) and its C_a -oxidized analogue (VBG-OxA_{ox}). Thus, overall, the addition of HBT to VBG- pCA incubations shifted the reaction outcome from polymerization to degradation. The (hydroxylated) p -coumaroyl moieties that were cleaved off were not detected in the RP-UHPLC-PDA-MS analysis, most likely due to further reactions (e.g. polymerization) of these moieties.

Based on the fact that the abundance of hydroxylated products decreased along with the formation of degradation products, it seems likely that VBG- pCA degradation occurred (mainly) after initial hydroxylation. As no hydroxylation was observed in incubations with laccase alone, it is clear that HBT is, somehow, involved in the hydroxylation reactions. A plausible route for hydroxylation of VBG- pCA is via formation of covalent HBT adducts as intermediates, as suggested earlier for hydroxylation of other phenolic molecules.³⁴ The HBT adducts could then decompose into hydroxylated VBG- pCA and either HBT or its degradation product benzotriazole (BT) (see **Fig. 7.4**). Corroborating evidence for the latter pathway is the remarkably high conversion of HBT to BT in VBG- pCA incubations (**Fig. S7.1**). Although reduction of HBT to BT is common in laccase/HBT incubations,^{21,23,35} and was also observed in incubations with VBG or VBG-CinA, this occurred to a substantially higher extent in incubations of VBG- pCA (see **Fig. S7.1**). Based on the above, we propose that the laccase/HBT system first hydroxylates VBG- pCA , after which subsequent degradation takes place, yielding VBG and VBG-OxA (**Fig. 7.3** and **7.4**). The latter two species may then undergo C_a -oxidation, as generally observed in laccase/HBT treatments,^{21,29} to form VBG_{ox} and VBG-OxA_{ox}.

Laccase-catalyzed conversion of VBG-CinA, a non-phenolic analogue of VBG- pCA , was only observed in the presence of HBT, with VBG-CinA_{ox} as the only reaction product detected (**Fig. 7.2C**, **Fig. 7.3**, **Table 7.1** and **7.2**). Neither degradation of the ester bond, nor hydroxylation was observed, as in the case of VBG- pCA , indicating that the phenolic character of the p -coumaroylated model plays a key role in its reactivity. Although VBG-CinA was converted slower than VBG- pCA , remarkably, its conversion was faster than that of VBG (**Table 7.2**).

Overall, the above described incubations show that p -coumaroylation increases, rather than decreases the reactivity of a non-phenolic lignin model in laccase and laccase/HBT treatments. Thus, the previously found accumulation of pCA groups in the residual fraction of laccase/HBT treated wheat straw and corn stover cannot be attributed to an intrinsic recalcitrance of the pCA moieties.¹⁶

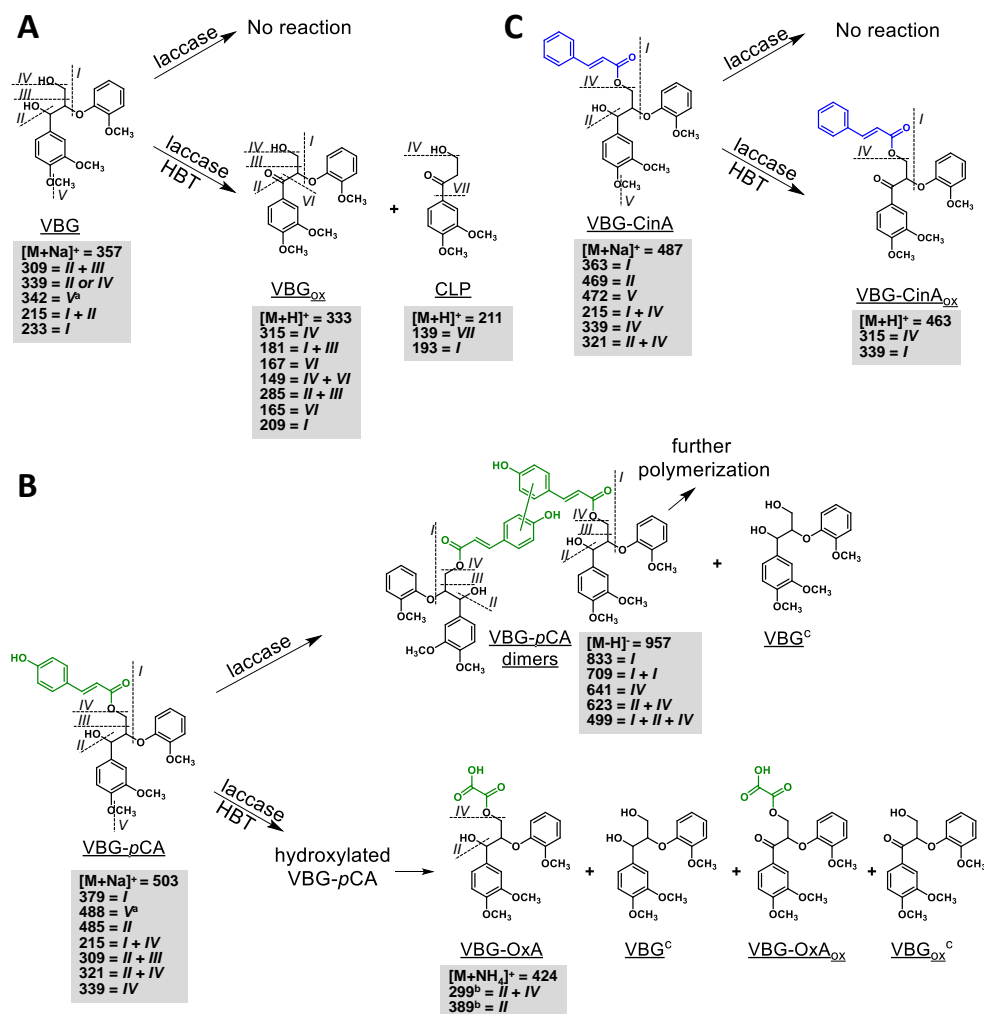


Fig. 7.3 Schematic overview of the final reaction outcomes of VBG (A), VBG-*p*CA (B) and VBG-CinA (C) incubations with laccase and laccase/HBT. Proposed fragmentation patterns of substrates and products resulting in the MS² fragments reported in Table 7.1 are shown in the grey boxes. Since multiple isomers of the VBG-*p*CA dimers are formed, the linkage type between the two VBG-*p*CA molecules is not specified in this figure. Hydroxylation of VBG-*p*CA (to VBG-*p*CA₀ and VBG-*p*CA₀₃) is suggested to occur prior to eventual degradation to VBG-OxA, VBG and VBG_{Ox}, but is not shown in the figure. ^a This fragmentation is suggested to be a radical fragmentation. ^b The NH₄⁺ ion is lost during this fragmentation. ^c For fragmentation pattern, see Fig. 7.3A.

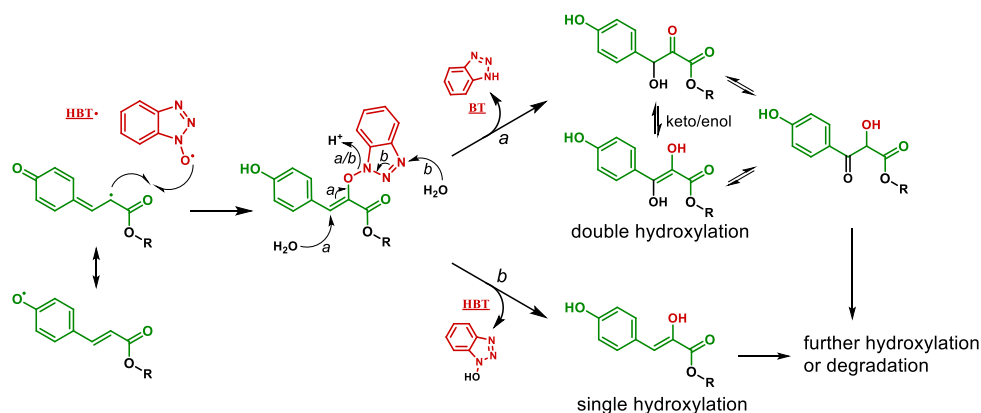
Table 7.1 Compounds detected with RP-UHPLC-PDA-ESI-FTMS and RP-UHPLC-PDA-ESI-ITMS after incubation of VBG, VBG-*p*CA or VBG-CinA with laccase in the presence or absence of HBT. MS² fragments were obtained by using RP-UHPLC-PDA-ESI-ITMS. All other values were obtained using RP-UHPLC-PDA-ESI-FTMS. Proposed fragmentation patterns are shown in Fig. 7.3. N.D. = Not determined.

RT (min)	Annot.	Mol. formula	Ion	Observed/ calculated mass (Da)	Mass error (ppm)	MS ² fragments
Substrates and mediator						
3.63	HBT	C ₆ H ₅ N ₃ O	[M+H] ⁺	135.04329/ 135.04326	0.23	119 (100), 80 (86), 91 (75), 53 (39), 116 (37)
6.64	BT	C ₆ H ₅ N ₃	[M+H] ⁺	119.04842/ 119.04835	0.30	92 (100), 102 (43), 65 (25)
15.00	VBG- <i>p</i> CA (<i>trans</i>)	C ₂₇ H ₂₈ O ₈	[M+Na] ⁺	480.17841/ 470.17842	-0.02	379 (100), 488 (27), 485 (25), 215 (26), 309 (24), 321 (15), 339 (11)
15.66	VBG- <i>p</i> CA (<i>cis</i>)	C ₂₇ H ₂₈ O ₈	[M+Na] ⁺	480.17841/ 480.17842	-0.02	379 (100), 488 (27), 485 (25), 215 (26), 309 (24), 321 (15), 339 (11)
19.71	VBG-CinA	C ₂₇ H ₂₈ O ₇	[M+Na] ⁺	464.18308/ 464.18350	-0.87	363 (100), 469 (40), 472 (38), 215 (28), 321 (23), 339 (18), 197 (16)
Reaction products						
5.40	CLP	C ₁₁ H ₁₄ O ₄	[M+H] ⁺	210.08961/ 210.08921	1.92	139 (100), 193 (18)
7.42	VBG-OxA	C ₂₀ H ₂₂ O ₉	[M+NH ₄] ⁺	406.12656/ 406.12639	0.41	299 (100), 389 (43)
8.61	VBG	C ₁₈ H ₂₂ O ₆	[M+Na] ⁺	334.14155/ 344.14164	-0.25	309 (100), 339 (22), 342 (14), 215 (6), 233 (6)
9.30	VBG-OxA _{ox}	C ₂₀ H ₂₀ O ₉	[M+H] ⁺	404.11146/ 404.11074	1.80	N.D.
10.68	VBG- <i>p</i> CA ₀₃	C ₂₇ H ₂₈ O ₁₁	[M-H] ⁻	528.16410/ 528.16316	1.7	509 (100)
10.75	VBG _{ox}	C ₁₈ H ₂₀ O ₆	[M+Na] ⁺	332.12586/ 332.12599	-0.37	315 (100), 181 (69), 167 (68), 149 (66), 285 (42), 165 (43), 209 (40)
11.20	VBG- <i>p</i> CA ₀₂	C ₂₇ H ₂₈ O ₁₀	[M+Na] ⁺	512.16904/ 512.16825	1.48	N.D.
13.36	VBG- <i>p</i> CA ₀	C ₂₇ H ₂₈ O ₉	[M-H] ⁻	496.17380/ 496.17334	-0.89	371 (100), 161 (14)
19.80-21.50	VBG- <i>p</i> CA dimers (multiple)	C ₅₄ H ₅₄ O ₁₆	[M-H] ⁻	958.34141/ 958.34119	1.42	833, 709, 641, 623, 499*
22.10-23.30	VBG- <i>p</i> CA trimers (multiple)	C ₈₁ H ₈₀ O ₂₄	[M+NH ₄] ⁺	1436.5061/ 1436.5040	1.47	N.D.
21.57	VBG-CinA _{ox}	C ₂₇ H ₂₆ O ₇	[M+H] ⁺	462.16774/ 462.16786	-0.24	315 (100), 339 (8)

* Abundance varies between dimer isomers

Table 7.2 Substrate recoveries and (estimated) product yields of VBG, VBG-*p*CA and VBG-CinA after 1 h and 24 h incubations with laccase or laccase/HBT. In control incubations without laccase, no conversion was observed in all cases. N.D. = Not determined.

Incubation		Substrate recovery (%)	Product yields (%)
VBG + laccase	1 h	100	-
	24 h	100	-
VBG + laccase/HBT	1 h	~100	VBG _{ox} (0.9)
	24 h	96	CLP (0.3); VBG _{ox} (3.7)
VBG- <i>p</i> CA + laccase	1 h	61	VBG (4.1); VBG- <i>p</i> CA dimers and trimers (N. D.)
	24 h	18	VBG (5.6); VBG- <i>p</i> CA dimers and trimers (N. D.)
VBG- <i>p</i> CA + laccase/HBT	1 h	29	VBG (5.3); VBG-OxA ^a (1.4); VBG- <i>p</i> CA ₀ (N.D.); VBG- <i>p</i> CA ₀₂ (N.D.); VBG- <i>p</i> CA ₀₃ (N.D.)
	24 h	3	VBG (24.7); VBG-OxA ^a (16.9); VBG _{ox} (N.D. ^b); VBG-OxA _{ox} (N.D.); VBG- <i>p</i> CA ₀₃ (N.D.)
VBG-CinA + laccase	1 h	100	-
	24 h	100	-
VBG-CinA + laccase/HBT	1 h	81	VBG-CinA _{ox} (1.1)
	24 h	63	VBG-CinA _{ox} (11.1)

^a Yields of VBG-OxA were estimated by assuming a molar extinction coefficient equal to VBG.^b In this incubation, VBG_{ox} could not accurately be quantified due to co-elution with VBG-*p*CA₀.**Fig. 7.4** Proposed reaction mechanism for the hydroxylation of VBG-*p*CA observed upon laccase/HBT treatment. R corresponds to VBG (without its primary hydroxyl group). It should be noted that the exact position of the hydroxyl groups is unknown, and that VBG-*p*CA₀₃ is expected to be hydroxylated at the aromatic ring.

7.3.2 Reactivity of *p*CA moieties upon laccase/HBT treatment of wheat straw and corn stover lignin isolates

As the relatively high reactivity of VBG-*p*CA conflicts with the apparent low reactivity of *p*CA groups upon laccase/HBT treatments of wheat straw and corn stover, we investigated whether, somehow, the cell wall matrices of wheat straw and corn stover could have selectively protected the *p*CA groups from laccase/HBT activity in our previous

study.¹⁶ Therefore, here, the reactivity of *p*CA groups in purified lignin isolates from corn stover (CSL) and wheat straw (WSL), lacking an intact cell wall matrix, was studied upon treatment with laccase/HBT. 2D HSQC NMR analysis revealed that the laccase/HBT treatment substantially altered the structure of lignin isolates, as shown by a 3 and 20-fold increased abundance of C_α-oxidized structures for CSL and WSL, respectively, and a ~37% decrease in interunit linkages (**Fig. 7.5** and **Table 7.3**). The relative abundance of *p*CA groups was shown to increase in both CSL and WSL (**Table 7.3**). These findings are in good agreement with those previously obtained in incubations of (unfractionated) CS and WS,¹⁶ indicating that the cell wall matrix does not play a major role in the reactivity of lignin *p*CA moieties in laccase/HBT treatments.

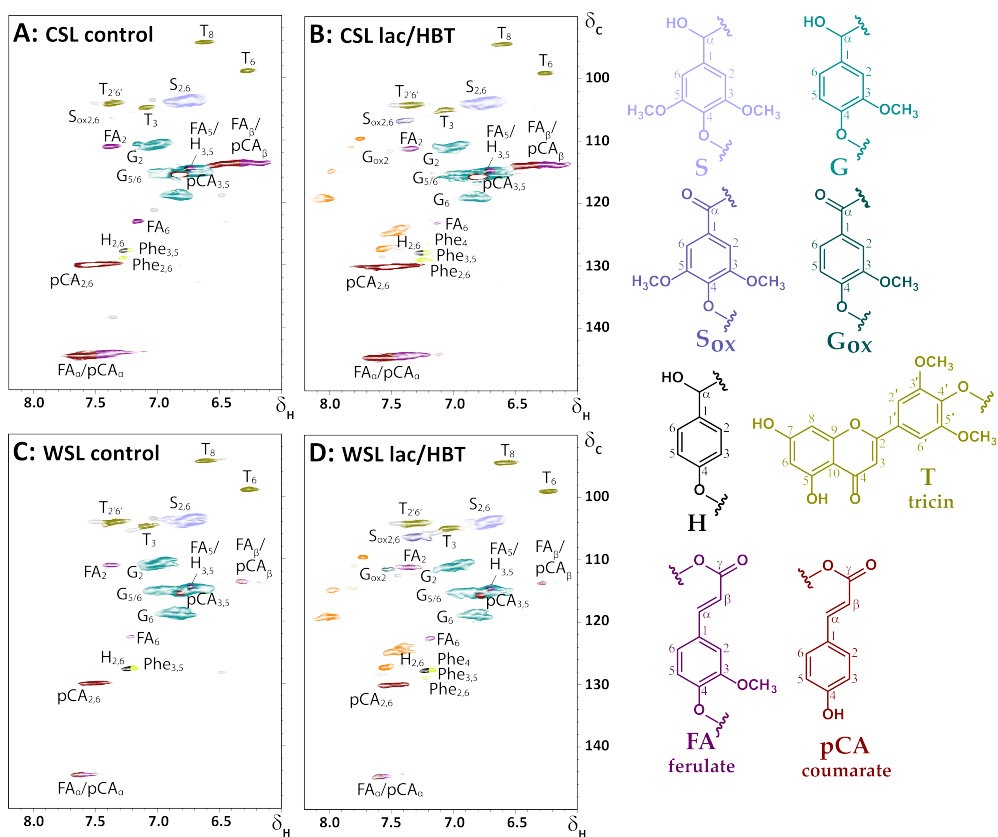


Fig. 7.5 Aromatic regions of HSQC spectra of CSL (A&B) and WSL (C&D) after incubation with buffer (A&C) or laccase/HBT (B&D). Lignin substructures corresponding to the colored annotations are shown on the right. Dashed lines correspond to -H or -OCH₃. Phe = phenylalanine. Correlations in grey are unannotated, those in orange correspond to signals from HBT.¹⁶ Annotation was performed based on literature.^{10,27,28} Aliphatic regions of the spectra can be found in Fig. S7.2

Table 7.3 Relative abundances of lignin subunits, hydroxycinnamates and interunit linkages in CSL and WSL after incubation with buffer (control) or laccase/HBT. ^aAmount per 100 lignin subunits (i.e. S+S_{ox}+G+G_{ox}+H).

	CSL control	CSL lac/HBT	WSL control	WSL lac/HBT
Lignin subunits (%)				
H	2	2	3	3
G	55	49	63	48
G _{ox}	1	4	1	10
S	39	39	33	30
S _{ox}	2	7	0	10
S/G	0.73	0.85	0.53	0.68
Hydroxycinnamates^a				
<i>p</i> CA	60	78	8	9
FA	11	9	5	10
Interunit linkages^a				
β-O-4'	32	23	43	28
β-5'	2	0	6	3
β-β'	1	0	0	0
β-β' (tetrahydrofuran)	5	2	0	0
Total	40	25	49	31

7.3.3 Potential explanations for the accumulation of *p*CA groups in residual lignin upon laccase/HBT treatment

From the above it is clear that, upon laccase/HBT treatment, *p*CA groups of *p*-coumaroylated model compounds were rapidly hydroxylated and degraded, whereas *p*CA groups in polymeric lignin isolates accumulated in the residue. Thus, the reactivity of *p*CA groups in polymeric lignin is not accurately reflected by the reactivity of VBG-*p*CA. In order to shine more light on this discrepancy and on the fate of *p*CA groups in polymeric lignin, two scenarios were investigated, which are discussed in detail below.

3.3.3.1. HSQC-undetectable radical coupling of *p*CA groups in lignin upon laccase/HBT treatment

Although, based on the accumulation of *p*CA groups in residual lignin, it seems that *p*CA groups in polymeric lignin are relatively unreactive upon laccase/HBT treatments, it could be speculated that *p*CA moieties underwent radical coupling to other *p*CA moieties or other types of lignin substructures, and that the result of this was undetectable in the HSQC NMR spectra. Based on reported chemical shifts of model compounds, it seems indeed possible that covalent coupling of *p*CA results in very small changes in chemical shifts (<1 ppm in the C-dimension and <0.1 ppm in the H-dimension), especially when coupling occurs via 5-5' bond formation or etherification of the *p*-OH group.³⁶

In order to investigate whether new ether or C-C bonds were formed upon laccase/HBT treatment, the residues of laccase/HBT treated CSL and WSL and control incubations were saponified (1 M NaOH, 30 °C, 24 h). The saponification residues were analyzed by

using HSQC NMR to determine the residual *p*CA content, and the supernatant was analyzed by using RP-UHPLC-PDA-MS to quantify the released *p*CA. If radical coupling between *p*CA and other lignin substructures occurred, saponification is expected to result in a lower removal of *p*CA from laccase/HBT treated lignin than from control treated lignin. In case of radical coupling between *p*CA groups, it can be expected that dicoumarates are released upon saponification.

In the case of CSL, HSQC analysis showed an almost equal removal of *p*CA groups from the laccase/HBT treated and control treated lignin upon saponification (**Table 7.4** and **Fig. S7.3**), suggesting that laccase/HBT treatment did not induce coupling between *p*CA groups and the lignin backbone to a substantial extent. This was, however, contradicted by the RP-UHPLC-PDA-MS analysis, which showed an 18% lower release of *p*CA from the laccase/HBT treated CSL than from the control sample (**Table 7.4**). In the case of WSL, both HSQC and RP-UHPLC-PDA-MS analysis showed an approximately 18% lower removal of *p*CA from laccase/HBT treated lignin than from the control (**Table 7.4**). Although it remains unclear why the HSQC and RP-UHPLC-PDA-MS data showed contradicting results in the case of CSL, the above suggest that part of the *p*CA groups may undergo coupling to other lignin substructures. In none of the samples, dicoumarates were detected by using RP-UHPLC-PDA-MS, suggesting that radical coupling between *p*CA moieties did not occur (data not shown).

Table 7.4 Relative abundance of *p*CA in CSL and WSL (control and laccase/HBT treated) before and after saponification, and absolute amounts of *p*CA released upon saponification. Saponification of *p*CA groups was complete in all samples (see Fig. S7.3). ^aDetermined by using HSQC NMR (see Fig. S7.5 for spectra). ^bDetermined by using RP-UHPLC-PDA-MS

	<i>p</i> CA / 100 Ar unsaponified ^a	<i>p</i> CA / 100 Ar saponified ^a	<i>p</i> CA released ($\mu\text{g}/\text{mg}$) ^b
CSL control	60	15	74.2
CSL + laccase/HBT	78	16	60.5
WSL control	8.1	0	12.0
WSL + laccase/HBT	9.4	1.7	9.9

3.3.3.2. *p*CA moieties as redox shuttles in lignin polymers

Another potential explanation for the apparent low reactivity of *p*CA groups in polymeric lignin could be that *p*CA groups are oxidized by laccase/HBT, but act as redox shuttles (or mediators) rather than undergoing coupling or degradation reactions. It has been suggested that, during lignin biosynthesis, lignin-*p*CA conjugates function as redox shuttles to assist in the formation of other lignin radicals, and that *p*CA radicals do not undergo oxidative coupling.³⁷ Possibly, *p*CA groups in polymeric lignin display similar reactivity when incubated with laccase/HBT. As it is challenging to prove such mediator activity in polymeric lignin or biomass, we tested whether VBG-*p*CA could act as a

mediator between laccase and other lignin model compounds. Hereto, incubations were performed in a centrifugal filter with a 10 kDa cut-off value. VBG-*p*CA solutions were loaded on top of the filter. Laccase was then added and the samples were immediately filtered onto a solution of VBG or its phenolic analogue GBG (guaiacylglycerol- β -guaiacyl ether). The filtrates were then analyzed by using RP-UHPLC-PDA-MS, to investigate whether VBG or GBG were oxidized by laccase-free oxidized VBG-*p*CA. In a control incubation, in which laccase (without VBG-*p*CA) was filtered onto an ABTS solution (1 mM), no color formation was observed, confirming that the filtrate was free of laccase (data not shown). Upon incubation of GBG, a new peak corresponding to C₃₄H₃₈O₁₂ was formed, which was annotated as a dimer of GBG (**Fig. 7.6C&D**), indicating that the produced VBG-*p*CA radicals were able to act as redox shuttles, and thereby oxidize GBG. Nevertheless, the newly formed GBG dimer accounted for only 7% of the UV₂₈₀ peak area, indicating that GBG was only converted to a limited extent. Upon incubation, also dimerization of VBG-*p*CA occurred, but the resulting products accumulated above the filter membrane (data not shown), and are therefore not visible in **Fig. 7.6**. Upon incubation of VBG with oxidized VBG-*p*CA, no conversion of VBG was observed (**Fig. 7.6A&B**). In an additional experiment, equimolar amounts of VBG and VBG-*p*CA were incubated with laccase (i.e. without filter membrane). After 24 h, extensive dimerization of VBG-*p*CA was observed, although also a minor conversion of VBG to VBG_{ox} (i.e. <1 %) occurred (data not shown). Overall, these results indicate that VBG-*p*CA could act as a redox shuttle towards other lignin structures, but preferentially undergoes radical coupling. Thus, based on these experiments, it seems not very likely that *p*CA groups in lignin act as *efficient* redox shuttles.

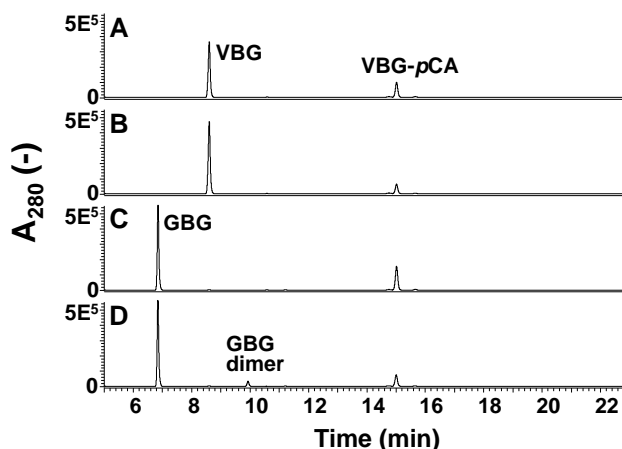


Fig. 7.6 RP-UHPLC-UV₂₈₀ chromatograms of VBG incubated with VBG-*p*CA (A), VBG incubated with oxidized laccase-free VBG-*p*CA (B), GBG incubated with VBG-*p*CA (C) and GBG incubated with oxidized laccase-free VBG-*p*CA (D). The GBG dimer was identified based on its molecular formula (C₃₄H₃₈O₁₂; mass error 0.06 ppm). VBG-*p*CA dimers were formed in the presence of laccase, but accumulated above the filter membrane, and were therefore not detected in the filtrates.

Nevertheless, there is an important difference between VBG-*p*CA and the *p*CA groups in polymeric lignin that is difficult to compensate for in model systems: whereas VBG-*p*CA molecules are soluble, and can rapidly diffuse through the incubation buffer, the *p*CA groups in polymeric lignin are covalently bound to the insoluble polymer, resulting in low mobility. Since oxidative coupling of *p*CA groups, and possibly also hydroxylation and degradation (see **Fig. 7.4**) require covalent bond formation to the *p*CA groups, it is not inconceivable that these reactions are very slow in case the *p*CA groups are immobile (i.e. in polymeric lignin). Possibly, these *p*CA groups undergo electron transfer instead, as this can occur rapidly over relatively long distances ($>15 \text{ \AA}$).³⁸ Based on the available data, this can, however, not be proven.

7.4 Conclusions

We studied the reactivity of *p*-coumaroyl groups in laccase and laccase/HBT treatments of lignin and lignin model compounds in detail. *p*-Coumaroyl moieties of lignin model compounds were shown to rapidly react in both laccase and laccase/HBT incubations, resulting in oxidative coupling (with laccase) and various degradation products (with laccase/HBT). The phenolic character of the *p*-coumaroyl moiety was found to be essential for these rapid conversions. Upon laccase/HBT treatment of polymeric lignin isolates, *p*CA groups accumulated in the residual lignin, implying that these groups do not undergo degradation, and thus, display different reactivity than *p*CA groups of model compounds. Although this discrepancy is still not fully resolved, we suggest that *p*CA groups in lignin polymers may be oxidized by laccase/HBT, but undergo HSQC-undetectable radical coupling or may act as redox shuttles instead of undergoing degradation reactions.

7.5 References

1. Li M, Pu Y and Ragauskas AJ. Current understanding of the correlation of lignin structure with biomass recalcitrance. *Frontiers in Chemistry* **2016**, *4*, 45.
2. Munk L, Sitarz AK, Kalyani DC, Mikkelsen JD and Meyer AS. Can laccases catalyze bond cleavage in lignin? *Biotechnology Advances* **2015**, *33* (1), 13-24.
3. Du X, Li J, Gellerstedt G, Rencoret J, Del Río JC, Martínez AT and Gutiérrez A. Understanding pulp delignification by laccase–mediator systems through isolation and characterization of lignin–carbohydrate complexes. *Biomacromolecules* **2013**, *14* (9), 3073-3080.
4. Kawai S, Nakagawa M and Ohashi H. Degradation mechanisms of a nonphenolic β -O-4 lignin model dimer by *Trametes versicolor* laccase in the presence of 1-hydroxybenzotriazole. *Enzyme and Microbial Technology* **2002**, *30* (4), 482-489.
5. Baiocco P, Barreca AM, Fabbrini M, Galli C and Gentili P. Promoting laccase activity towards non-phenolic substrates: a mechanistic investigation with some laccase–mediator systems. *Organic & Biomolecular Chemistry* **2003**, *1* (1), 191-197.
6. Vanholme R, Demedts B, Morreel K, Ralph J and Boerjan W. Lignin biosynthesis and structure. *Plant Physiology* **2010**, *153* (3), 895-905.
7. Ralph J, Lapierre C and Boerjan W. Lignin structure and its engineering. *Current Opinion in Biotechnology* **2019**, *56*, 240-249.
8. Lu F, Karlen SD, Regner M, Kim H, Ralph SA, Sun R-C, Kuroda K-i, Augustin MA, Mawson R and Sabarez H. Naturally *p*-hydroxybenzoylated lignins in palms. *BioEnergy Research* **2015**, *8* (3), 934-952.
9. Morreel K, Ralph J, Kim H, Lu F, Goeminne G, Ralph S, Messens E and Boerjan W. Profiling of oligolignols reveals monolignol coupling conditions in lignifying poplar xylem. *Plant Physiology* **2004**, *136* (3), 3537-3549.
10. Del Río JC, Rencoret J, Prinsen P, Martínez AT, Ralph J and Gutiérrez A. Structural characterization of wheat straw lignin as revealed by analytical pyrolysis, 2D-NMR, and reductive cleavage methods. *Journal of Agricultural and Food Chemistry* **2012**, *60* (23), 5922-5935.
11. Del Río JC, Lino AG, Colodette JL, Lima CF, Gutiérrez A, Martínez ÁT, Lu F, Ralph J and Rencoret J. Differences in the chemical structure of the lignins from sugarcane bagasse and straw. *Biomass and Bioenergy* **2015**, *81*, 322-338.
12. Lundquist K and Parkäs J. Different types of phenolic units in lignins. *BioResources* **2011**, *6* (2), 920-926.
13. Hilgers R, Van Dam A, Zuilhof H, Vincken J-P and Kabel MA. Boosting degradation of lignin β -O-4' linkages by laccase/HBT: the overlooked effect of buffer properties. *Submitted for publication* **2020**.
14. Rico A, Rencoret J, Del Río JC, Martínez AT and Gutiérrez A. In-depth 2D NMR study of lignin modification during pretreatment of Eucalyptus wood with laccase and mediators. *BioEnergy Research* **2015**, *8* (1), 211-230.
15. Rencoret J, Pereira A, Del Río JC, Martínez AT and Gutiérrez A. Delignification and saccharification enhancement of sugarcane byproducts by a laccase-based pretreatment. *ACS Sustainable Chemistry & Engineering* **2017**, *5* (8), 7145-7154.
16. Hilgers R, Van Erven G, Boerkamp V, Sulaeva I, Potthast A, Kabel MA and Vincken J-P. Understanding laccase/HBT-catalyzed grass delignification at the molecular level. *Green Chemistry* **2020**, *22*, 1735-1746.
17. Ralph J, Hatfield RD, Quideau S, Helm RF, Grabber JH and Jung H-JG. Pathway of *p*-coumaric acid incorporation into maize lignin as revealed by NMR. *Journal of the American Chemical Society* **1994**, *116* (21), 9448-9456.
18. Sun R, Sun XF, Wang SQ, Zhu W and Wang XY. Ester and ether linkages between hydroxycinnamic acids and lignins from wheat, rice, rye, and barley straws, maize stems, and fast-growing poplar wood. *Industrial Crops and Products* **2002**, *15* (3), 179-188.
19. Bourbonnais R and Paice MG. Oxidation of non-phenolic substrates: an expanded role for laccase in lignin biodegradation. *FEBS Letters* **1990**, *267* (1), 99-102.
20. Crestini C and Argyropoulos DS. The early oxidative biodegradation steps of residual kraft lignin models with laccase. *Bioorganic & Medicinal Chemistry* **1998**, *6* (11), 2161-2169.

21. Hilgers R, Twentyman-Jones M, van Dam A, Gruppen H, Zuilhof H, Kabel MA and Vincken J-P. The impact of lignin sulfonation on its reactivity with laccase and laccase/HBT. *Catalysis Science & Technology* **2019**, 9(6), 1535-1542.
22. Hilgers R, Vincken J-P and Kabel M. Facile enzymatic Cy-acylation of lignin model compounds. *Catalysis Communications* **2019**, 105919.
23. Hilgers RJ, Vincken J-P, Gruppen H and Kabel MA. Laccase/mediator systems: Their reactivity towards phenolic lignin structures. *ACS Sustainable Chemistry & Engineering* **2018**, 6(2), 2037-2046.
24. Masarin F, Gurgilhães DB, Baffa DCF, Barbosa MHP, Carvalho W, Ferraz A and Milagres AMF. Chemical composition and enzymatic digestibility of sugarcane clones selected for varied lignin content. *Biotechnology for Biofuels* **2011**, 4(1), 55.
25. Mansfield SD, Kim H, Lu F and Ralph J. Whole plant cell wall characterization using solution-state 2D NMR. *Nature Protocols* **2012**, 7(9), 1579.
26. Guo H, Miles-Barrett DM, Neal AR, Zhang T, Li C and Westwood NJ. Unravelling the enigma of lignin OX: can the oxidation of lignin be controlled? *Chemical Science* **2018**, 9(3), 702-711.
27. Zeng J, Helms GL, Gao X and Chen S. Quantification of wheat straw lignin structure by comprehensive NMR analysis. *Journal of Agricultural and Food Chemistry* **2013**, 61(46), 10848-10857.
28. Van Erven G, Hilgers R, De Waard P, Gladbeek E-J, Van Berkel WJH and Kabel MA. Elucidation of *in situ* ligninolysis mechanisms of the selective white-rot fungus *Ceriporiopsis subvermispora*. *ACS Sustainable Chemistry & Engineering* **2019**, 7(19), 16757-16764.
29. Heap L, Green A, Brown D, van Dongen B and Turner N. Role of laccase as an enzymatic pretreatment method to improve lignocellulosic saccharification. *Catalysis Science & Technology* **2014**, 4(8), 2251-2259.
30. Mattinen M-L, Maijala P, Nousiainen P, Smeds A, Kontro J, Sipilä J, Tamminen T, Willför S and Viikari L. Oxidation of lignans and lignin model compounds by laccase in aqueous solvent systems. *Journal of Molecular Catalysis B: Enzymatic* **2011**, 72(3-4), 122-129.
31. Kort R, Vonk H, Xu X, Hoff W, Crielgaard W and Hellingwerf K. Evidence for trans-cis isomerization of the p-coumaric acid chromophore as the photochemical basis of the photocycle of photoactive yellow protein. *FEBS Letters* **1996**, 382(1-2), 73-78.
32. Mitani T, Mimura H, Ikeda K, Nishide M, Yamaguchi M, Koyama H, Hayashi Y and Sakamoto H. Process for the purification of *cis-p*-coumaric acid by cellulose column chromatography after the treatment of the *trans* isomer with ultraviolet irradiation. *Analytical Sciences* **2018**, 34(10), 1195-1199.
33. Ramalingam B, Sana B, Seayad J, Ghadessy FJ and Sullivan MB. Towards understanding of laccase-catalysed oxidative oligomerisation of dimeric lignin model compounds. *RSC Advances* **2017**, 7(20), 11951-11958.
34. Sealey J and Ragauskas AJ. Investigation of laccase/N-hydroxybenzotriazole delignification of kraft pulp. *Journal of Wood Chemistry and Technology* **1998**, 18(4), 403-416.
35. Potthast A, Rosenau T and Fischer K. Oxidation of benzyl alcohols by the laccase-mediator system (LMS) a comprehensive kinetic description. *Holzforschung* **2001**, 55(1), 47-56.
36. Ralph SA, Ralph J and Landucci L. NMR database of lignin and cell wall model compounds. **2009**, available at URL www.glbrc.org/databases_and_software/nmrdatabase/.
37. Hatfield R, Ralph J and Grabber JH. A potential role for sinapyl *p*-coumarate as a radical transfer mechanism in grass lignin formation. *Planta* **2008**, 228(6), 919.
38. Kuss-Petermann M and Wenger OS. Electron transfer rate maxima at large donor-acceptor distances. *Journal of the American Chemical Society* **2016**, 138(4), 1349-1358.

7.6 Supporting Information

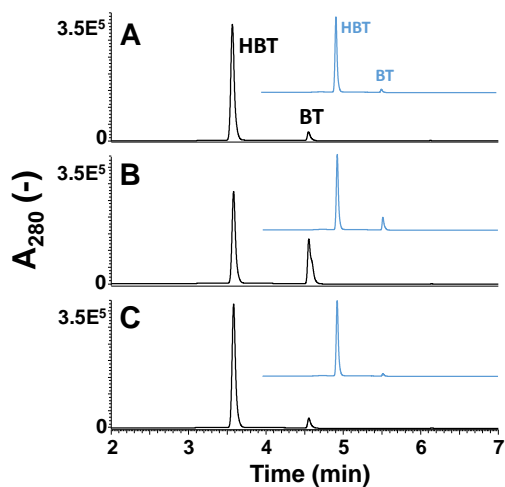


Fig. S7.3 Early regions of RP-UHPLC-UV₂₈₀ chromatograms of VBG (A), VBG-*p*CA (B) and VBG-CinA (C) after 24 h of laccase/HBT treatment (black lines). Blue lines correspond to incubation times of 1 h.

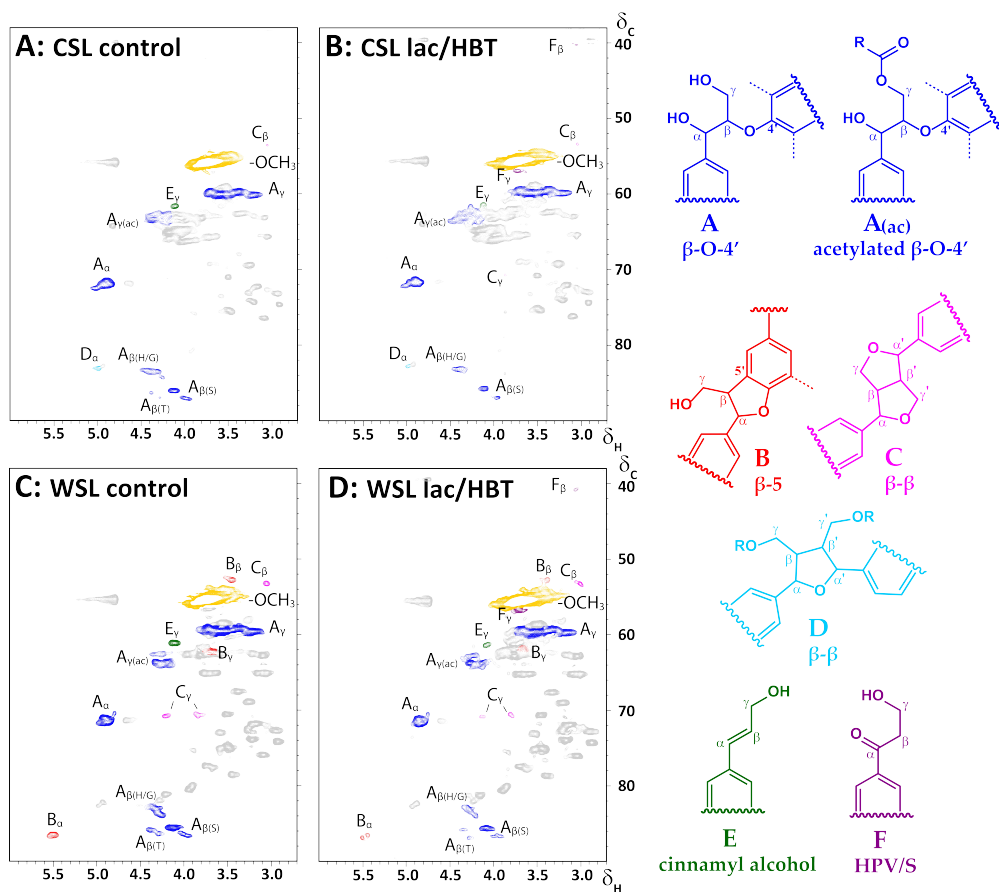


Fig. S7.2 Aliphatic regions of HSQC spectra of residues of CSL (A&B) and WSL (C&D) after incubation with buffer (A&C) or laccase/HBT (B&D). Lignin substructures corresponding to the colored annotations are shown on the right. HPV/S = hydroxypropiovanillone/hydroxypropiosyringone. Dashed lines correspond to $-H$ or $-OCH_3$. Correlations in grey are unannotated, and mainly belong to proteins.¹ Annotation was performed based on literature.²⁻⁴

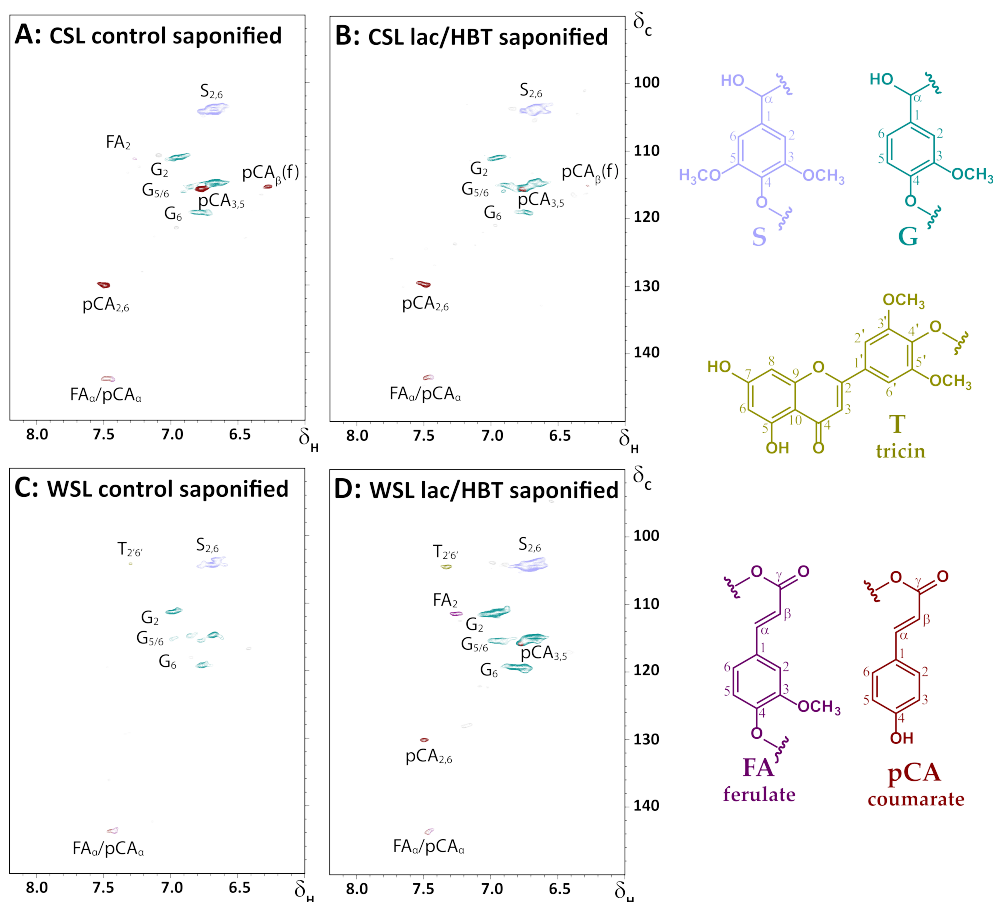
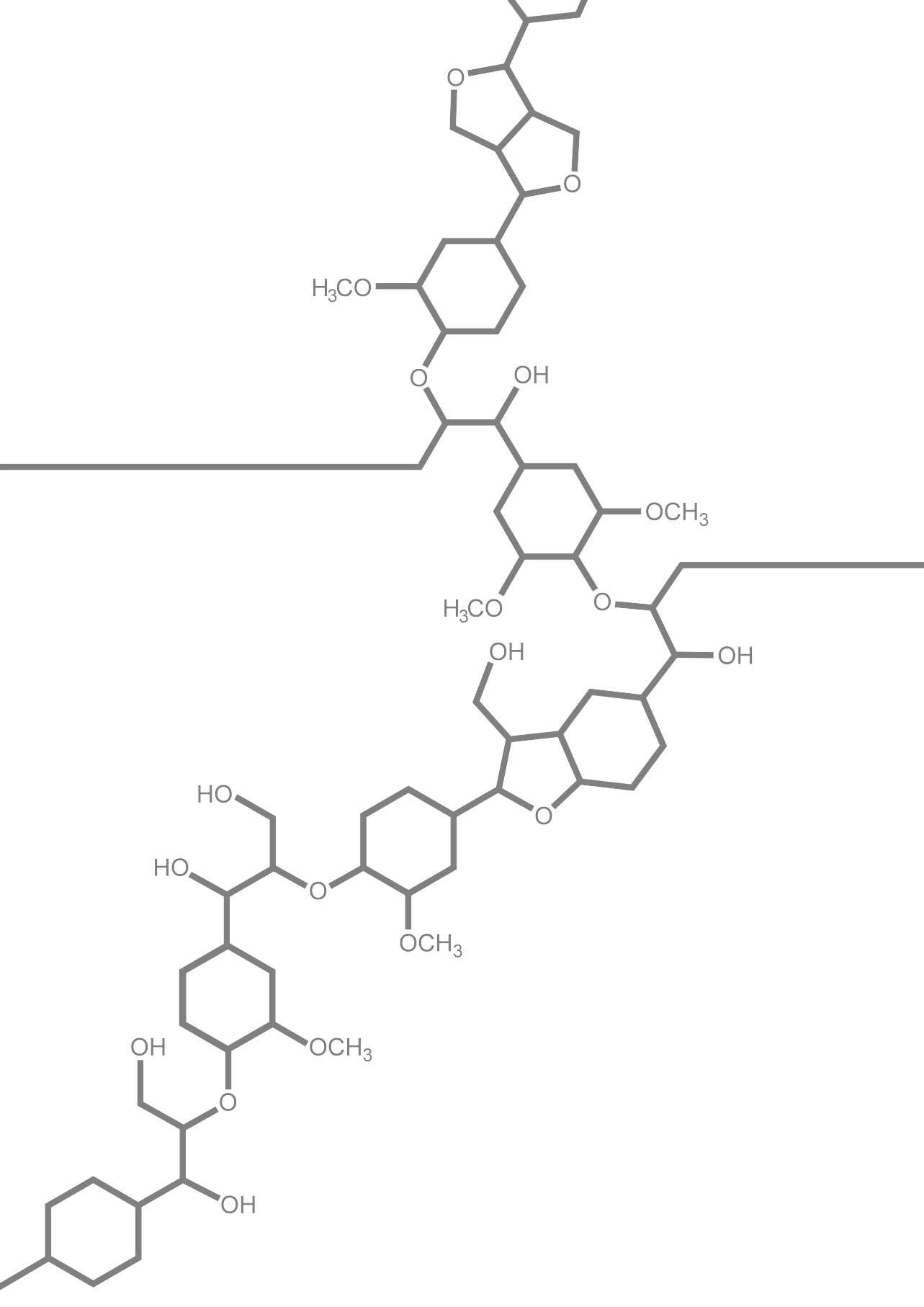


Fig. S7.3 Aromatic regions of HSQC spectra of residues of lignin isolates after saponification. A = CSL control, B = laccase/HBT treated CSL, C = WSL control and D = laccase/HBT treated WSL. Lignin substructures corresponding to the colored annotations are shown on the right. Annotation was performed based on literature.^{10,27,282-4} As the abundance of *p*CA was determined by integration of the C_{2,6}-H_{2,6} correlation, a value of 0 was found for the WSL control sample. It should be noted, however, that still a small peak was visible corresponding to the C_α-H_α correlation of *p*CA or FA, indicating that still small amounts of *p*CA may be present. Even in samples where *p*CA groups were still present, saponification was complete, as evidenced by the shift of C_α-H_α and C_β-H_β correlations of *p*CA to 143.8/7.48 and 115.1/6.28, which are diagnostic for *p*CA moieties with free carboxyl groups.

References Supporting Information

1. Hilgers R, Van Erven G, Boerkamp V, Sulaeva I, Potthast A, Kabel MA and Vincken J-P. *Green Chemistry* **2020**, 22, 1735-1746.
2. Van Erven G, Hilgers RJ, De Waard P, Gladbeek E-J, Van Berkel WJH and Kabel MA. *ACS Sustainable Chemistry & Engineering* **2019**, 7 (19), 16757-16764.
3. Del Río JC, Rencoret J, Prinsen P, Martínez AT, Ralph J and Gutiérrez A. *Journal of Agricultural and Food Chemistry* **2012**, 60 (23), 5922-5935.
4. Zeng J, Helms GL, Gao X and Chen S. *Journal of Agricultural and Food Chemistry* **2013**, 61 (46), 10848-10857.
5. de Menezes FF, Rencoret J, Nakanishi SC, Nascimento VM, Silva VFN, Gutiérrez A, del Río JC and de Moraes Rocha GJ. *ACS Sustainable Chemistry & Engineering* **2017**, 5 (7), 5702-5712.



CHAPTER

8

General discussion

8.1. Outline of this discussion

In this thesis we aimed to enhance the understanding of lignin degradation and modification by laccase and laccase/mediator systems (LMS). To this end, the reactivity of both (novel) lignin model compounds and polymeric lignin was investigated upon laccase and LMS treatments. In this chapter, the obtained insights from the previous chapters and literature are combined in a discussion on four main topics: (i) the reactions of the mediator in LMS-catalyzed lignin modification, (ii) the impact of lignin structure on its reactivity in LMS treatments, (iii) the (non-)sense of lignin model compound studies, and (iv) whether and how LMS-catalysis could become a sustainable tool for lignin degradation or modification at industrial scale.

8.2. The reactions of the mediator in LMS-catalyzed lignin modification

8.2.1. A critical reflection on the oxidation mechanisms of laccase/HBT and laccase/ABTS systems

Lignin, majorly composed of non-phenolic substructures, can be oxidized by using LMS. Oxidation of lignin structures by mediators can occur via different mechanisms, such as electron transfer (ET), hydrogen atom transfer (HAT) and ionic mechanisms (as described in detail in **Chapter 1**). The most common mediators, i.e. HBT and ABTS, have been thoroughly investigated and suggested to operate via HAT and ET, respectively.² These mechanisms were proposed based on three types of experiments, which are depicted in **Table 8.1**. Although, it is a widespread idea that the mediators HBT and ABTS operate via HAT and ET, respectively, not all experimental data reported in this thesis and in literature corroborate these suggestions, as discussed below in detail.

8.2.1.1. The laccase/HBT system

A HAT mechanisms has been proposed for lignin oxidation by laccase/HBT, based on the following experimental observations:

- Oxidation of monomeric C₆-monodeuterated benzyl alcohols by laccase/HBT resulted in large C₆-H/D kinetic isotope effects (KIEs), suggesting that cleavage of the C₆-H/D bond occurs during the rate-limiting step.²
- Upon oxidation of various substituted benzyl alcohols by laccase/HBT, a relatively small negative Hammett reaction constant was found (i.e. -0.64), which is expected in the case of HAT (see **Table 8.1**).^{2,3}
- Oxidation of a 'probe substrate' (see **Table 8.1**) resulted in ketone formation exclusively, which also occurred under *bona fide* HAT conditions.²

Table 8.1 Experiments used for mechanistic investigations of lignin oxidation by LMS and corresponding expected outcomes as reported in literature.^{2,4-6} It should be noted that the appropriateness of the experiments and correctness of the expectations is partly disputed, as further discussed in the main text. EWG = electron-withdrawing group. EDG = electron-donating group.

Experiment	Expected outcome
Determination of intramolecular C_α-H/D KIE	
<p>KIE = [D-aldehyde]/[H-aldehyde]</p> <p>D-aldehyde H-aldehyde</p>	<p>ET : small KIE²</p> <p>HAT : large KIE²</p> <p>Ionic : small KIE^{4,5}</p>
Determination of Hammett reaction constant (ρ)	
<p>Measure rate constant (k) relative to X=H Determine ρ^a</p> <p>X = Me, MeO, Cl, NO₂, other</p>	<p>ET : negative ρ^2</p> <p>HAT : slightly negative ρ^2</p> <p>Ionic (X=EWG) : slightly negative ρ^6</p> <p>Ionic (X=EDG) : positive ρ^6</p>
Oxidation of probe substrate	
<p>aldehyde or ketone</p>	<p>ET : aldehyde²</p> <p>HAT : ketone²</p> <p>Ionic : unknown</p>

^a ρ is the slope of the curve obtained by plotting k_X/k_H vs. the substitution constants (σ), which are positive for EWGs and negative for EDGs.

Indeed, most reactions reported in literature and in this thesis support a HAT mechanism, and we also confirmed HAT oxidation by observation of a large *intermolecular* C_α-H/C_α-D KIE upon oxidation of VBG (**Chapter 4**, see **Fig. 4.2** for structure of VBG). Nonetheless, it has been shown that one of the results of laccase/HBT treatment of non-phenolic model dimers and polymeric lignin (**Chapter 4** and **5**) is *O*-4' cleavage of β -*O*-4' linkages.⁷ Such a reaction is difficult to envision starting from a benzylic radical, the initial product of HAT, whereas it is reasonably logic starting from a radical cation, formed via ET (see **Fig. 5.7** for mechanisms).⁷ It seems, therefore, plausible that HBT (and probably also other N-OH type mediators), can operate via both HAT and ET. The balance between those mechanisms, and, thereby, the overall outcome of the LMS treatment, may be influenced by the exact structure of the substrate, as further discussed in section 8.3.

8.2.1.2. The laccase/ABTS system

It is a generally accepted idea that the laccase/ABTS system oxidizes non-phenolic lignin structures via ET, also based on the experiments depicted in **Table 8.1**.² Indeed, the KIE

observed for ABTS-mediated oxidation of benzyl alcohols was lower than that of HBT-mediated oxidation, and similar to that obtained by using a *bona fide* ET oxidant, suggesting that ABTS operates via ET.² The reported Hammett reaction constant of laccase/ABTS was, however, similar to that of a laccase/N-hydroxyphthalimide system, which was suggested to operate via HAT.² In addition, the authors claimed that oxidation of a probe substrate allows unambiguous identification of either ET or HAT oxidations (**Table 8.1**). This, however, assumes that mediators only interact with the substrate during oxidation, and not after oxidation. This assumption is tricky, e.g. because ABTS has been shown to interact with phenoxyl radicals (see **Chapter 2**). It cannot be excluded that ABTS also interacts with e.g. benzylic radicals, and thereby influences the reaction pathway after the initial substrate oxidation. In addition, if the product profile of a LMS treatment were indicative for the oxidation mechanism, it should be noted that product profiles obtained from other substrates contradict ET as the mechanism involved. For instance, treatment of VBG with *bona fide* ET oxidants mainly results in C α -C β cleavage,⁸ whereas laccase/ABTS treatment results in C α -oxidation exclusively (**Fig. 8.1** in text box 8.1).

Thus, in fact, the presented evidence for an ET mechanism in laccase/ABTS-catalyzed oxidation of non-phenolic lignin structures is largely limited to the relatively low *intramolecular* KIEs obtained upon oxidation of benzyl alcohols.

Another finding that is difficult to reconcile with an ET mechanism, is that the laccase/ABTS system has been shown to be unreactive towards benzyl ethers, even though it can oxidize benzyl alcohols with similar or even higher redox potentials.² Laccase/ABTS was also unable to convert the C α -sulfonated analogue of VBG, lacking a benzylic hydroxyl group (SVBG, see **Fig 3.1**). These observations suggest that the laccase/ABTS is only able to oxidize benzyl alcohols. In case of an ET oxidation mechanism, such a specificity towards benzyl alcohols would not be expected.

Lastly, it should be noted that the relatively low C α -H/D KIEs (i.e. 3.1-3.6) for laccase/ABTS reported by Baiocco et al.² were obtained from *intramolecular* competition experiments (see **Table 8.1**). Although the obtained values hinted at an ET mechanism, it should be noted that only *intermolecular* KIEs obtained from parallel incubations provide direct evidence for the involvement of C α -H or C α -D cleavage in the rate-limiting step (which is the case for HAT, but not for ET).⁹ When we performed such parallel incubations of VBG and C α -deuterated VBG with laccase/ABTS, we found a KIE of 6.2 \pm 0.3 (data not shown).¹⁰ Admittedly, this value was only obtained from a single incubation time (i.e. 24 h), so its accuracy could be questioned. Nevertheless, the high value suggests that the C α -H bond is involved in the rate-limiting step of VBG oxidation by laccase/ABTS, which conflicts with an ET mechanism.

Although the above-mentioned findings seem to conflict with an ET mechanism, other mechanisms, such as HAT or an ionic mechanism also do not match perfectly with the set of observations described above. Based on the observed specificity for benzyl

alcohols, it is tempting to suggest an ionic mechanism, similar to that of the laccase/TEMPO system (see **Chapter 1**). This would also explain the fact that laccase/ABTS treatment of VBG results in C_α-oxidation exclusively (**Fig. 8.1**), and could match with a relatively large KIE (in case C_α-H deprotonation is rate-limiting).⁶ Nevertheless, as indicated by Baiocco et al., oxidation of substrates by laccase/ABTS seems to decrease with increasing redox potential of the substrate,² which is not expected for an ionic mechanism, and, indeed, not found in the case of laccase/TEMPO.¹¹

A HAT mechanism does not seem to be completely impossible. As mentioned above, the Hammett reaction constant of laccase/ABTS reported by Baiocco et al., was similar to that of laccase/hydroxyphthalimide, a LMS suggested to operate via HAT.² In addition, a HAT mechanism would explain the large KIE obtained from parallel incubations of VBG and its C_α-deuterated analogue. Nevertheless, if HAT were the oxidation mechanism of laccase/ABTS, it remains difficult to explain that Baiocco et al. reported *intramolecular* KIEs that perfectly match with a *bona fide* ET oxidant. Moreover, a specificity towards benzyl alcohols would not be expected in the case of HAT.¹²

Overall, the above shows that laccase/ABTS-catalyzed oxidation of non-phenolic lignin structures is not yet fully understood. In fact, even the exact structure of the oxidizing ABTS species is still unclear.¹³ Although it is a widespread idea that laccase/ABTS oxidized non-phenolic lignin structures via ET, many data have been presented that are difficult to reconcile with this mechanism, and thus, the oxidation mechanism should be reconsidered. In addition, it cannot be excluded that a single mediator operates via multiple mechanisms.

8.2.2. The potential of natural mediators

Although the synthetic molecules HBT and ABTS are still the most widely used mediators, over the past years, several phenolic molecules have been described and promoted as natural alternatives.^{14,15} Many of those molecules are lignin-derived monomers. Although referred to as 'efficient mediators', the actual potential of these natural mediators has only been tested to a very limited extent.^{14,15} Camarero et al. reported that various lignin-derived monomers, especially acetosyringone and syringaldehyde, are efficient mediators for laccase-catalyzed decolorization of recalcitrant dyes.¹⁵ Nevertheless, the only analysis performed was spectrophotometric monitoring of the decolorization of dye solutions. As the recovery of phenolic monomers was not determined, it actually remains unclear whether these small phenolics are 'efficient' mediators. In fact, since the mechanism of dye decolorization was not investigated at all, it is even unknown whether these phenolic monomers act as 'mediators' or decolorize the dyes via non-redox mechanisms. Another phenolic monomer, methyl syringate (MeS), has also been described as a promising natural mediator.¹⁴ Indeed, MeS has been shown to enable laccase-catalyzed oxidation of veratryl alcohol, a non-phenolic lignin model monomer, with reasonably high yields

(31% after 24 h).¹⁴ Nevertheless, when we repeated these incubations with VBG as substrate, extensive degradation of MeS was observed, and only a marginal conversion of VBG to VBG_{ox} occurred (~2%), which is much lower than in laccase/HBT or laccase/ABTS incubations (see **Fig. 8.2** in text box 8.1).

Text box 8.1

In various chapters of this thesis, the incubation of VBG with laccase/HBT has been described. To investigate the effectiveness of alternative mediators in oxidation of VBG, similar incubations were performed with ABTS and methyl syringate (MeS) as mediators. In the case of ABTS, C_α-oxidation was observed as the only reaction outcome. In addition, extensive hydroxylation of ABTS was observed (**Fig. 8.1**). In the case of MeS, extensive degradation of MeS was observed, with only very minor VBG oxidation (**Fig. 8.2**).

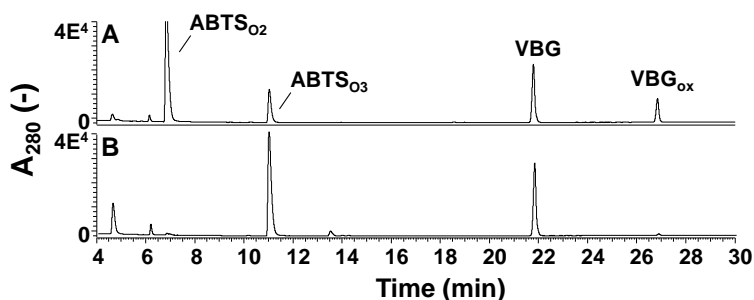


Fig. 8.1 RP-UHPLC-UV₂₈₀ chromatograms of VBG incubated with laccase/ABTS for 24 h at pH 4 (A) and pH 6 (B). ABTS_{O_n} = ABTS with n additional oxygen atoms.

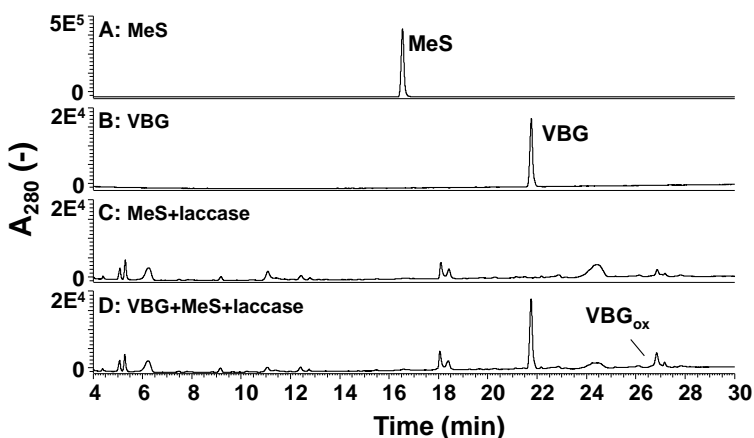


Fig. 8.2 RP-UHPLC-UV₂₈₀ chromatograms of MeS (A), VBG (B), MeS+laccase (C) and VBG+MeS+laccase (D) after incubation for 48 h at pH 6 (A-D).

A laccase/MeS system has also been used for delignification of Eucalyptus feedstock, but also in this case its effectiveness was found to be lower than that of a laccase/HBT system.^{16,17} Overall, although some phenolic compounds seem to be natural alternatives for synthetic laccase mediators, they are prone to degradation, resulting in a relatively low efficiency.

8.2.3. Side-reactions of mediators

An ideal mediator acts as a diffusible redox shuttle without undergoing secondary reactions. Clearly, none of the mediators reported in this thesis showed such ideal behavior. In **Chapter 2**, it was shown that in presence of a phenolic lignin structure, ABTS undergoes extensive coupling to the phenolic compound, followed by cleavage of the ABTS moiety. Also in absence of a radical coupling partner, ABTS undergoes side-reactions, such as hydroxylation (**Fig. 8.1**). When laccase is used in combination with HBT, covalent bonds can be formed between lignin structures and the mediator (**Chapter 2 and 5**), although to a lower extent than in the case of ABTS. Furthermore, HBT undergoes degradation to benzotriazole (BT) in the presence of laccase, as shown in **Chapter 2-5 and 7**. This conversion is accelerated in the presence of *p*-coumaroyl groups, presumably via the formation of covalent HBT-coumarate adducts (**Chapter 7**). So far, it remains unknown how HBT is converted to BT in incubations containing only laccase and HBT.

Despite its degradation and coupling reactions, HBT still seems to be one of the most effective mediators for oxidation of lignin, as it oxidizes non-phenolic lignin structures with relatively high yields, and its degradation and coupling reactions are slower than that of ABTS and natural mediators, such as MeS.

8.3. The impact of lignin structure on its reactivity upon laccase and LMS treatments

8.3.1. The reactivity of phenolic vs. non-phenolic lignin substructures

Although, in native lignin, phenolic subunits are far less abundant than non-phenolic subunits, their high reactivity might result in a relatively large contribution to the overall incubation outcome. In addition, it seems likely that ether cleavage of non-phenolic β -O-4' linked structures results in the formation of phenoxyl radicals (see **Chapter 4**), which are, in fact, oxidized phenolic structures. Thus, although the initial abundance of phenolic subunits is low, they may be formed *in situ* upon cleavage of non-phenolic structures.

In incubations with laccase alone, the difference in reactivity between phenolic and non-phenolic subunits is relatively simple: phenolic structures are readily converted (as further discussed in section 8.3.2), whereas non-phenolic structures are recalcitrant.

Nevertheless, as incubations of polymeric lignin are generally performed by using laccase in combination with a mediator, it is also important to understand the reactivity of both phenolic and non-phenolic substructures upon such LMS treatments. Hitherto, the reactivity of phenolic lignin substructures upon LMS treatments had, however, hardly been investigated. In **Chapter 2**, we showed that addition of a mediator may substantially affect the reactions that a phenolic lignin model compound (GBG) undergoes when incubated with laccase. Whereas GBG polymerized in incubations with laccase alone, treatment with a laccase/ABTS system resulted in extensive substrate-ABTS coupling (also referred to as grafting). The latter was not observed upon laccase/ABTS treatment of VBG, a non-phenolic lignin model (**Fig. 8.1**).¹⁸ Overall, whereas VBG mainly underwent C_α-oxidation and ether cleavage upon LMS treatments (**Chapter 3** and **4**), GBG underwent oxidative coupling, grafting and C_α-oxidation, illustrating that phenolic and non-phenolic structures undergo completely different reactions upon LMS treatment.

8.3.2. The reactivity of S and G-type lignin structures

With a few exceptions, most lignin model compound studies have focused on the reactivity of one or two model compounds, probably due to the limited commercial availability of lignin model compounds. Consequently, the difference in reactivity of S, G and H-type models has hardly been investigated. In fact, the reactivity of model dimers containing H-rings upon laccase and LMS treatments has, so far, not been investigated at all. Nevertheless, combining results from this thesis and from literature allows to create an overview of the reactivity of various S and G-type lignin model dimers upon laccase and LMS treatment (**Fig. 8.3**). From this overview, it is clear that the reaction pathways of lignin model compounds are strongly dependent on the type of subunits (i.e. S or G) of the model.

In the case of non-phenolic β-*O*-4' linked model dimers, it has been observed that G-G type dimers (i.e. VBG) mainly undergo C_α-oxidation and C_β-*O* cleavage upon laccase/HBT treatment, whereas G-S type dimers also undergo C_α-C_β cleavage and aromatic ring cleavage (**Fig. 8.4**).^{7,19,20} The reason behind this difference, most likely, lies in the oxidation mechanisms involved. Whereas the laccase/HBT system oxidizes VBG primarily via HAT, it can be postulated that it oxidizes the G-S analogue of VBG via both HAT and ET. The latter is facilitated by an increased electron density at the S-ring, due to an extra electron-donating methoxyl substituent.⁷

Also in the case of phenolic β-*O*-4' linked model dimers, different reactions have been observed for G and S-type aromatic rings. Whereas G-G dimers (GBG) primarily undergo radical coupling upon incubation with laccase, S-G dimers (SBG) undergo C_α-oxidation and alkyl-aryl cleavage (**Fig. 8.3** and **8.4**). As the only difference between GBG and SBG is the presence of an extra methoxyl substituent at C₅ in SBG, this raises the question whether phenolic G-rings, after substitution of C₅ (e.g. via radical coupling), show reactivity similar to S-rings. At first sight, the fact that GBG undergoes coupling to form

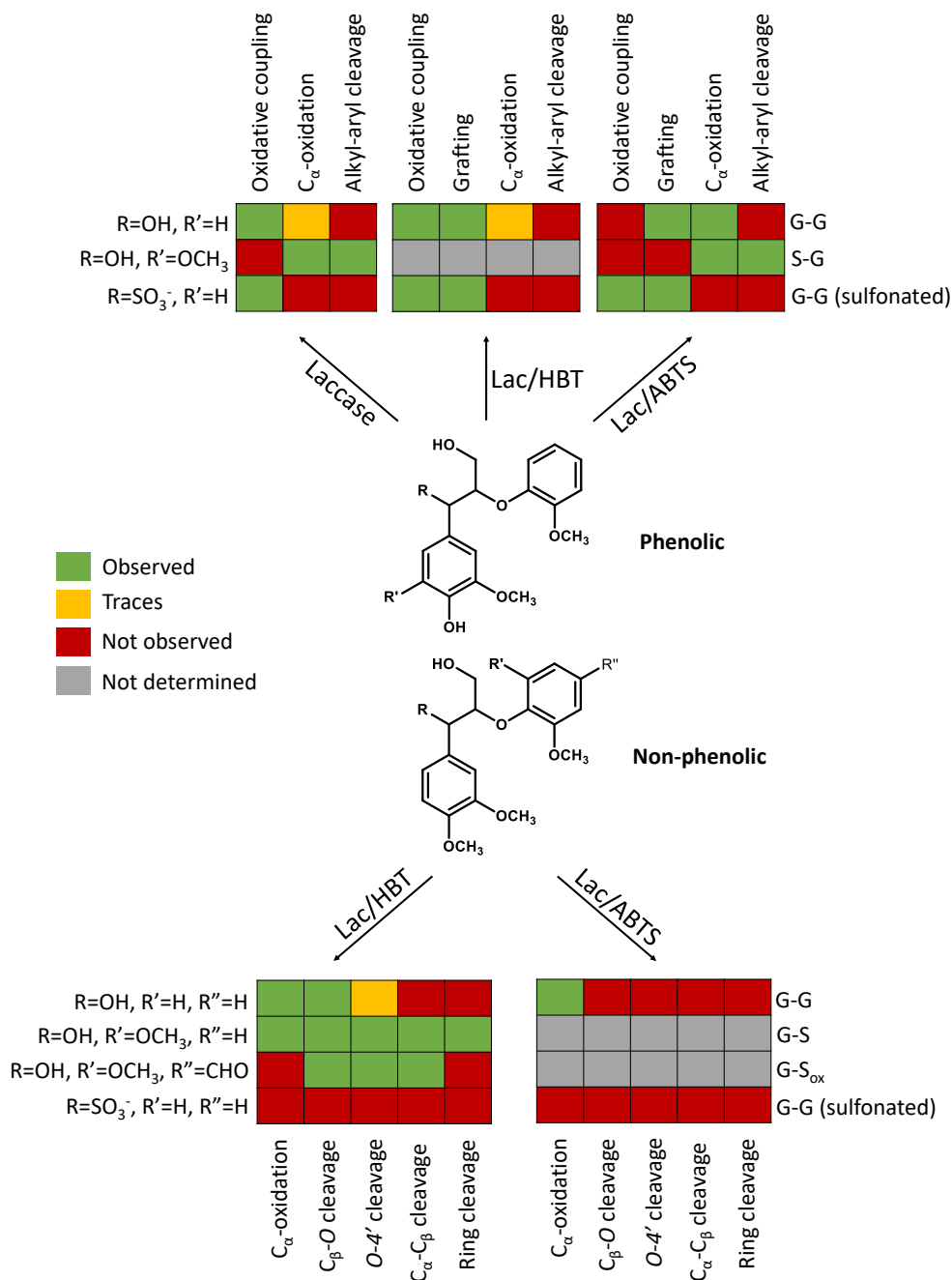


Fig. 8.3 Overview of reported reaction outcomes upon incubation of phenolic and non-phenolic β -O-4' linked model compounds in this thesis and literature.^{7,19,20} All data were obtained at pH 4-5. Although other types of β -O-4' linked model dimers could be synthesized (e.g. non-phenolic S-G dimers), no reports of their reactivity with laccase or LMS are known.

GBG trimers, tetramers and even larger oligomers, with only traces of C_α-oxidation and no detectable alkyl-aryl cleavage (**Chapter 2**) suggests that this is not the case. Nevertheless, when the 5-5' linked dimer of GBG was purified and incubated with laccase, no oxidative coupling, but alkyl-aryl cleavage and C_α-oxidation were observed (**Fig. 8.4**). Thus, we concluded that C₅-substituted phenolic G-units show reactivity similar to that of phenolic S-units. Furthermore, these findings indicated that oligomerization of GBG starts with 5-5' coupling (see **Chapter 2**), and then continues via 4-*O*-5' coupling to GBG radicals, as 5-5' coupling to dimerized GBG is not possible (**Fig. 8.4**). Radical coupling between phenolic groups can, thus, occur between two G-units, between G and S-units, but not between two S-units.

8.3.3. Other effects of lignin structure on its reactivity

In addition to the type of aromatic rings of the model dimers, other structural properties of lignin model compounds have been shown to affect their reactivity in laccase and LMS incubations. For instance, whereas a non-phenolic G-S model dimer undergoes aromatic ring cleavage upon laccase/HBT treatment, this is not observed when the S-ring is substituted with an aldehyde group, indicating that C_α-oxidation affects the reactivity of adjacent rings. It has been proposed that this is caused by a decreased electron density at the S-ring, due to the electron-withdrawing nature of the aldehyde group. The exact reason is, however, unknown. Another example has been discussed in **Chapter 3**, where we investigated the effect of C_α-sulfonation of phenolic and non-phenolic lignin models, to understand the reactivity of lignosulfonate in more detail. Upon incubation with laccase and laccase/HBT, sulfonated GBG followed a reaction pathway similar to that of GBG (i.e. radical coupling), whereas sulfonated VBG was completely unreactive upon both treatments. This was explained by an increased C_α-H bond dissociation energy after sulfonation.

The above described examples show that the reactivity of lignin cannot simply be predicted based on the abundance of S, G and H-units, and that also other structural properties may affect the reactions pathway of a lignin substructure upon LMS treatment.

It should also be noted that, hitherto, only insights have been obtained into the reactivity of β-*O*-4' linked substructures. Based on the above, it seems obvious that other linkages, such as phenylcoumarans and resinols, will display reactivity different from that of β-*O*-4' linkages. As we have shown that phenylcoumaran (β-5') and resinol (β-β') linkages are reactive upon LMS treatment (**Chapter 5**), it would be interesting to study the reactivity of β-5' and β-β' linked model dimers in more detail. Such models are, however, not commercially available, and therefore need to be synthesized first.

Text box 8.2

As a lignin dimer with a phenolic G-type ring (GBG) was found to undergo polymerization upon incubation with laccase, presumably via the C₅ position (**chapter 2**),¹ we investigated whether a lignin model dimer with a phenolic S-type ring, in which the C₅ atom is substituted, would show different reactivity. The results indicated that SBG undergoes C_α-oxidation, as well as alkyl-aryl cleavage (**Fig. 8.4**). Polymerization was not observed at all. In addition, we investigated the reactivity of 5-5' dimerized GBG upon laccase treatment. This compound underwent the same reactions as SBG, albeit substantially slower.

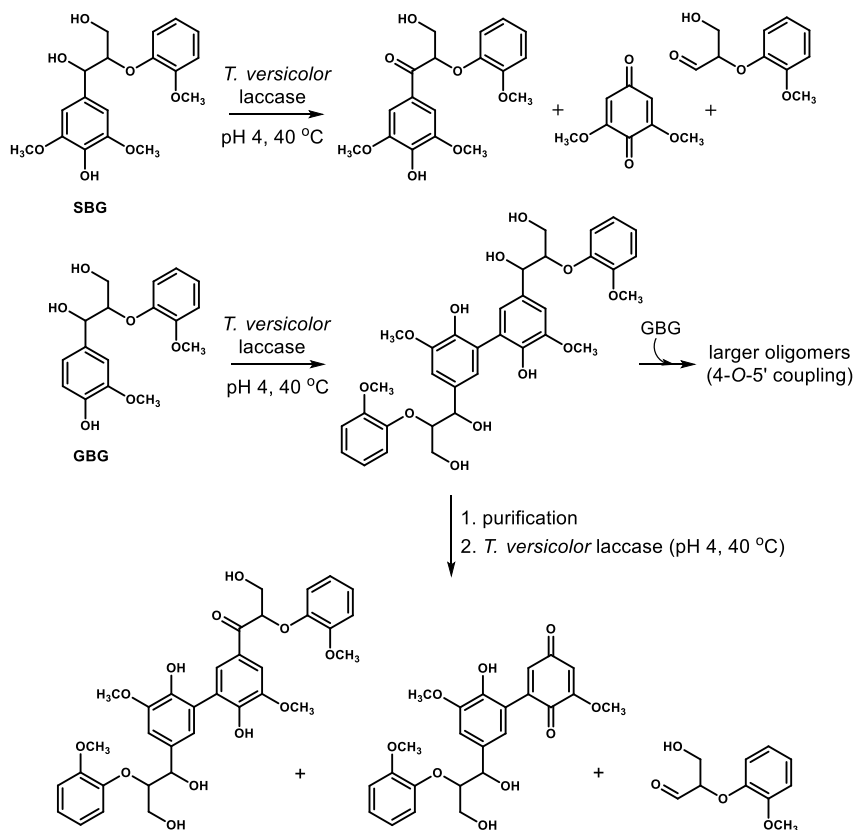


Fig. 8.4 Schematic overview of the reaction outcomes of treatment of SBG (ABCR, Karlsruhe, Germany), GBG and a purified 5-5' linked dimer of GBG with laccase (pH 4, 40 °C), as determined by using RP-UHPLC-PDA-MS (see Chapter 2 for detailed method). For product annotation of GBG, see Chapter 2. Annotation of other reaction products was performed based on high resolution RP-UHPLC-MS (mass error <0.5 ppm for all products) and MS² fragmentation (not shown).

8.4. What can we (not) learn from lignin model compound studies?

8.4.1. The (non)-sense of studying lignin monomers, dimers and oligomers

As lignin model compounds are much more simple than polymeric lignin, the relevance of model compound studies in understanding lignin reactivity could be questioned. In other words: to what extent can we extrapolate the findings obtained from model compound studies to polymeric lignin?

An important factor related to this question is the size, or degree of polymerization, of the model compound. Whereas only dimeric (or larger) lignin model compounds have been used in this thesis, many studies reported in literature have investigated (chemo-) enzymatic lignin conversion by using monomeric model compounds, even though a few dimeric model compounds have become commercially available.^{14,21-24} Although, from a biochemistry perspective, it could be interesting to study the interaction between an enzyme and a monomeric substrate, understanding reactivity of lignin based on a model compound that does not even possess an interunit linkage does not make much sense. In fact, one might even question whether the term 'lignin model compound' is appropriate for monomeric compounds. Admittedly, many studies do not aim to understand the reaction pathways underlying lignin conversion in detail, but, for example, aim to demonstrate new tools for lignin oxidation. Nevertheless, even in those cases it is tricky to draw conclusions based on monomeric model compounds. This is, for instance, illustrated by the fact that a laccase/MeS system effectively oxidizes veratryl alcohol, whereas it is rather ineffective in oxidizing VBG (**Fig. 8.2**).¹⁴ Thus, it is essential to select appropriate model compounds, even in studies that aim to demonstrate, rather than understand (novel) tools for lignin conversion. As dimeric models reflect the structure of lignin much better than monomers do, the use of monomeric lignin models should be avoided as much as possible. It should be noted that, even when dimeric model compounds are used, the obtained results can only be used to understand the reactivity of lignin polymers with matching substructures. For example, the reactivity of S-type lignin models is unlikely to be a good predictor of softwood lignin, which essentially only contains G-subunits. And, VBG is not a suitable model compound to mimic the reactivity of heavily sulfonated lignin.

Now that many reactions of phenolic and non-phenolic lignin model dimers have been described, it would be interesting to also employ more complex oligomers as model substrates for laccase and LMS treatments. For instance, trimeric model compounds containing two different interunit linkages could be used,²⁵ which would provide insight into which substructure is preferentially attacked. Such information contributes to a more reliable extrapolation of the reactivity of model compounds to that of lignin polymers.

8.4.2. Model compound studies as key steps to explore and understand reactivity of polymeric lignin

The use of lignin model compounds offers several advantages as compared to polymeric lignin. Firstly, it provides a facile approach for initial testing of novel lignin modification and/or degradation methods. In general it can be stated that, if an approach is not effective on a model compound, it will also not be effective on polymeric lignin.²⁶ In the past years, several innovative strategies for lignin degradation have been published, that were initially tested on model dimers. After successful results, the approaches were extended to polymeric lignin.^{27,28}

Also in this thesis, model compound studies have been proven highly useful in understanding the reactions of polymeric lignin upon LMS treatment. For instance, in **Chapter 5**, we identified C_β-O cleavage, O-4' cleavage and C_α-oxidation of lignin as major reaction outcomes of laccase/HBT treatment of wheat straw and corn stover. The elucidation of these reaction outcomes was facilitated by our earlier studies of VBG treatment with laccase/HBT, in which the same reactions were observed (**Chapter 4**). In fact, the purified reaction products of VBG were even used for annotation of HSQC correlations that appeared after laccase/HBT treatment of wheat straw and corn stover. Thus, lignin model compounds have predicting value for the reactivity of lignin, but can also be used to facilitate analysis of polymeric lignin.

Lastly, insights into reaction mechanisms underlying degradation and/or modification, such as presented in **Chapter 4**, can only be obtained when a well-defined substrate is used, which is not possible in case of polymeric lignin. Such fundamental understanding of reaction mechanisms is a stepping stone for optimization of existing approaches for lignin conversion, or even the development of novel approaches (see section 8.5).

8.4.3. The issue of different mobility of model compounds and polymeric lignin

In contrast to the fact that model compounds do not perfectly reflect the structure of polymeric lignin, another drawback of using model compounds has received little attention in literature: Model compounds are much more mobile than lignin polymers. Whereas model compounds tend to be readily soluble in aqueous solutions, this is not the case for lignocellulosic biomass and polymeric lignin isolates. As various reactions of model compounds require that radicals can approach each other, it could be questioned whether these reactions also play a major role in LMS treatment of insoluble lignin polymers. Examples of such reactions are oligomerization (**Chapter 2, 3 and 7**), and possibly also hydroxylation and degradation of *p*-coumaroyl groups (**Chapter 7**). In **Chapter 7**, we compared the reactivity of *p*-coumaroylated VBG with that of *p*-coumaroyl groups in lignin isolates, and found that *p*-coumaroylated VBG underwent extensive hydroxylation and degradation upon laccase/HBT treatment, whereas *p*-coumaroyl groups in polymeric lignin accumulated in the residue. Thus, in this case, the reactivity

of the model compound was not a good predictor of the reactivity *p*-coumaroyl groups in polymeric lignin, and it seems possible that this is due to a difference in mobility of model compounds and polymeric lignin (see **Chapter 7**). To investigate the importance of mobility in more detail, it would be interesting to study the reactivity of immobilized lignin model compounds. Nevertheless, to the best of our knowledge, no suitable methods for such immobilization have been reported. The use of oligomeric model compounds with relatively high DP could also be a solution here, although it should be noted that such structures may still be partly soluble in aqueous solutions, as evidenced by the detection of GBG tetramers, having eight aromatic rings, in RP-UHPLC-PDA-MS analysis (**Chapter 2**).

Overall, it can be concluded that, in order to obtain reliable insights into the reactivity of lignin, it is essential to select suitable and relevant model compounds. Even then, model compound studies have limitations. Nevertheless, obtaining in-depth understanding of the reactivity of lignin without using model compounds is highly challenging, if not impossible.

8.5. Blue enzymes for green lignin degradation and valorization: challenges and potential solutions

8.5.1. Issues of LMS-catalyzed biomass delignification strategies

Based on our results presented in **Chapter 5**, and a few studies reported in literature, it can be concluded that substantial delignification can be obtained by treating lignocellulosic biomass with a laccase/HBT system.²⁹⁻³¹ Nevertheless, several issues have been reported that may limit industrial applicability of LMS-catalyzed biomass delignification. Firstly, as shown in several chapters of this thesis, (re)polymerization of phenolic groups may occur. Even though it is not fully known to which extent such (re)polymerization occurs in polymeric lignin (see **Chapter 7**), this issue has also been reported by others,³²⁻³⁴ and negatively influences the overall degradation of lignin. Although we reported substantial delignification (up to 51%) in **Chapter 5**, this was obtained by using relatively high laccase and mediator concentrations. Probably, by preventing (re)polymerization of phenolic groups, a higher delignification extent could be obtained, or the laccase and mediator concentration could be decreased. Secondly, LMS-catalyzed lignin oxidation may not only result in cleavage of interunit linkages, but also in C_α-oxidation, as shown in various chapters of this thesis. After C_α-oxidation, interunit linkages are still intact and non-phenolic substructures are not oxidized by LMS anymore. Thus, it is of interest to prevent C_α-oxidation and steer the overall outcome of the LMS treatment towards bond cleavage. Lastly, it should be noted that in essentially all reports of successful LMS-catalyzed delignification, ball milled biomass was used as a substrate. Although, hitherto, the effect of substrate accessibility on the extent of delignification has not been studied, it is very likely that substrate accessibility plays a large role in the

effectivity of LMS treatments. After all, in order to achieve HAT (or ET) between the mediator and lignin, these species should be able to approach each other.

8.5.2. Approaches for improvement of LMS-catalyzed biomass delignification

8.5.2.1. Solubilization of lignin

As mentioned above, the accessibility of lignin to the LMS may be an important factor contributing to the efficiency of the LMS treatment. As ball-milling on industrial scale is rather challenging, an alternative and possibly more effective strategy could be solubilization of lignin prior to LMS treatment. One method for the solubilization of lignin is the use of alkali. At high pH, lignin can be largely solubilized, even at low temperature. This approach is, for instance, used to solubilize lignin for size-exclusion chromatography,³⁵ and also in a recently published laccase-based lignin degradation process.³⁶

Another approach for lignin solubilization could be the use of ionic liquids. In various studies it has been reported that ionic liquids are promising solvents for (selective) solubilization of native or technical lignins.^{37–40} In addition, recent publications showed that several laccases retain high activity in case ionic liquids are used as co-solvents,^{41,42} indicating that ionic liquids may also be compatible with laccase-based conversion strategies. However, at high ionic liquid concentrations, laccase activity is diminished.^{41,43} In addition, attention should be paid to the solubility of molecular oxygen in the solvent, as this has been reported to be limited in various ionic liquids.⁴⁴

8.5.2.2. Prevention of (re)polymerization

As discussed above, (re)polymerization of lignin upon LMS treatment may be an issue that limits the overall degradation of lignin. From the results shown in **Fig. 8.3**, it seems likely that (re)polymerization is mainly an issue when G-type (or H-type) phenolic structures are abundant, as these substructures can undergo radical coupling via their C₅ atom. Therefore, it seems likely that 'blocking' C₅-positions of phenoxyl radicals would be a suitable strategy to prevent (re)polymerization. In fact, the proof-of-principle for this approach has already been shown in **Chapter 2**, where we reported that covalent coupling of ABTS to GBG prevents laccase-induced polymerization of GBG. As ABTS also promotes (undesired) C₆-oxidation (see **Fig. 8.1**), and undergoes rapid side-reactions, especially under alkaline conditions, it would be beneficial to use alternative 'C₅-capping' molecules. Potentially interesting candidates are e.g. 2,4,6-substituted monomeric phenols such as 4-*tert*-butyl-2,6-dimethylphenol (TBDMP).⁴⁵ Such molecules do not undergo polymerization upon oxidation by laccase, and may undergo radical coupling to the C₅ atom of a lignin G-unit, forming a 2,4,6-substituted phenolic lignin substructure. In case the resulting structure is still oxidized by LMS, it is expected to undergo C₆-oxidation or alkyl-aryl cleavage, rather than radical coupling (**Fig. 8.5**).

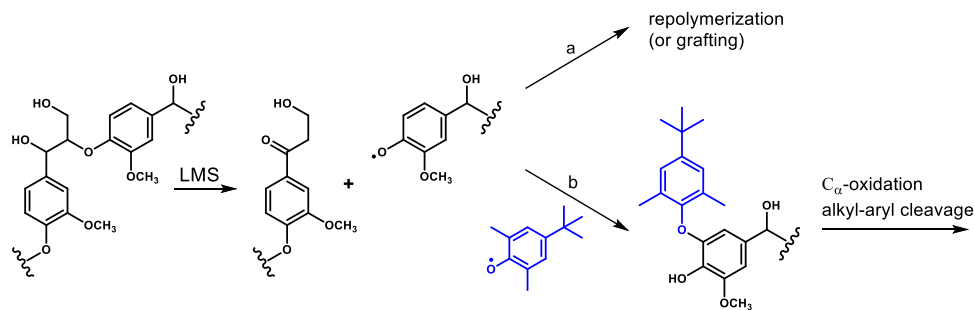


Fig. 8.5 Proposed 'C₅-capping' strategy to counteract (re)polymerization of lignin upon laccase or LMS treatment. In the figure, 4-*tert*-butyl-2,6-dimethylphenol (TBDMP) is shown in blue as an example of a C₅-capping molecule.

Another approach to prevent repolymerization of phenoxyl radicals could be combining LMS with enzymes that reduce phenoxyl radicals to phenols. Several enzymes have been reported to show such activity, such as aryl alcohol oxidases and glucose oxidases, and it has even been speculated that this is also their role in fungal lignin degradation.^{46,47} An alternative and innovative approach was recently published by Salvachúa et al.³³, wherein lignin was incubated with a combination of fungal secretomes, rich in laccases, and bacteria that were able to catabolize low-molecular weight lignin. It was shown that the bacteria successfully prevented repolymerization of lignin. Possibly, such bacteria could also be effective in counteracting repolymerization upon LMS treatments of lignin.³³

Lastly, (re)polymerization could also be prevented by using a more process-oriented approach. For example, LMS treatments could be combined with ultrafiltration membranes in a continuous process. Such a process has recently been developed and has been reported to successfully counteract (re)polymerization.³⁶

8.5.2.3. Bond cleavage vs. C_α-oxidation: maximizing degradation

As C_α-oxidation of lignin results in substructures that are unreactive towards LMS activity, and not in bond cleavage, this reaction counteracts effective LMS-catalyzed degradation of lignin. To increase the effectiveness of LMS treatments, two approaches can be followed: (i) an additional processing step could be introduced that cleaves C_α-oxidized interunit linkages, or (ii) the competition between C_α-oxidation and interunit cleavage could be steered towards the latter.

In line with the first approach, a widely used strategy is to combine LMS treatments with alkaline peroxide treatments. During the latter step, C_α-oxidized β-O-4' linkages undergo a rearrangement that results in C_α-C_β cleavage.⁴⁸ This way, unproductive C_α-oxidation is converted into productive bond cleavage, and a higher extent of lignin degradation.³⁰ Nevertheless, this strategy would require an additional processing step. Alternatively, it

would be of interest to explore the possibility to combine LMS with β -etherase, either in a cocktail or in sequential treatments. β -Etherases are glutathione-dependent enzymes, produced by various bacteria and fungi, that catalyze ether cleavage of C_α -oxidized β -O-4' linkages. Although their effectivity has mainly been tested on lignin model dimers, they also have been shown to be active on synthetic and technical lignins.⁴⁹⁻⁵¹

In line with the second approach, an interesting strategy is optimization of reaction conditions or even exploration of other solvent systems to steer the follow-up reactions of the initial lignin oxidation towards bond cleavage. In **Chapter 4**, we described that the outcome of a laccase/HBT treatment of a non-phenolic lignin model dimer is highly dependent on the buffer properties. Whereas mainly C_α -oxidation, and only small extents of ether cleavage were found at low pH and low buffer strength (regular conditions), this balance shifted towards a main outcome of ether cleavage at near-neutral pH and high buffer strengths. Based on several experiments and observations, we proposed that this competition between C_α -oxidation and ether cleavage is dependent on the extent and strength of H-bonding of the C_α -OH groups of the lignin structure to the buffer anions present. In case of strong H-bonding between the C_α -OH proton and buffer anions, C_α -oxidation is suggested to be impaired, resulting in relatively more ether cleavage. Although it remains to be investigated whether degradation of polymeric lignin can also be enhanced in concentrated buffers around neutral pH, it seems a promising and facile strategy.

Lignin dissolution in ionic liquids has been proposed to be driven by H-bond formation between the ionic liquid and lignin, disrupting intra and intermolecular H-bonds involved in lignin-lignin or lignin-polysaccharide association.⁵²⁻⁵⁴ By using Density Functional Theory (DFT) studies on the interaction between lignin model compounds and various ionic liquids, it was demonstrated that strong H-bonds are formed between the anions of the ionic liquid and the C_α -OH proton of the lignin model dimer.⁵² As we proposed that this is exactly the interaction required for shifting C_α -oxidation to ether cleavage upon LMS treatments (**Chapter 4**), it seems possible that the use of ionic liquids promotes ether cleavage, at the cost of C_α -oxidation, in a way similar to that of buffer ions. In that case, ionic liquids would not only increase the accessibility of lignin, but also steer the overall incubation outcome towards degradation.

In theory, another possibility would be to introduce a pretreatment step to modify the lignin structure, in such a way that C_α -oxidation is prevented or bond cleavage is promoted upon LMS treatment. For example, a formaldehyde pretreatment could be introduced to etherify the C_α -OH group.²⁸ Such etherification is expected to prevent C_α -oxidation, whereas ether cleavage might still occur (**Fig. 8.6**). Nevertheless, it remains to be investigated whether this strategy indeed works. Furthermore, the use of formaldehyde is undesirable, as it is harmful and toxic. Thus, the approaches described above are preferred over this one.

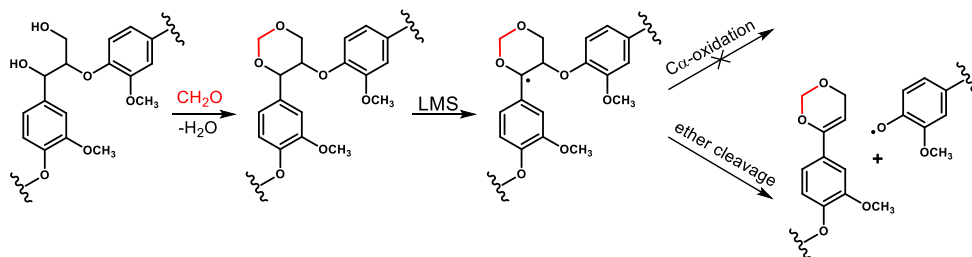


Fig. 8.6 Possible effect of formaldehyde pretreatment on the outcome of LMS treatments of non-phenolic β -O-4' linked lignin structures.

8.5.2.4. A proposed strategy for LMS-catalyzed lignin degradation based on the current knowledge

Based on the issues and potential solutions discussed above, a process for LMS-catalyzed lignin degradation is proposed (**Fig. 8.7**). To maximize effectivity of lignin degradation, several potential solutions discussed above have been combined. The first step is solubilization of lignin. Hereto, alkali or ionic liquids could be used. The dissolved lignin is then transferred to a continuous process involving a degradative treatment with laccase/HBT and a suitable C₅-capping molecule, and ultrafiltration to remove low-molecular-weight lignin. The use of a suitable ionic liquid or alkaline conditions with high phosphate concentrations is expected to limit C₆-oxidation and promote ether cleavage. It should be noted that, instead of phosphate, other anions could be used. A potential issue of using ionic liquids is the relatively high viscosity of such solvents, which could be problematic upon ultrafiltration. Nevertheless, several ionic liquids with relatively low viscosity are known, and the viscosity could be decreased substantially by addition of small amounts of organic co-solvents.^{55,56}

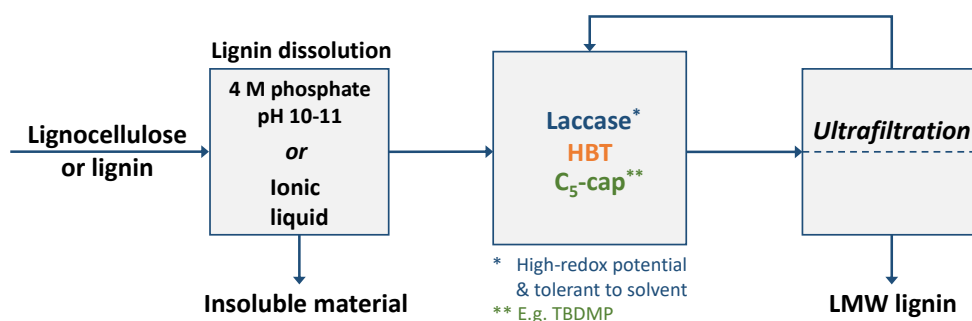


Fig. 8.7 Proposed future process for LMS-catalyzed lignin degradation. First, lignin is solubilized in alkali (containing high phosphate concentrations) or ionic liquid. The dissolved lignin then enters a continuous process wherein treatment with laccase, HBT and a suitable C₅-capping molecule and ultrafiltration occur simultaneously. The laccase should be of high enough redox potential to oxidize HBT, and should be sufficiently active and stable in the used solvent.

The above described future process contains three suggested improvements compared to the LMS treatment performed in **Chapter 5**: the use of concentrated buffer/ionic liquid as solvent, addition of C₅-capping molecules, and ultrafiltration. It should be noted that the combined effect of these improvements remains to be investigated, and that combining two improvements might be more cost-effective than combining all three improvements.

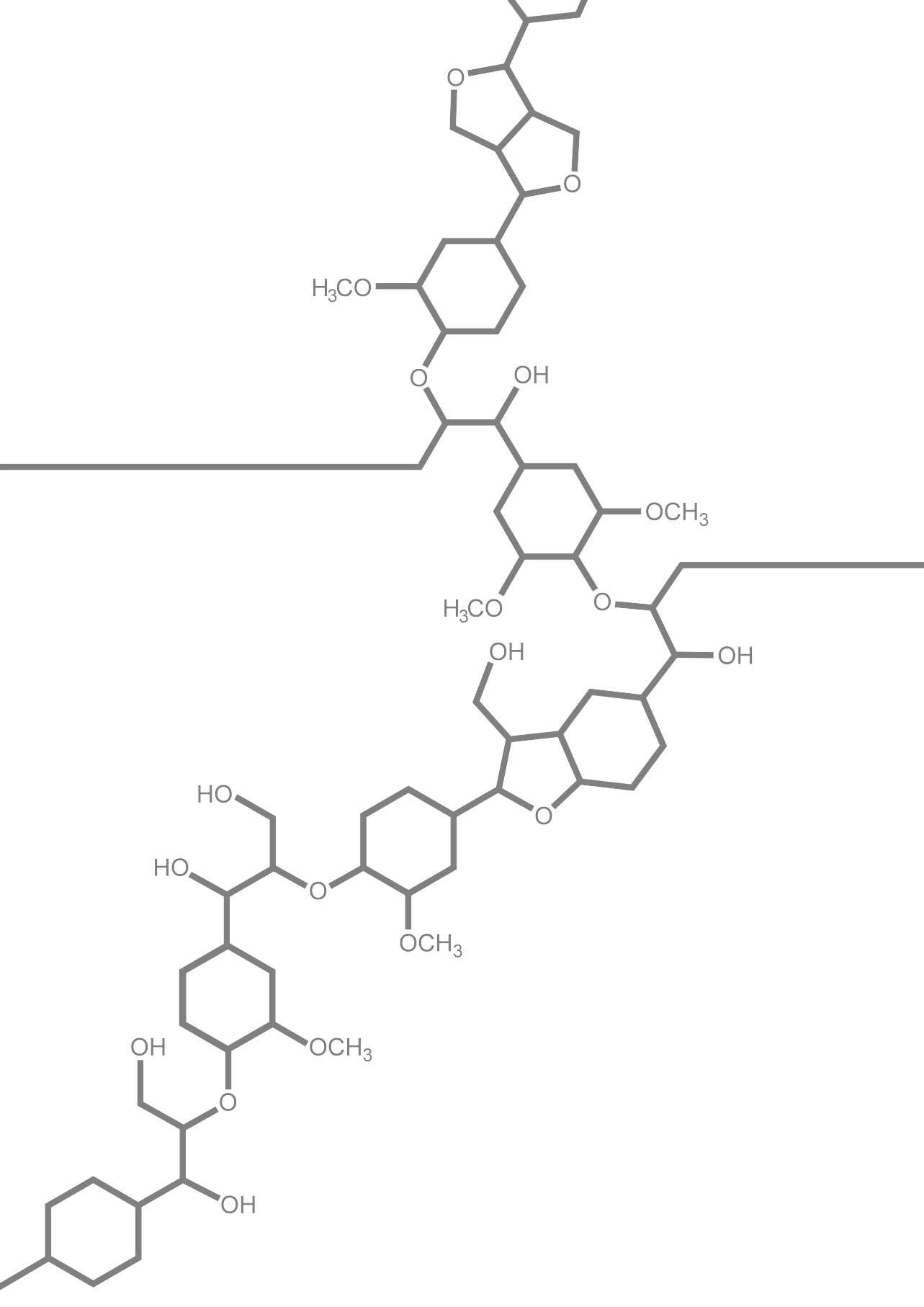
Lastly, it should be noted that this future process requires a laccase that is active and stable under non-mainstream conditions (i.e. in ionic liquid or at highly alkali pH). Although several laccases have been described to maintain high activity and stability when ionic liquids are used as co-solvents, the activity is generally impaired at high ionic liquid concentrations.^{41,43} In contrast, alkali-tolerant laccases with high pH optima (up to pH 10) have been reported, which makes lignin solubilization in alkali a more realistic approach (at least in the short term).^{14,36,57} Nevertheless, also here lies a challenge, as such alkali-tolerant laccases are of bacterial origin and, consequently, have relatively low redox potentials (400-500 mV vs. NHE).⁵⁸ Thus, it is unlikely that these laccases are able to oxidize mediators of high redox potential, such as HBT. An optimistic note is that, over the past years, several successful reports have been published on the increase of pH optima of fungal (high redox potential) laccases via directed evolution.^{59,60} Thus, it does not seem impossible that laccases can be engineered that are compatible with the process described in **Fig. 8.7**.

8.6. References and notes

1. Ramalingam B, Sana B, Seayad J, Ghadessy FJ and Sullivan MB. Towards understanding of laccase-catalysed oxidative oligomerisation of dimeric lignin model compounds. *RSC Advances* **2017**, 7 (20), 11951-11958.
2. Baiocco P, Barreca AM, Fabbrini M, Galli C and Gentili P. Promoting laccase activity towards non-phenolic substrates: a mechanistic investigation with some laccase–mediator systems. *Organic & Biomolecular Chemistry* **2003**, 1 (1), 191-197.
3. d'Acunzo F, Baiocco P, Fabbrini M, Galli C and Gentili P. The radical rate-determining step in the oxidation of benzyl alcohols by two N–OH-type mediators of laccase: the polar N-oxyl radical intermediate. *New Journal of Chemistry* **2002**, 26 (12), 1791-1794.
4. Galli C and Gentili P. Chemical messengers: mediated oxidations with the enzyme laccase. *Journal of physical organic chemistry* **2004**, 17 (11), 973-977.
5. Arends IW, Li Y-X, Ausan R and Sheldon RA. Comparison of TEMPO and its derivatives as mediators in laccase catalysed oxidation of alcohols. *Tetrahedron* **2006**, 62 (28), 6659-6665.
6. d'Acunzo F, Baiocco P, Fabbrini M, Galli C and Gentili P. A mechanistic survey of the oxidation of alcohols and ethers with the enzyme laccase and its mediation by TEMPO. *European Journal of Organic Chemistry* **2002**, 2002 (24), 4195-4201.
7. Kawai S, Nakagawa M and Ohashi H. Degradation mechanisms of a nonphenolic β -O-4 lignin model dimer by *Trametes versicolor* laccase in the presence of 1-hydroxybenzotriazole. *Enzyme and Microbial Technology* **2002**, 30 (4), 482-489.
8. Bohlin C, Persson P, Gorton L, Lundquist K and Jönsson LJ. Product profiles in enzymic and non-enzymic oxidations of the lignin model compound erythro-1-(3, 4-dimethoxyphenyl)-2-(2-methoxyphenoxy)-1, 3-propanediol. *Journal of Molecular Catalysis B: Enzymatic* **2005**, 35 (4-6), 100-107.
9. Simmons EM and Hartwig JF. On the interpretation of deuterium kinetic isotope effects in C-H bond functionalizations by transition-metal complexes. *Angewandte Chemie International Edition* **2012**, 51 (13), 3066-3072.
10. Incubations were performed for 24 h in 20/40 mM citrate/phosphate buffer (pH 4, 40 °C, 400 rpm shaking) with 0.04 mM substrate, 0.4 mM ABTS and 2 U/mL laccase. Analysis was performed as described in Chapter 4.
11. Fabbrini M, Galli C and Gentili P. Comparing the catalytic efficiency of some mediators of laccase. *Journal of Molecular Catalysis B: Enzymatic* **2002**, 16 (5), 231-240.
12. d'Acunzo F, Baiocco P and Galli C. A study of the oxidation of ethers with the enzyme laccase under mediation by two N–OH-type compounds. *New Journal of Chemistry* **2003**, 27 (2), 329-332.
13. Branchi B, Galli C and Gentili P. Kinetics of oxidation of benzyl alcohols by the dication and radical cation of ABTS. Comparison with laccase–ABTS oxidations: an apparent paradox. *Organic & Biomolecular Chemistry* **2005**, 3 (14), 2604-2614.
14. Rosado T, Bernardo P, Koci K, Coelho AV, Robalo MP and Martins LO. Methyl syringate: an efficient phenolic mediator for bacterial and fungal laccases. *Bioresource Technology* **2012**, 124, 371-378.
15. Camarero S, Ibarra D, Martínez MJ and Martínez ÁT. Lignin-derived compounds as efficient laccase mediators for decolorization of different types of recalcitrant dyes. *Applied and Environmental Microbiology* **2005**, 71 (4), 1775-1784.
16. Rico A, Rencoret J, Del Río JC, Martínez AT and Gutiérrez A. Pretreatment with laccase and a phenolic mediator degrades lignin and enhances saccharification of Eucalyptus feedstock. *Biotechnology for Biofuels* **2014**, 7 (1), 6.
17. Rico A, Rencoret J, Del Río JC, Martínez AT and Gutiérrez A. In-depth 2D NMR study of lignin modification during pretreatment of Eucalyptus wood with laccase and mediators. *BioEnergy Research* **2015**, 8 (1), 211-230.
18. Bourbonnais R and Paice MG. Oxidation of non-phenolic substrates: an expanded role for laccase in lignin biodegradation. *FEBS Letters* **1990**, 267 (1), 99-102.
19. Kawai S, Asukai M, Ohya N, Okita K, Ito T and Ohashi H. Degradation of a non-phenolic β -O-4 substructure and of polymeric lignin model compounds by laccase of *Coriolus versicolor* in the presence of 1-hydroxybenzotriazole. *FEMS Microbiology Letters* **1999**, 170 (1), 51-57.

20. Heap L, Green A, Brown D, van Dongen B and Turner N. Role of laccase as an enzymatic pretreatment method to improve lignocellulosic saccharification. *Catalysis Science & Technology* **2014**, 4 (8), 2251-2259.
21. Areskog D, Li J, Nousiainen P, Gellerstedt G, Sipilä J and Henriksson G. Oxidative polymerisation of models for phenolic lignin end-groups by laccase. *Holzforschung* **2010**, 64 (1), 21-34.
22. Lahtinen M, Heinonen P, Oivanen M, Karhunen P, Kruus K and Sipilä J. On the factors affecting product distribution in laccase-catalyzed oxidation of a lignin model compound vanillyl alcohol: experimental and computational evaluation. *Organic & Biomolecular Chemistry* **2013**, 11 (33), 5454-5464.
23. Majjala P, Mattinen M-L, Nousiainen P, Kontro J, Asikkala J, Sipilä J and Viikari L. Action of fungal laccases on lignin model compounds in organic solvents. *Journal of Molecular Catalysis B: Enzymatic* **2012**, 76, 59-67.
24. Qin X, Sun X, Huang H, Bai Y, Wang Y, Luo H, Yao B, Zhang X and Su X. Oxidation of a non-phenolic lignin model compound by two *Irpex lacteus* manganese peroxidases: evidence for implication of carboxylate and radicals. *Biotechnology for Biofuels* **2017**, 10 (1), 103.
25. Lahive CW, Deuss PJ, Lancefield CS, Sun Z, Cordes DB, Young CM, Tran F, Slawin AMZ, de Vries JG, Kamer PC, Westwood NJ and Barta K. Advanced model compounds for understanding acid-catalyzed lignin depolymerization: identification of renewable aromatics and a lignin-derived solvent. *Journal of the American Chemical Society* **2016**, 138 (28), 8900-8911.
26. Rinaldi R, Jastrzebski R, Clough MT, Ralph J, Kennema M, Bruijninx PC and Weckhuysen BM. Paving the way for lignin valorisation: recent advances in bioengineering, biorefining and catalysis. *Angewandte Chemie International Edition* **2016**, 55 (29), 8164-8215.
27. Rahimi A, Ulbrich A, Coon JJ and Stahl SS. Formic-acid-induced depolymerization of oxidized lignin to aromatics. *Nature* **2014**, 515 (7526), 249-252.
28. Shuai L, Amiri MT, Questell-Santiago YM, Héroguel F, Li Y, Kim H, Meilan R, Chapple C, Ralph J and Luterbacher JS. Formaldehyde stabilization facilitates lignin monomer production during biomass depolymerization. *Science* **2016**, 354 (6310), 329-333.
29. Chen Q, Marshall MN, Geib SM, Tien M and Richard TL. Effects of laccase on lignin depolymerization and enzymatic hydrolysis of ensiled corn stover. *Bioresource Technology* **2012**, 117, 186-192.
30. Rencoret J, Pereira A, Del Río JC, Martínez AT and Gutiérrez A. Laccase-mediator pretreatment of wheat straw degrades lignin and improves saccharification. *BioEnergy Research* **2016**, 9 (3), 917-930.
31. Du X, Li J, Gellerstedt G, Rencoret J, Del Río JC, Martínez AT and Gutiérrez A. Understanding pulp delignification by laccase-mediator systems through isolation and characterization of lignin-carbohydrate complexes. *Biomacromolecules* **2013**, 14 (9), 3073-3080.
32. Munk L, Sitarz AK, Kalyani DC, Mikkelsen JD and Meyer AS. Can laccases catalyze bond cleavage in lignin? *Biotechnology Advances* **2015**, 33 (1), 13-24.
33. Salvachúa D, Katahira R, Cleveland NS, Khanna P, Resch MG, Black BA, Purvine SO, Zink EM, Prieto A, Martínez MJ, Martínez AT, Simmons BA, Gladden JM and Beckham GT. Lignin depolymerization by fungal secretomes and a microbial sink. *Green Chemistry* **2016**, 18 (22), 6046-6062.
34. Roth S and Spiess AC. Laccases for biorefinery applications: a critical review on challenges and perspectives. *Bioprocess and Biosystems Engineering* **2015**, 38 (12), 2285-2313.
35. Constant S, Wienk HLJ, Frissen AE, de Peinder P, Boelens R, Van Es DS, Grisel RJH, Weckhuysen BM, Huijgen WJJ, Gosselink RJA and Bruijninx PCA. New insights into the structure and composition of technical lignins: a comparative characterisation study. *Green Chemistry* **2016**, 18 (9), 2651-2665.
36. Hämäläinen V, Grönroos T, Suonpää A, Heikkilä MW, Romein B, Ihalainen P, Malandra S and Birikh KR. Enzymatic processes to unlock the lignin value. *Frontiers in Bioengineering and Biotechnology* **2018**, 6 (20).
37. Hart WE, Harper JB and Aldous L. The effect of changing the components of an ionic liquid upon the solubility of lignin. *Green Chemistry* **2015**, 17 (1), 214-218.
38. Merino O, Fundora-Galano G, Luque R and Martínez-Palou R. Understanding microwave-assisted lignin solubilization in protic ionic liquids with multiaromatic imidazolium cations. *ACS Sustainable Chemistry & Engineering* **2018**, 6 (3), 4122-4129.

39. Pu Y, Jiang N and Ragauskas AJ. Ionic liquid as a green solvent for lignin. *Journal of Wood Chemistry and Technology* **2007**, 27 (1), 23-33.
40. Prado R, Erdocia X and Labidi J. Lignin extraction and purification with ionic liquids. *Journal of Chemical Technology & Biotechnology* **2013**, 88 (7), 1248-1257.
41. Stevens JC, Das L, Mobley JK, Asare SO, Lynn BC, Rodgers DW and Shi J. Understanding laccase-ionic liquid interactions toward biocatalytic lignin conversion in aqueous ionic liquids. *ACS Sustainable Chemistry & Engineering* **2019**, 7 (19), 15928-15938.
42. Wallraf A-M, Liu H, Zhu L, Khalfallah G, Simons C, Alibiglou H, Davari MD and Schwaneberg U. A loop engineering strategy improves laccase lcc2 activity in ionic liquid and aqueous solution. *Green Chemistry* **2018**, 20 (12), 2801-2812.
43. Shipovskov S, Gunaratne HN, Seddon KR and Stephens G. Catalytic activity of laccases in aqueous solutions of ionic liquids. *Green Chemistry* **2008**, 10 (7), 806-810.
44. Anthony JL, Anderson JL, Maginn EJ and Brennecke JF. Anion effects on gas solubility in ionic liquids. *The Journal of Physical Chemistry B* **2005**, 109 (13), 6366-6374.
45. Longe LF, Couvreur J, Leriche Grandchamp M, Garnier G, Allais F and Saito K. Importance of mediators for lignin degradation by fungal laccase. *ACS Sustainable Chemistry & Engineering* **2018**, 6 (8), 10097-10107.
46. Marzullo L, Cannio R, Giardina P, Santini MT and Sannia G. Veratryl alcohol oxidase from *Pleurotus ostreatus* participates in lignin biodegradation and prevents polymerization of laccase-oxidized substrates. *Journal of Biological Chemistry* **1995**, 270 (8), 3823-3827.
47. Szklarz G and Leonowicz A. Cooperation between fungal laccase and glucose oxidase in the degradation of lignin derivatives. *Phytochemistry* **1986**, 25 (11), 2537-2539.
48. Gierer J, Imsgard F and Noren I. Studies on the degradation of phenolic lignin units of the β -aryl ether type with oxygen in alkaline media. *Acta Chemica Scandinavica B* **1977**, 31 (7), 561-572.
49. Gall DL, Ralph J, Donohue TJ and Noguera DR. A group of sequence-related sphingomonad enzymes catalyzes cleavage of β -aryl ether linkages in lignin β -guaiacyl and β -syringyl ether dimers. *Environmental Science & Technology* **2014**, 48 (20), 12454-12463.
50. Picart P, Liu H, Grande PM, Anders N, Zhu L, Klankermayer J, Leitner W, De María PD, Schwaneberg U and Schallmey A. Multi-step biocatalytic depolymerization of lignin. *Applied Microbiology and Biotechnology* **2017**, 101 (15), 6277-6287.
51. Picart P, Müller C, Mottweiler J, Wiermans L, Bolm C, Domínguez de María P and Schallmey A. From gene towards selective biomass valorization: bacterial β -etherases with catalytic activity on lignin-like polymers. *ChemSusChem* **2014**, 7 (11), 3164-3171.
52. Zhang Y, He H, Dong K, Fan M and Zhang S. A DFT study on lignin dissolution in imidazolium-based ionic liquids. *RSC Advances* **2017**, 7 (21), 12670-12681.
53. Janesko BG. Modeling interactions between lignocellulose and ionic liquids using DFT-D. *Physical Chemistry Chemical Physics* **2011**, 13 (23), 11393-11401.
54. Casas A, Palomar J, Alonso MV, Oliet M, Omar S and Rodriguez F. Comparison of lignin and cellulose solubilities in ionic liquids by COSMO-RS analysis and experimental validation. *Industrial Crops and Products* **2012**, 37 (1), 155-163.
55. MacFarlane DR, Golding J, Forsyth S, Forsyth M and Deacon GB. Low viscosity ionic liquids based on organic salts of the dicyanamide anion. *Chemical Communications* **2001**, (16), 1430-1431.
56. Yang F, Wang X, Tan H and Liu Z. Improvement the viscosity of imidazolium-based ionic liquid using organic solvents for biofuels. *Journal of Molecular Liquids* **2017**, 248, 626-633.
57. Chauhan PS, Goradia B and Saxena A. Bacterial laccase: recent update on production, properties and industrial applications. *3 Biotech* **2017**, 7 (5), 323.
58. Chandra R and Chowdhary P. Properties of bacterial laccases and their application in bioremediation of industrial wastes. *Environmental Science: Processes & Impacts* **2015**, 17 (2), 326-342.
59. Mate DM, Gonzalez-Perez D, Falk M, Kittl R, Pita M, De Lacey AL, Ludwig R, Shleev S and Alcalde M. Blood tolerant laccase by directed evolution. *Chemistry & Biology* **2013**, 20 (2), 223-231.
60. Torres-Salas P, Mate DM, Ghazi I, Plou FJ, Ballesteros AO and Alcalde M. Widening the pH activity profile of a fungal laccase by directed evolution. *ChemBioChem* **2013**, 14 (8), 934-937.



Summary

One of the major challenges in biorefinery is the degradation and valorization of lignin, a complex aromatic heteropolymer, highly abundant in plant cell walls. Although various strategies for lignin degradation have been described, most of these processes require large amounts of chemicals or high energy input. Therefore, green alternatives are searched for.

A potential sustainable approach for lignin degradation is by using laccase/mediator systems (LMS). Laccases (E.C. 1.10.3.2) are oxidases, produced by various lignin-degrading microorganisms. Due to their relatively low redox potentials, laccases can only oxidize the phenolic substructures of lignin, which typically account for 10-20% of the lignin polymer. Nevertheless, in combination with a mediator, a small molecule that operates as a redox shuttle, laccases can also oxidize non-phenolic lignin substructures (80-90%). Such oxidation may, eventually, result in lignin degradation, modification or even polymerization. Despite various mechanistic studies on the effect of LMS treatments on the structure of lignin, the exact outcome of such LMS treatments remains hard to predict. This is partly caused by the fact that lignin has a complex and heterogeneous structure and that structural analysis of lignin is highly challenging.

In this thesis, we aimed to enhance the understanding of laccase and LMS-catalyzed lignin degradation and modification at the molecular level. To this end, we used various (novel) β -O-4' linked lignin model dimers to study, in detail, the reactivity of multiple important lignin substructures upon laccase and LMS treatments. β -O-4' linked model dimers were used, as the β -O-4' linkage is, by far, the most abundant interunit linkage in native lignin. In addition, lignocellulosic biomass and lignin isolates were used, to investigate to what extent the findings obtained in model compound studies can be extrapolated to LMS treatments of polymeric lignin.

In **Chapter 2**, we investigated the reactivity of a phenolic β -O-4' linked lignin model dimer guaiacylglycerol- β -guaiacyl ether (GBG) with laccase alone, and in the presence of the mediators 1-hydroxybenzotriazole (HBT) or 2,2'-azino-bis(3-ethylbenzothiazoline-6-sulfonic acid (ABTS). Although phenolic lignin structures, such as GBG, can be oxidized by laccase without a mediator, polymeric lignin substrates are generally treated with LMS rather than with laccase alone, to broaden the substrate range of the laccase. Thus, it is important to understand how the addition of a mediator influences the reaction pathway of phenolic lignin structures. We show, based on RP-UHPLC-PDA-MSⁿ and MALDI-TOF-MS, that GBG polymerizes extensively upon incubation with laccase alone. In the presence of HBT, radical coupling between GBG and HBT was observed, although only to a minor extent. Polymerization in presence of HBT occurred to a similar extent as in the incubation with laccase alone. In contrast, in the presence of ABTS, no polymerization of GBG was observed. Instead, extensive coupling between GBG and ABTS occurred, as well as C_o-oxidation of the GBG moiety. This indicates that the selection of a mediator has a large impact on the outcome of LMS treatments of lignin.

In **Chapter 3**, we aimed to provide insights into the reactivity of lignosulfonate upon laccase and LMS treatments. Lignosulfonate is a major by-product from pulp and paper industry, and is extensively sulfonated at the C₆-positions. Although various studies aimed to modify lignosulfonate by using LMS, it remained unclear whether and how sulfonation of lignin influenced the reaction outcome of LMS treatments. To overcome this knowledge gap, we investigated the reactivity of multiple model dimers, resembling the structure of native or sulfonated lignin, upon laccase and laccase/HBT treatments. It was observed that a sulfonated phenolic model dimer was converted slower by laccase and laccase/HBT than its non-sulfonated 'native' analogue. Nevertheless, the reaction pathways of the phenolic model dimers were similar: Upon both laccase and laccase/HBT treatments, extensive polymerization was observed. A larger impact of sulfonation was found upon incubation of non-phenolic model dimers. Whereas a 'native' non-phenolic lignin model dimer underwent C₆-oxidation and ether cleavage upon laccase/HBT treatment, its sulfonated analogue was completely unreactive. Based on Density Functional Theory (DFT) calculations, we proposed that this inertness was caused by the fact that sulfonation of lignin increases the C₆-H bond dissociation energy by 9 kcal/mol, which would make hydrogen atom abstraction by the mediator (HBT) too endergonic to occur. As sulfonation did not impede polymerization (of phenolic substructures), but completely prevented cleavage of the non-phenolic structures, we concluded that sulfonation of lignin steers the overall outcome of LMS treatments towards polymerization.

In **Chapter 4**, we zoomed in on the competition between C₆-oxidation and ether cleavage of non-phenolic β -O-4' linked lignin structures upon laccase/HBT treatments. Although ether cleavage, and not C₆-oxidation, contributes to degradation of lignin, C₆-oxidation is generally the main result of LMS treatments. In this study, we report that this balance between C₆-oxidation and ether cleavage can be shifted in favor of the latter by altering the properties of the incubation buffer. Whereas ether cleavage products accounted for <10% of the reaction products under standard conditions (i.e. weak buffer at pH 4), this was enhanced to 80% in concentrated buffers at pH 6. By performing DFT calculations, we proposed, for the first time, detailed reaction mechanisms for C₆-oxidation and ether cleavage of non-phenolic β -O-4' linked lignin structures. Based on additional experiments and computational insights, we propose that increasing buffer pH and strength enhances H-bonding between the C₆-OH group of lignin structures and buffer anions, and that such H-bonding drives the overall reaction outcome towards ether cleavage.

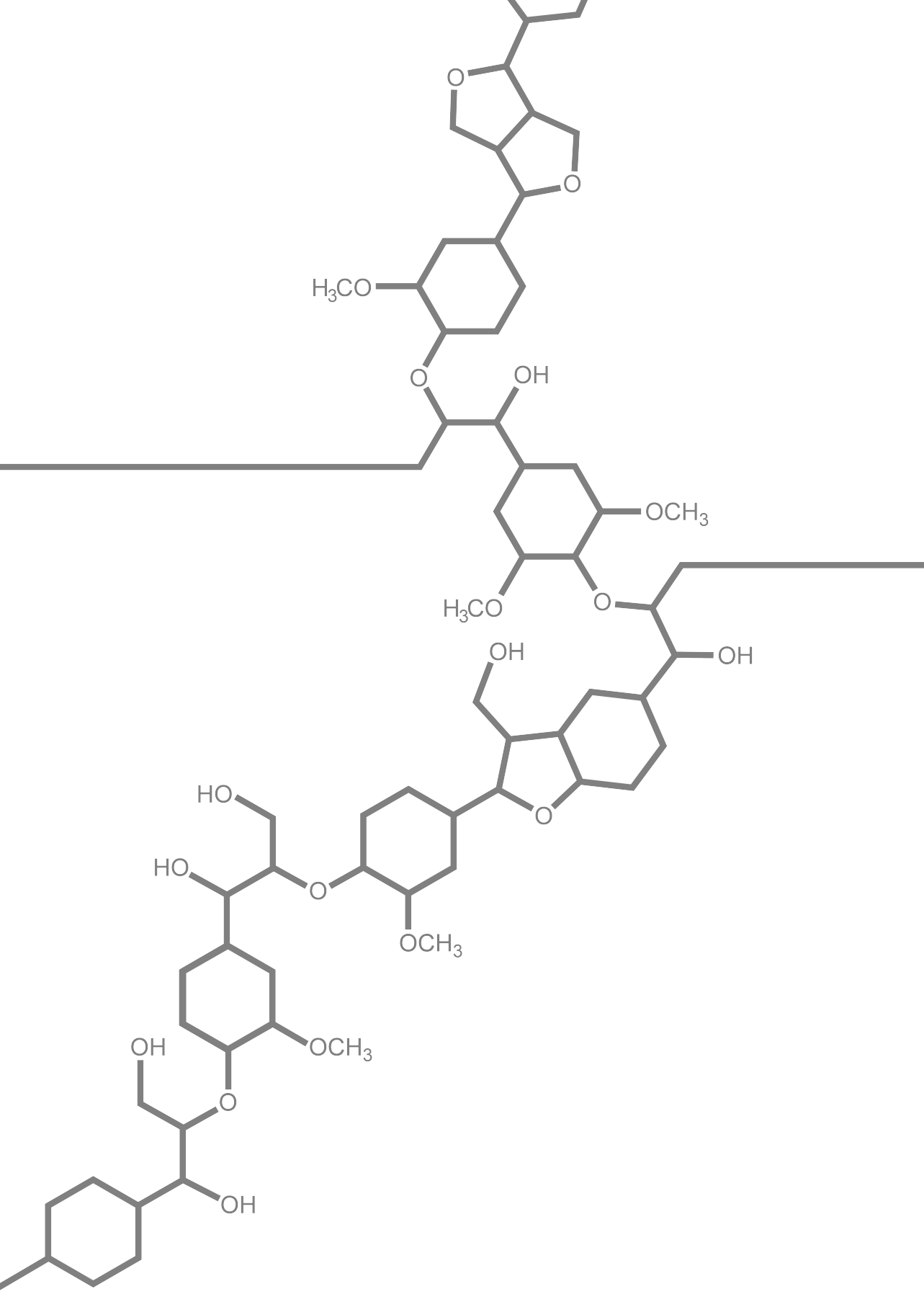
In **Chapter 5**, laccase/HBT-catalyzed degradation of lignin in wheat straw and corn stover was studied. Comprehensive fractionation and purification allowed to study the effect of laccase/HBT treatment on native lignin at an unprecedented level of detail. To this end, 2D NMR spectroscopy, py-GC-MS and several other techniques were used. Laccase/HBT treatment was found to result in up to 51% biomass delignification. Furthermore, by using various analytical techniques and insights obtained from model

compound studies, we were able to show, for the first time, that laccase/HBT treatment of wheat straw and corn stover resulted in C_α-oxidation and cleavage of C_β-O, O-4' and C_α-C_β bonds. Remarkably, upon laccase/HBT treatment, *p*-coumaroyl groups accumulated in the residue, suggesting that they are relatively unreactive, despite their free-phenolic character.

In **Chapter 6**, a facile procedure was reported for C_V-acylation of (non-phenolic) lignin model dimers, by using a lipase from *Candida antarctica* as a catalyst. Following this procedure, lignin model compounds were acylated at the C_V-position with *p*-coumaroyl, cinnamoyl, *p*-hydroxybenzoyl and acetyl groups. The resulting novel model compounds mimic highly abundant substructures of grass and hardwood lignins, and, thereby, enable to study the reactivity of such lignins in more detail.

In **Chapter 7**, we zoomed in on the reactivity of *p*-coumaroyl groups in lignin upon laccase and laccase/HBT treatments. Hereto, the reactivity of *p*-coumaroylated and cinnamoylated lignin model dimers (Chapter 6) was studied by using RP-UHPLC-PDA-MSⁿ. In addition, the effect of laccase/HBT treatment on lignin isolated from wheat straw and corn stover was investigated by using HSQC NMR spectroscopy. The *p*-coumaroylated lignin dimers were rapidly converted by laccase and laccase/HBT, resulting in dimerization and HBT-mediated degradation, respectively. The high reactivity was clearly related to the phenolic nature of the *p*-coumaroyl moiety, as non-acylated and non-phenolic analogues showed low or no reactivity. Upon laccase/HBT treatment of the lignin isolates, *p*-coumaroyl groups accumulated in the residue, indicating that *p*-coumaroyl groups in polymeric lignin display different reactivity than those in model compounds. Based on additional experiments, we proposed that *p*-coumaroyl groups in lignin polymers are oxidized by laccase/HBT, but undergo HSQC-undetectable radical coupling or redox reactions rather than degradation.

In **Chapter 8**, the insights obtained from previous chapters were combined in a general discussion. We reflected on the role of the mediator in LMS treatments of lignin, and concluded that the mechanisms underlying LMS-catalyzed lignin oxidations should be partly reconsidered. In addition, based on additional (unpublished) data and literature, we argued that natural phenolic molecules may be used as alternatives for synthetic mediators like HBT, but that such natural alternatives are less effective and less efficient than HBT. We also discussed, in detail, how (small) differences in lignin structure can result in large differences in reactivity upon laccase and LMS treatments, and how lignin model compound studies contribute to the understanding of such reactivity. Lastly, we pointed out the main challenges related to LMS-catalyzed lignin degradation on industrial scale, and provided a potential future approach to tackle these challenges, based on the insights obtained from this thesis.



Acknowledgements

Zo. Dat was het dan. Vier jaar verder, en tijd om een mooi hoofdstuk van mijn leven af te sluiten. Dat het zo'n mooi hoofdstuk was komt vooral door alle mensen die mij de afgelopen jaren binnen en buiten de WUR hebben ondersteund. Die mensen wil ik hieronder graag bedanken.

In 2010 begon ik met studeren in Wageningen. Het idee: iets met voedsel op een universiteit. Misschien dat ik daar wel iets zou leren over moleculaire gastronomie, dan een eigen restaurant zou beginnen, of wellicht productontwerper worden. Het is anders gelopen. In 2013 deed ik mijn BSc afstudeeronderzoek bij FCH. Daar sloeg een wetenschappelijke vonk op mij over die niet meer is verdwenen. Tomas en Jean-Paul, jullie enthousiasme en persoonlijke begeleiding destijds hebben daar een grote rol in gespeeld. Anderhalf jaar later deden Roy en Peter daar nog een schepje bovenop tijdens mijn MSc thesis, en toen wist ik het zeker: ik wil AIO worden, en het liefst bij FCH.

In 2015 kwam er een project vrij bij Mirjam op lignine. Uiteindelijk gooiden we een muntje op om te beslissen of Gijs of ik daarop als AIO zou worden. Het lot bepaalde dat dit project naar Gijs ging, en dat is een uiterst gelukkige combinatie gebleken. Harry, ondanks dat het muntje voor mij niet goed viel, besloot je mij aan te nemen bij FCH, in eerste instantie als onderzoeks- en onderwijsmedewerker, en later als AIO. Aangezien er op dat moment geen goedgekeurde projectvoorstellen lagen, was dat laatste verre van vanzelfsprekend. Het is jammer dat jij zelf het FCH-schip vroegtijdig hebt moeten verlaten, maar ik ben je enorm dankbaar dat je mij aan boord hebt gelaten. Dat zal ik altijd onthouden.

Zodoende belandde ik begin 2016 aan tafel bij Mirjam en Jean-Paul. Jullie wilden wel eens samen een project begeleiden, en zagen mogelijkheden om dat binnen mijn interessegebied te doen. Het begon met een half A4-tje waarop enkel een aantal steekwoorden stonden. Eigenlijk hadden we alle drie nog geen duidelijk beeld waar deze reis heen zou gaan. Uiteindelijk kristalliseerde dat uit in een proposal waarin laccase, mediator en lignine de boventoon voerden. Mirjam, bedankt voor de uitzonderlijke combinatie van gedrevenheid en luchtigheid die je mij vier jaar lang als voorbeeld hebt gesteld. Soms snap ik nog steeds niet hoe je het doet, maar ik hoop diezelfde balans ook te bereiken. Qua onderzoek zal ik met name je enzym-gerichte mindset meenemen. Terwijl ik in al mijn enthousiasme al het lab in was gedoken om met een 7-staps synthese gecoumaroyleerde lignine modelcomponenten te maken, kwam jij doodleuk met de vraag of zo iets niet in 1 stap met een lipase zou kunnen. De rest is geschiedenis (en hoofdstuk 6). Jean-Paul, ik herinner me dat Tomas in zijn dankwoord schreef dat het een voorrecht is om jou als co-promotor te hebben. 'Co' is inmiddels verdwenen, maar bij de rest kan ik me alleen maar aansluiten. De manier waarop jij mensen leest is bewonderingswaardig. Je voelt je als AIO gezien en begrepen, en dat maakt FCH een fantastische plek om te werken. Hoeveel comments of vragen je ook hebt bij presentaties en manuscripten, de boodschap is altijd positief geladen (geen wonder dat je zo'n fan bent van anthocyanen).

Mirjam en Jean-Paul, bedankt voor de houvast die jullie me gaven toen het in het begin van mijn PhD nog vrij lang onzeker bleef hoe mijn project er uit kwam te zien. Evenveel bedankt voor de grote vrijheid die jullie me gaven toen de rode draad beter zichtbaar werd. Het was voor mij een heel goede balans!

Jolanda, het is moeilijk om nog iets origineels over jou te schrijven, want alle lof die andere AIO's jou al hebben toegeschreven kan ik enkel onderschrijven. Bedankt voor het constant draaiende houden van de FCH-motor en voor al je geduld bij het oplossen van organisatorische problemen (#vliegticketgate).

To all FCH (ex-)colleagues: It has been an absolute privilege to work in such a nice team. With many of you, I've had many good laughs and conversations during coffee and lunch breaks and FCH activities. Despite the fact that we are a group of many different characters, I think FCH is a place where everybody feels respected. I hope that this will never change (I'm quite confident about this)!

Gijs, naast alle woordgrapsessies zijn we elkaar de afgelopen jaren steeds vaker gaan opzoeken om inhoudelijk te sparren over onze onderzoeken. Waar ik mijn project aangevlogen was met een focus op reactiviteit van lignine substructuren en het begrijpen daarvan, was jij volop in de analyse en structuuropheldering van lignine gedoken. Ik heb met name in de laatste twee jaar van mijn project veelvuldig gebruik gemaakt van jouw kennis. Mooi dat we ook tot twee gezamenlijke publicaties zijn gekomen! Dank voor alle ligninspiratie!

Willem, een lignine-maatje had ik al, maar toen jij bij FCH kwam werken kreeg ik er ook een mede-laccase-enthousiast bij. Ondanks dat je nooit direct betrokken bent geweest bij mijn project hebben we meerdere malen discussies gehad over laccase en andere enzymen, vaak tijdens koffiepauzes en borrels. Dit heeft mijn blik op laccase en biocatalyse sterk verruimd. Dank daarvoor!

Ook wil ik graag alle technicians van FCH bedanken voor alle ondersteuning en het draaiende houden van de labs. In het bijzonder Mark, van wie ik veel heb geleerd over de UHPLC-MS systemen.

Thanks to my office mates at FCH: Matthias, Madelon, Zhibin and Frederik in my first office, Sylvia, Loes and Eleni in my second office. I really liked the balance between social contact and focus on work I experienced in both offices. Sylvia, αλσο θανκς φορ ιμπροβινγ μαι Γρεεκ. Ι θινκ ιτ ρεαλλι παιδ οφφ! Μιλλαλοττε!

Also thanks to my lab mates at FCH: Peter, Melliana, Fangjie, Junfeng, Jianli, Loes and Lorenz. I think we never won the prize for 'tidiest lab', but I very much appreciated the relaxed vibe in X0229!

Dear Pauline, Napon, Joran, Xinyue, Megan, Florence, Kim and Vincent, thanks for all your direct and indirect contributions to my PhD project. I enjoyed supervising your BSc and MSc thesis projects, and I definitely learned a lot from this. Vincent, heel mooi dat je ervoor hebt gekozen terug te keren naar FCH voor een PhD project. Ik ben ervan overtuigd dat je het 'vet' goed gaat doen!

Han en Annemieke (ORC), enorm bedankt voor al jullie berekeningen en andere input tijdens mijn PhD. Het heeft twee mooie manuscripten opgeleverd, die zonder jullie bijdrage niet mogelijk waren geweest. Misschien nog wel belangrijker: ik heb ontzettend veel geleerd en genoten van de discussies met jullie. Soms op het Helix, en vaak ook via mail met Annemieke. Het is voor mij echt een verrijking van mijn project geweest! Antje and Irina, thank you very much for performing the SEC-MALS analyses!

Wouter, de afgelopen jaren zijn we steeds meer met elkaar opgetrokken, op het Axis, maar ook daarbuiten. Het samen begeleiden van Advanced Molecular Gastronomy was elk jaar een feest. Ook heb ik genoten van alle etentjes en speciaalbieravonden. Jouw toekomst is al wat zekerder dan die van mij, maar ik hoop dat we dit links- of rechtsom kunnen blijven doen in de toekomst. Bedankt dat je mijn paranimf bent op 4-9-2020!

Judith, een paar jaar geleden zat je nog als student in het practicum dat Wouter en ik samen begeleidden. Inmiddels lever je als AIO op meerdere vlakken een 'ijzersterke' bijdrage aan FCH. Ik heb genoten van alle discussies die we hebben gehad (van ijzercomplexen tot feminisme), en hoop dat er ook in de toekomst nog bezoeken aan jullie boerderij in zitten! Bedankt dat ook jij mijn paranimf bent op 4-9-2020!

Ook naast het WUR-leven hebben veel mensen me op verschillende manieren ondersteund de afgelopen jaren. Manu, Maarten, Wouter, Steef, Jochem en Bram, ik mag me echt rijk rekenen met vrienden als jullie. We zijn na de middelbare school allemaal ons eigen ding gaan doen, maar het gevoel van verwantschap is met de jaren alleen maar gegroeid. Dank voor alle goede discussies (vaak gekatalyseerd door een speciaalbiertje), vriendenweekenden, skivakanties, enzovoort. Steef, het wekelijkse quizuitje op dinsdag was een heerlijke afleiding van het PhD-leven. Lang leve PV de Wijnkelder!

David, het opboksen tegen zo'n talentvolle grote broer was niet altijd even makkelijk, maar het heeft me gepusht om zoveel mogelijk uit mezelf te halen en de wereld te laten zien wie ik ben. Gelukkig is die competitie inmiddels wel verdwenen;) Bedankt voor het voorbeeld dat je me gegeven hebt!

Mam, bedankt voor alle onvoorwaardelijke steun die je mij de afgelopen 29 jaar gegeven hebt, in goede maar vooral ook in minder goede tijden. Ik vraag me af of dit boekje er zonder die steun überhaupt was geweest.

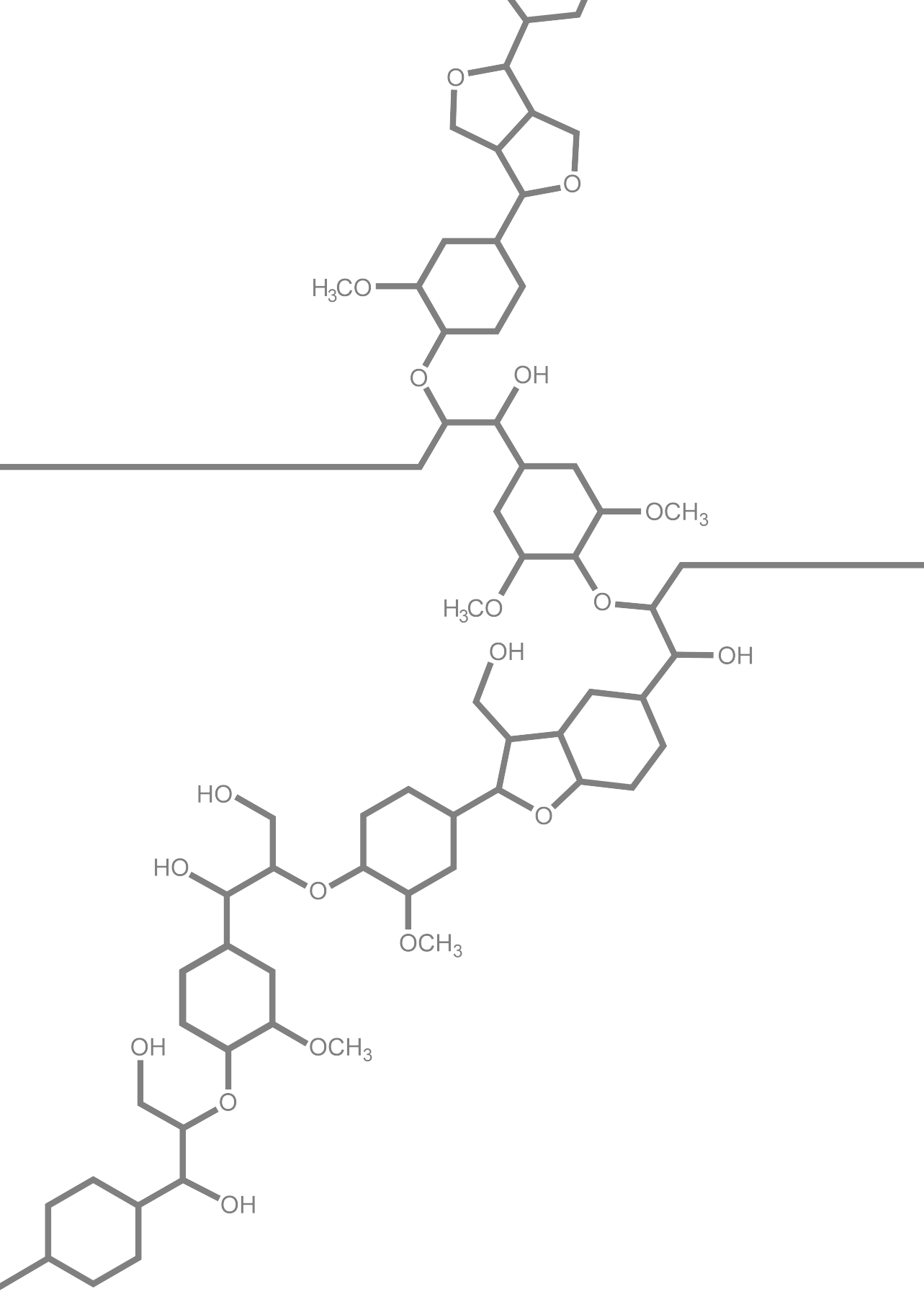
Pap, bedankt voor alle wijze lessen die je me geleerd hebt. Ik heb er veel aan gehad de afgelopen jaren. Ik hoop dat je trots bent man!

Lotte en Ted, jullie hebben het familiegevoel in ons gezin weer helemaal teruggebracht. Bedankt voor alle fijne etentjes, uitjes en gesprekken!

Ook mijn 'grote' zussen en broer en de gezinnen daaromheen: Bedankt voor al jullie betrokkenheid, zorgzaamheid en gezelligheid de afgelopen jaren! Marcelle, enorm bedankt voor het ontwerpen van de cover! Ik ben er heel blij mee!

Lieve Bianca, ik ben dankbaar dat ik jou heb mogen leren kennen tijdens mijn PhD. Door onze gesprekken en de spiegel die je me regelmatig voorhoudt leer ik mezelf en de wereld om me heen elke dag iets beter kennen. Bedankt ook voor alle flexibiliteit die je toont als ik weer eens in het weekend 'pieken ga checken' in het Axis, omdat ik te ongeduldig ben. Die flexibiliteit is niet vanzelfsprekend en waardeer ik enorm. Om in wetenschapstermen te blijven: Je bent met afstand de grootste Impact Factor die ik aan mijn PhD heb overgehouden. Op naar nog veel mooie jaren samen!

Roelant



About the author

Curriculum vitae

Roelant Jan Hilgers was born on June 11th 1991 in Ooij, The Netherlands. After graduating from high school (Stedelijk Gymnasium Nijmegen), he started his studies in Food Technology at Wageningen University. In 2013 he obtained his BSc degree after finishing a thesis entitled 'Tyrosinase-induced reactions between phenolics and nucleophiles' at the Laboratory of Food Chemistry in Wageningen. In the same year he started his master studies in Food Technology at Wageningen university, during which he mainly specialized in the chemistry and physics of food. In 2015, he finished his MSc thesis entitled 'The influence of pH and protein concentration on emulsion flocculation' and did a six-month internship at Corbion, Gorinchem, The Netherlands, during which he focused on UHPLC-MS based impurity profiling. After obtaining his MSc degree (cum laude), he worked for six months as a research & education co-worker at the Laboratory of Food Chemistry, after which he started as a PhD candidate at the same laboratory under the supervision of Dr. Mirjam Kabel and Prof. Jean-Paul Vincken. The results of his PhD research are presented in this thesis. Roelant currently works as a researcher at the Laboratory of Food Chemistry.



List of publications

Hilgers R, Van Dam A, Zuilhof H, Vincken J-P, Kabel MA. Controlling the competition: boosting laccase/HBT-catalyzed cleavage of a β -O-4' linked lignin model. *ACS Catalysis*. 2020, 10, 8650-8659.

Hilgers R, Kabel MA and Vincken J-P. On the reactivity of *p*-coumaroyl groups in lignin upon laccase and laccase/HBT treatments. *ACS Sustainable Chemistry & Engineering*. 2020, 8(23), 8723-8731.

Hilgers R, Van Erven G, Boerkamp V, Sulaeva I, Potthast A, Kabel MA, Vincken J-P. Understanding laccase/HBT-catalyzed grass delignification at the molecular level. *Green Chemistry*. 2020, 22(5), 1735-1746.

Hilgers R, Vincken J-P, Kabel MA. Facile enzymatic C_γ-acylation of lignin model compounds. *Catalysis Communications*. 2020, 136; 105919.

Hilgers R, Twentyman-Jones M, Van Dam A, Zuilhof H, Kabel MA, Vincken J-P. The impact of lignin sulfonation on its reactivity with laccase and laccase/HBT. *Catalysis Science & Technology*. 2019, 9(6), 1535-1542.

Hilgers R, Vincken J-P, Gruppen H, Kabel MA. Laccase/mediator systems: their reactivity toward phenolic lignin structures. *ACS Sustainable Chemistry & Engineering*. 2018, 6(2), 2037-2046.

Van Erven G, **Hilgers R**, De Waard P, Gladbeek E-J, Van Berkel WJH, Kabel MA. Elucidation of in situ ligninolysis mechanisms of the selective white-rot fungus *Ceriporiopsis subvermispora*. *ACS Sustainable Chemistry & Engineering*. 2019, 7(19), 16757-16764.

Frommhagen M, Westphal AH, **Hilgers R**, Koetsier MJ, Hinz SWA, Visser J, Gruppen H, Van Berkel WJH, Kabel MA. Quantification of the catalytic performance of C1-cellulose-specific lytic polysaccharide monooxygenases. *Applied Microbiology and Biotechnology*. 2018, 102(3), 1281-1295.

Vissers A, Kiskini A, **Hilgers R**, Marinea M, Wierenga PA, Gruppen H, Vincken J-P. Enzymatic browning in sugar beet leaves (*Beta vulgaris* L.): influence of caffeic acid derivatives, oxidative coupling, and coupled oxidation. *Journal of Agricultural and Food Chemistry*. 2017, 65(24), 4911-4920.

Delahaije RJBM, **Hilgers R**, Wierenga PA, Gruppen H. Relative contributions of charge and surface coverage on pH-induced flocculation of protein-stabilized emulsions. *Colloids and Surfaces A: Physicochemical and Engineering Aspects*. 2017. 521, 153-160.

Overview of completed training activities

Discipline specific activities		
<i>Courses</i>		
Ion Trap operations course	Thermo Scientific, Wageningen	2016
Structure & Reactivity	ORC, WUR, Wageningen	2016
<i>Conferences</i>		
OxiZymes	VLAG/BIC, Wageningen	2016
GRC Lignin Conference	Gordon Research Conferences, Easton MA, USA	2018 ^a
CHAINS (CHemistry As INnovative Science)	NWO, Veldhoven	2019 ^{a,b}
General courses		
Brain Training	WGS, Wageningen	2016
The Essentials of Scientific Writing & Presenting	WGS, Wageningen	2016
Project & Time Management	WGS, Wageningen	2017
Scientific Writing	WGS, Wageningen	2018
Career Perspectives	WGS, Wageningen	2019
Optional activities		
Preparation research proposal	FCH, Wageningen	2016
PhD study trip 2016	FCH, Japan	2016 ^{a,b}
PhD study trip 2018	FCH, Italy & Austria	2018 ^{a,b,c}
BSc & MSc thesis student supervision, presentations and colloquia	FCH, Wageningen	2016- 2020
PhD presentations	FCH, Wageningen	2016- 2020

^a Poster presentation. ^b Oral presentation. ^c Organizing committee.

Abbreviations: ORC, Laboratory of Organic Chemistry (WUR); VLAG, Graduate School for Advanced studies in Food Technology, Agrobiotechnology, Nutrition and Health Science; BIC, Laboratory of Biochemistry (WUR); NWO, Nederlandse Organisatie voor Wetenschappelijk Onderzoek; WGS, Wageningen Graduate Schools; FCH, Laboratory of Food Chemistry (WUR).

The work described in this thesis was performed at the Laboratory of Food Chemistry of Wageningen University & Research, The Netherlands.

Financial support from Wageningen University for printing this thesis is gratefully acknowledged.

Cover design by Marcelle Hilgers and Revi Bloemendal
Printed by Proefschrift-AIO
Edition: 250 copies

Roelant Hilgers, 2020

